

# THESE de l'Université de Lyon

Délivrée par l'Ecole Centrale de Lyon

Specialité: **Materiaux - Ecole Doctorale EDML**

Soutenue le 18 Decembre 2015 à Lyon

par

**De Feo Modestino**

preparée au Laboratoire de Tribologie et Dynamique des Systèmes

Impact of thermo-oxidative degradation of MoDTC additive on its tribological performances for steel-steel and DLC-steel contacts

*“Impact du vieillissement de l’additif MoDTC sur ses propriétés tribologiques pour les contacts acier-acier et DLC-acier”*

Composition du jury:

DR	Christophe <b>GEANTET</b>	CNRS	Rapporteur
Dr.	Ali <b>ERDEMIR</b>	Argonne National Laboratory	Rapporteur
Pr.	Christophe <b>DONNET</b>	Lab. Hubert Curien	Examineur
Pr.	Anne <b>NEVILLE</b>	Université de Leeds	Examineur
Pr.	Martin <b>DIENWIEBEL</b>	Karlsruhe Institute of Technology (KIT)	Examineur
MCF HDR	Maria Isabel <b>DE BARROS</b>	LTDS Lyon	Directrice de these
MCF	Clotilde <b>MINFRAY</b>	LTDS Lyon	Co-Encadrante



This study was funded by the FP7 program through the Marie Curie Initial Training Network (MC- ITN) entitled “**ENTICE** - Engineering Tribochemistry and Interfaces with a Focus on the Internal Combustion Engine” [290077]





# Table of contents

GENERAL INTRODUCTION.....	9
---------------------------	---

## CHAPTER 1: State of Art

1. Lubricant degradation causes: Overview.....	19
2. Base oil oxidation and Additive oxidation reactions.....	25
2.1. Base oil oxidation.....	25
2.2. Additive degradation.....	27
2.2.1. Molybdenum-containing friction modifiers.....	28
2.2.2. Molybdenum disulfide (MoS <sub>2</sub> ) .....	28
2.2.3. Molybdenum dithiocarbamate (MoDTC) .....	29
2.2.4. MoDTC degradation.....	31
3. Conclusions.....	32
4. Bibliography.....	33

## CHAPTER 2: Ageing impact on tribological properties of MoDTC-containing base oil

1. Introduction.....	41
2. Experimental details.....	41
2.1. Materials.....	41
2.2. Protocol of oxidative procedure.....	42
2.3. Tribological experiments.....	43
2.3.1. Friction Coefficient.....	43
2.3.2. Wear Measurement.....	43
2.4. X-ray Photoelectron Spectroscopy (XPS) analysis.....	44
2.5. Raman spectroscopy analyses.....	44
2.6. Transmission Electron Microscopy (TEM) analysis.....	45
3. Results.....	45
3.1. Optical observations of the ageing effects.....	45
3.2. Tribological tests.....	46
3.2.1. Friction coefficient.....	46
3.2.2. Wear.....	47
3.3. X-ray Photoelectron Spectroscopy (XPS) analysis.....	48

3.3.1.	First fitting based on a progressive chemical shift of Mo (IV) peak.....	49
3.3.2.	Second fitting based on three contributions in Mo3d peak.....	52
3.4.	Raman Spectroscopy.....	55
3.5.	Transmission Electron Microscopy (TEM) .....	56
4.	Discussion.....	59
5.	Conclusions.....	63
6.	Bibliography.....	64

### **CHAPTER 3: MoDTC chemical changes in bulk oil due to degradation process**

1.	Introduction.....	69
2.	Methodology.....	70
2.1.	Degradation procedure.....	70
2.2.	High Performance Liquid Chromatography (HPLC) .....	70
2.3.	Mass Spectroscopy (MS) .....	71
2.4.	Fourier Transform Infra-Red Spectroscopy (FT-IR) .....	71
3.	Results.....	71
3.1.	Degraded oil: visual inspection.....	71
3.2.	MoDTC additive depletion by HPLC.....	72
3.3.	Study of MoDTC molecular transformations by Mass Spectroscopy.....	74
3.4.	Study of MoDTC thermo-oxidative degradation by FT-IR.....	80
4.	Discussion.....	82
5.	Conclusions.....	84
6.	Bibliography.....	85

### **CHAPTER 4: Investigation of solid-like particles generated by the ageing degradation: chemical composition, morphological structure and tribological properties**

1.	Introduction.....	89
2.	Methods.....	90
2.1.	Particles extraction.....	90
2.2.	Particles size.....	91
2.3.	Chemical and morphological analysis (XPS and TEM) .....	91
2.4.	Tribometry study.....	91

2.4.1.	Linear reciprocating tribometer.....	91
2.4.2.	MTM.....	93
3.	Results.....	94
3.1.	Visual inspection.....	94
3.2.	Particle size.....	94
3.3.	TEM characterization.....	95
3.4.	XPS analysis.....	96
3.5.	Tribological results.....	98
3.5.1.	Linear reciprocating tribometer.....	98
3.5.2.	MTM.....	92
4.	Discussion.....	103
5.	Conclusions.....	105
6.	Bibliography.....	106

## **CHAPTER 5: DLC-involving contact**

1.	Introduction.....	109
2.	Material and Methods.....	111
2.1.	DLC coatings.....	111
2.2.	Tribological experiments.....	111
2.3.	Surface post-mortem analysis.....	111
3.	Results.....	112
3.1.	Friction performance.....	112
3.2.	(DLC) Wear measurements.....	113
3.3.	(DLC) X-ray photoelectron spectroscopy (XPS).....	115
3.4.	(DLC) Scanning Electron Microscopy/Energy Dispersive X-ray (SEM/EDX).....	116
3.5.	(Ball) X-ray photoelectron spectroscopy (XPS).....	117
3.6.	(Ball) Scanning Electron Microscopy/Energy Dispersive X-ray (SEM/EDX).....	119
3.7.	(Ball) Transmission Electron Microscopy/Energy Dispersive X-ray (TEM/EDX).....	120
4.	Discussion.....	125
4.1.	Experimental results.....	125
4.2.	Proposal of new wear mechanism.....	126

4.3.	Model Validation.....	128
4.3.1.	a-C:H DLC vs. a-C:H:Si:O DLC.....	128
4.3.2.	Characterization of pristine a-C:H:Si:O DLC coating.....	129
4.3.3.	XPS analysis on DLC coating prior the tribological experiments...	130
4.3.4.	TEM observations.....	130
4.3.5.	Variable duration tests.....	133
4.4.	Questions arising from the results presenting above.....	135
4.4.1.	PEELS analysis.....	135
4.4.2.	Nano-indentation.....	137
4.4.3.	TEM characterization of wear debris.....	138
4.4.4.	Tribological behavior of DLC/DLC tribo-pairs.....	141
4.5.	Influence of MoDTC degradation on DLC/steel-involving contact.....	144
4.5.1.	Friction and wear performance.....	144
5.	Conclusions.....	147
6.	Bibliography.....	149

## **CHAPTER 6: Binary Additive Combinations**

1.	Introduction.....	155
1.1.	Zinc Dialkyl Dithiophosphate (ZDDP) .....	155
1.2.	Antioxidant.....	156
1.3.	Dispersant.....	156
2.	Objectives.....	157
3.	Materials.....	158
4.	Methods.....	159
5.	Results.....	159
5.1.	Visual Inspection.....	159
5.2.	Liquid Chromatography (LC) .....	160
5.3.	Mass Spectroscopy (MS) .....	162
5.4.	Tribological Experiments.....	165
5.4.1.	Steel/Steel Contact.....	166
5.4.2.	DLC/Steel Contact.....	168
6.	Discussion.....	173
7.	Conclusions.....	175
8.	Bibliography.....	177

# General Introduction

---

In order to conserve natural resources, to have less exhaust emission, to protect the environment, to improve energy efficiency, to extend equipment durability and to reduce operating cost, it is necessary to find a solution for the fuel efficiency of automobiles and new engine designs. Significant improvements on this point have been achieved by vehicle weight reduction [1-3], combustion optimization [4], and enhancement of vehicle design [5]. During the last decades, the reduction in frictional loss in the Internal Combustion Engine (ICE) has given a great contribution to solve the problem. In fact, it is estimated that approximately one third of all energy used in industrial countries goes to overcome friction [6,7]. High friction often results in high wear and machinery breakdown, and more than 30% of the production in industry goes to replace worn out products with new ones [8]. The breakdown of machinery may, in addition, result in safety risks and environmental pollution. Furthermore, increasing engine efficiency leads to a lower consumption of fuel and oil; which in turn decreases the emission of pollutants. Therefore, decreasing friction and wear is one major challenge in order to have a sustainable society with low energy consumption and reduced environmental climate change effects [8].

To date, research has been focused primarily on lubricant specifications and on the development of new materials [3, 8-10], low friction coatings [11-13] and new surface finishing techniques [14]. In the latter, the influence of contaminants [15] and the effect of the oil degradation over time [16] were studied as well.

Moving parts in industrial devices require lubrication and the efficiency of a process depends on the type and quality of the lubricant used. For this reason, oils employed in lubricating applications must show widely different specifications, while also having one requirement in common: they should not undergo a significant change during usage.

Among the wide variety of lubricants employed in the large range of industrial automotive applications, engine lubricants have a crucial role. They can be considered as a “multi-tasking” lubricants: their principal duties are to provide lubrication of moving parts of the internal combustion engine, to control the engine temperature and to give the right level of cleaning (preventing carbon and varnishes from accumulation) and corrosion protection, maximizing the power output of the engine. For this reason, it is extremely important to study their behavior in order to optimize the equipment’s efficiency. One fundamental aspect to consider is that engine oils operate in a very hostile environment. They are

subjected to high temperatures, high shear stress, oxidation and chemical attack by fuel combustion products and the combination of these factors might result in changes in the oil properties. These chemical and physical changes give rise to oil with lower lubricant functionality, leading to lubricant additives unfit for their purpose.

The possibility to know the lifetime of a lubricant under a range of conditions, both by reproducing the environment of an engine in a laboratory environment, and modeling the oil degradation processes, would provide aid in designing the lubricant for a particular purpose, or to schedule maintenance before to have mechanical failure of moving parts. For these reasons, understanding of the ageing process starting from simpler model lubricant with base oil and one single additive can provide significant benefits.

The molybdenum dithiocarbamate (MoDTC) additive promotes the energy efficiency and reduces the friction coefficient under boundary lubrication conditions in automotive engines, making evaluation of its performance very important. It has already been reported that this friction modifier has extremely good tribological performance [17-20]. However, the performance loss of MoDTC-containing lubricants due to oil degradation has also been published [20-21] and it remains unclear how the MoDTC behaves when subjected to ageing. For this reason, more work needs to be done in this area before any conclusions can be made. To date, several investigations have been undertaken to determine the parameters effecting MoDTC friction reduction [18, 22] and hypotheses [20, 23] have been made for mechanisms occurring inside the tribological contacts. All these studies provide strong support to the theory that the formation of layered molybdenum disulfide ( $\text{MoS}_2$ ) material is the main mechanism governing the friction reduction whereas the presence of molybdenum trioxide ( $\text{MoO}_3$ ) on the rubbing surfaces tends to decrease the tribological performance. However, due to the extremely complex chemical reaction pathway of MoDTC molecules, the current understanding of its behavior and the effect of its degradation on the tribological properties are still not fully identified. This is particularly true for tribological contacts involving DLC coatings.

The work presented in this thesis is multi-disciplinary, drawing on understanding from three scientific research areas: tribology, lubricant chemistry and degradation mechanisms.

In the **first opening chapter** the main lubricant ageing causes have been briefly discussed, focusing attention on the general background of the molybdenum dithiocarbamate (MoDTC) additive.

Each of the ensuing chapters has the following structure:

- brief overview on the current understanding of the subject, highlighting current knowledge gaps;
- description of the analytical methodologies employed for characterization;
- principal findings resulting from these methods to date are discussed.

**Chapter 2** discusses the impact of MoDTC degradation on tribological properties and a new model about the MoDTC additive behavior in the tribological contact during ageing has been proposed.

**Chapter 3** reports the chemical characterization of MoDTC blended to base oil when subjected to thermo-oxidative degradation. The findings obtained in this chapter led to the proposal of new hypothetical chemical pathway followed by the MoDTC molecule during the ageing process.

The influence of the solid-like particles formed during the degradation process is reported in **Chapter 4**. It focuses on the chemical characterization of these particles and their influence on the friction behavior, in both sliding and rolling/sliding motion.

In the **Chapter 5**, a new DLC coating wear model for the MoDTC-involving lubrication is proposed. At the end of the chapter, the impact of lubricant degradation on the tribological properties of steel/DLC contact is reported.

**Chapter 6** investigates the MoDTC behavior in the presence of ZDDP, antioxidant or dispersant. Particularly, in the first portion of the chapter, the impact of these binary combinations on the chemical bulk degradation is examined. Following that, their tribological behavior in both steel/steel and DLC/steel contact is investigated.

Finally, the conclusions arising from this research work are listed in the **conclusion chapter**, along with future **perspectives**.

# Introduction générale

---

Afin de préserver les ressources naturelles, d'avoir moins d'émission de gaz d'échappement, de protéger l'environnement, d'étendre la durabilité des systèmes mécaniques et de réduire les coûts d'opération d'entretien, il est nécessaire de trouver des solutions pour optimiser les performances énergétiques des véhicules. Des améliorations significatives ont déjà été atteintes via la réduction du poids du véhicule [1-3], l'optimisation du processus de combustion [4], et avec l'optimisation de la conception mécanique des véhicules [5], mais des progrès sont encore à effectuer.

Concernant le moteur à combustion interne, durant les dernières décennies un intérêt particulier a été porté sur la réduction des pertes par frottement et sur l'augmentation de la durée de vie des pièces mécaniques en contact. À ce jour, de nombreux travaux de recherche portent sur le développement de nouveaux matériaux (nouveaux revêtements, nouvel état de surface etc..) et de nouveaux lubrifiants [3, 8-14] permettant d'obtenir les meilleurs résultats tribologiques possibles tout en respectant les normes environnementales. Récemment, l'influence des contaminants [15] et l'effet de la dégradation de l'huile [16] ont fait l'objet de recherches ayant pour but d'améliorer la durabilité du lubrifiant.

Le lubrifiant utilisé dans un véhicule automobile peut être considéré comme "multifonctions" c'est-à-dire qu'il devra permettre de lubrifier les pièces du moteur, de contrôler la température de celui-ci, de le maintenir propre (prévenir l'accumulation de carbone et la formation de vernis) et de le protéger contre la corrosion. Un aspect fondamental à considérer est que les huiles pour moteur opèrent dans un environnement très hostile. Elles sont soumises à des températures élevées, à une sollicitation en cisaillement importante, à de l'oxydation, à des attaques chimiques par les produits de combustion et à la combinaison de tous ces facteurs qui peuvent entraîner une évolution des propriétés physico-chimiques du lubrifiant occasionnant une perte de performance avec le temps.

La possibilité de connaître la durée de vie d'un lubrifiant utilisé dans des conditions précises reproduisant l'environnement d'un moteur (par l'expérience ou par la simulation numérique) serait une aide considérable au développement de nouveaux lubrifiants plus performants. Dans un premier temps, la compréhension du processus de vieillissement d'un lubrifiant modèle simplifié composé d'une huile de base et d'un additif unique serait intéressante à effectuer. Grâce à ses bonnes propriétés réductrices de frottement en régime de lubrification limite dans un contact acier/acier, le dithiocarbamate de molybdène (MoDTC) est un additif



particulièrement intéressant à étudier [17-20]. Cependant, la perte de performance de l'additif MoDTC au cours du temps a été mentionnée à plusieurs reprises [20-21] sans que le processus de dégradation de la molécule ne soit clairement compris. À ce jour, plusieurs études ont été menées pour déterminer les paramètres qui affectent la capacité de réduction du frottement du MoDTC [18, 22] et des hypothèses [20, 23] ont été émises pour tenter d'expliquer les mécanismes de décomposition de l'additif dans le contact tribologique. Il a été montré que deux composés peuvent principalement se former en présence de MoDTC dans un contact acier/acier : i) le bisulfure de molybdène lamellaire ( $\text{MoS}_2$ ) qui permet la réduction du frottement, et ii) le trioxyde de molybdène ( $\text{MoO}_3$ ) qui tend à augmenter l'usure. Toutefois, en raison des réactions chimiques extrêmement complexes suivies par les molécules de MoDTC au cours du vieillissement de l'huile, la compréhension de l'effet de sa dégradation sur les propriétés tribologiques n'est pas clairement identifiée. Cela est particulièrement vrai pour les contacts tribologiques impliquant les revêtements DLC.

Le travail présenté dans cette thèse est centré sur la compréhension des mécanismes de dégradation de la molécule de MoDTC et sur l'impact de cette dégradation sur les propriétés tribologiques dans le cas de contact acier/acier et DLC/acier.

Ce manuscrit est articulé de la manière suivante :

Dans le premier chapitre, les principales causes du vieillissement d'un lubrifiant formulé sont brièvement discutées avec un focus sur le cas particulier de l'additif MoDTC.

Le chapitre 2 traitera de l'impact de la dégradation de la molécule de MoDTC sur les propriétés tribologiques dans un contact acier/acier. L'évolution en terme de composition et d'organisation des tribofilms formés pour différentes conditions de vieillissement est discutée au regard des résultats tribologiques.

Le chapitre 3 focalisera sur l'étude de l'évolution de la composition chimique d'un lubrifiant contenant du MoDTC soumis à différentes conditions de dégradation ( $\text{O}_2$ , température etc...).

Au cours du chapitre 3, la présence de particules solides formées au cours du processus de dégradation du MoDTC a été mise en évidence. Dans le chapitre 4, les résultats de caractérisation de ces particules seront présentés. L'influence de ces particules sur le comportement en frottement pour un contact acier/acier est également étudiée (conditions de glissement pur et de roulement-glissement).

Dans le chapitre 5, c'est le comportement tribologique de contact DLC/acier en présence de MoDTC qui est étudié. Le problème d'usure des revêtements DLC quand ils sont lubrifiés par une huile contenant du MoDTC a été mis en évidence confirmant ainsi la littérature. Un

modèle expliquant cet endommagement spécifique est proposé. A la fin de ce chapitre, les effets de dégradation du lubrifiant sur les propriétés tribologiques du contact acier / DLC est brièvement abordé.

Le chapitre 6 portera sur l'étude de l'influence de la dégradation de mélanges binaires (MoDTC + additif autre) et de leurs impacts sur les propriétés en frottement. Trois mélanges binaires ont été étudiés contenant tous du MoDTC associé soit à du ZDDP (Zinc Dithiophosphate), soit à un antioxydant ou un dispersant. La première partie de ce chapitre portera sur les effets de la dégradation chimique de ces combinaisons binaires (chimie du lubrifiant). Ensuite, le comportement tribologique de tels mélanges dégradés a été étudié en considérant à la fois le contact acier/acier et le contact DLC/acier.

Enfin, les conclusions ainsi que des perspectives tirées de ces travaux de recherche sont présentées dans le dernier chapitre.

## BIBLIOGRAPHY

- [1] Yukihiisa K., Manabu T., Hiroshi O., Basic technology for vehicle weight reduction. Trend of car weight reduction using high-strength steel; Journal of the Society of Automotive Engineers of Japan, Volume 55, Issue 4; Pages 51-57, (2001).
- [2] Magnante S., Lose weight now part II, hot rod magazine, February, (2009).
- [3] Fukuoka S., Hara N., Mori A., Ohtsubo K., Friction loss reduction by new lighter valve train system, JSAE Review, Volume 18, Issue 2, Pages 107–111, (1997).
- [4] McAllister C.D. and Simpson T.W., Multidisciplinary robust design optimization of an internal combustion engine, ASME Journal of Mechanical Design, Volume 125, Pages 124-130, (2003).
- [5] Zheng S., Tang H., Han Z., and Zhang Y., Controller design for vehicle stability enhancement, Control Engneeng Practice, Volume 14, Pages 1413–1421, (2006).
- [6] Stachowiak G., Batchelor A.W., Engineering Tribology Third Edition, Elsevier Butterworth-Heinemann, Oxford 77, (2005).
- [7] Holmberg K., Friction science saves energy, VVT Impulse, (2009).
- [8] Holmberg K., Andersson P., Erdemir A., Global energy consumption due to friction in passenger cars, Tribology International, Volume 47, Pages 221–234, (2013).
- [9] Eyre T.S., Crawley B., Camshaft and cam follower materials, Tribology International, Volume 13, Pages 147-152, (1980).
- [10] Gangopadhyay A.K., McWatt D.G., The effect of novel surface textures on tappet shims on valvetrain friction and wear, Tribology Transactions, Volume 51, Pages 221–230, (2008).
- [11] Vengudusamy B., Green J.H., Lamb G.D., Spikes H.A., Tribological properties of tribofilms formed from ZDDP in DLC/DLC and DLC/steel contacts, Tribology International, Volume 44, Pages 165-174, (2011).
- [12] Vengudusamy B., Green J.H., Lamb G.D., Spikes H.A., Behavior of MoDTC in DLC/DLC and DLC/steel contacts. Tribology International, Volume 54, Pages 68-76, (2012).
- [13] Kano M., Super low friction of DLC applied to engine cam follower lubricated with ester-containing oil, Tribology International, Volume 39, Pages 1682-1685, (2006).

- [14] Katoh A., Yasuda Y., An analysis of friction reduction techniques for the direct acting valve train system of a new generation lightweight 3-Liter V6 Nissan Engine, SAE Paper No. 940992, (1994).
- [15] Abner E., Lubricant deterioration in service, CRC Handbook of lubrication (Theory and Practice of Tribology) Volume I: Practice, Booser, E.R., Ed., CRC Press, (1983).
- [16] Aranzabe A., Aranzabe E., Marcaide A., Ferret R., Terradillos J., Ameye J., Shah R., Comparing different analytical techniques to monitor lubricating grease degradation, NLGI Spokesman, Volume 70, Issue 6, Pages 17–30, (2006).
- [17] Graham J., Spikes H., Korcek S., The friction reducing properties of molybdenum dialkyldithiocarbamate additives: part I-factors influencing friction reduction. Tribology Transactions; Volume 44, Pages 626–36, (2001).
- [18] Spengler G., and Webber A., On the lubricating performance of organic molybdenum compounds. Chem. Ber. Volume 92, Pages 2163-2171, (1939).
- [19] Grossiord C., Varlot K., Martin J.M., Le Mogne Th., Esnouf C., Inoue K., MoS<sub>2</sub> single sheet lubrication by molybdenum dithiocarbamate. Tribology International; Volume 31, Pages 737–43. (1998).
- [20] Kubo K., Mitsuhiro N., Shitamichi T., Motoyama K., The effect of ageing during engine running on the friction reduction performance of oil soluble molybdenum compounds, Proceeding of the international tribology conference, Yokohama, (1995).
- [21] De Barros Bouchet M.I., Martin J.M., Le Mogne Th., Bilas P., Vacher B., Yamada Y., Mechanisms of MoS<sub>2</sub> formation by MoDTC in presence of ZnDTP. Effect of oxidative degradation. Wear, Volume 258, Pages 1643, (2005).
- [22] Graham J., Spikes H., Korcek S., The friction reducing properties of molybdenum dialkyldithiocarbamate additives: part I-factors influencing friction reduction. Tribology Transactions; Volume 44, Pages 626–36, (2001).
- [23] Grossiord C., Varlot K., Martin J.M., Mogne T.L., Esnouf C., Inoue K., MoS<sub>2</sub> single sheet lubrication by molybdenum dithiocarbamate. Tribology International, Volume 31, Pages 737–43. (1998).



# Chapter 1

---

## State of art

---

*The first section of this chapter presents a short overview on the causes of engine lubricant degradation, with emphasis on the oxidation mechanisms of both base oil and additives.*

*The characteristics and functionalities of molybdenum-containing friction modifiers are then discussed, focusing on molybdenum dithiocarbamate additive (MoDTC). The last section points out the lack of knowledge about MoDTC degradation impact on its tribological properties and the importance of further studies.*

# Chapitre 1

---

## Etat de l'art

---

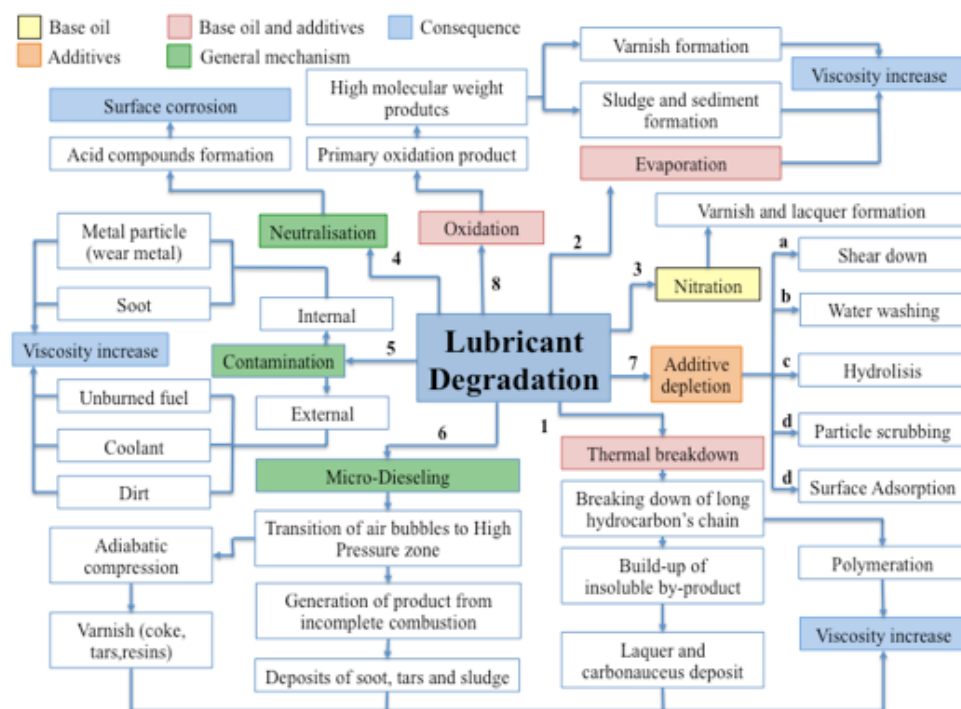
*La première partie de ce chapitre présente un bref aperçu des principales causes de la dégradation d'un lubrifiant moteur, en mettant l'accent sur les mécanismes d'oxydation des huiles de base et des additifs.*

*Les caractéristiques et les performances des modificateurs de frottement contenant du molybdène sont ensuite discutées, mettant l'accent sur le dithiocarbamate de molybdène (MoDTC), additif réducteur de frottement très connu. La dernière partie de ce chapitre souligne le manque de connaissances concernant les mécanismes de dégradation de la molécule de MoDTC et leurs impacts sur les propriétés tribologiques.*

# 1. Lubricant degradation causes: Overview

The alterations in oil properties during operation are due to extraneous contamination, chemical and physical changes in the lubricant molecules themselves. These changes, in both base oil and additives, have a significant effect on the lubricant performance and, just a slight loss of lubricating properties can lead to a decrease in the production efficiency through an increase in production costs, on advanced degradation or even a decomposition of a lubricant with serious failures of devices causing production delay and high repair cost. The understanding of the lubricant ageing mechanism, however, is extremely complex because many factors and changes in several parameters are involved and because there are many competing mechanisms which can occur simultaneously. For this reason, a careful analysis of “state of the art” has to be in order to build sufficient knowledge of the topic, and to acquire an accurate and deep comprehension of the subject. It is important to gain insight into the chemistry behind lubricant ageing and in the changes of the physical and tribological properties during operation, in order to be able to understand when the lubricant becomes unsuitable for its intended purpose and to take the necessary precautions. In order to ensure excellent engine performance and reliability, it is necessary to classify all of the degradation causes, responsible for several lubricant-related problems.

In the following paragraph, the current state of topic is reviewed. In order to summarize the main oil aging mechanisms a block diagram has been built in **Figure 1.1**.



**Fig. 1.1. Chart for the lubricant degradation causes.**

The degradation processes presented in **Figure 1.1** can be classified into four different categories:

- reactions involving the base oil (yellow);
- reactions involving the additives (orange);
- reactions involving both base oil and additives (red);
- general mechanisms (green).

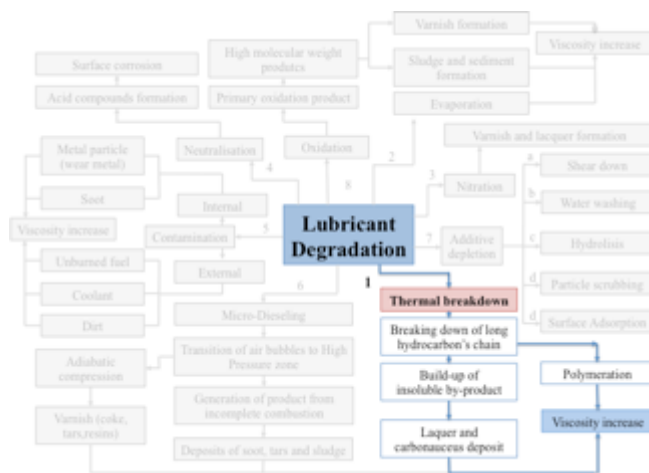
The chart presented in **Figure 1.1** is explained point by point below, reporting again the path to follow in the image on the side.

**1.** In a mechanical working environment, the temperature of the lubricant is a fundamental parameter. In fact, the main purpose of lubrication is to reduce friction and wear, but the lubricant must also be able to dissipate heat and to cool down the engine. In some cases, in fact, it is possible to reach a temperature above that which

maintains lubricant stability. This scenario can lead to the so-called thermal degradation process and involves the breaking down of the lubricant's long hydrocarbon chains and the additive molecules into shorter compounds with lower boiling points or with decomposition process leading to a deposit of reaction products. When the complications due to this breakdown are studied, both additive and base oil degradation must be considered.

The thermal degradation is often combined with oxidation processes and the oxidative life of a lubricant relative to temperature generally follows the Arrhenius Law - one of the best-known models for assessing the lifetime of lubricant, commonly used to predict the combined effects of temperature and time (it shows that the rate of a chemical reaction increases exponentially with the absolute temperature). It suggests that short-term tests conducted at elevated temperatures can be representative of long-term exposures at low temperatures. The oxidation process will be further explained later (point 8).

The lubricant loses thickening capabilities in service because the reduction on the weight/size of the polymer molecules, due to chain-breaking, facilitates the lubricant mobility. At the same time, it tends to thicken due to two different phenomena, both responsible of viscosity increasing. The high temperature can cause some of these compounds to chemically react resulting in higher molecular weight compounds

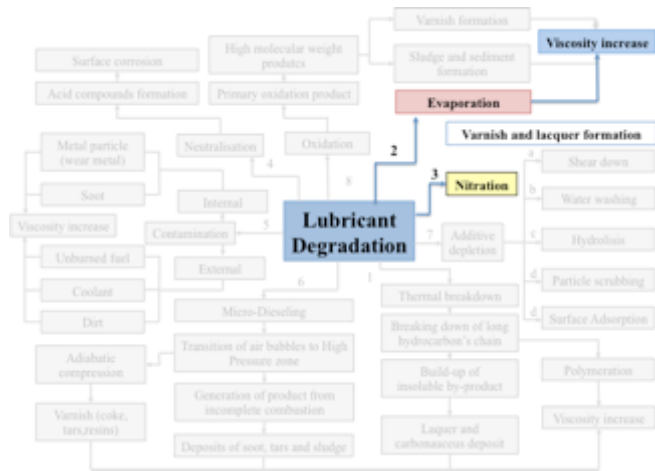




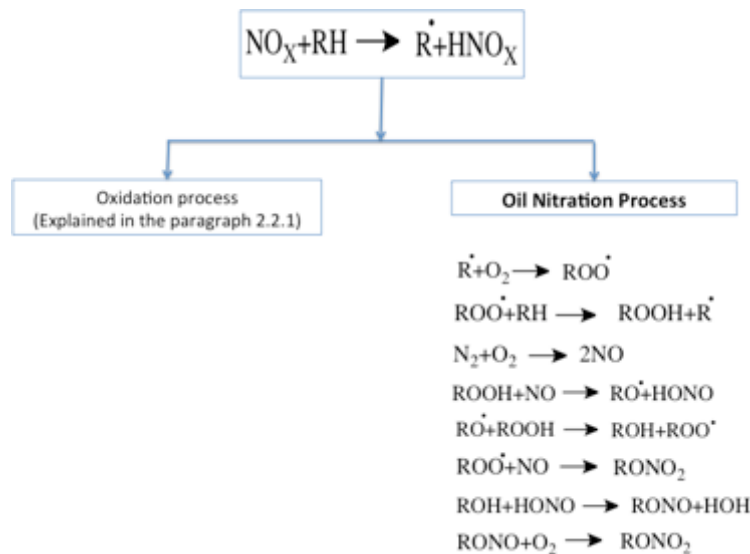
(polymerization and reticulation) [1, 2]. These compounds might evaporate, resulting in thickening of the lubricant and higher shear resistance [3].

2. In fact, the low weight molecules (formed after breaking) are more sensible to evaporation because of their lower boiling points (higher volatility) [4-8].

3. The major cause of lacquer and varnish formation is the nitration, which is the reaction of hydrocarbon chains with nitrogen oxides (NO, NO<sub>2</sub> and N<sub>2</sub>O<sub>4</sub>) produced during the combustion.



**Figure 1.2** represents the two mechanisms of deposit formation due to nitration process.

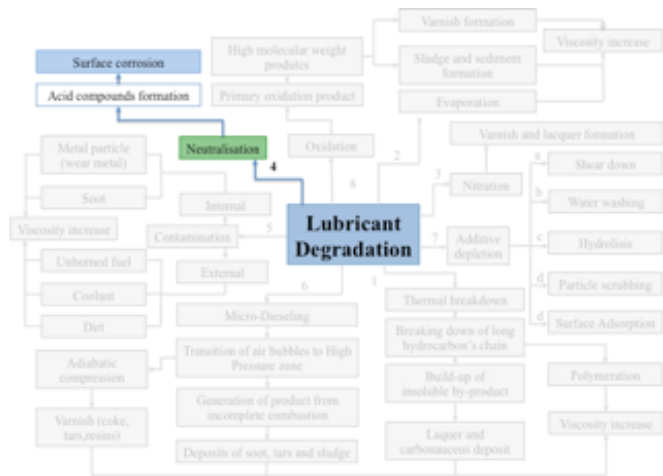
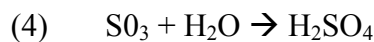
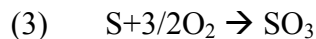
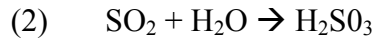
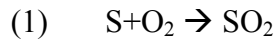


**Fig 1.2. Nitration mechanisms**

The products of these reactions are chemically reactive and they can polymerize via individual precursors. The result is an increase in molecular weight and in size and final compounds are insoluble in the oil and forming engine deposits.

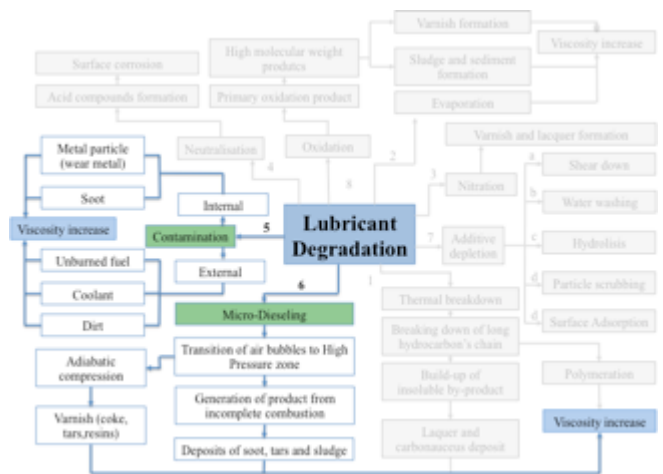
The organic nitrates are decomposed at high temperatures; the nitration of the oil film progressively decreases as the temperature increases. [9].

4. Since the last decade it has been observed a significant reduction on the sulphur content in the lubricants [10] although a relatively small amount of S is still present. During the combustion the sulphur oxidises and sulphur acids are produced due to the reaction with water vapour, as reported in the following reactions:



The overbased detergent present in the package of additives of the lubricant is used to neutralize acid compounds such as the sulphuric acid, resulting normally in the formation of metallic sulphates (neutralisation) [11].

5. The degradation rate is also influenced by the presence of extraneous substances inside the lubricant. The internal contamination, such as metal particle (iron or copper), acts as catalyst for the degradation [12] or the soot [13, 14], which are produced as a by-product from fuel combustion in engines and significantly impact on the oil viscosity.



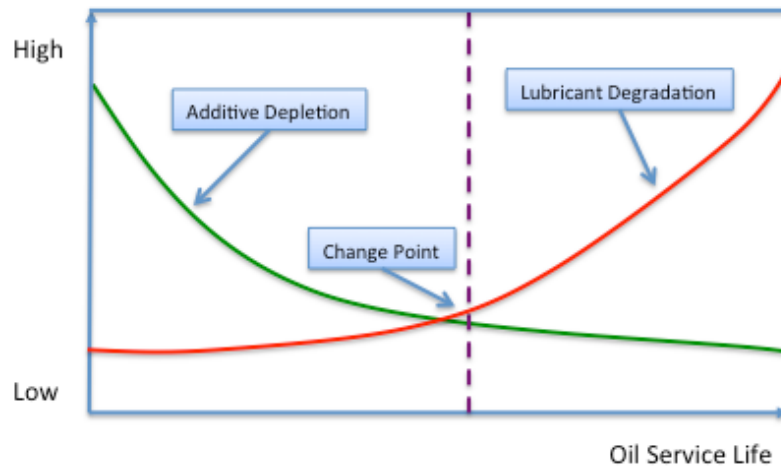
The external contaminants, such as moisture or unburned fuel, might accelerate the degradations process as well;

6. The pressure-induced thermal degradation, called micro-dieseling, is mainly caused by the bubbles of air in the oil. They can move from a high-pressure zone to a low-pressure one and, according with the Boyle's law, causing an adiabatic compression. The result is, thus, the generation of a substantial temperature increase on a microscopic scale that accelerates the oil degradation and it forms carbonaceous by-products [15].

7. As already underlined, the changes of the lubricant's properties during ageing can significantly influence the performance, reliability and durability of technological systems.

Initially, the degradation rate is slow due to the protective action of the additives; however, the rate dramatically increases as soon as the additives package is depleted.

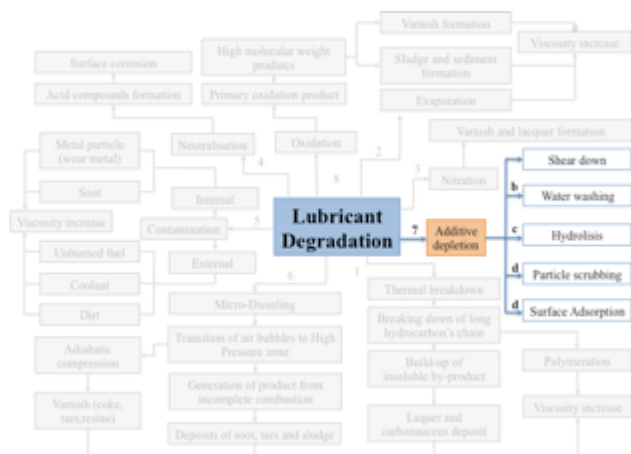
**Figure 1.3** shows the evolutions of additive depletion and lubricant degradation versus time.



**Fig. 1.3. Degradation rate vs. additives depletion over time**

Over time, additives depletion is well visible and the lubricant requires service to restore the performance properties, which usually occurs in the form of an oil change. The rate at which additives deplete depends on the chemistry of the additive and on the operating/ambient conditions, particularly temperature and presence of water.

a) Sustained mechanical work might affect the ageing process causing the polymeric additive depletion [16] mostly, if the engine lubricant does not contain viscosity index improvers. These additives are long chain of organic polymer, which are unstable under high shear rate at high temperature. They are added to the lubricant formulation in order to reduce the rate of change of viscosity with changes in temperature. During the operation, in some zones of the engine (in the oil pump, cam shaft area, piston rings, etc.), the lubricant is subjected to high shear stresses, causing polymer breakdown and thus viscosity decrease. This process speeds up the lubricant degradation process.

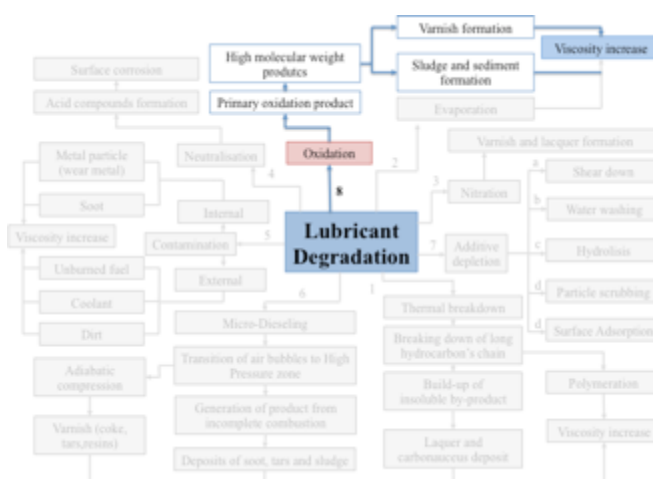


b) The physical depletion of the additive can occur due to the water washing: some additives are soluble in the water and a dilution is possible [17, 18];

c) The additive molecules or the base stock chains can be broken into two parts because of the reaction with a molecule of water (hydrolysis). One part gives an hydrogen ion ( $H^+$ ) while the other one becomes the hydroxyl group ( $OH^-$ ) [17, 18];

d) Surface active additives might react with wear debris in the bottom of the sump (particle scrubbing) or might be adsorbed on other surfaces of the device (surface adsorption) resulting in a decrease of their concentration;

8. The leading phenomenon influencing the lubricant lifetime is the oxidation process. It is a complicated sequence of chemical reactions, chemical changes and formulation of new unwanted molecules [19]. Originally, oxidation was considered as a chemical reaction involving oxygen but the meaning has been extended involving any reactions providing electron transfer, which in general occurs when hydrocarbons and additives start to react with oxygen.



Oxidation is often simulated in laboratory environment using high temperature. The rate of the oxidation reaction become roughly double for every 10°C increase in temperature. It means that the oil life is critically dependent on the temperature at which that reaction takes place: the higher the temperature, the faster the oil will oxidise and it will be reduced by one-half for every 10°C increase in temperature.

This section showed that lubricant degradation is mostly determined by temperature, reactions between the hydrocarbon chains and/or the additives molecules with the oxygen dissolved in the lubricant and by the local stresses at which the oil system is subjected. It results in the production of primary oxidation products, which could further react to form long chain molecules. As described before, as these reactions continue over time, the molecular weight and the concentration of the resulting molecules increase until a solubility limit is obtained and these materials will come out as deposits and sludge.

At the same time, because of the high temperature, the evaporation of the volatile product occurs, speeding up the increase of the viscosity.

The formation of high molecular weight polymeric products and the evaporation of the low weight/length molecules might significantly decrease the engine performance, inhibiting the circulation of the liquid lubricant, resulting in a decreasing of lubricity in the system and accelerating the machine elements wear up to failure.

## 2. Base oil oxidation and Additive oxidation reactions

As already said, it is widely understood that oxidation is the primary mechanism of lubricant degradation and it is the primary cause of increase in viscosity, sludge, lacquer formation and enhanced engine corrosion.

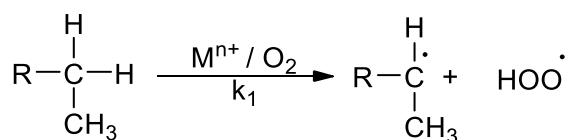
The main key to understand lubricant oxidation is the fundamental comprehension of the chemistry of lubricants and their degradation process. In order to simplify the problem, it is possible to distinguish base oil oxidation and additive oxidation.

### 2.1. Base oil oxidation

The hydrocarbons of mineral oils undergo a self-accelerating oxidation process called auto-oxidation [20], consisting of four stages: initiation, propagation, chain branching and termination. The understanding of the main causes of each of these steps is required on the development of technologies/methodologies to improve lubricant oxidation resistance. It suggests that it is possible to monitor the oxidation mechanisms through the control of one or more of these stages. For example, limiting the source of oxygen (the initiation), shortening the number of reaction cycles (the propagation) or adding alternate stopping methods (increasing termination).

#### Initiation

During the initiation, free radicals are formed which are molecular fragments having one or more electrons accessible to easily react with other hydrocarbons. Because they are highly reactive, they have usually relative short life. The predominant source of free radicals is oxygen but there are several others such as nitro-oxides, ultraviolet light and flow electrification (electrostatic discharge). The initiation of the chain reaction (**Scheme 1.1**) is a really slow process ( $k_1 = 10^{-9} - 10^{-10} \text{ l mol}^{-1} \text{ s}^{-1}$ ).

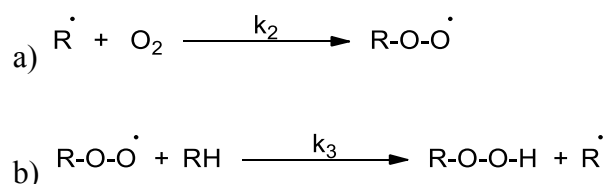


**Scheme 1.1.** The initiation reaction of the free radical mechanism of mineral oil oxidation.

Where R refers to a alkyl chain substituent and  $\text{M}^{n+}$  refers to a transition metal ion that acts as a catalyst.

## Propagation

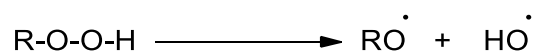
Propagation occurs when an alkyl radical (R) is formed, as it irreversibly and very quickly ( $k_2 = 10^7 - 10^9 \text{ l mol}^{-1} \text{ s}^{-1}$ ) reacts with oxygen to create an alkyl peroxy radical, which can form hydroperoxide able to extract hydrogen from another hydrocarbon. These reactions are slower ( $k_3 = 10^{-1} - 10^{-5} \text{ l mol}^{-1} \text{ s}^{-1}$ ) and respectively shown in **Scheme 1.2a** and **1.2b**.



**Scheme 1.2.** The propagation reactions of the free radical mechanism of mineral oil oxidation – a) Creation of peroxy radical. b) Hydrogen extraction from another hydrocarbon.

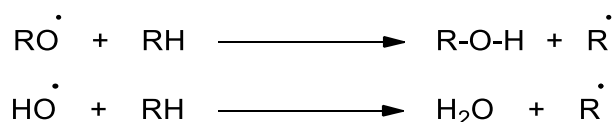
## Chain branching

Chain branching step can occur by different mechanisms depending on the concentration of hydroperoxides present. At low concentrations, the hydroperoxide group can produce alkoxy and hydroxyl radicals (**Scheme 1.3**).



**Scheme 1.3.** The production of alkoxy and hydroxyl radicals for the chain branching stage.

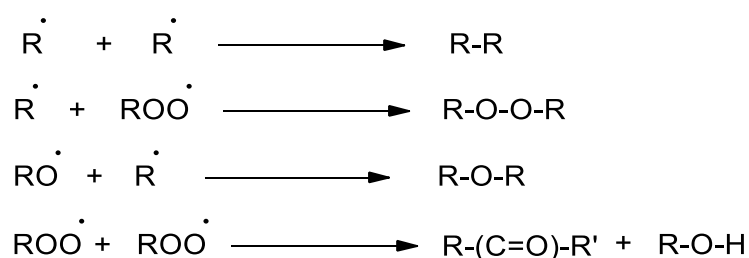
Because of the high activation energy required, this reactions will only occur at temperatures above 120 °C. These radicals can then react further (**Scheme 1.4**) producing more alkyl radicals, which contribute to the propagation reaction.



**Scheme 1.4.** Chain branching reactions of alkoxy and hydroxyl radicals, which produce alkyl radicals.

## Termination

The termination reactions occur at the end of the oxidation process, preventing the hydrocarbon from further degradation. During this stage oxidation products, such as ketones and sludge, are formed. Because numerous products are possible, there is a wide range of radicals present (**Scheme 1.5**).



**Scheme 1.5.** Termination reactions producing a variety of products – a) Long chain hydrocarbons. b) Dialkyl peroxides. c) Ethers. d) Ketones and alcohols.

## 2.2. Additive degradation

Modern lubricants are, in general, formulated with base oil and an additive package (anti-wear, anti-oxidant, dispersants, and viscosity and friction modifier agents, etc.). The additives enhance various aspects of lubricant performance and they can effectively increase the mechanical efficiency, decrease the energy consumption, and reduce friction and wear of machinery equipment.

As aforementioned, one of the most important aspects of lubricating oils is their oxidant stability. Exposure of hydrocarbons and additives to oxygen and heat will accelerate the oxidation process. The internal combustion engine could be considered as a chemical reactor for catalyzing the process of oxidation, where also the metal parts of engine (copper and iron) act as oxidation catalysts. For this reason, engine oils are probably the lubricant more susceptible to oxidation than any other lubricant application. Antioxidant additives play a critical role in preventing lubricant degradation. The main role of these additives, in fact, is essentially the protection of the base oil. In fact, they will degrade first while minimizing any degradation to the base oil molecular properties. At the same time, the other additive

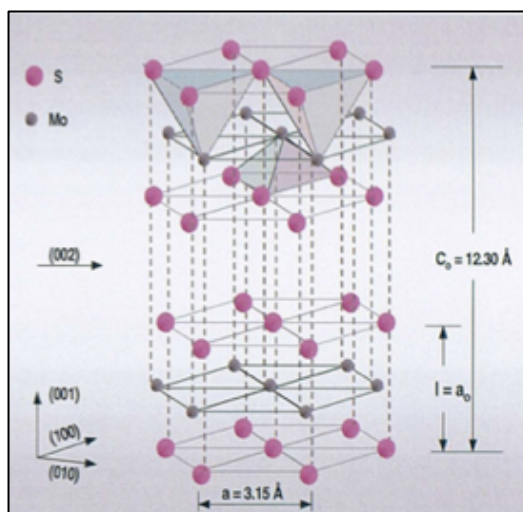
present in the package are protected as well but, after antioxidant content is consumed by operational processes, the integrity of the hydrocarbon base oil and the additive package becomes compromised. At this point the additive package oxidation and the consequent additive depletion start.

### 2.2.1. Molybdenum-containing friction modifiers

Nowadays, it is common to blend the engine lubricant with organomolybdenum-based friction-reducing additives. The exact mechanism by which these additives lower the friction coefficient is still not completely well understood, though as will be described in this paragraph, recent studies on MoDTC additives are giving insights into the behavior of this friction modifier capability. These additives are generally believed to form  $\text{MoS}_2$  in the contacts and thereby reduce friction in boundary lubrication conditions.

### 2.2.2. Molybdenum disulfide ( $\text{MoS}_2$ )

The molybdenum disulfide ( $\text{MoS}_2$ ) is an important inorganic compound, able to provide friction reduction in boundary lubrication conditions to low value (0.05-0.07) [21]. It can have two different crystalline structures [22]. Both are regular layered structures with the molybdenum layer sandwiched between two sulfur layers and it can be two-layer hexagonal (2H- $\text{MoS}_2$ ) or three-layer rhombohedral (SR- $\text{MoS}_2$ ) respectively. Cell dimensions of 2H hexagonal  $\text{MoS}_2$  are  $a = 3.160 \text{ \AA}$  and  $c = 12.295 \text{ \AA}$ , 3R rhombohedral structure has  $a = 3.164 \text{ \AA}$  and the  $c = 18.371 \text{ \AA}$ . The crystal structure of natural  $\text{MoS}_2$  commonly found is the molybdenite 2H- $\text{MoS}_2$  structure (**Figure 1.4**) [22, 23].



**Figure 1.4.** Lamellar crystal structure of 2H- $\text{MoS}_2$ .



As mentioned above, the detailed mechanisms for the excellent lubricant properties of MoS<sub>2</sub> sheets are still unclear. Since the beginning, it was widely believed that using MoS<sub>2</sub> it is possible to lower the friction coefficient thanks to the low interactions between layers. In fact, it was supposed that the ability to reduce friction coefficient is an intrinsic property of the MoS<sub>2</sub> crystal structure, where covalently bonded layers are joined by weak Van der Waals attraction forces between the (002) planes, which lead to low shear strength in the parallel direction to the atomic pla. However, recent theoretical investigations by means of computational chemistry method have shown that the predominant interaction between two sulfur layers in different MoS<sub>2</sub> sheets is Coulombic repulsion [24]. It has been demonstrated, in fact, that this force is the main responsible for the low friction obtained when MoS<sub>2</sub> species are produced on the rubbing surfaces.

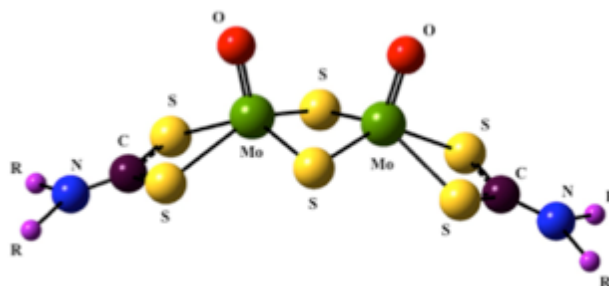
It has been reported that the MoS<sub>2</sub> additive can be used as solid lubricant, obtaining beneficial effects by reducing friction and wear [25]. However in some circumstances MoS<sub>2</sub> can become ineffective or it can even have negative performance. For example, the MoS<sub>2</sub> particles may interfere with lubricant flow blocking the lubricant entry into the contact [26]. It has been found also that the wear rate of the rubbing surfaces could be more important with high concentration of solid lubricant dispersed in oil, high load conditions or large particles size [27]. For these reasons and, due to its insolubility problem [28] in oil this compound is not widely used as it is in liquid lubrication and, during the last decades, it has been a growing concern to use oil-soluble molybdenum-containing additives, able to decompose giving MoS<sub>2</sub> species in the contact.

### **2.2.3. Molybdenum dithiocarbamate (MoDTC)**

The molybdenum-containing compounds were first studied as potential lubricant additives in the 50's [29] but were initially used mainly as antiwear [30, 31]. They were considered, in fact, as friction modifiers for the first time in the late 70's [25, 32].

Different types of Mo-based additive have been applied in oil formulation [29, 32-34]. The one that shows the best performance in modern engine lubricant is the molybdenum dithiocarbamate (MoDTC) widely used to improve fuel efficiency by acting as friction modifier.

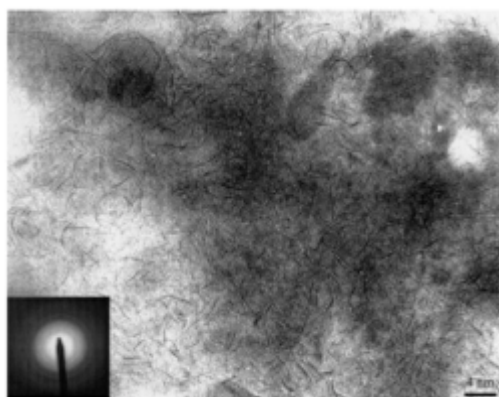
The general chemical structure of MoDTC is shown in **Figure 1.5**.



**Figure 1.5.** Chemical structure of MoDTC additive.

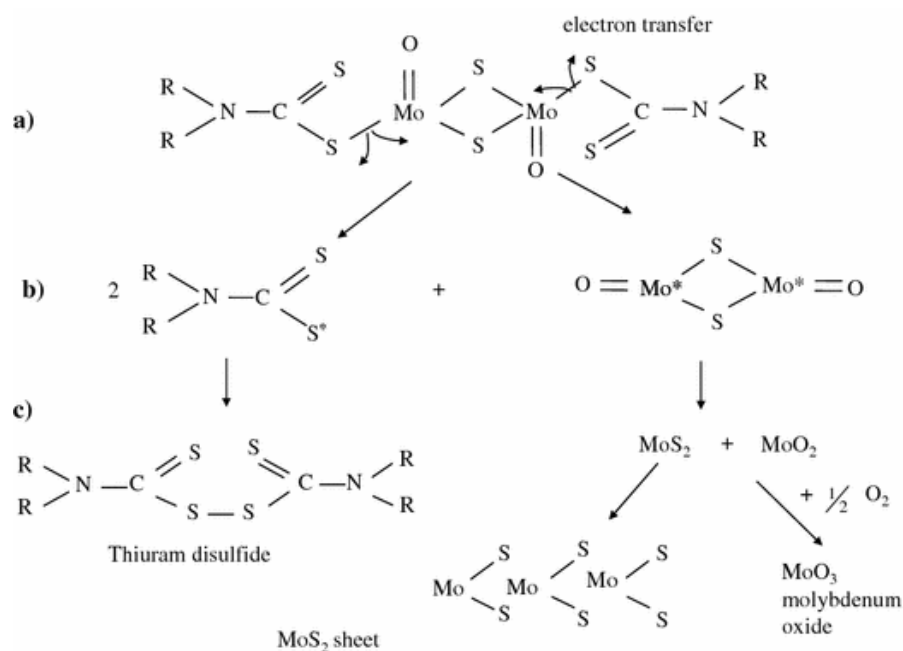
Over the last forty years, a large number of research work have been devoted to this friction modifier additive and different techniques have been adopted in order to understand its action mechanisms. A consistent number of friction tests have been carried out using MoDTC containing lubricants. To identify the products formed on the surface during friction different analyses have been used to investigate the mechanisms by which soluble molybdenum additives lower the friction coefficient. The detailed studies carried out by means of electron diffraction techniques [41, 42], X-ray techniques such as XPS [43, 44] and XANES [45] or Raman spectroscopy [46-48], allowed to believe that the reduction by such additive is mainly due to the formation of reaction film containing MoS<sub>2</sub> individual sheets, as a result of complex tribo-chemical reactions.

The morphology of this tribofilm formed on the rubbed surfaces and the physical nature of wear debris have been intensely studied by J.M. Martin *et al.* employing high-resolution transmission electron microscopy (HR-TEM). The presence of tiny flake-like particles with approximately 10 nm diameter and ca. 1 nm thick, characteristic of the MoS<sub>2</sub> structure [49, 50] is underlined (**Figure 1.6**).



**Fig. 1.6.** Transmission electron micrograph of wear debris showing the presence of MoS<sub>2</sub> 'nano-sheets' from [49].

Combining all these results, it has been proposed a schematic chemical breakdown of MoDTC molecule happening in the steel/steel contact (**Figure 1.7**) [49, 51]. The reaction starts with the formation of three free radicals due to an electron transfer (**Figure 1.7a** and **1.7b**). At the end, the part corresponding to the center of MoDTC molecule decomposes into MoS<sub>2</sub> and MoO<sub>2</sub>, which can further react to produce MoO<sub>3</sub> that is more stable than MoO<sub>2</sub> (experimentally detected), while the parts corresponding to the chain ends of MoDTC molecule are synthesized to thiuram disulfide.



**Fig. 1.7. MoS<sub>2</sub> formation mechanism** [51, 52].

## 2.2.4. MoDTC degradation

The use of effective friction reducing additives to achieve low boundary friction coefficient is not enough to have great engine fuel efficiency. In addition, in fact, it is needed also to maximize their durability, preventing premature consumption or depletion of these additives. It has been shown that the friction reduction performance of MoDTC is sensitive to engine operating time and that is related to the degradation of MoDTC itself. In the case of aged oils, lower concentration of MoDTC is detected, the formation of layers of MoS<sub>2</sub> is reduced and poor reducing-friction properties are observed. Due to the oxidation, a decrease in MoDTC concentration is obtained, leading to the formation of different MoS<sub>2</sub> sheets in size, number and shape [51, 52]. It has been previously reported that it is possible to slow down consumption of this compound by addition of an other antioxidant. In fact, it has been found

that the MoDTC degradation can be delayed by adding ZDDP [38, 39], methylphenol (MPH) [44] or by an addition of disulfide [53]. All these works clearly show that further improvements in energy conservation and optimization of fuel efficiency of engine oils are possible. A better understanding of the mechanisms occurring during the lubricants usage and the investigation of the impact of both the chemical and the physical changes on the tribological properties are strongly required in order to obtain the maximum benefit from friction reducing additives.

### **3. CONCLUSIONS**

This introduction chapter highlights many of the important findings from the last years concerning degradation causes of lubricants for internal combustion engine applications. The main aim was not to exhaust all the literature but provide a summary of the state of art about the complexity of degradation mechanisms. In the first part, the lubricant degradation roots has been described while the second part provides information about the well-known molybdenum dialkyldithiocarbamate (MoDTC) additive. At the end it underlines the needed to carry out new experiments going in different direction, where important data are still lacking, especially for the impact of lubricant degradation on the tribological properties.

## 4. BIBLIOGRAPHY

- [1] Chen C.I., Hsu S.M., A chemical kinetics model to predict lubricant performance in a diesel engine. Part I: simulation methodology, *Tribology Letters*, Volume 142, Issue 2, Pages 83-90, (2003).
- [2] Livingstone G.J., Muennich D.J., Understanding and addressing varnish, *Paper Machine Systems, TAPPI/PIMA/Coating Conference*, (2008).
- [3] Stachowiak G., Batchelor A. W, *Engineering Tribology Third Edition*; Elsevier Butterworth-Heinemann, Oxford 77, (2005).
- [4] Fingas M.F., A Literature review of the physics and predictive modelling of oil spill evaporation, *Journal of Hazardous Materials*, Volume 42, Pages 157-175, (1995).
- [5] Fingas M.F., Studies on the evaporation of crude oil and petroleum products: I. The relationship between evaporation rate and time, *Journal of Hazardous Materials*, Volume 56, Pages 227-236, (1997).
- [6] Fingas M., *Evaporation modeling in oil spill science and technology*, Fingas, M. Editor, Gulf Publishing, NY, Chapter 9, Pages 201-242, (2011).
- [7] Goodwin S.R., Mackay D., Shiu W.Y., Characterization of the evaporation rates of complex hydrocarbon mixtures under environmental conditions, *Canadian Journal of Chemical Engineering*, Volume 54, Pages 290-294, (1976).
- [8] Li Y.Y., Zheng X.L., Li B., Ma Y.X., Cao J.H., Volatilization behaviors of diesel oil from the soils, *Journal of Environmental Science (China)*, Pages 1033-1038, (2004).
- [9] Broman E., Factors affecting the formulation of engine oils for LP-Gas Service, *LP-Gas Engine Fuels: A Symposium Presented at the Seventy-Fifth Annual Meeting, ASTM*, Los Angeles, CA, 7, Pages 3-17, (1972).
- [10] Kilcarr S., *Truck engine emissions update: the road to '07*, (2004).
- [11] Steijns M., The role of sulfur trapped in micropores in the catalytic partial oxidation of hydrogen sulfide with oxygen, *J Catal* (1974).
- [12] Abner E., Lubricant deterioration in service, *CRC Handbook of lubrication (Theory and Practice of Tribology) Volume I: Practice*, Booser, E.R., Ed., CRC Press, (1983).
- [13] Gautam M., Chitoor , Durbha M., Summers J.C., Effect of diesel soot contaminated oil on engine wear – investigation of novel oil formulations, *Tribol. Int.*, Volume 32, Pages 687–699, (1999).
- [14] Miyaji T., Taya H., Tamoto Y. The influence of diesel soot in oil on viscosity increase, *Proc. Int. Tribology Conf. Yokohama*, Pages 823-828, (1995).

- [15] Khemchandani G., Non-varnishing and tribological characteristics of polyalkylene glycol-based synthetic turbine fluid, *Lubrication Science*, Volume 24, Issue 1, Pages 11–21, (2012).
- [16] Kudish II, Airapetyan RG, Covitch MJ, Modeling of kinetics of strain induced degradation of polymer additives in lubricants, *Journal of Mathematical Models and Methods in Applied Sciences*, Volume 12, Issue 6, Pages 835–856, (2002).
- [17] Sander J., Water contamination: management of water during the lubricant life cycle, *Technology, Lubrication Engineers*, (2009).
- [18] Eachus A., The trouble with water, *Tribology & Lubrication Technology*, Society of Tribologists and Lubrication Engineers Publishing, Ridge Park, IL, (2005).
- [19] Wootton D., The Lubricant's Nemesis - Oxidation, *Practicing Oil Analysis*, (2007).
- [20] Rasberger M., Chemistry and technology of lubricants, ed. R.M. Mortier, M.F. Fox and S.T. Orszulik, Springer, New York, 2nd ed., Chapter 4, Pages 99-143, (1996).
- [21] Greene A.B. and Ridsen T.J., Effect of Mo-containing pil soluble friction modifiers on engine fuel economy and gear oil efficiency", *SAE Tech. Paper 811 187*, (1981).
- [22] Levy F. (ed.), *Crystallography and crystal chemistry of materials with layered structures*, Reidel, Dordrecht, (1976).
- [23] Farr J.P.G., Molybdenum disulfide in lubrication. A review, *Wear*, Volume 35, Pages 1-22, (1975).
- [24] Onodera T., Morita Y., Nagumo R., Miura R., Suzuki A., Tsuboi H., Hatakeyama N., Endou A., Takaba H., Dassenoy F., Minfray C., Joly-Pottuz L., Kubo M., Martin J.M., and Miyamoto A., A Computational Chemistry Study on Friction of h-MoS<sub>2</sub>. Part I. Mechanism of Single sheet lubrication, *J. Phys. Chem. B*, 113, (2009).
- [25] Braithwaite E.R. and Greene A.B., A critical analysis of the performance of molybdenum compounds in motor vehicles, *Wear*, Volume 46, Pages 405, (1978).
- [26] Wan G.T.Y. and Spikes H.A., The behavior of suspended solid particles in rolling and sliding elasto-hydrodynamic contacts, *Trib. Transactions*, Volume 31 (1), Pages 12-21. (1988).
- [27] Bartz, W.J., Some investigations on the influence of particle size on the lubrication effectiveness of molybdenum disulfide, *ASLE Transactions*, Volume 15, Pages 207-215, (1972).
- [28] Cusano C. and Sliney H.E., Dynamics of solid dispersions in oil during the lubrication of point contacts, Part II - Molybdenum Bisulfide, *STLE Transactions*, Volume 25, Pages 190-197, (1981).

- [29] Mitchell D., Oil-soluble Mo-S compounds as lubricant additives, *Wear*, Volume 100, Pages 281-300, (1984).
- [30] Vanderbilt R.T., Molybdenum-containing dithiophosphoric ester compounds, UK Patent 1144145, (1966).
- [31] Sakurai T., Okabe H. and Isoyama H., The synthesis of di-m-thio-dithio-bis(dialkyldithiocarbamates) dimolybdenum (V) and their effects on boundary Lubrication, *Bull. Japan Petr. Inst.*, Volume 13, Pages 308-314, (1971).
- [32] Passut C.A. and Kollman R.E., Laboratory techniques for evaluation of engine oil effects on fuel economy, *SAE Tech. Paper 780601*, (1978).
- [33] Tang Z. and Li S., A review of recent developments of friction modifiers for liquid lubricants (2007-present), *Current Opinion in Solid State and Materials Science*, (2014).
- [34] Yamamoto Y., Seigo G., Friction and wear characteristics of molybdenum dithiocarbamate and molybdenum dithiophosphate. *Tribology Transactions*, Volume 32, Pages 251-257, (1989).
- [35] Sorab J., Korcek S., Bovington C, “Friction reduction in lubricated components through engine oil formulation”, *SAE*, (1998).
- [36] Morina A., Neville A., Priest M., Green J.H., ZDDP and MoDTC interactions and their effect on tribological performance-tribofilm characteristics and its evolution, *Tribology Letters*, Volume 24, 243–56, (2006).
- [37] Graham J., Spikes H., Korcek S., The friction reducing properties of molybdenum dialkyldithiocarbamate additives: part I - factors influencing friction reduction, *Tribology Transaction*, Volume 44, Pages 626-636, (2001).
- [38] Morina A., Neville A., Priest M., Green J.H., ZDDP and MoDTC interactions in boundary lubrication - The effect of temperature and ZDDP/MoDTC ratio, *Tribology International*, Volume 39, Issue 12, Pages 1545–1557, (2006).
- [39] Morina A., Haque T., Neville A., MoDTC low friction tribofilm durability - Effect of interactions with ZDDP and their dependence on substrate material, *Society of Tribologists and Lubrication Engineers - 62<sup>nd</sup> Annual Meeting of the Society of Tribologists and Lubrication Engineers*, Volume 2, Pages 1044-1046, (2007).
- [40] Muraki M., Yanagi Y. and Sakaguchi K., Synergistic effect on frictional characteristics under rolling-sliding conditions due to a combination of molybdenum dialkil dithiocarbamate and zinc dithiophosphate, *Trib. Intern*, Volume 30, Pages 69-75, (1997).

- [41] Graham J., Jensen R. and Spikes H., The friction reducing properties of molybdenum dialkyldithiocarbamate additives: Part II - durability of friction reducing capability, Trib. Transactions, Volume 44, Pages 637-647, (2001).
- [42] Ming Feng I., Perilstein W.L. and Adams M.R., Solid film deposition and non-sacrificial boundary lubrication, ASLE Transactions, Volume 6, Pages 60-66, (1963).
- [43] Gondo S. and Konishi M., Organoamine and organophosphate molybdenum complexes as lubricant additives, Wear, Volume 120, Pages 51-60, (1987).
- [44] Korcek S., Jensen R.K., Johnson M.D., Clausing E.M., International Tribology Conference, Yokohama, Pages 733-737, (1996).
- [45] Kasrai M., Cutler J.N., Gore K., Canning G., Bancroft G.M., The chemistry of antiwear films generated by the combination of ZDDP and MoDTC examined by X-RAY absorption spectroscopy, Trib. Trans. Volume 41, Pages 69-77, (1998).
- [46] McDevitt N.T., Donley M.S., Zabinski J.S., Utilization of raman-spectroscopy in tribochemical studies, Wear, Volume 166, Pages 65-72, (1993).
- [47] Zabinski J.S., Donley M.S., Waick S.D., Schneider T.R. and McDevitt N.T., The effects of dopants on the chemistry and tribology of sputter-deposited MoS<sub>2</sub> films, Trib. Transactions, Volume 38, Pages 894-904, (1995).
- [48] Willermet P.A., Carter R.O., Schmitz P.J., Everson M., Scholl D.J., and Weber W.H, Formation, structure and properties of lubricant-derived antiwear films, Lubr. Science, Volume 9, Pages 325-347, (1997).
- [49] Grossiord C., Martin J.M., Le Mogne Th., Palermo T., In situ MoS<sub>2</sub> formation and selective transfer from MoDPT films, Surface and Coatings Technology, Volume 108-109, Issue 10, Pages 352-359, (1998).
- [50] Martin, J.M., Belin M., Mansot J.L, Dexpert H., and Lagarde P., Friction-induced amorphization with ZDDP - an EXASF study, ASLE Transactions, Volume 29, Pages 523-531, (1986).
- [51] De Barros Bouchet M.I., Martin J.M., Le Mogne Th., Bilas P., Vacher B. and Yamada Y., Mechanisms of MoS<sub>2</sub> formation by MoDTC in presence of ZnDTP. Effect of oxidative degradation, Wear, Issue 258, Pages 1643, (2005).
- [52] Kubo K., Mitsuhiro N., Shitamichi T., Motoyama K., The effect of ageing during engine running on the friction reduction performance of oil soluble molybdenum compounds, Proceeding of the international tribology conference, Yokohama, (1995).



- [53] Arai K., Yamada M., Asano S., Yoshizawa S., Lubricant technology to enhance the durability of low friction performance of gasoline engine oils, SAE Technical Paper 952533, (1995).
- [54] Bec S., Tonck A., Georges J.M., Roper G.W., Synergistic effects of MoDTC and ZDTP on frictional behavior of tribofilms at the nanometer scale, Tribol Lett, Volume 17, Pages 797, (2004).



## Chapter 2

---

# Ageing impact on tribological properties of MoDTC-containing base oil

---

*Since last decades, there is an industry-wide need for the comprehension of how degradation process affects lubricant tribological performance.*

*This chapter focuses on the impact of MoDTC ageing on its tribological properties.*

*Ageing tests were carried out with a device built in the laboratory based on CEC-L-48-A00 standard. The lubricating performances of the fresh and aged oils have been assessed using a ball-on-flat reciprocating tribometer, under boundary lubrication conditions. The chemical composition of the surface of the tribofilm has been investigated by means of X-ray Photoelectron Spectroscopy (XPS), while its structure and thickness have been studied using Transmission Electron Microscopy (TEM).*

*An induction period increasing with the degradation time was evidenced on the friction behavior when Mo-containing base oil was subjected to the degradation process. Moreover, the formation of a tribofilm rich in molybdenum oxi-sulfides compounds and the impact of ageing on the sheet morphology have been documented.*

*All the results found are discussed to clarify the correlation between degradation time, tribological performance and tribofilm characterizations.*

## Chapter 2

---

# Ageing impact on tribological properties of MoDTC-containing base oil

---

*D'un point de vue industriel, il est important de comprendre comment la dégradation du lubrifiant affecte ses performances tribologiques. Ce chapitre se concentre donc sur l'étude et la compréhension de l'impact du vieillissement de la molécule de MoDTC sur sa capacité à réduire le frottement dans un contact acier/acier.*

*Les essais de vieillissements ont été réalisés avec un dispositif développé au laboratoire, selon la norme CEC-L-48-A00. Les performances tribologiques des huiles neuves et vieilles ont été évaluées en utilisant un tribomètre alternatif bille/plan, dans des conditions de lubrification limite. La composition chimique du tribofilm formé sur la surface a été étudiée grâce à la spectroscopie de photoélectron (XPS), tandis que sa structure et son épaisseur ont été étudiées en utilisant la microscopie électronique à transmission (MET) sur des lames minces obtenues par FIB (Focused Ion Beam).*

*Les résultats montrent que lorsque l'huile contenant du MoDTC est soumise au processus de dégradation, il y a une période d'induction qui augmente avec le temps de dégradation. Le vieillissement du lubrifiant a donc un impact sur la composition et morphologie du tribofilm puisque la composition (présence d'oxi-sulfures de molybdène) et la morphologie des feuillettes peut varier ( $\text{MoS}_2/\text{MoS}_{2-x}\text{O}_x$ ).*

*Tous les résultats sont discutés afin de clarifier la corrélation entre le temps de dégradation, les performances tribologiques et la composition des tribofilms.*

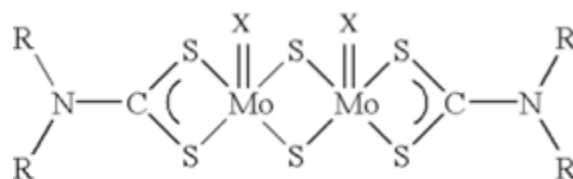
## 1. INTRODUCTION

One of the major drawbacks of MoDTC additive is that its lubricating ability is greatly degraded in severe conditions such as high temperature, shear stress and chemical attack by fuel combustion products [10,11]. For this reason, chemical and physical changes are usually noticeable in the engine, in both base oil and additive, having a significant effect on their tribological properties. The knowledge of the MoDTC decomposition under relative high temperature and the understanding of the MoDTC-containing lubricant degradation play a key role in lubricant optimization and to extend the longevity of the friction reducing performance and long drain intervals. Previous work [17] showed that the MoDTC concentration depletion due to the lubricant ageing mechanisms leads to the formation of poor reducing friction-properties tribofilm. The correlation between the oxidation time and the decrease of the  $\text{MoS}_2$  sheets formed inside the tribofilm, and to the formation of  $\text{MoS}_{2-x}\text{O}_x$  oxi-sulfide species, was highlighted. The same authors examined the antioxidant effect of phosphorous-containing compound ZnDTP when lubricant degradation occurs and  $\text{MoS}_{2-x}\text{O}_x$  oxi-sulfide species are present in the tribofilm [11]. It has been experimentally demonstrated [23] that the concentration of oxygen into the oxi-sulfide tribofilm significantly influences both the friction coefficient and the endurance of tribofilm. The aim of this chapter is to give a better understanding on the impact of the MoDTC containing base oil degradation on its tribological performance, correlating the deterioration of the friction-reducing property to surface chemistry and to tribofilm morphology.

## 2. EXPERIMENTAL DETAILS

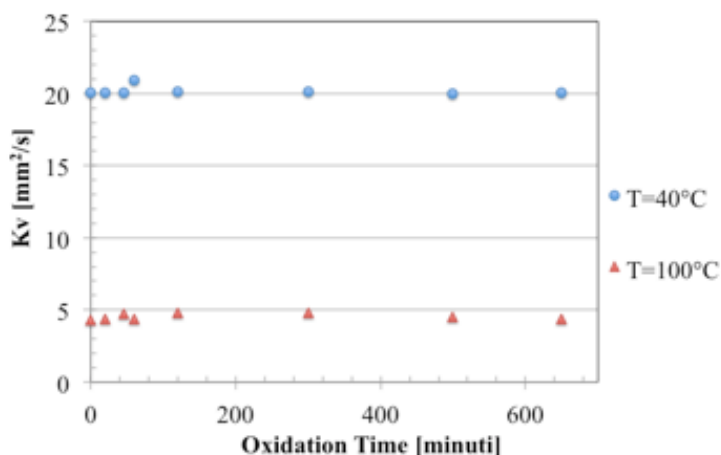
### 2.1. Materials

The molybdenum dithiocarbamate (MoDTC) additive studied in this thesis is blended into the mineral base oil (III group), supplied by TOTAL Company. The chemical structure of the MoDTC compound is shown schematically in **Figure 2.1**, where X can be S or O atoms (mainly S) and R are alkyl chains which can be  $4\text{C}_8$ ,  $4\text{C}_{13}$  or a mixture of  $2\text{C}_8$  and  $2\text{C}_{13}$ .



**Fig 2.1. Chemical structure of molybdenum dithiocarbamate (MoDTC).**

All the results shown in this thesis are performed by heating 1% by weight of MoDTC in mineral base oil. The solution is prepared in a beaker on a stirrer hot plate at a nominal temperature of 65°C, whilst stirring for 10 min. The addition of friction modifier in the base oil and the degradation process did not change the viscosity of the sample (**Figure 2.2**).



**Fig 2.2. Viscosity changes over degradation time**

## 2.2. Protocol of oxidative procedure

Laboratory oil aging procedure was conducted considering the CEC-L-48-A00 standard. The base oil and the additive was heated to 160°C using an in-house built system, consisting of a thermo-controlled heater and a round-bottom flask containing 300 mL oil sample, connected to a condenser in order to reduce the evaporation losses of the more volatiles components. To simulate the degradation process two choices were done differing from the standard:

- samples were not withdrawn at intervals. It was preferred to collect the entire sample for the successive analyses in order to have enough oil for the various characterizations and to avoid differences due to the changing in sample volume;
- samples were not exposed to any gas stream during the heating at 160°C. It was decided to carry out the oxidative test under atmospheric condition because the amount of oxygen present in the air in the flask has been assumed adequate to reach the degradation level required, although an inlet of air (or oxygen) would certainly speed up the degradation process.

## 2.3. Tribological experiments

### 2.3.1. Friction Coefficient

Tribological testing was performed using reciprocating linear ball-on-flat tribometer, with both ball (radius = 12.7 mm) and flat made of AISI 52100 steel and both surfaces had roughness of 25 nm in  $R_q$ . The tribometer configuration is described in ANNEX A.

Boundary lubrication conditions were achieved using appropriate combination of load, speed and temperature: a load of 32 N, ensured a maximum Hertz contact pressure of 800 MPa and an average linear sliding speed of 50 mm/s were set. The stroke length was 10 mm and the frequency was set to 5 Hz. The test duration was 1 hour corresponding to about 18000 cycles. Before starting the friction tests, the whole system (friction pairs and oil) was immersed in a about 8 ml of oil and heated to 100°C and about 30 minutes were needed to reach a stable temperature value. The tests were replicated three times to ensure the relative error as small as possible.

### 2.3.2. Wear measurement

The wear scar diameter on the ball was measured by using an optical microscope at 100 times magnification, before removing the balls from the sample holder. The wear volume was measured using a two dimensional analysis using the equations 2.1a and 2.1b [14,15].

$$V = \frac{1}{3} \pi h^2 (3R - h) \quad (a)$$

$$h = R - \sqrt{\left(R^2 - \frac{D^2}{4}\right)} \quad (b)$$

**Equation 2.1. Wear volume calculation.**

Where V is the volume material removed, R is the ball radius and D is the wear scar diameter on the ball resulting from the average of five measurements.

The wear produced on the flat samples was calculated by means of interferometry (Bruker).

## 2.4. X-ray photoelectron spectroscopy (XPS) analysis

XPS analyses for the tribofilms formed on the flat counterpart were carried out using an ULVAC-PHI VersaProbe II spectrometer equipped with a monochromatized  $\text{AlK}_\alpha$  X-ray source (1486.6 eV). The size of the X-ray spot was 50  $\mu\text{m}$ . A charge neutralization system using a dual beam is used to limit the charging effect that can occur on insulating materials. An additional correction to compensate the charge effect is performed on all spectra by setting the C1s line peak used as an internal reference at BE = 284.8 eV. Before performing XPS analyses, the flat was cleaned by several immersions in pure *n*-heptane and then left in ultrasonic bath for 10 minutes. The analysis chamber pressure is lower than  $10^{-8}$  Pa. Standardization in binding energy (BE) is achieved by analysing gold standard sample to locate the well-known energy positions of  $\text{Au}4f_{5/2}$  and  $\text{Au}4f_{7/2}$  at 84.0 eV and 87.7 eV. First, XPS measurements were performed by taking a survey spectrum covering a range of 1200 eV, permitting to identify all peaks and the presence of contaminants. Afterwards, a scanning of the individual peaks in more detail over a smaller range of 15-25 eV was undertaken. The detailed spectra of C1s, O1s, S2p, Mo3d and Fe2p were acquired to identify the different chemical states of the species and to perform a quantitative analysis using PHI multipack software. The chemical species corresponding to each binding energy have been attributed using standard materials and XPS handbook [18]. Photo-peaks of XPS were fitted with a Shirley background, and the quantification is calculated with sensitivity factors [24]. All the parameters needed for the fitting such as the peak area ratio, the difference between doublets binding energies and the Full-Width at Half-Maximum (FWHM) were fixed to obtain the most rigorous chemical tribofilm characterization.

## 2.5. Raman spectroscopy analyses

In order to elucidate the chemistry of the tribofilm formed by MoDTC-containing base oil lubrication, the XPS data must be combined with data from another analytical technique in order to provide a complete investigation of the tribofilm composition.

Raman spectroscopy is a very useful technique for the determination of the structure of the tribofilm formed on the steel surface, especially for  $\text{MoS}_2$  and  $\text{MoO}_3$  structures. Moreover, when interpreting Raman spectra, the laser excitation parameters (both wavelength and intensity) must be considered because modifications in the tribofilm structure can be caused.



The Raman used in this work operates at 488 nm wavelength. The spectral energy window used covered approximately  $1000\text{ cm}^{-1}$  and the beam was focused with a 50x objective. All Raman spectra were obtained under ambient conditions, using 50% laser power, and were accumulated for 3 times over 20 seconds. All the spectra were recorded 3 times in 3 different zones of the tribofilm, under identical instrument conditions in order to make comparisons between them. The standard deviation for the peak values was less than 1%. The Raman analysis has been carried out at **Leeds University**.

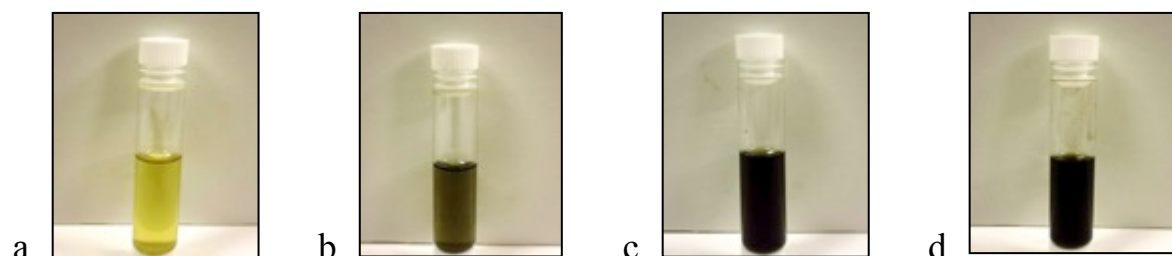
## 2.6. Transmission Electron Microscopy (TEM) analysis

To provide samples for Transmission Electron Microscopy (TEM) investigations of surface features of cross-sectional samples, Focused Ion Beam (FIB) technique has been employed. The area to be cross-sectioned was first covered with protection layers of platinum and tungsten before FIB milling, in order to protect the original surface from damage during the sample preparation. The FIB cross-sections were then placed on a copper grid covered by a holey carbon film and analyzed in a JEOL 2010F TEM operating at 200 kV acceleration voltage and equipped with Energy Dispersive X-Ray Spectroscopy (EDX).

## 3. RESULTS

### 3.1. Optical observations of the ageing effects

The color change was one of the clearest sign of the degradation process. **Figure 2.3** compares the fresh sample containing 1% in weight of MoDTC and the same mixture after different oxidative process durations.



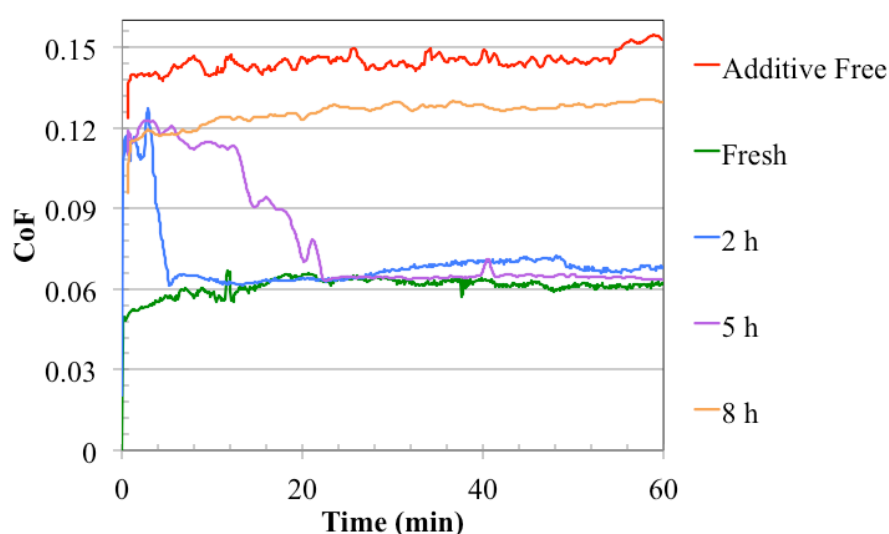
**Fig 2.3. Optical images of base oil plus 1% in weight of MoDTC (a) fresh, (b) after 2 hours oxidation, (c) after 5 hours oxidation and (d) after 8 hours oxidation.**

It can be clearly seen that the color of the sample becomes darker and darker along with the oxidation time. After 5 hours oxidation, the oil seems to be already black, and this is due to the formation of black solid-like particles as we will explain in the following. As the oxidation proceeded, in fact, solid suspension progressively increased in the liquid phase resulting in the strong color changes from original yellow-green color of the MoDTC mixture.

## 3.2. Tribological tests

### 3.2.1. Friction coefficient

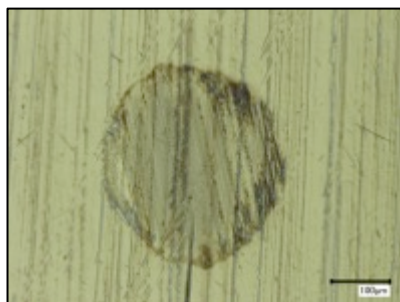
The evolution of the friction coefficients as a function of sliding time obtained for pure base oil and MoDTC-base oil blends with different ageing time are presented in **Figure 2.4**. The friction coefficient obtained using additive-free base oil is approximately 0.14 for the entire test, whereas the addition of 1% in weight of MoDTC additive drastically decreases the friction level to 0.06 in the steady state throughout the test. This result is in agreement with values previously reported in the literature [5,12]. For the oil aged for 2 hours, there is an induction time of about 5 minutes before friction coefficient dropped to the same value as the fresh MoDTC-containing base oil. The friction coefficient obtained using 5 hours aged oil reaches the same steady state value of 0.06 after a longer induction time of approximately 20 minutes. However, for 8 hours aged oil, the friction is still reduced (0.12) but it never reaches similar values obtained with fresh oil (0.06).



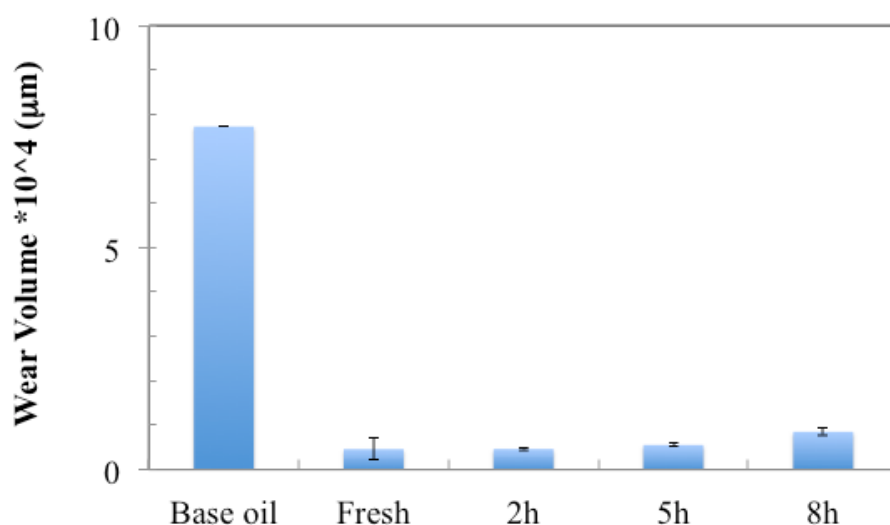
**Fig 2.4.** Friction coefficient of the steel/steel tribo-pairs lubricated with pure mineral base oil (black curve) and 1% in weight MoDTC-base oil blends after different duration of oxidation process (green-fresh, violet-2 hours of oxidation, blue - 5 hours of oxidation and red - 8 hours of oxidation).

### 3.2.2. Wear

The impact of lubricant degradation on wear is examined comparing the wear scar diameter on the rubbed balls. The wear scar obtained for fresh lubricant is shown in **Figure 2.5**. The wear volumes of the steel balls obtained for the different lubricants tested are compared in **Figure 2.6**.



**Fig 2.5.** Optical microscopy image (100x) of the wear scar on steel ball after friction test in the presence of fresh 1% wt. MoDTC- base oil blend.

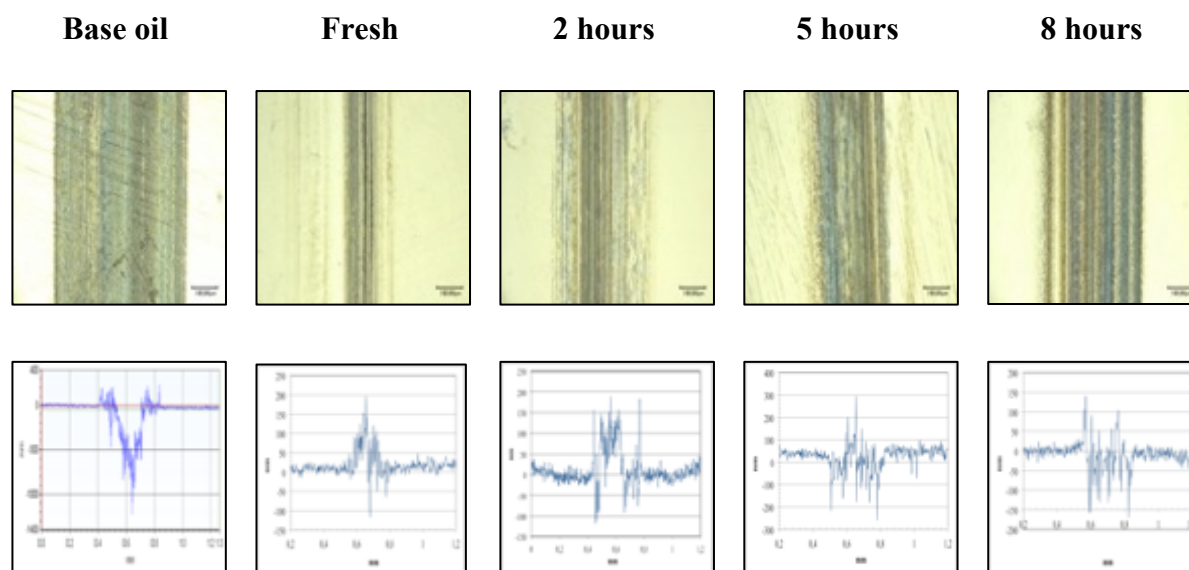


**Fig 2.6.** Comparison of the calculated wear volumes obtained for all the ball samples tested.

After the friction experiments, the steel flats were cleaned in *n-heptane* to clearly observe the tribofilms formed and to further be able to analyze them chemically. **Figure 2.7** shows the tribofilms formed on the steel flats specimen and the wear track profile obtained by means of interferometry.

Looking to the profiles, it is possible to affirm that the difference in color for the wear tracks formed on the flat sample may be due to the presence/absence of tribofilm. It can be seen, in fact, that the wear track profiles obtained using fresh and low oxide oils seem to have thicker

tribofilm while the wear for the 8 hours aged MoDTC-containing oil seems to be more severe.



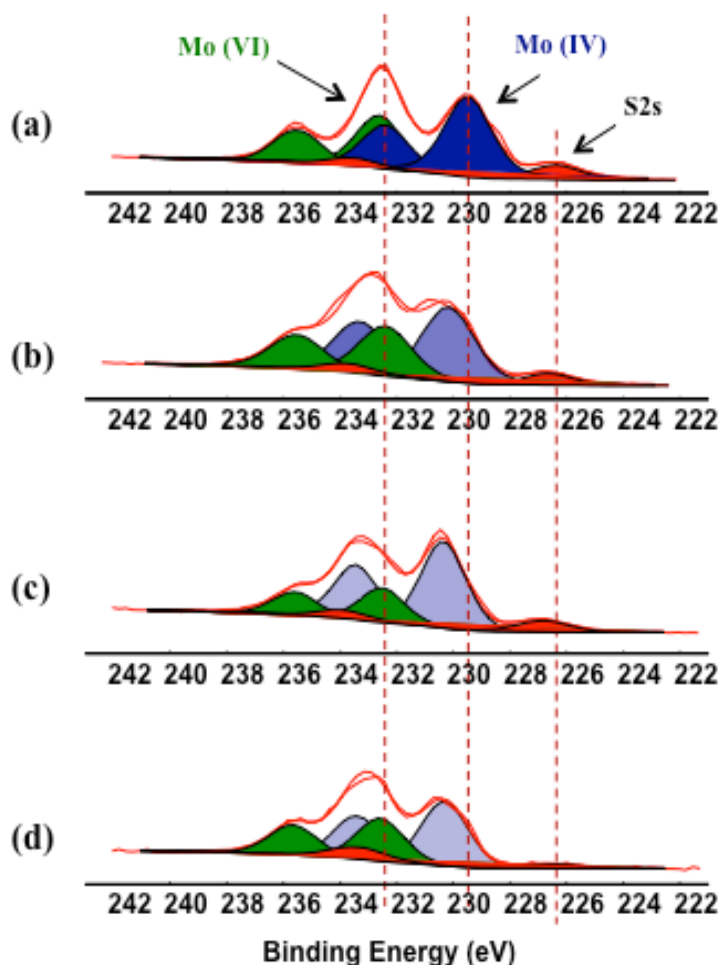
**Fig 2.7. Optical microscopy images of steel flats after friction tests carried out with different oils and their corresponding wear track profiles.**

### 3.3. X-ray photoelectron spectroscopy (XPS) analysis

The chemical composition of the extreme surface (maximum 10 nm depth) of tribofilm formed on the steel flat sample was studied by XPS. The narrow scans gave detailed information on each element present on the tribofilm. To perform an accurate fitting of the recorded data, the pure standard materials  $\text{MoS}_2$  and  $\text{MoO}_3$  were analyzed by XPS in order to have references. From the Mo3d spectra recorded on the tribofilms obtained with aged oil, two possible fittings can be proposed and this is explained in the following.

### 3.3.1. First fitting based on a progressive chemical shift of Mo (IV) photoelectron peak

As previously described, from the Mo3d spectra recorded on the tribofilms obtained with aged oil, two possible fittings can be proposed. **Figure 2.8** shows the first proposed fitting of Mo3d spectra for the solution base oil plus MoDTC additive fresh (a), 2 hours aged (b), 5 hours aged (c) and 8 hours aged (d) samples.



**Fig 2.8.** XPS High-resolution Mo3d spectra changes as a function of the oxidation time considering two contributions for fresh oil (a), 2 hours aged (b), 5 hours aged (c) and 8 hours aged (d) samples.

The tribofilm obtained with fresh sample (**Figure 2.8a**) is composed of large amount of MoS<sub>2</sub> (blue peaks, oxidation state of molybdenum IV) and MoO<sub>3</sub> (green peaks, oxidation state of molybdenum VI). Our result is in good agreement with the proposed reaction pathways of degradation of MoDTC in the contact, as described in the literature [10,11].

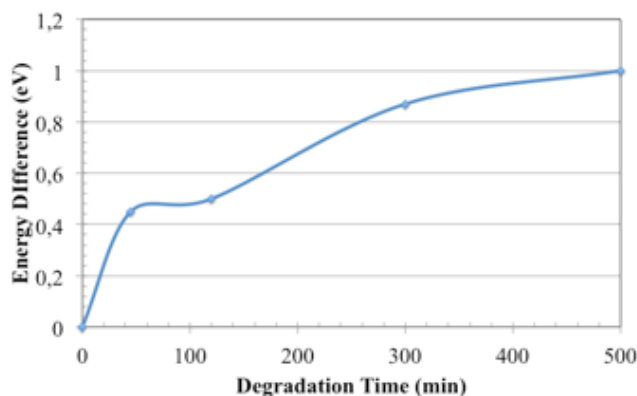
The binding energy, the FWHM and the atomic percentage for each contribution are reported in the **Table 2.2**.

Element	Binding energy (eV)	FWHM (eV)	Atomic %
<b>Fresh</b>			
<b>Mo3d<sub>5/2</sub></b>	229.5	2.2	9
	232.5	1.4	7
<b>S2p</b>	162.2	1.5	13
	168.7	1.6	2
<b>O1s</b>	530.5	1.7	27
	531.5	1.7	31
	532.5	1.8	10
<b>2 hours aged</b>			
<b>Mo3d<sub>5/2</sub></b>	230.2	2.2	6
	232.5	2.1	5
<b>S2p</b>	162.4	1.4	7
	169.0	1.4	13
<b>O1s</b>	531.1	1.7	19
	532.1	1.7	51
<b>5 hours aged</b>			
<b>Mo3d<sub>5/2</sub></b>	230.4	1.9	6
	232.5	1.5	7
<b>S2p</b>	162.5	1.4	8
	168.7	1.4	11
<b>O1s</b>	531.2	1.8	26
	532.0	1.7	41
<b>8 hours aged</b>			
<b>Mo3d<sub>5/2</sub></b>	230.5	2.0	9
	232.5	1.7	6
<b>S2p</b>	162.4	1.4	7
	168.8	1.4	11
<b>O1s</b>	531.3	1.7	26
	532.1	1.6	41

**Tab. 2.2.** The binding energies ( $\pm 0.1$  eV), FWHM ( $\pm 0.1$  eV) and atomic percentage of species measured on Mo3d and S2s photoelectron peaks recorded on tribofilms formed on steel flats by fresh and aged base oil plus 1% in weight MoDTC when two contributions are used to fit the Mo 3d peak.

While the molybdenum oxide peaks are always at the same binding energy (about 232.5 eV), for the Mo (IV) we observe a progressive chemical shift of the Mo3d photopeak to higher values as the degradation time increases (**Figure 2.9**).

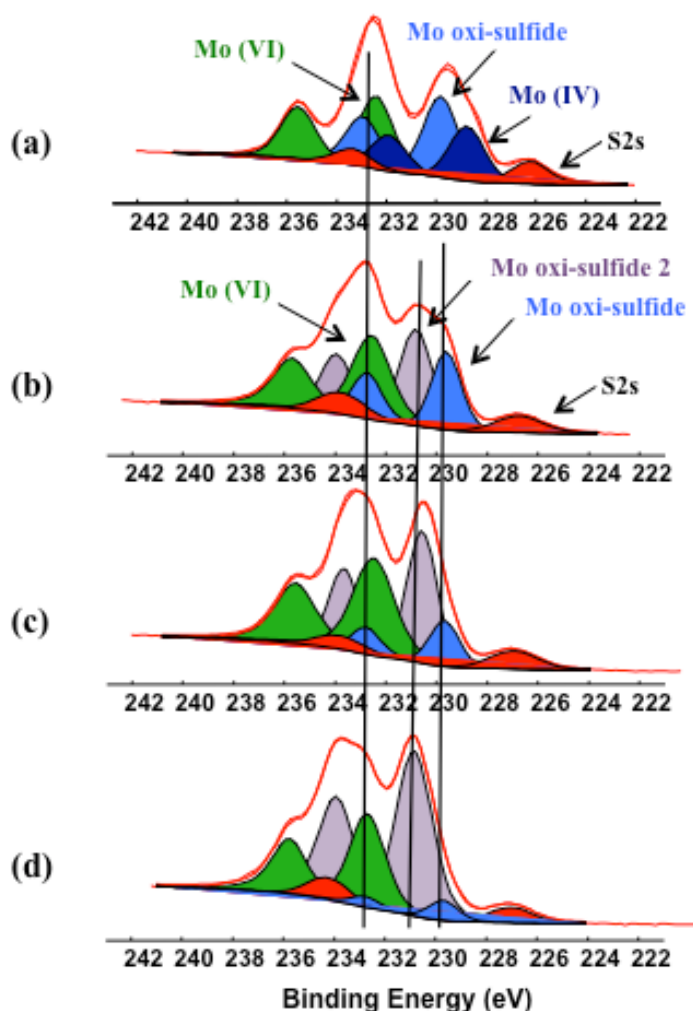
Peak interpretation for the spectra obtained with aged oil will be discussed in more detail in the section 4.



**Fig 2.9.** Chemical shift in the binding energy of the Mo (IV) line between fresh and aged oil as a function of oxidation time.

### 3.3.2. Second fitting based on three contributions in Mo3d photoelectron peak

The second possibility for analyzing the Mo3d photoelectron peak is to fit it with three different contributions, as shown in **Figure 2.10**.



**Fig 2.10.** XPS High-resolution Mo3d spectra changes in the tribofilm as a function of the oxidation time considering three contributions for fresh sample (a), 2 hours aged (b), 5 hours aged (c) and 8 hours aged (d) oil.

In this second case, the binding energies of Mo3d peaks for the fresh oil were found at 228.8 eV and 232.4 eV. The first one can be attributed to MoS<sub>2</sub> (dark blue peak) while the second can be assigned to MoO<sub>3</sub> (green peak at 232.6 eV). To fit the experimental spectrum a third contribution, located at 229.8 eV (light blue peak), was needed. Also, in the case of the photoemission peak obtained for aged oils, it is possible to notice the presence of the three contributions, located at about the same binding energy for the three ageing time (no chemical shift). Differently from the fresh sample, the MoS<sub>2</sub> contribution located at 228.8



eV disappears and only the two different photoemission peaks are observed: the first one at about 229.6 eV (light blue peak) decreasing as the degradation time increases and, the second one (violet peak) at about 230.6 eV increasing in intensity if the lubricant is aged for longer time. These two contributions could be interpreted as molybdenum oxi-sulfide species, with low and high oxygen content respectively. This hypothesis will be explained in detail in the discussion paragraph. The binding energy peak, the FWHM and the atomic percentage for each contribution are reported in the **Table 2.3**.

Element	Peak (eV)	FWHM	%
<b>Fresh</b>			
<b>Mo3d<sub>5/2</sub></b>	228.6	1.1	2
	229.8	2.0	9
	232.6	1.5	7
<b>S2p</b>	162.2	1.5	13
	168.7	1.6	2
<b>O1s</b>	530.5	1.7	27
	531.5	1.7	31
	532.5	1.8	10
<b>2 hours aged</b>			
<b>Mo3d<sub>5/2</sub></b>	229.6	1.4	3
	230.8	1.5	4
	232.6	1.8	4
<b>S2p</b>	162.4	1.4	6
	169.0	1.4	13
<b>O1s</b>	531.1	1.7	19
	532.1	1.7	51
<b>5 hours aged</b>			
<b>Mo3d<sub>5/2</sub></b>	229.6	1.4	2
	230.5	1.4	5
	232.4	2.0	6
<b>S2p</b>	162.5	1.4	8
	168.7	1.4	11
<b>O1s</b>	531.2	1.8	26
	532.0	1.7	41
<b>8 hours aged</b>			
<b>Mo3d<sub>5/2</sub></b>	229.4	1.4	1
	230.6	1.7	9
	232.5	1.7	5
<b>S2p</b>	162.4	1.4	7
	168.8	1.4	11
<b>O1s</b>	531.3	1.7	26
	532.1	1.6	41

**Tab. 2.3 The binding energies ( $\pm 0.1$  eV), FWHM ( $\pm 0.1$  eV) and atomic percentage of species measured on Mo3d and S2s photoelectron peaks recorded on tribofilms formed on steel flats by fresh and aged oils with 1% in weight of MoDTC when three contributions are used to fit the Mo 3d peak.**

### 3.4. Raman spectroscopy

In order to have a better interpretation of the tribofilm composition, it is needed to establish a reference spectrum for the  $\text{MoS}_2$  and  $\text{MoO}_3$  powders, scanned from a deposit on a steel disc (**Figure 2.11**). The Raman shift for the  $\text{MoS}_2$  (**Figure 2.11a**) shows well-defined bands at 382 and 408  $\text{cm}^{-1}$  [22], while the one for the  $\text{MoO}_3$  (**Figure 2.11b**) has the intense band at 819  $\text{cm}^{-1}$  [22]. **Figure 2.12** displays the spectra of fresh and aged oils.

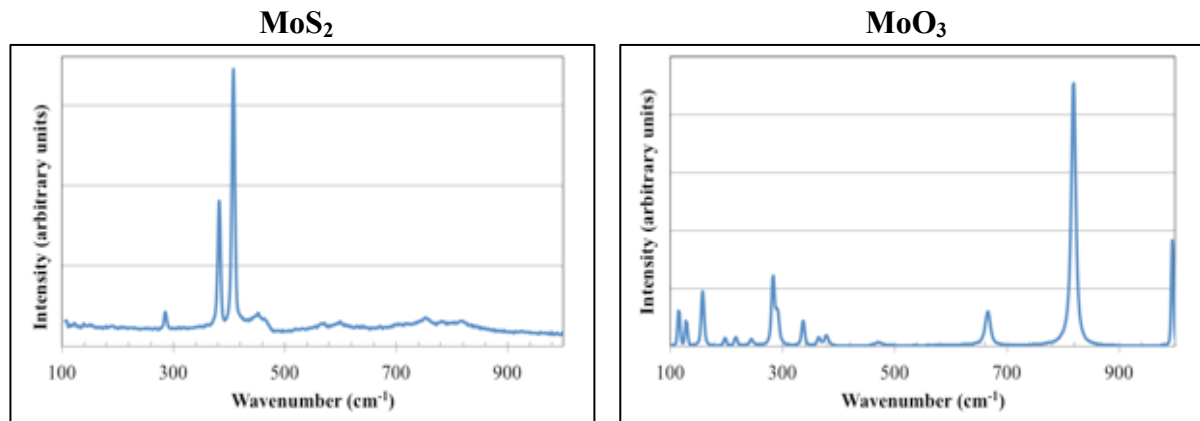


Fig 2.11. Raman spectra of  $\text{MoS}_2$  and  $\text{MoO}_3$  reference materials.

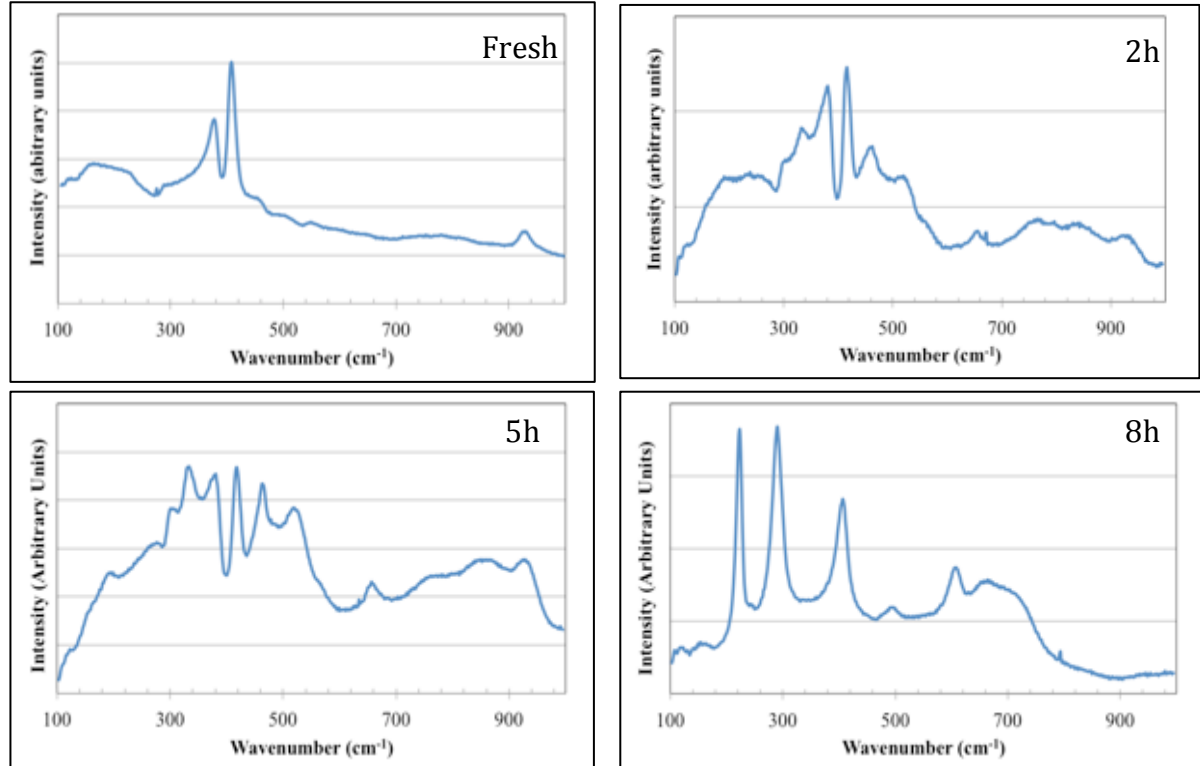


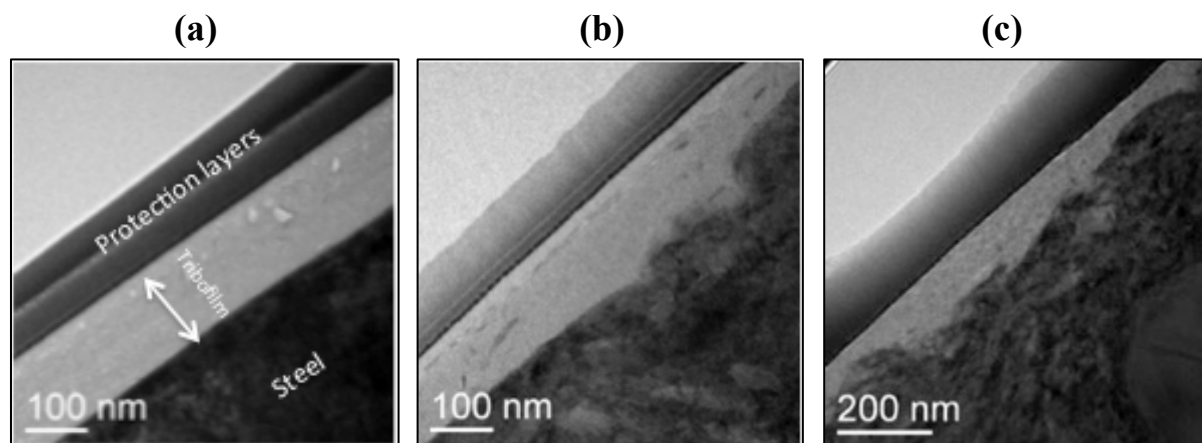
Fig 2.12. Raman spectra obtained on the wear track for fresh and aged MoDTC-containing samples.

It can be clearly observed that the fresh oil shows the typical two MoS<sub>2</sub> bands. On the contrary, although the spectra obtained using 2 and 5 hours exhibit bands that can be assigned to vibrational modes within the S–Mo–S layer, the peaks are not well defined and, in the same range there are new peaks appearing. The spectrum obtained for 8 h aged lubricant (**Figure 2.12(d)**) shows that practically no peaks related to MoS<sub>2</sub> compound are present and the Raman peaks in this case could be assigned to Fe<sub>2</sub>O<sub>3</sub> [21].

It is interesting to note that in all the spectra is not present any peak related to MoO<sub>3</sub>. This could be explained considering that the MoO<sub>3</sub> species in the tribofilm are in amorphous phase, reason why the peaks obtained analyzing the crystalline MoO<sub>3</sub> powder [20] are not detected.

### 3.5. Transmission Electron Microscopy (TEM) observations

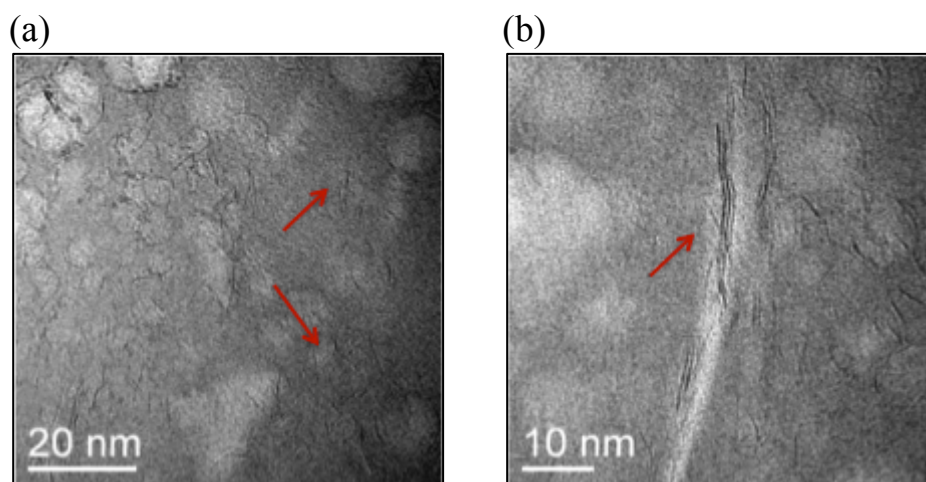
In order to investigate the microstructure of the tribofilm formed on the steel surface using fresh, 2 hours and 8 hours aged oil (**Figure 2.13a, 2.13b and 2.13c**) thin cross-sections were prepared by the Focused Ion Beam (FIB) technique and studied by means of Transmission Electron Microscopy (TEM). The results are given here only for fresh, 2 hours and 8 hours aged lubricants, respectively (**Figure 2.13a, 2.13b and 2.13c**).



**Fig 2.13.** TEM pictures of the longitudinal cross sections on the tribofilm formed on the steel plates after the test using 1% wt MoDTC in mineral base oil fresh (a), 2 hours aged (b) and 8 hours aged;

For the fresh oil, a 140 nm thick tribofilm (**Figure 2.13a**) is clearly distinguished between the steel substrate and the multi protective FIB multilayers used to protect the tribofilm before the nanomachining by Ga<sup>+</sup> ions beam. In this case, the steel interface with tribofilm seemed to be smooth and no significant wear was visible within the substrate.

The 2 hours aged oil case shows a thinner tribofilm, around 110 nm thick, and some wear of the steel surface was sometimes observed (**Figure 2.13b**). Using 8 hours aged oil, a much thinner tribofilm was formed (its thickness ranged between 30 and 90 nm). Moreover in this case, the steel surface seemed to be quite damaged and a relative high wear was obvious. The observations at higher magnification of the tribofilm derived from fresh lubricant (**Figure 2.14a** and **2.14b**) clearly show the presence of lamellar MoS<sub>2</sub> sheets embedded inside an amorphous matrix.

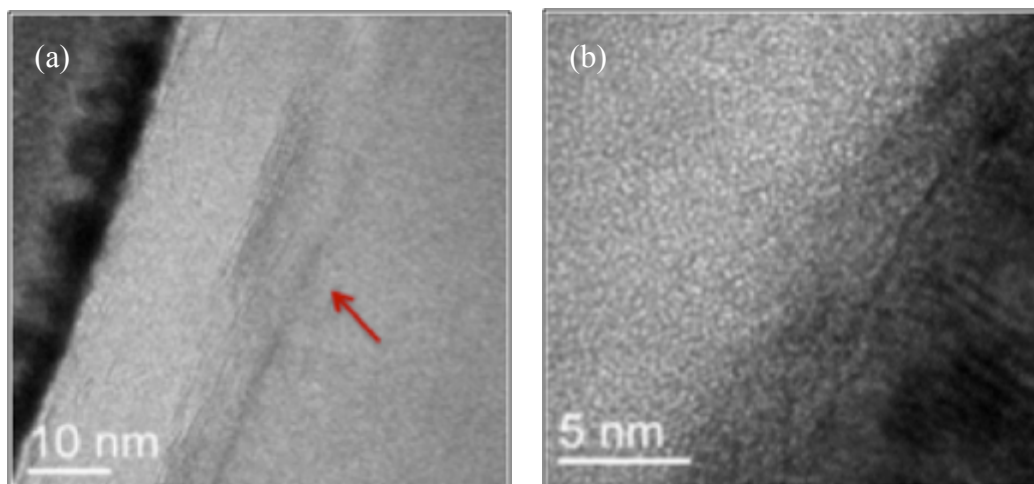


**Fig 2.14.** TEM micrographs of the cross-section of the tribofilm formed on steel after friction test using fresh 1% wt MoDTC in mineral base oil, evidencing the dispersed single MoS<sub>2</sub> sheets (a) and some MoS<sub>2</sub> sheets agglomeration (b).

This is characteristic of the MoS<sub>2</sub> compounds formation and such sheet structures were observed previously by other authors inside wear debris collected on the tribofilms surface [5, 11]. The MoS<sub>2</sub> sheets appeared as dispersed all over the tribofilm and they are organized in two different forms:

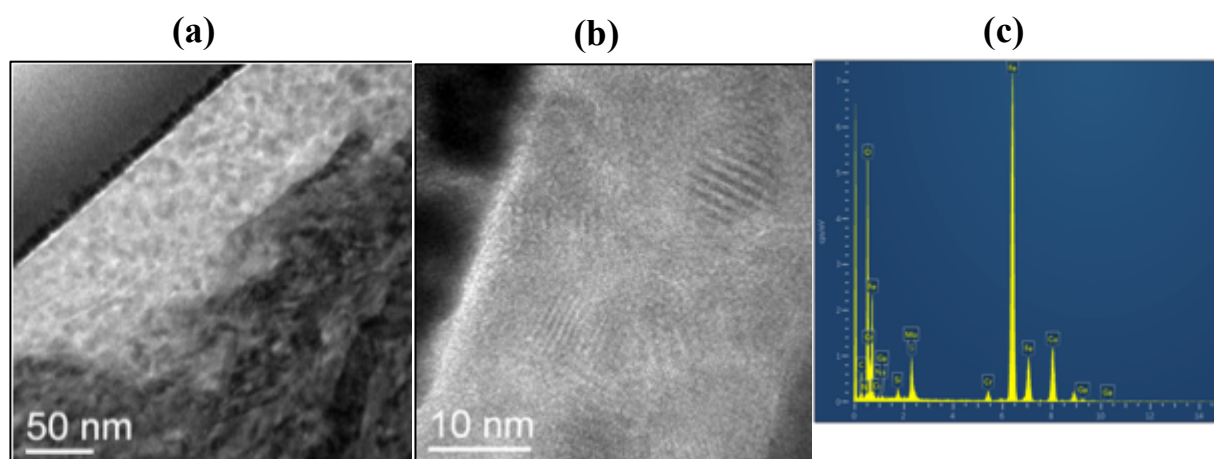
- single and isolated sheets with mean length of 3 nm (**Figure 2.14a**);
- long and compact bundles stacking naturally with a variable length from 8 to 16 nm (**Figure 2.14b**).

The higher magnification TEM images obtained for the 2 hours aged oil tribofilm (**Figures 2.15a and 2.15b**), indicated the presence of sheet structures similar to fresh oil but, in that case, they are well organized on the top part of the tribofilm and oriented parallel to the surface in the direction of motion.



**Fig 2.15.** TEM micrographs of the cross-section of the tribofilm formed on steel after friction test using 1% wt MoDTC in mineral base oil aged for 2 hours, showing the well-aligned  $\text{MoS}_2$  sheets located on top part of the tribofilm (a) while no chevron-like structure of S-Mo-S sandwich was visible (b).

Examining the tribofilm obtained with the 8 hours aged sample, see **Figures 2.16(a) and 2.16(b)**, it is observed that no more  $\text{MoS}_2$  sheets are present in the tribofilm. Moreover, the tribofilm is mainly composed of crystallized iron oxides particles and presence of carbon, molybdenum and sulfur, was identified by energy dispersive x-ray (EDX) spectroscopy analysis (**Figure 2.16(c)**).



**Fig 2.16.** TEM micrographs of the cross-section of the tribofilm formed on steel after friction test using 1% wt MoDTC in mineral base oil aged for 8 hours, where no  $\text{MoS}_2$  sheet structures are visible (a) and the iron oxides particles are present in the tribofilm (b, c).

## 4. DISCUSSION

Tribological tests and *post mortem* surface analysis (XPS and TEM) were performed to investigate the relation between the tribological performance of MoDTC-containing base oil and the degradation time. A significant reduction in friction coefficient was observed when adding 1% by weight of MoDTC in mineral base oil and, when the fresh mixture was used, the reduction in friction was obtained all over the tribological test. When this blend was aged, an induction period was necessary to obtain the reduction in friction coefficient and the delay to reach the steady-state value increased as the ageing time increases. Friction experiments indicated also that the friction-reducing properties of the sample were less important after 8 hours of ageing (**Figure 2.4**).

The wear volume loss calculated with the equations shown above (**Figure 2.6**) suggests that a significant reduction in wear volume loss was obtained when MoDTC is blended into base oil, confirming its good antiwear performance [16]. Moreover, considering the calculation done using the wear scar diameter on the ball, it is possible to note that the size of the worn areas do not significantly change with the degradation time. This means that the calculated worn volume on the ball is not related to the amount or the nature of the molybdenum oxysulfide  $\text{MoS}_{2-x}\text{O}_x$  compounds, suggesting that the MoDTC anti-wear property is mainly related to the amorphous carbon-rich matrix formed. However, the wear rate seems to be dependent to the degradation time when evaluated from the wear scars obtained on the steel plates. In fact, although it is difficult to exactly link wear rate and degradation time, it seems that the more the oil is aged the higher the wear produced on the flat it is, as shown in **Figure 2.7**.

A correlation between the chemical composition of tribofilm and the tribological properties can be established. If the attention is focused on the detailed inspection of the Mo3d XPS lines, it is possible to note that two distinct fits were possible to identify chemical composition of the tribofilm. In both cases, the two peaks related to molybdenum oxide ( $\text{MoO}_3$ ) for fresh and aged oils were always detected. Different hypotheses can be done to assign the other peaks. Considering that these peaks are located at binding energies between Mo (IV) and Mo (VI), De Barros *et al* [11] suggested that this contribution is associated to Mo (V), corresponding to the oxidation state of the molybdenum present in the MoDTC molecule. The authors assumed that some residual MoDTC molecule is adsorbed on the steel sample during the tribological tests. If so, a photoemission peak at the same binding energy should be detected when the analysis is made outside the wear track, assuming that

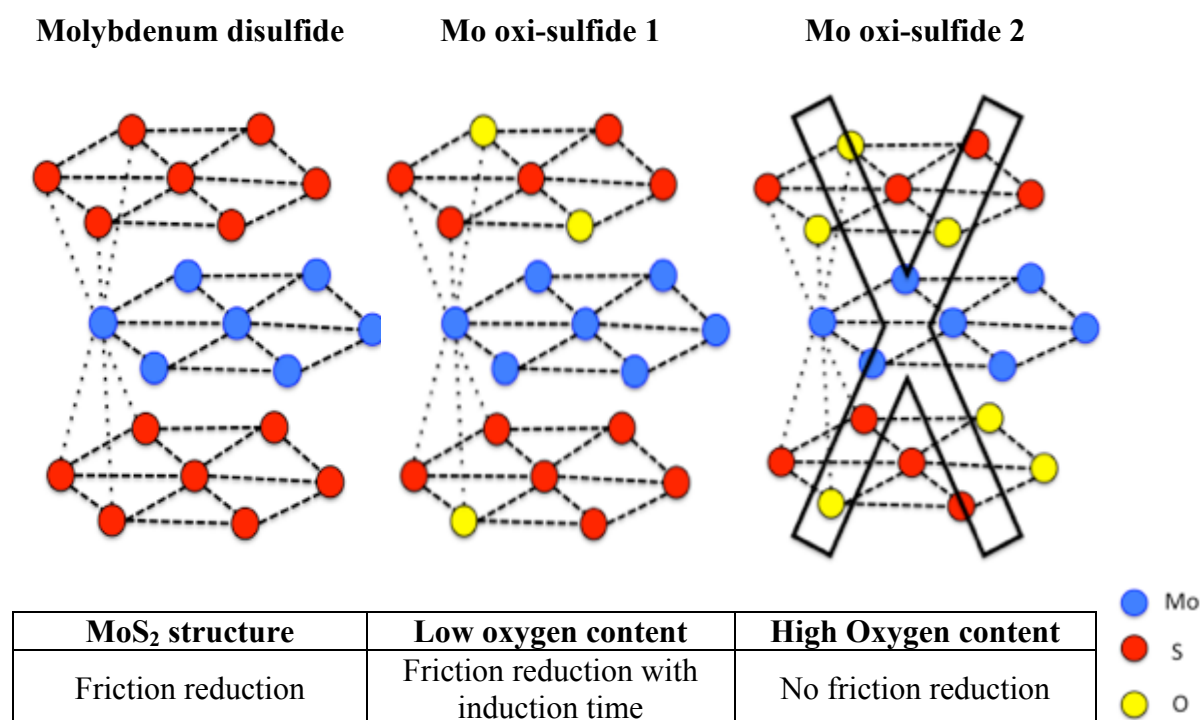
the adsorption is the same than inside, but it is not the case in this work. The same authors considered that the peak may come from molybdenum oxo-sulfide species ( $\text{MoS}_{2-x}\text{O}_x$ ) and that there is a chemical shift in its position to higher binding energy, which became greater and greater as the oxygen replaces sulfur in the molybdenum oxo-sulfide structure (**Figure 2.8**). Also this second assumption appeared to be not consistent in our case because of the S/Mo ratio. Indeed, the stoichiometry of the different species present into the tribofilm was not well respected. Another probable hypothesis was obtained when a third contribution was added to the fitting procedure. It may be assumed that two different molybdenum oxo-sulfide species are present in the tribofilms generated in the presence of aged oils. They can be identified as oxo-sulfide 1 ( $\text{MoS}_{2-x}\text{O}_x$ ) and oxo-sulfide 2 ( $\text{MoS}_{2-y}\text{O}_y$ ), where  $x < y$ , that is to say, one poor in oxygen and another with higher oxygen content. Considering the tribofilm atomic composition, in this case, the stoichiometry was found to be relatively well respected. In fact, while the S/Mo ratio is less than two, the ratio of the sum of sulfur plus oxygen (subtracting the oxygen in the  $\text{MoO}_3$ ) to molybdenum is two, within experimental error. To further validate this last XPS results interpretation, the chemical composition of the tribofilm was linked to the reduction in friction. It was seen that the position of the two peaks were almost degradation time independent and that the intensity of the peak corresponding to the oxo-sulfide 1 ( $\text{MoS}_{2-x}\text{O}_x$ ) decreased over degradation time, until it practically disappeared for the 8 hours of ageing. On the other hand, the oxo-sulfide 2 ( $\text{MoS}_{2-y}\text{O}_y$ ) concentration increased until it became the main contribution when the oil is aged for 8 hours. This trend correlates appropriately with the friction behavior. Indeed, until enough quantity of low oxygen content oxo-sulfide ( $\text{MoS}_{2-x}\text{O}_x$ ) compound is detected inside the tribofilm, a significant friction reduction is observed. In the opposite way, when the oil employed is aged for 8 hours, the XPS analysis shows that the tribofilm is mainly formed of high oxygen content molybdenum oxo-sulfide specie ( $\text{MoS}_{2-y}\text{O}_y$ ) compound, resulting in a significant decrease in friction reduction property. The validity of such hypothesis is supported by the results reported in literature. It has already been shown, in fact, that it is still possible to obtain the friction reduction till a certain oxygen level, approximately 15%, is detected inside the  $\text{MoS}_2$  lamellar structure [13].

In order to monitor the differences between the molybdenum oxidation states and to confirm the hypothesis done for the XPS results interpretation, Raman spectroscopy technique has been employed. The spectrum obtained with the fresh MoDTC-containing base oil clearly shows that  $\text{MoS}_2$  is formed, although it can be supposed that there is a small disorder in the crystal structure, which leads to the slightly broad and asymmetrical peaks



compared to pure MoS<sub>2</sub> powder. New peaks are detected for the film obtained using aged oils, probably due to some bond-angle disorder in the crystal structure. In fact, it is difficult to say with certainty that pure MoS<sub>2</sub> is present in the tribofilm formed with 2 h and 5 h aged oils. However, it is evident that the more the oil is aged the more the crystal structure is distorted. The peaks present in the same region at slightly higher frequencies could be due to strain introduced to the stacking layer of the crystal, while the frequency shifts at lower energy can be caused by possible distortions in the site symmetry of the atoms in the x-y plane. All these changes can be assigned to the presence of oxygen atoms in the lamellar structure of oxi-sulfide MoS<sub>2-x</sub>O<sub>x</sub>, confirming the hypothesis done using XPS results. Furthermore, the spectrum obtained for the 8 h degraded oil do not present peaks related to molybdenum-based species and the peaks detected can be assigned to iron oxide species. The Raman technique gave results in accordance to the tribological test and to the XPS analysis, indicating that, for the oil aged for 8 hours, only a relative small decrease in friction value is obtain. This can be related to the fact that the tribofilm is mainly made of iron oxide. This result is also confirmed by the TEM micrographs that revealed the presence of sheets inside the tribofilm generated in the presence of the 2 hours aged oil, while no sheets are detected after 8 hours of ageing. On the other hand, TEM studies revealed that if the friction test is carried out using fresh oil, a smooth interface between steel and tribofilm, without relevant damage, is observed. On the contrary, when aged samples are used, wear on the steel surface is noticeable, becoming more obvious with the presence of iron oxide particles into the tribofilm as the lubricant degradation time increases. This could be related to the presence of the induction period, where the friction value is relatively high before to drop to lower level.

In **Figure 2.18** it has been schematized the hypothesis done in this study about the coexistence between the two kind of molybdenum oxi-sulfides.



**Fig 2.18.** Schematic hypothesis about the coexistence of two oxi-sulfides into the tribofilms formed using aged MoDTC-containing oils.

## 5. CONCLUSIONS

Friction-reducing performances of molybdenum dithiocarbamate MoDTC containing base oil have been investigated as a function of degradation time (static oxidation test).

Considering the above results and discussions, the following conclusions can be drawn:

- (1) When lubricated by MoDTC-containing base oil, friction coefficient of the steel rubbing surface was reduced to 0.06 value throughout the test, generating more uniform and effective tribofilm without important wear on the steel surface;
- (2) For aged samples, the interface between the steel and the tribofilm appeared increasingly damaged as the degradation time of the lubricant increases. This can be correlated to the fact that an induction time was needed to obtain low friction coefficient;
- (3) When the lubricant is aged for 8 hours, the friction reduction property is less significant than for the fresh oil, whereas the wear scar remains relatively small thanks to the amorphous carbon-rich matrix of the tribofilm;
- (4) Between the 2 different hypotheses about MoDTC tribofilm chemical composition, the one about the concomitance of two molybdenum oxi-sulfides compounds (with low and high oxygen content) has been found more relevant. Although it is difficult to be sure about this new model because only the XPS cannot accurately conclude on the different species tribo-formed, it seems that also Raman spectroscopy validate this hypothesis.

Significant differences on the structure of the tribofilms formed using fresh and aged oil samples in term of thickness, orientation, size, shape and amount of MoS<sub>2</sub> sheets, have been observed. The possible explanations of these differences are reported in the previous chapters.

## 6. BIBLIOGRAPHY

- [1] Stachowiak G.W. and Batchelor A.W., Engineering tribology, Elsevier Butterworth Heinemann, Oxford, 3<sup>rd</sup> ed., (2005).
- [2] Graham J., Spikes H., Korcek S., The friction reducing properties of molybdenum dialkyldithiocarbamate additives: part I - factors influencing friction reduction. Tribology Transactions; Volume 44, Pages 626–36, (2001).
- [3] Yue W., Sun X.J., Wang C.B., Fu Z.Q., Liu J.J., A comparative study on the tribological behaviors of nitrided and sulfur-nitrided 35CrMo steel lubricated in PAO base oil with MoDTC additive. Tribology International, Volume 44, Pages 2029–34, (2011).
- [4] Harvey S.S.K and Blackwell J., An exploratory investigation of lubricant soluble molybdenum sulfur additives under conditions of rolling contact, Wear, Volume 63, Pages 183-188, (1980).
- [5] Grossiord C., Varlot K., Martin J.M., Le Mogne Th., Esnouf C., Inoue K., MoS<sub>2</sub> single sheet lubrication by molybdenum dithiocarbamate. Tribology International, Volume 31, Pages 737–43, (1998).
- [6] Schriver, Atkins and Langford, Inorganic Chemistry 2nd Edition, publ. Oxford University Press 2nd Ed., (1994).
- [7] Spengler G., and Webber A., On the lubricating performance of organic molybdenum compounds. Chem. Ber, Volume 92, Pages 2163-2171, (1939).
- [8] Rydberg H., Dion M., Jacobson N., Schröder E., Hyldgaard P., Simak S.I., Langreth D.C., Lundqvist B.I., Van der Waals Density Functional for Layered Structures. Phys. Rev. Lett. Volume 91, (2003).
- [9] Onodera T., Morita Y., Nagumo R., Miura R., Suzuki A., Tsuboi H., Hatakeyama N., Endou A., Takaba H., Dassenoy F., Minfray C., Joly-Pottuz L., Kubo M., Martin J.M., Miyamoto A., A Computational Chemistry Study on Friction of h-MoS<sub>2</sub>. Part I. Mechanism of Single sheet lubrication. J. Phys. Chem. B, Volume 113, (2009).
- [10] Kubo K., Nagakari M., Shitsmichi T., Motoyama K., The effect of ageing during engine running on the friction reduction performance of oil soluble molybdenum compounds. Proc. Intern. Trib. Conf. Yokohama, Pages 745-750, (1995).
- [11] De Barros Bouchet M.I., Martin J.M., Le Mogne Th., Bilas P., Vacher B., Yamada Y., Mechanisms of MoS<sub>2</sub> formation by MoDTC in presence of ZnDTP. Effect of oxidative degradation. Wear, 258, Pp. 1643, (2005).

- [12] Morina A., Neville A., Priest M., Green J.H. ZDDP and MoDTC interactions and their effect on tribological performance-tribofilm characteristics and its evolution. *Tribology Letters*; Volume 24(3), Pages 243–56, (2006).
- [13] Martin J.M., Superlubricity of molybdenum disulphide, *Superlubricity*, Edited by A. Erdemir and J.M. Martin, Pages 207-225, (2007).
- [14] Blau P.J. and Jun Q., An efficient method for accurately determining wear volume of sliders with non-flat wear scars and compound curvatures. *Wear*, 261, (2006).
- [15] Blau P.J., *Friction science and technology: from concepts to applications*, CRC press, Boca Raton, (2009).
- [16] Braithwaite E.R. and Greene A.B., A critical analysis of the performance of molybdenum, *Wear*, Volume 46, Pages 405-43, (1978).
- [17] Martin J.M., Le Mogne Th., Bilas P., Vacher B., Yamada, Effect of oxidative degradation on mechanisms of friction reduction by MoDTC, *Proceedings of the 28<sup>th</sup> Leeds-Lyon Symposium on Tribology*, Vienne, Austria, (2001).
- [18] Moulder J.F., Bomben K.D., Sobol P.E., Stickle W.F., *Handbook of X-Ray Photoelectron Spectroscopy. A Reference Book of Standard Spectra for Identification and Interpretation of XPS data*. Phy. Electr., Eden Prairie, MN, (1992).
- [19] Willermet P.A., Carter R.O., Schmitz P.J., Everson M., Scholl D.J., and Weber W.H., *Formation, Structure and Properties of Lubricant-Derived Antiwear Films*, *Lubrication Science*, Volume 9, Pages 325-347, (1997).
- [20] Ajito K., Nagahara L., Tryk D., Hashimoto K., Fujishima, A., Study of the photochromic properties of amorphous MoO<sub>3</sub> films using Raman microscopy, *The Journal of Physical Chemistry*, Volume 99 (44), Pages 16383-16388, (1995).
- [21] Shim S. and Duffy T., Raman spectroscopy of Fe<sub>2</sub>O<sub>3</sub> to 62 GPa, *American Mineralogist*, Volume 87, Pages 318–326, (2001).
- [22] Khaemba D.N., Neville A., Morina A., A methodology for Raman characterization of MoDTC tribofilms and its application in investigating the influence of surface chemistry on friction performance of MoDTC lubricants, *Trib. Letters*, 59:38, (2015).
- [23] Fleischauer P.D., Lince J.R. A comparison of oxidation and oxygen substitution in MoS<sub>2</sub> solid film lubricants. *Tribol. Int.* 32(11), 627–636, (1999).
- [24] Wagner C.D., Davis L.E., Zeller M.V., Taylor J.A., Raymond R.H., Gale L.H., Empirical atomic sensitivity factors for quantitative analysis by electron spectroscopy for chemical analysis, *Surface and Interface Analysis*,. Volume 3(5), Pages 211-225, (1981).



## Chapter 3

---

# MoDTC chemical changes in bulk oil due to degradation process

---

*Due to the complexity of the processes, the degradation mechanisms of molybdenum dithiocarbamate (MoDTC)-containing oil are still not fully understood. In order to get a better understanding of how a MoDTC additive works at the molecular level, correlation between its chemical behavior in the bulk oil during thermo-oxidative degradation and its ability to reduce friction has been investigated. The combination of using High-Performance Liquid Chromatography (HPLC), Fourier Transform Infrared Spectroscopy (FT-IR) and Mass Spectroscopy (MS) techniques has provided much detailed information about the complex chemistry involved in the degradation process.*

*At the end of this chapter, the link between MoDTC additive depletion and its effectiveness to lower the friction has been studied and a hypothesis on the chemical pathway followed by MoDTC during a thermo-oxidative degradation process has been proposed.*

## Chapter 3

---

### MoDTC chemical changes in bulk oil due to degradation process

---

*Les mécanismes de dégradation du MoDTC dans un moteur thermique étant particulièrement complexes, ils ne sont pas encore totalement compris. Afin d'obtenir une meilleure compréhension de l'évolution de la composition chimique du MoDTC, une caractérisation des huiles dégradées a été réalisée. La combinaison de l'utilisation de la chromatographie liquide (LC), la spectroscopie infra-rouge (FT-IR) et la spectroscopie de masse (MS) a permis d'obtenir des informations détaillées sur l'évolution de la composition chimique de la molécule lors du processus de dégradation.*

*A la fin de ce chapitre, nous avons étudié le lien entre l'appauvrissement en MoDTC et sa capacité à réduire le frottement. L'effet des produits de dégradation obtenus à partir du MoDTC sur une possible réduction du frottement a également été étudié. En se basant sur ces résultats, un mécanisme de dégradation thermo-oxydative du MoDTC a été proposé.*



## 1. INTRODUCTION

In chapter 2, it has been reported the extremely good tribological performance of MoDTC additive, able to reduce the friction coefficient to relatively low value. However, it has been also shown the performance loss of this friction modifier due to oil degradation. Nevertheless, it is still unclear how the MoDTC molecule behaves in the bulk oil when subjected to ageing. For this reason more work needs to be done in this area before any conclusion can be made. In fact, many investigations have been already undertaken to determine the parameters affecting its friction reduction property [1,2] and the mechanisms occurring inside the tribological contacts when MoDTC-containing oil is employed have been hypothesized [3, 4]. However, due to the extremely complex chemical pathway involving the MoDTC molecules, the current understanding of its chemical behavior in the bulk oil when subjected to thermo-oxidative degradation is still not fully identified. In fact, in the knowledge of the authors, any work has been done to accurately understand the MoDTC compound degradation process.

To date, the only investigations undertaken relating to the additive depletion evaluation on the bulk oil characterization have been performed using High-Performance Liquid Chromatography (HPLC). The authors, De Barros *et al.* [5], followed the MoDTC and ZDDP concentration during lubricant degradation process and hypothesized that the oxidation process significantly affects the exchange reaction supposed between MoDTC and ZDDP. The interaction of these two additives has also been analyzed by Kubo *et al.* [4]. The authors evaluated the effect of lubricant ageing on the friction reduction performance during engine testing. In this instance the remaining concentrations of zinc and molybdenum compounds were determined by HPLC, coupled with Fourier Transform Infrared Spectroscopy (FT-IR). It was shown that the addition of an antioxidant additive delayed the MoDTC depletion and consequently maintained the friction reduction over a longer time period. The synergistic effects between MoDTC and ZDDP and their lubricating performances have also been analyzed by Graham *et al.* [6]. Again, it has been confirmed that MoDTC additives can be protected against thermo-oxidative degradation by adding ZDDP additive. On the other side, these papers did not carried out the detailed bulk oil analysis to study the molecular behavior of additives. For this reason additional investigations are clearly needed to further understand the MoDTC chemical reactions taking place during the degradation process and their impact on the friction reduction efficiency. Considering that it is not possible to infer the decomposition mechanisms

followed by MoDTC molecule using a single technique, in this chapter we have extended our analytical strategy to obtain a deeper insight into the MoDTC friction modifier additive chemical changes under thermo-oxidative degradation. High-performance liquid chromatography (HPLC), Fourier Transform Infrared Spectroscopy (FT-IR) and mass spectroscopy (MS) have been included to follow the concentration of the remaining MoDTC and the nature of the decomposition products formed after the time-controlled degradation procedure. Finally the reaction pathway of a MoDTC additive when subjected to thermo-oxidative degradation is hypothesized and the link between the chemical changes subjected by the MoDTC molecules with the degradation process and the MoDTC ability to lower the friction is discussed.

## **2. METHODOLOGY**

### **2.1. Degradation Procedure**

The mixture of MoDTC in the base oil was degraded as described in the previous chapter but, for the analysis reported in this chapter, the additivated oil samples of 25 ml were withdrawn in steps of 1 hour up to a maximum of 8 hours of thermo-oxidative degradation. In this way it has been possible to evaluate the possible MoDTC depletion more precisely and to monitor the chemical pathway followed by the additive molecule.

### **2.2. High Performance Liquid Chromatography (HPLC)**

A UHPLC system (Water Acquity) was used in reversed-phase mode, equipped with a module LC pump, auto-sampler and photodiode-array (PDA) detector. The HPLC parameters run according to TOTAL's internal procedure.

Samples were first weighed into a 100 ml vial and then diluted in *n-heptane* to obtain an oil/solvent ratio of ca. 1:20. Part of this solution was filtered through 0.2  $\mu\text{m}$  micropore filter prior to analysis (in order to remove any particles present in the aged oil) and added in a 20 ml vial. At the end the diluted and filtrated samples were placed in auto-sampler racks. The spectrum intensity is used to determine the MoDTC concentration after a suitable calibration of the additive content.

## 2.3. Mass Spectroscopy (MS)

The Xevo G2 Q-TOF mass spectrometer was used both in positive and negative ESI mode for data acquisition and analyzed the filtered fresh and aged oil. Typical source conditions for maximum intensity of precursor ions and the parameters set for the scan function used for the data acquisition were set according to TOTAL's internal procedure.

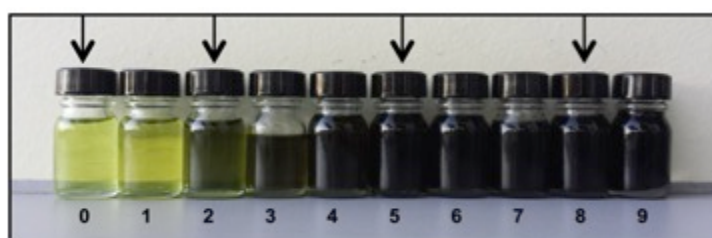
## 2.4. Fourier Transform Infra-Red Spectroscopy (FTIR)

Absorbance spectra were recorded with Nicolet 380 FTIR spectrometer, with  $4\text{ cm}^{-1}$  resolution. The spectral range of the measurement set-up was to  $(4000-400)\text{ cm}^{-1}$  with 30 scans. A background spectrum of the Potassium Bromide (KBr) window was taken before the measurement and automatically subtracted from the sample spectrum in order to obtain peaks related specifically to the lubricant sample (filtered oil).

# 3. RESULTS

## 3.1. Degraded oil: visual inspection

As already underlined in the previous chapter, during the degradation process, pronounced color changes - suggesting chemical modifications – were observed in all samples (**Figure 3.1**). Here it is even clearer how the light green color of the freshly additivated oil (0 hours degradation time) became darker and darker until resulting completely black when the oil is aged for longer time (8 hours).



**Fig 3.1. MoDTC-containing base oil color changes with degradation time (0 hour to 8 hours ageing).**

### 3.2. MoDTC additive depletion by HPLC

The HPLC chromatograms for both fresh and aged oils are characterized by the presence of two peaks characteristic values of molybdenum dithiocarbamate additive. This is due to the presence of three types of MoDTC molecules in the additive used in this work (hydrocarbon chain with  $4R=C_8$ ,  $4R=C_{13}$  or  $2R=C_8$  and  $2R=C_{13}$ ). To accurately correlate the peak areas to the MoDTC concentration, calibration solutions with 8 different known concentrations in the mobile phase were prepared and injected in duplicate. Linear regression analysis was carried out on the curve generated by plotting the peak area response (x) versus the known concentration of MoDTC (y) expressed in ppm (**Figure 3.2a, 3.2b**).

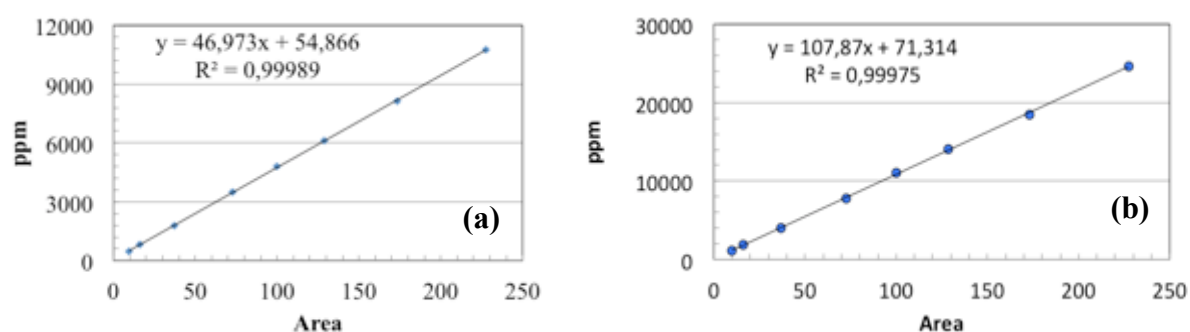


Fig 3.2. Calibration curves for MoDTC with  $4R=C_8$  (a) and MoDTC with  $2R=C_8$  and  $2R=C_8$  (b).

Subsequently, experiments were carried out on several oils having 9 progressive degradation times, starting from 0 hours (fresh oil), over a period of 8 hours with an evaluation made every hour. The presence of MoDTC in solution has been quantified by measuring the peak volume of the characteristic retention time for the two peaks for the MoDTC-containing base oil with the results plotted in **Figure 3.3a and 3.3b**.

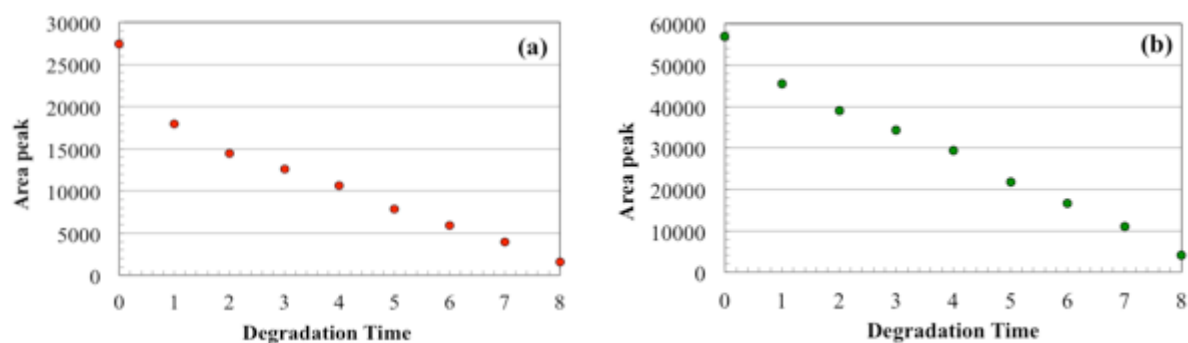
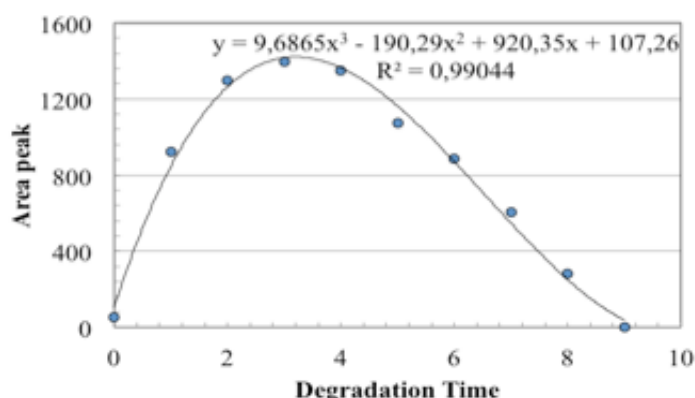


Fig 3.3. Additive depletion considering the MoDTC with  $4R=C_8$  (a) and with  $2R=C_8$  and  $2R=C_8$  (b).

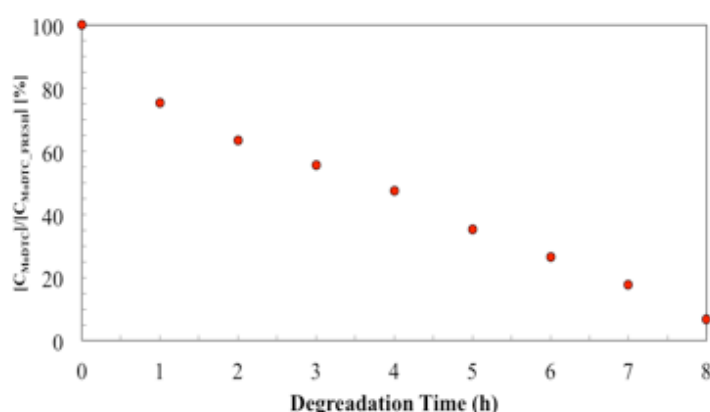
The presence of another small peak was detected and, in the same way, its areas were plotted as function of degradation time (**Figure 3.4**).



**Fig 3.4. Additive depletion against the degradation time, taking in consideration the third new peak.**

The area of this peak seems to increase during the initial early degradation periods and then to gradually decrease. It is possible that a reaction product is formed in the beginning of the ageing process, followed by other chemical changes the lead to the consumption of this new compound. These results will be discussed more carefully within the next paragraph.

All the HPLC results relate to the fresh oil concentration at 100% and the MoDTC depletion is reported in percentage. The additive depletion of MoDTC additive, given by the sum of the two characteristic peaks is shown in **Figure 3.5**. In the graph ( $C_{\text{MoDTC\_FRESH}}$ ) corresponds to the MoDTC concentration of fresh oil while the amount of remaining MoDTC in the base oil at the degradation time considered is called ( $C_{\text{MoDTC}}$ ).

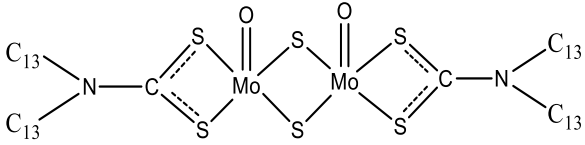
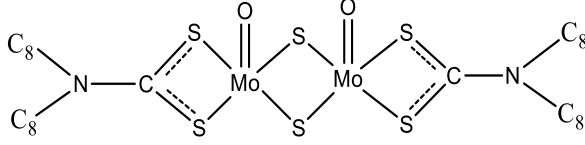
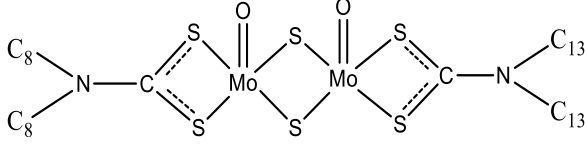
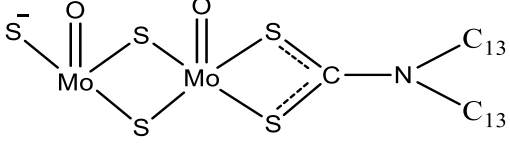
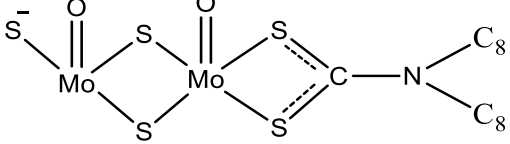
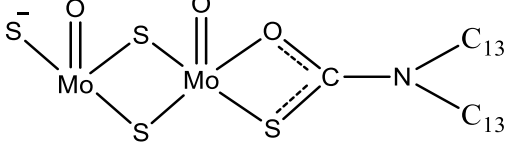
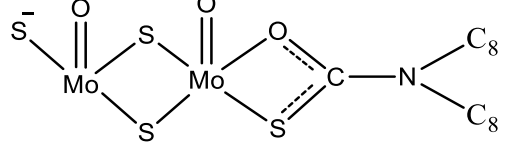
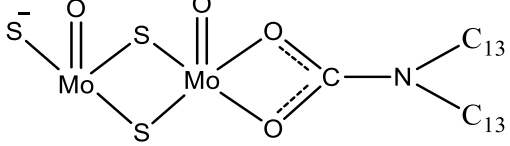
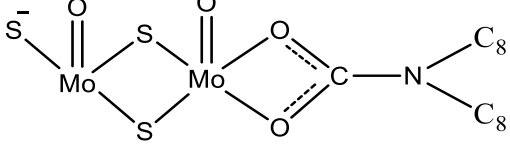


**Fig 3.5. MoDTC additive depletion considering the sum of the two MoDTC characteristic peaks.**

When the MoDTC-additivated base oil is aged, a linear reduction (kinetic zero order) of the MoDTC compound concentration is visible up to 8 hours degradation, at which point virtually all the MoDTC has become consumed.

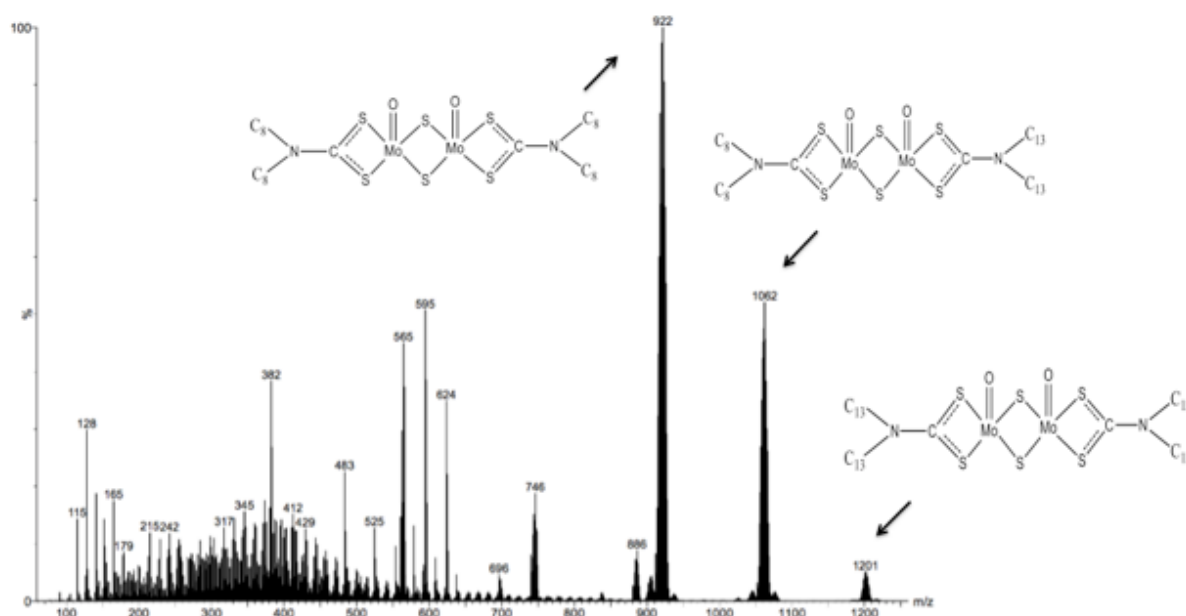
### **3.3. Study of MoDTC molecular transformations by Mass Spectroscopy**

Mass spectroscopy (MS) was used to obtain information about the molecular transformations of MoDTC present into the base oil and the degradation products formed during the ageing process. In order to ease the interpretation of the MS spectra, the fractional groups and their molecular weight, important for the understanding of the results presented in the current paper are reported in the **Table 3.1**.

MoDTC molecules and fragments		MW
	Starting molecule having 4 R=C <sub>13</sub>	1202
	Starting molecule having 4 R=C <sub>8</sub>	922
	Starting molecule having 2 R=C <sub>13</sub> and 2 R=C <sub>8</sub>	1062
	<b>Fragment A</b> , having 2 radical group C <sub>13</sub>	778
	<b>Fragment B</b> , having 2 radical group C <sub>8</sub>	636
	<b>Fragment C</b> , having 1 sulfur atom replaced by an oxygen atom compared to the fragment A	762
	<b>Fragment D</b> , having 1 sulfur atom replaced by an oxygen atom compared to the fragment B	620
	<b>Fragment E</b> , having 2 sulfur atoms replaced by 2 oxygen atoms compared to the fragment A	746
	<b>Fragment F</b> , having 2 sulfur atoms replaced by 2 oxygen atoms compared to the fragment B	604

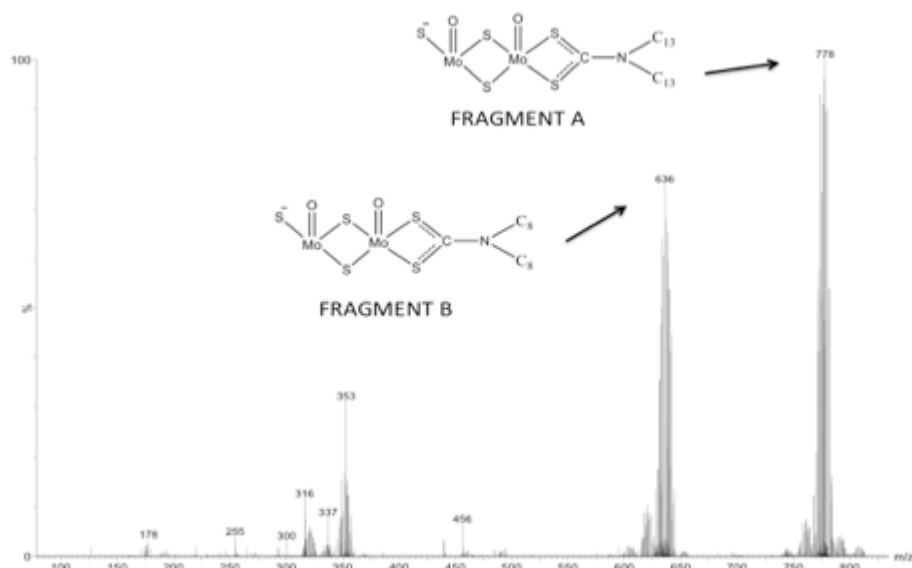
Tab. 3.1 MoDTC molecular fragments obtained by mass spectroscopy.

Considering that the radical group present in the MoDTC molecule analyzed in this work is a mixture of C<sub>8</sub> and C<sub>13</sub> hydrocarbon chains, the MS results obtained using the positive mode confirmed the presence of MoDTC additive in the oils and the possibility to monitor its chemical change. In fact, the measured molecular weights observed in **Figure 3.6** are in good agreement with the theoretical values presented in the **Table 3.1**.



**Fig 3.6.** Mass spectrum obtained for fresh MoDTC-containing base oil in positive ion mode.

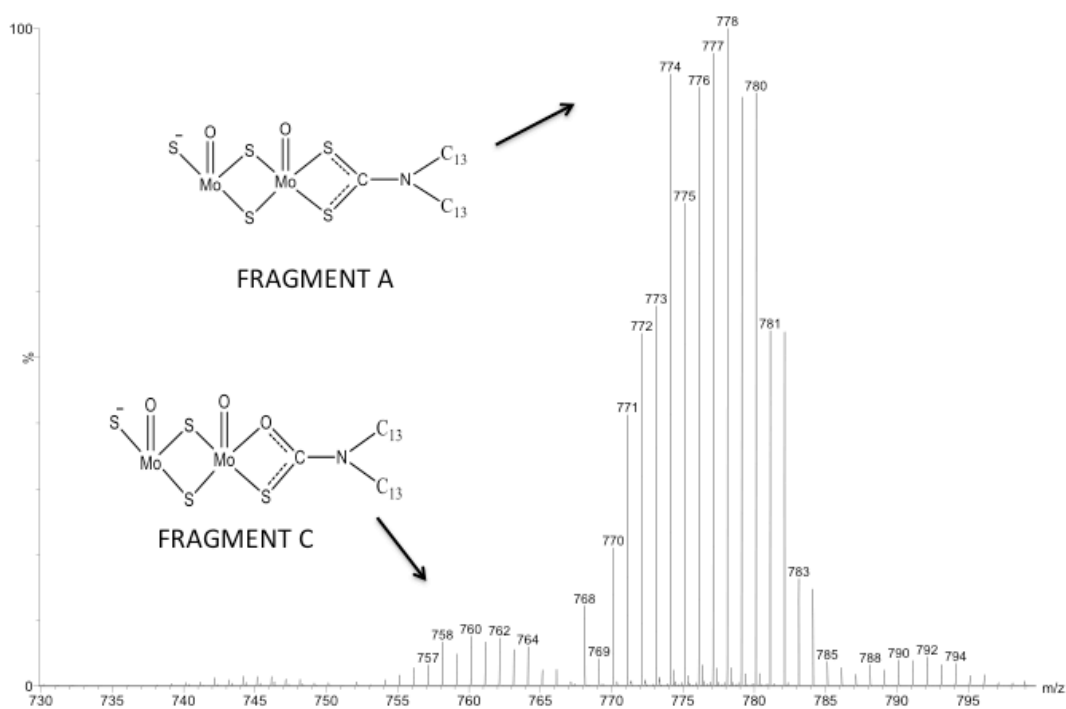
In the same way, the m/z spectrum obtained analyzing the fresh sample under negative ionization conditions showed dominant ions with m/z at 636 and 778, which are consistent with the deprotonated molecular fragment (M-H-) (**Figure 3.7**).



**Fig 3.7.** Mass spectrum obtained for fresh MoDTC-containing base oil in negative ion mode.

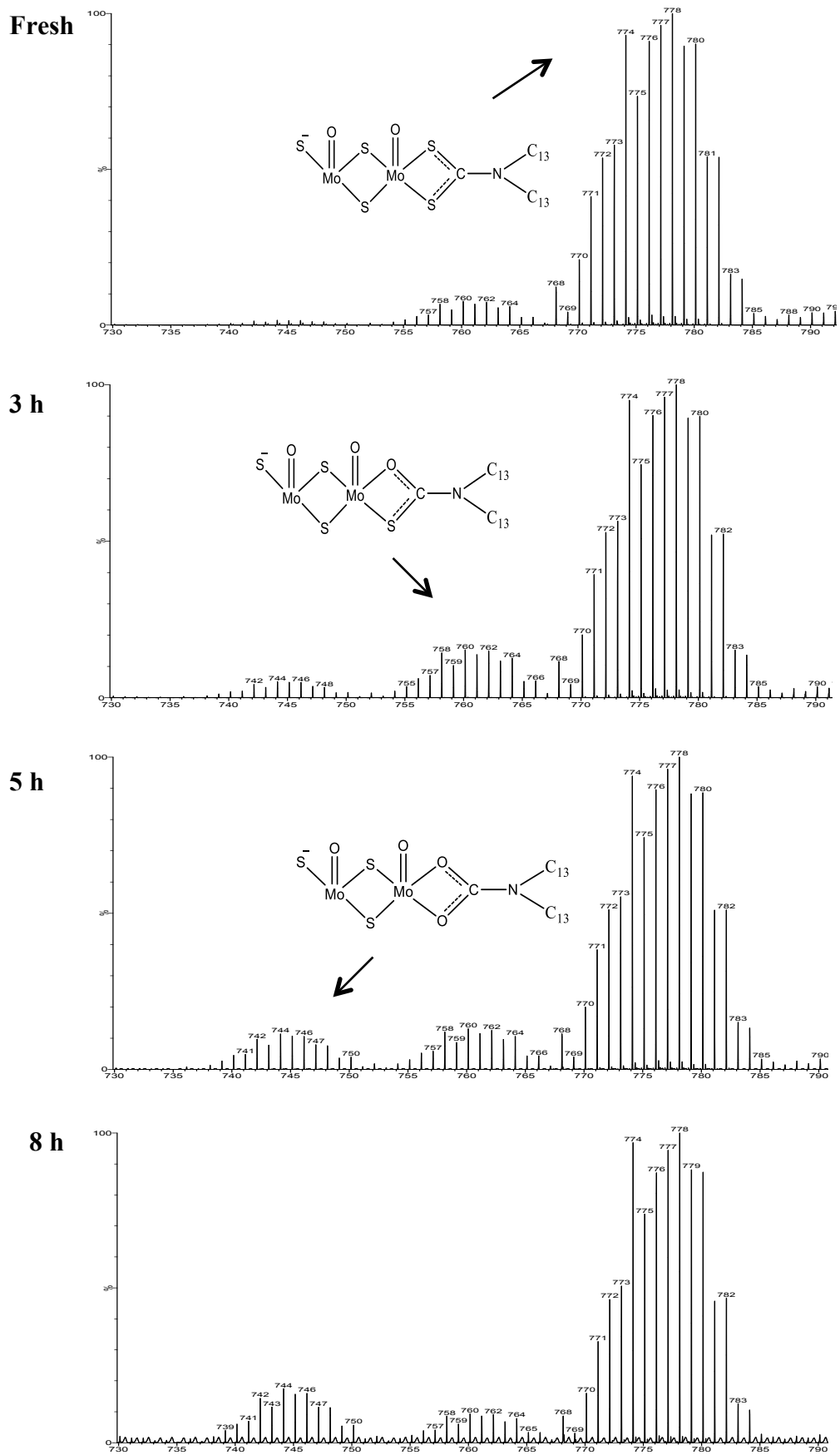


**Figure 3.8** shows the spectrometer for the oil aged for 1 hour. It is interesting to notice that the spectrum relating to both fresh and aged oils contains other ions at  $m/z$  620 and 762, thus 16 Da lower than the characteristic masses of MoDTC (**Figure 3.8**). These lower masses could be identified as the same molecular fragments but having sulfur atom replaced by an oxygen atom.



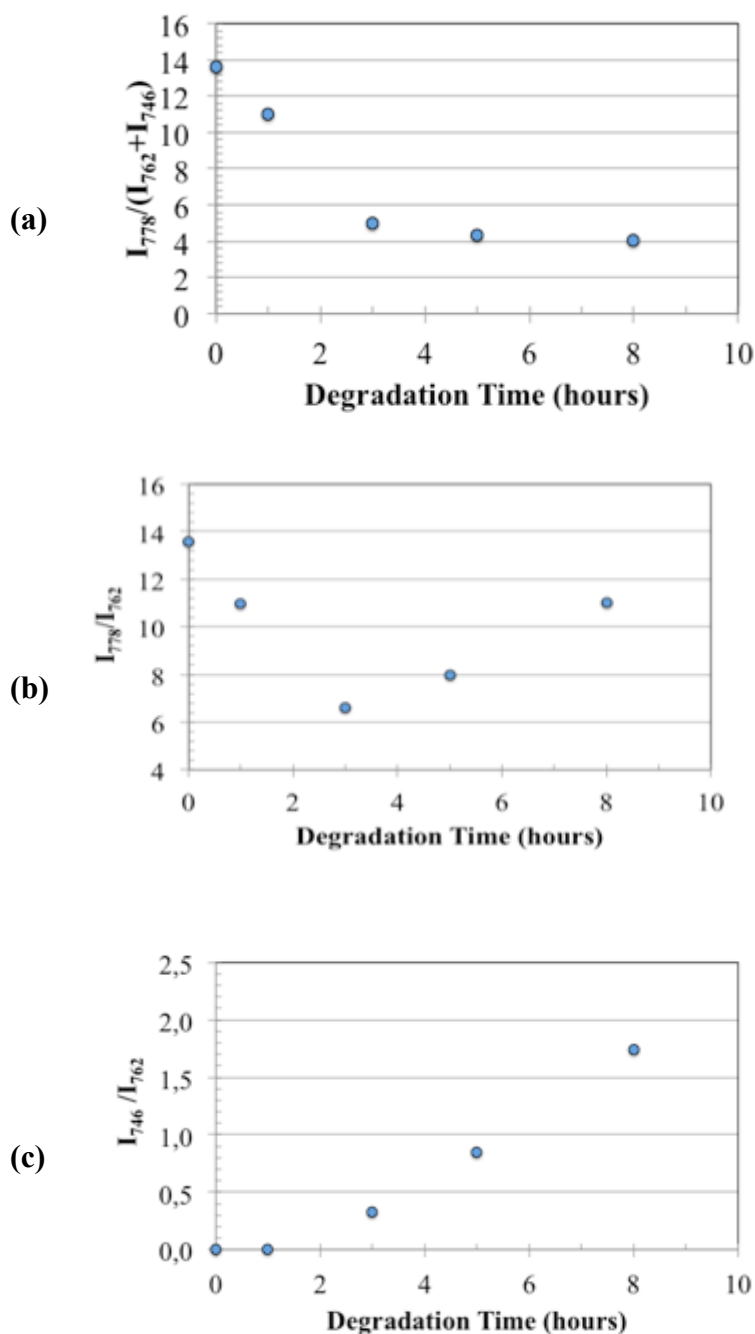
**Fig 3.8.** Mass spectrum obtained for 1h aged MoDTC-containing base oil in negative ion mode.

If the same analysis is extended to the full degradation period (**Figure 3.9**), it can be observed that after approximately 3 ageing hours, an additional reaction product peak appears, having 32 Da difference with the main peak. This trend is common to all the MoDTC fragments.



**Fig 3.9.** Mass spectra obtained for different aged MoDTC-containing base oil in negative ion mode.

To confirm the assumption of the sulfur-oxygen replacement, the relative ratio between the main peak ( $I_{778}$ ) intensity, corresponding to the molecular weight of the starting molecule fragment, and the sum ( $I_{762} + I_{746}$ ) related to the other two reaction products peaks was calculated (**Figure 3.10(a)**).



**Fig 3.10.** Relative ratio between (a) the main peak intensity (778 m/z) and the sum of the two reaction products (762 and 746 m/z); (b) the main peak intensity (778 m/z) and the first reaction product (762 m/z) intensity; (c) the second reaction product (746 m/z) intensity and the first reaction product (762 m/z) intensity.

A marked reduction in the ratio value was obtained during the early ageing hours, confirming that the main fragment (778 m/z) is converting in the first reaction product (762 m/z), considering it is the only new species in the beginning of the degradation process. In other words, the results reported in **Figure 3.10(a)** suggests that when the degradation process starts, there is a decrease in the 778 m/z intensity peak (main fragment) and the intensity of new peak appeared (762 m/z) increases. For higher degradation time, the ratio value reaches a plateau, indicating that changes do not happen anymore in the additive molecule but in the first reaction product, which reacts giving the second reaction product (746 m/z). It appears that having one sulfur atom replaced by an oxygen atom the MoDTC molecule becomes more reactive to substitution by further oxygen compared to MoDTC itself.

The ratios ( $I_{778}/I_{762}$ ) and ( $I_{746}/I_{762}$ ) indicate the same behavior: in the **Figure 3.10(b)** it is possible to see that when the oil starts to degrade, the main fragment (778 m/z) concentration decreases while the first reaction product with 762 m/z as molecular weight increases. Following the same line of reasoning, the first reaction product concentration after few degradation hours reacts giving the second reaction product with 746 m/z as molecular weight and, for this reason, the ratio in **Figure 3.10(b)** increases after 3 hours of degradation. Interpretation of **Figure 3.10(c)** in the same way gives a coherent result: as the oil is degraded the increase of the second reaction product (746 m/z) -which is missing during the first ageing phase, is seen coincides with the decrease of the first reaction product (peak 762 m/z).

### 3.4. Study of MoDTC thermo-oxidative degradation by FTIR

**Figure 3.11(a)** shows the results of analysis of pure MoDTC diluted in base oil. The strong absorption bands seen within the area  $2800-3000\text{ cm}^{-1}$ , corresponding to the comprising of C-H asymmetric stretch and C-H symmetric stretch of  $\text{CH}_2$  and  $\text{CH}_3$  bonds originate from the base oil hydrocarbon structure [9]. These plus the absorbance bands relating to chemical bonds present in the MoDTC molecule are detailed on the graph in the absorption region  $400\text{ cm}^{-1} - 1600\text{ cm}^{-1}$  (**Figure 3.11(b)**).

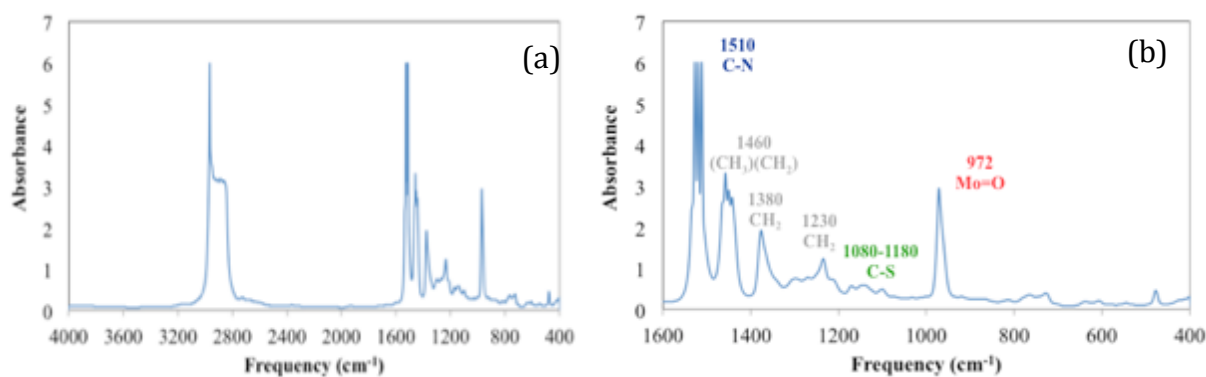


Fig 3.11. FT-IR spectrum of fresh pure MoDTC (a) and zoom in the region 400-1600  $\text{cm}^{-1}$  (b).

The group of absorption bands assigned to the alkane chains lies at 1380  $\text{cm}^{-1}$  and 1460  $\text{cm}^{-1}$ . They originate from  $\text{CH}_3$  umbrella bends,  $\text{CH}_2$  scissors and the CH vibrational modes of short alkanes and a small amount of branched polymeric chains [9].

The two typical absorption bands relating to the MoDTC compound are the one at 1510  $\text{cm}^{-1}$  and at 972  $\text{cm}^{-1}$ . The assignment of these bands has been already discussed in literature. A similar compound to the MoDTC studied in this work has also been analyzed and the contribution at 1523  $\text{cm}^{-1}$  has been attributed to the vibration of a partial CN bond in a CNS conformation [7]. However the same bands have been assigned also to a full C=N double bond [8]. The strong peak present at 972  $\text{cm}^{-1}$  in this work was assigned to Mo=O, referring to previous studies [7]. Subtraction spectra between fresh and aged oils have been calculated and they are plotted in **Figure 3.12**. These have been separated into two parts to better underline the differences between the peaks, a shift in y-direction has also been added for better clarity.

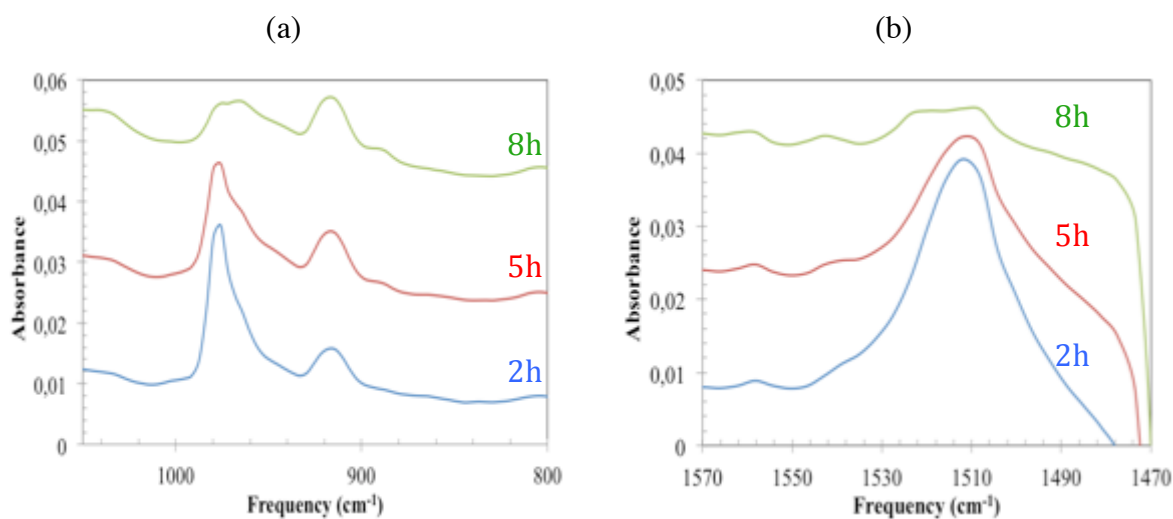


Fig 3.12. The resultant absorbance spectra after subtraction with the fresh oil in the area (800-1040)  $\text{cm}^{-1}$  corresponding to Mo=O bond (a) and in the area (1470-1570)  $\text{cm}^{-1}$  corresponding to C-N bond (b).

In the spectra reported in **Figure 3.12**, a number of different intensity bands are detected. The details of these peaks are reported in the **Table 3.2**, highlighting only the peaks related to MoDTC sample, rather than to the base oil.

Band (cm <sup>-1</sup> )	Contribution	Trend as the degradation time increases
976	Mo=O	Decrease
1510	C-N	Decrease

**Tab. 3.2. FTIR absorption bands related to MoDTC.**

## 4. DISCUSSION

Comprehensive research into the bulk MoDTC-containing lubricant degradation has not yet been undertaken; understanding the MoDTC additive behavior in lubricant base stock when subjected to thermo-oxidative degradation was clearly needed. Chromatographic and spectroscopic techniques were employed to establish the fundamental differences between the fresh and aged oils by monitoring the chemical changes during the degradation process.

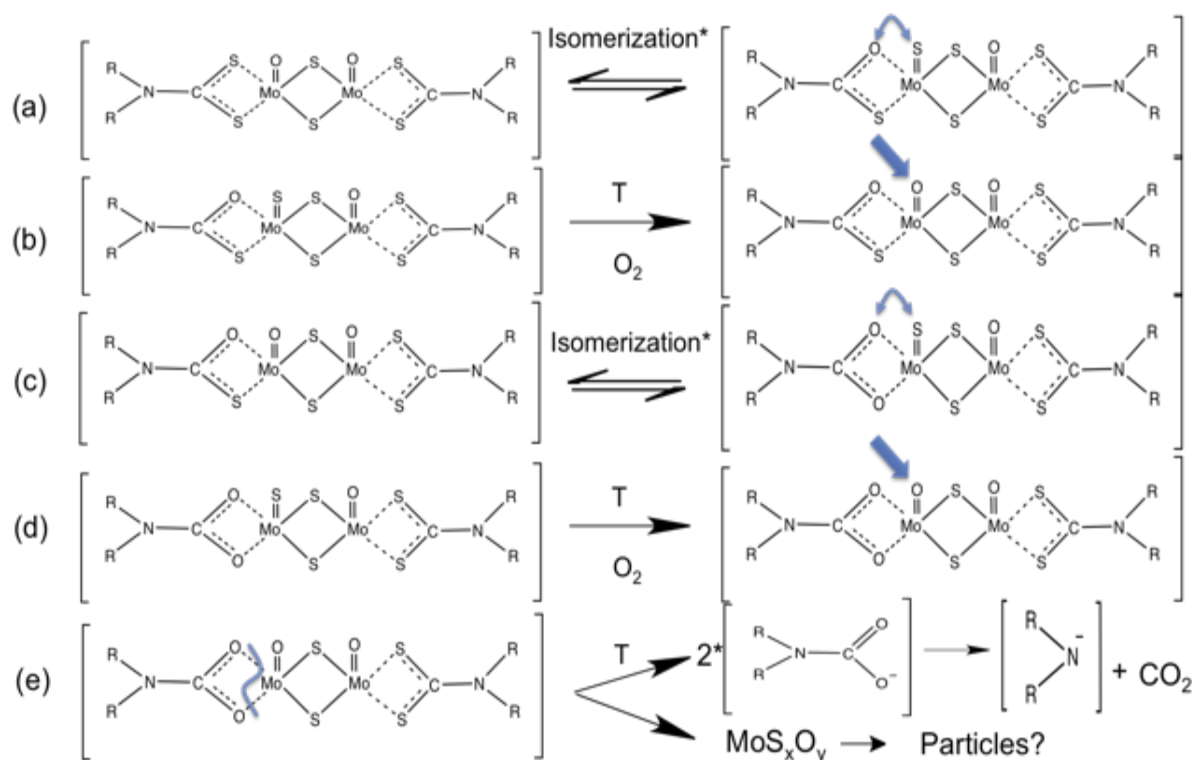
As reported in the previous paragraph, 8 solutions of MoDTC additive in base oil with known concentration were analyzed by means of liquid chromatography.

Considering the amount of MoDTC additive in the fresh sample to be 100% concentration, it has been possible to follow the additive depletion caused by the ageing process. The MoDTC almost completely disappeared from the oil after 8 hours and this result is exactly as anticipated given that no friction reduction was obtained when testing this aged oil.

Previous works showed that the friction reducing property depends on the MoDTC concentration [1]. For this reason as the quantity of MoDTC in the oil is continually decreasing during oxidation (**Figure 3.5**), it was anticipated that the friction coefficient would also linearly increase. This theory is in disagreement with our previous results [12] where it was shown that employing 5 hours aged oil, after an induction time, the friction drops to the same low value obtained for the fresh oil (0.06). This suggests that the reduction in the friction value is not proportional to the MoDTC concentration; there is a minimum critical concentration required for achieving a low friction coefficient.

Using FT-IR technique, it was possible to obtain information about the chemical bonds present in the oil. The thermo-oxidative degradation process was found to impact the C-N and Mo=O peaks, the intensity of these bond peaks decreasing with the degradation time.

Consolidating all the data obtained from the HPLC, MS and FT-IR it is possible to hypothesize the chemical pathway followed by the MoDTC during thermo-oxidative degradation (**Figure 3.13**).



The MoDTC decomposes via a multi-stage reaction pathway:

- firstly an isomerization reaction occurs - a thiol-diolo rearrangement - characterized by the exchange between the sulfur and oxygen positions (a) [10];
- the sulfur atom double bonded to the molybdenum is then replaced by an oxygen atom (b);

- a second isomerization reaction takes place with the sulfur atom changing its position with the oxygen linked to the central molybdenum (c);
- this sequence is then repeated resulting in the second substitution between an oxygen atom and the sulfur (d);
- the last step is the loss of the  $R_2NCO_2$  group producing the amino group  $R_2N$  and carbon dioxide ( $CO_2$ );
- the core of MoDTC molecule ( $Mo_xS_yO_z$ ) becomes incorporated into the solid-like particles formed when the additive decomposes, this precipitates out during the degradation process.

The characterization of these particles and their effect on the tribological properties merits further investigations. Furthermore, if we consider the behavior of the HPLC new peak that appears (**Figure 3.4**) it seems that following the first degradation period during which a new chemical species is produced, there is then a subsequent depletion of this new reaction product and this is in line with our hypothesis. Also, if we assume that this new peak corresponds to the MoDTC molecule with a sulfur atom replaced by an oxygen atom, it is observed that this subsequently converts into another molecule, where a further sulfur atom is substituted by an oxygen atom.

## 5. CONCLUSIONS

The results from the complete characterization studies performed in this chapter have provided a valuable insight into the changes of the MoDTC friction modifier during thermo-oxidative degradation. Quantification of the additive within the samples has been achieved from a calibration curve using HPLC measurement techniques. In addition with the combined FTIR and MS results a hypothesis for the MoDTC thermo-oxidative degradation chemical pathway has now been proposed.

Our analytical results support the theory that the additive depletion is due to a sulfur-oxygen atom substitution, this then leads to the oxidation and finally the breaking up of the MoDTC molecule itself. Furthermore the oxygen-sulfur replacement within a partially oxidized product molecule appears to take place in an easier way than in fresh MoDTC itself. These findings support our theory that the MoDTC friction performance is primarily due to the presence of partially oxidized MoDTC molecules, which remain still able to decrease friction coefficient thanks to the production of molybdenum oxi-sulfides.



## 6. BIBLIOGRAPHY

- [1] Graham J., Spikes H., Korcek S., The friction reducing properties of molybdenum dialkyldithiocarbamate additives: part I - factors influencing friction reduction. *Tribology Transactions*; Volume 44(4), Pages 626–36, (2001).
- [2] Spengler G., and Webber A., On the lubricating performance of organic molybdenum compounds. *Chem. Ber.*, Volume 92, Pages 2163-2171, (1939).
- [3] Grossiord C., Varlot K., Martin J.M., Le Mogne Th., Esnouf C., Inoue K., MoS<sub>2</sub> single sheet lubrication by molybdenum dithiocarbamate. *Tribology International*, Volume 31, Pages 737–43, (1998).
- [4] Kubo K., Mitsuhiro N., Shitamichi T., Motoyama K., The effect of ageing during engine running on the friction reduction performance of oil soluble molybdenum compounds, *Proceeding of the international tribology conference*, Yokohama, (1995).
- [5] De Barros Bouchet M.I., Martin J.M., Le Mogne Th., Bilas P., Vacher B., Yamada Y., Mechanisms of MoS<sub>2</sub> formation by MoDTC in presence of ZnDTP. Effect of oxidative degradation. *Wear*, Volume 258, Pages 1643, (2005).
- [6] Jocelyn Claire Herries Graham PhD thesis, Imperial College (2001).
- [7] Musha K., Ohashi Y., Yamazaki, S., Toda S., and Tanaka S., Structural analysis of dinuclear molybdenum (V) dibutyldithiocarbamate complexes and crystal structure of di- $\mu$ -sulphido-bis(oxodibutyldithiocarbamate) Mmolybdenum (V), *Journal of the Chemical Society of Japan*, Volume 5, Pages 636-658, (1983).
- [8] Moore F.W., and Larson M. L., Dialkyldithiocarbamate Complexes of Molybdenum (V) and Molybdenum (VI), *Inorg. Chem.*, Volume 6, Pages 998-1003, (1967).
- [9] Cronauer D.C., Snyder R.W. and Painter P.C., Characterization of oil shale by FTIR spectroscopy ACS division of Fuel Chemistry Proceedings, Symposium on Processing of Oil Shale Tar Sands and Heavy Oils, Meeting 183, Las Vegas, NV, Volume 27(2), Pages 122-130, (1982).
- [10] Onodera T., Morita Y., Nagumo R., Miura R., Suzuki A., Tsuboi H., Hatakeyama N., Endou A., Takaba H., Dassenoy F., Minfray C., Joly-Pottuz L., Kubo M., Martin J.M., Miyamoto A., A Computational Chemistry Study on Friction of h-MoS<sub>2</sub>. Part I. Mechanism of Single sheet lubrication. *J. Phys. Chem. B*, Volume 113, 15832-8 (2009).
- [11] Carangelo R.M., Solomon P.R. and Gerson D.J., Application of TG-FTIR to study hydrocarbon structure and kinetics, *Fuel*, Volume 66, Pages 960, (1987).

- [12] De Feo M., Minfray C., De Barros Bouchet M.I., Thiebaut B., Le Mogne Th., Vacher B., Martin J.M., Ageing impact on tribological properties of MoDTC-containing base oil, *Tribology International*, Volume 92, Pages 126–135, (2015).

## Chapter 4

---

### Investigation of solid-like particles generated by the ageing degradation: chemical composition, morphological structure and tribological properties.

---

*In this chapter is reported the investigation of the solid-like particles formed during the thermo-oxidative degradation. The particles recuperated by means of centrifugation are physically and chemically characterized using Dynamic Light Scattering (DLS), XPS and TEM. Afterwards, it has been considered their influence on the friction coefficient, using two different tribometers, linear reciprocating ball-on flat tribometer and Mini Traction Machine (MTM), for sliding and rolling/sliding motions.*

*As main results it has been found that the particles are mainly composed of carbon as determined by XPS and TEM/EDX analyses. However, the chemical characterization revealed also the presence of molybdenum, sulfur and oxygen. The key role of these particles in friction reduction has been proved in both sliding and rolling/sliding motion.*

## Chapter 4

---

### Investigation of solid-like particles generated by the ageing degradation: chemical composition, morphological structure and tribological properties.

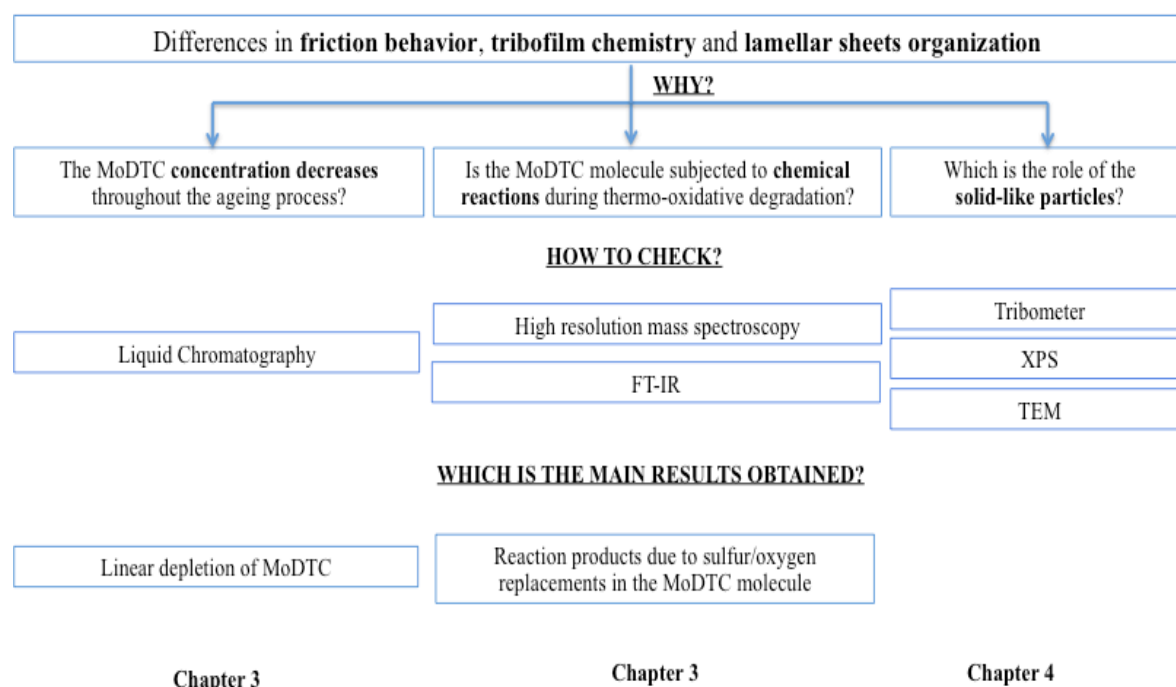
---

*Dans ce chapitre, nous avons rapporté la caractérisation des particules solides formées au cours de la dégradation thermo-oxydative du MoDTC. Les particules récupérées par centrifugation ont été caractérisées physiquement et chimiquement en utilisant la Dynamic Light Scattering (DLS), la spectroscopie de photoelectron (XPS) et la microscopie électronique à transmission (MET). Ensuite, l'influence de ces particules solides contenant du molybdène sur le comportement en frottement a été étudiée, en utilisant deux tribomètres différents : le tribomètre linéaire alternatif bille/plan (glissement pur) et la mini-traction machine (MTM) pour étudier un contact fonctionnant sous roulement et glissement.*

*Il a été montré que les particules sont majoritairement composées de carbone (analyse XPS et MET/EDX). Cependant, la caractérisation chimique a révélé aussi la présence de molybdène, de soufre et d'oxygène. Un rôle clé de ces particules dans la réduction du frottement a été mis en évidence, à la fois dans le cas du glissement pur et dans le cas de roulement/glissement.*

# 1. INTRODUCTION

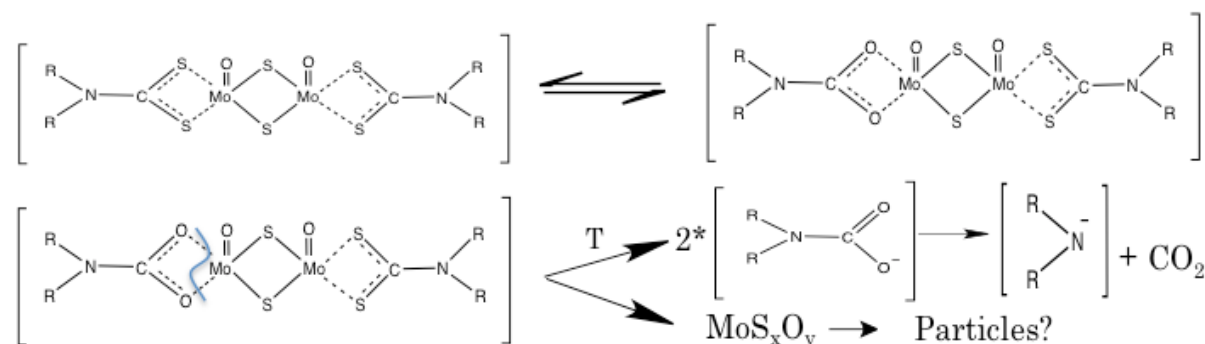
As already underlined in the previous chapters, the degradation process of MoDTC additive blended to base oil leads to the production of black solid-like particles. The chapter 2 reports the main differences in the tribological behavior of fresh and aged MoDTC-containing base oil. It has been shown that the oil subjected to thermo-oxidative degradation process provides different friction performance (after 8 hours it does not reduce friction anymore), different tribofilm chemistry (the presence of two kind of oxi-sulfide species has been supposed) with different MoS<sub>2</sub> lamellar sheets organization. Several hypotheses could be proposed to explain these differences (**Figure 4.1**).



**Fig. 4.1. Summary of the main difference between the results obtained with fresh and aged oil underlined in the chapter 2 and the possible explanations shown in chapter 3.**

As experimentally demonstrated in the chapter 3, the MoDTC is linearly depleted during the thermo-oxidative degradation and is subjected to chemical reactions. The additive depletion and the changes in the chemistry of the molecule could strongly affect the tribological behavior of aged MoDTC-containing base oil. Moreover, in the same chapter, it has been hypothesized that the MoDTC molecule during thermo-oxidation ageing follows a chemical pathway characterized by the replacement of two sulfur atoms by two oxygen atoms. These mechanisms lead to the formation of reaction by-products that may correspond to the core of

the MoDTC molecule, which can be schematized as  $\text{Mo}_x\text{S}_y\text{O}_z$ . However, it has not been detected such species when the bulk oil has been analyzed by means of mass spectroscopy technique (**Figure 4.2**).



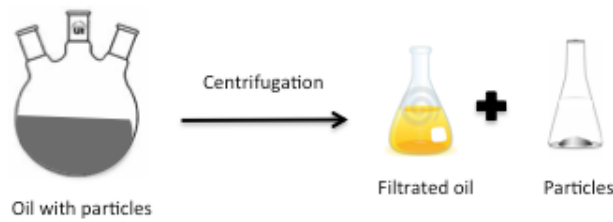
**Fig. 4.2.** Chemical pathway followed by MoDTC molecule during thermo-oxidative degradation hypothesized in chapter 3.

In this chapter, special attention has been paid to the study of the non-soluble solid particles to validate the hypothesis done on the reactions occurring when MoDTC is subjected to thermo-oxidative degradation. At the same time, it will be investigate the impact of these particles on the tribological behavior.

## 2. METHODS

### 2.1. Particles extraction

To extract the solid particles from the oil (**Figure 4.3**) it has been used the centrifugation technique. The oil sample is spun for approximately 30 minutes in a test tube at 3000 rpm causing the particles deposition on the bottom of the tube. After a carefully separation of particles from the centrifuged oil, a second centrifugation is done using pure *n-heptane* solvent in order to clean these particles from possible rest of oil. All the experiments presented in this chapter are carried out on the particles collected from the oil aged for 8 hours. Similar results have been obtained also investigating the particles recuperated from the oil aged for 2 and 5 hours. It has been seen, in fact, that they had same chemical composition and same morphology. The only thing that changed during degradation time is the amount of particles in the sample.



**Fig. 4.3. Particles extraction from the degraded oil done by means of centrifugation.**

## 2.2. Particles size

The granulometric analyses were performed by Dynamic Light Scattering (DLS) using Zeta Sizer, which allowed to measure both the size and the size dispersity of the particles. Using a DLS principle, the Brownian motions are related to the particles size by illuminating them with a laser and analyzing the intensity fluctuations in the scattered light.

## 2.3. Chemical and morphological analyses (XPS and TEM)

Because DLS technique evaluates the particle's hydrodynamic diameter, this measurement may be strongly influenced by particles agglomeration [1]. The ability to image the particles agglomeration means of TEM analyses have been used to assess if the observed particle's hydrodynamic diameter could be affected by changes in agglomeration state and to evaluate the particle's dimensions. Moreover, to get information about chemical composition of the particles, X-ray photoelectron spectroscopy (XPS) and TEM/EDX analyses were employed. Samples are prepared for TEM imaging by drying the particles on a copper grid that is coated with a thin carbon layer.

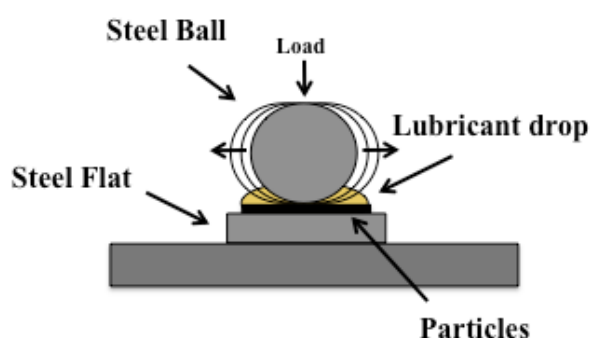
## 2.4. Tribometry study

The aim of tribological experiments is to investigate how the presence of the solid particles affects the MoDTC performance in two types of contact, linear sliding and sliding/rolling. In both cases, repeated tests carried out following the protocol described in the following paragraphs, showed an overall good repeatability.

### 2.4.1. Linear reciprocating tribometer

In the tribometer used in the previous chapters, the steel plate was fixed into a stationary oil bath, which keeps the sample fully immersed into the lubricant during the whole experiment. Considering that all the tribological experiments are carried out at 100°C and that the system

takes approximately 30 minutes to reach the set temperature, during this period all the particles are susceptible of sedimentation on the bottom of the sample holder, preventing the particles to stay in the contact during the test. For this reason, using this configuration, weak reproducibility of the results has been obtained. Hence, in order to investigate the real role of the solid-like particles, the tribometer chosen among all the homemade tribometers available at ECL is the one that needs only a drop of lubricant in the contact (**Figure 4.4**) using a small ball (radius = 3 mm). In this way the problem of particles sedimentation has been reduced and it is much more probable to have these particles into the contact. The tribometer configuration is described in more detail in **ANNEX B**.



**Fig. 4.4.** Scheme of the reciprocating tribometer used for the study on the tribological behavior of solid particles obtained during MoDTC ageing process.

The main parameters set for these experiments are listed in **Table 4.1**.

Parameter	Value
Ball properties	AISI 52100 steel; D = 6 mm
Load	2 N
Maximum Hertzian Pressure	800 MPa
Speed	5 mm/s
Test duration	1 hours
Temperature	100°C

**Tab. 4.1.** Main parameters set for the tribological experiments carried out with the reciprocating tribometer.



## 2.4.2. MTM

### Tribological experiment methodology

To avoid the running in effect on the MoDTC-containing lubricant performance, a film-forming rolling-sliding test at constant speed was first carried out, followed by a slide to roll test. The 2 steps procedure carried out are described in the following:

- **Step 1 (tribofilm formation):** 180 minutes test under linear rolling-sliding (mean entrainment speed = 50 mm/s and SRR = 5%) at 100°C with a normal load of 18 N. During each test, the ball is loaded several times against the layer-coated window in order to capture the image to estimate the tribofilm thickness. The MTM employed for the experiments was equipped with a space layer imaging method (SLIM), which allows (*in situ*) to monitor the tribofilm formation on the steel ball and to evaluate its thickness.
- **Step 2 (measurement of Stribeck curves):** The friction coefficient is measured as a function of mean velocity. During each test the friction coefficient was recorded adjusting the rotational speed of the ball and disc in order to have the mean velocity changing from 10 mm/s to 3000 mm/s in 100 steps and the SRR equal to 5%. To protect the tribofilm formed during the step 1 from possible damages occurring when the asperities of the surfaces are in a shearing contact, it has been decided to set the acquisition of the Stribeck curves starting from the highest speed (3000 mm/s) going till the lowest (10 mm/s).

The friction measurements were performed using fixed parameter chosen because representing of typical values in bearing applications [2]. The ball and disk samples were made of AISI 52100 steel, finished to 0.01  $\mu\text{m}$  Ra, with 800-920 Hv and 720-780 Hv hardness, respectively. The diameters of the ball and the disk were 18 mm and 46 mm respectively. To investigate the difference in lubricant behavior at different speeds, the coefficient of friction versus the mean velocity plots were obtained. The disk and the ball are independently driven allowing to set 5% SRR. The conditions of testing are summarized in the **Table 4.2**.

Parameter	Value
Ball properties	AISI 52100 steel; D=19 mm; $R_a < 0.01 \mu\text{m}$
Disc properties	AISI 52100 steel; D=46 mm; $R_a < 0.01 \mu\text{m}$
Speed for step 1	50 mm/s
Entrainment speed for step 2	From 3000 mm/s to 10 mm/s
Load (Contact Pressure)	18 N (800 MPa)
SRR	5%
Temperature	100°C

Tab. 4.2. Main parameters set for the MTM experiments

These experiments have been carried out at **SKF research center (Netherlands)** and at **Ljubljana University**.

### 3. RESULTS

#### 3.1. Visual inspection

The degradation process has a marked effect on the resulting clarity and color of the oil. The formation of insoluble particles, in fact, sharply darkens the samples. After centrifuging the samples, it was possible to separate most of these black particles and the oil color changes were even more evident (**Figure 4.5**).

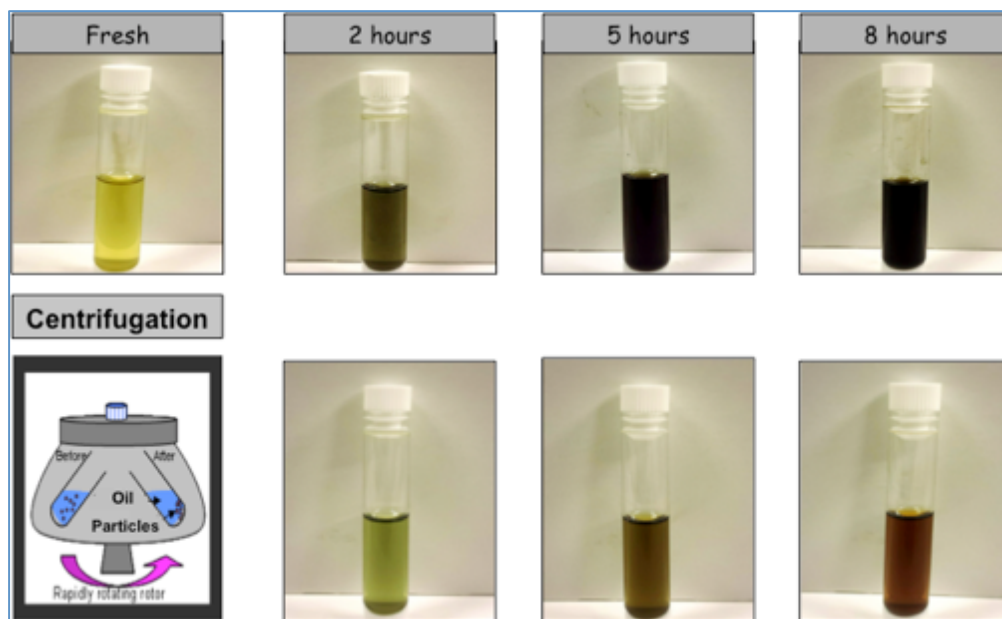
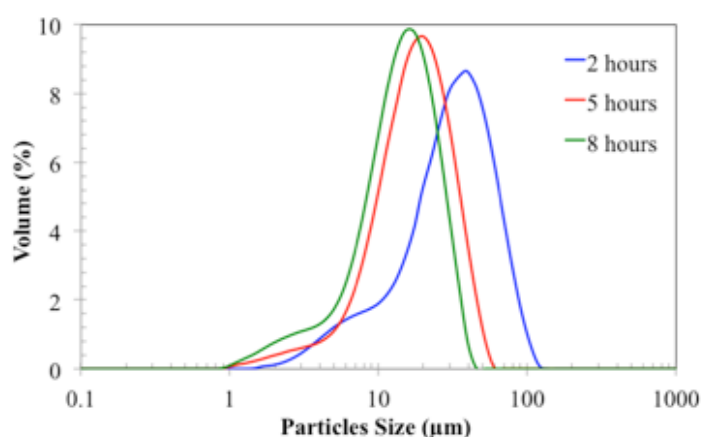


Fig 4.5. Visual inspection of mixture base oil plus 1% wt of MoDTC at different oxidation time before and after centrifugation.

### 3.2. Particles size

The size of the particles was examined by DLS. Prior the test, the samples containing the particles were placed into ultra-sonic water bath for ca. 30 minutes, in order to disrupt aggregates and to facilitate their dispersion. DLS measurements (**Figure 4.6**) on the particles recuperated after 2 hours degradation revealed a scattered-light intensity average particle of 37  $\mu\text{m}$ . Surprisingly, the diameter of particles produced during longer degradation periods decreased, becoming approximately 20  $\mu\text{m}$  smaller. In fact, the average diameter for the particles collected for the oil degraded for 5 hours is ca. 20  $\mu\text{m}$ , while those after 8 hours degradation test decreased to approximately 15  $\mu\text{m}$ . The distributions of particle diameters are approximately Gaussian for the three different particles analyzed.

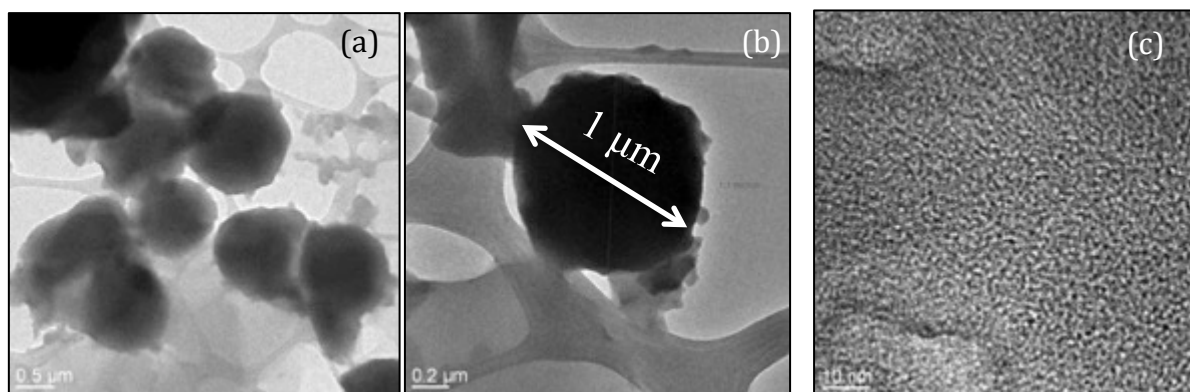


**Fig. 4.6.** DLS distribution for the particles collected from the aged oils. The oil samples were submitted to 30 minutes of ultra-sonic bath.

### 3.3. TEM Characterization

In order to study the particles dispersion state, TEM observations have been carried out. **Figure 4.7** shows a series of TEM images of particles collected from the aged oil. As mentioned before, the only findings shown in this chapter are those related to the oil aged for 8 hours. Indeed, apart from the particles number, any big difference was observed in their size or chemical composition considering the other degradation times.

The oil sample has been submitted to sonication for approximately 30 minutes before the deposition on the carbon grid. Nevertheless, the spherical amorphous particles are highly agglomerated, with a size of about 1 micron.



**Fig. 4.7.** TEM images showing the particles (8 hours aged oil) agglomeration (a); a single particle (b); High-Resolution image showing the amorphous state of the particles (c).

Elemental composition of these particles was also evaluated by EDX analysis (**Table 4.3**).

Element	at (%)
C	77.2
O	14.2
S	4.1
Mo	4.5

**Tab. 4.3.** TEM/EDX elemental quantification for the particles collected from the 8 hours degraded oil.

### 3.4. XPS Analysis

The core levels of molybdenum (Mo3d), oxygen (O1s) and sulfur (S1s) elements detected on the extreme surface of the particles produced after 8 hours are depicted in **Figure 4.8**. The photo-peak corresponding to molybdenum compound clearly shows two contributions. The blue peak at 231.4 eV suggests the presence of molybdenum oxy-sulfide species ( $\text{MoS}_{2-x}\text{O}_x$ ) onto the particles, while the peak at 232.9 eV can be attributed to molybdenum oxide ( $\text{MoO}_3$ ). Coherent results are obtained with the fitting of oxygen and sulfur photo-peaks, showing sulfate and oxi-sulfide contributions.

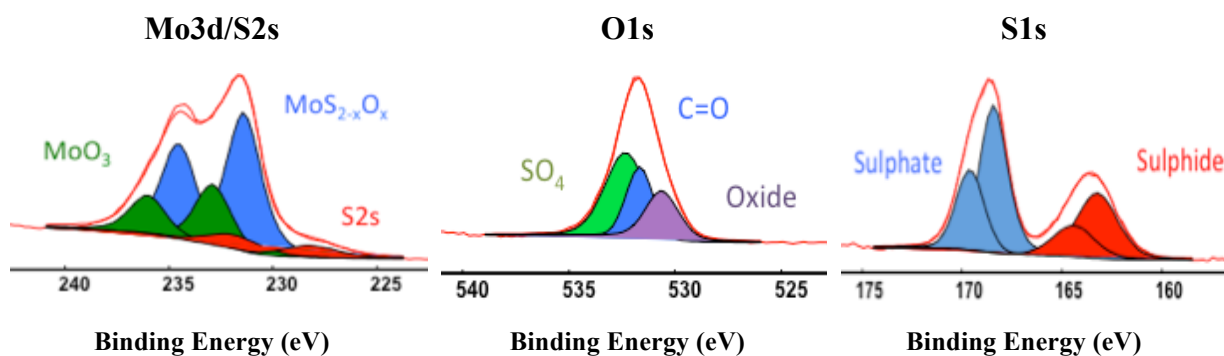


Fig. 4.8. Mo3d/S2s, O1s and S1s XPS photo-peaks of particles collected from the oil aged for 8 hours

Table 4.4 reports the atomic concentration obtained from the spectra, coherent to the hypothetical fits done.

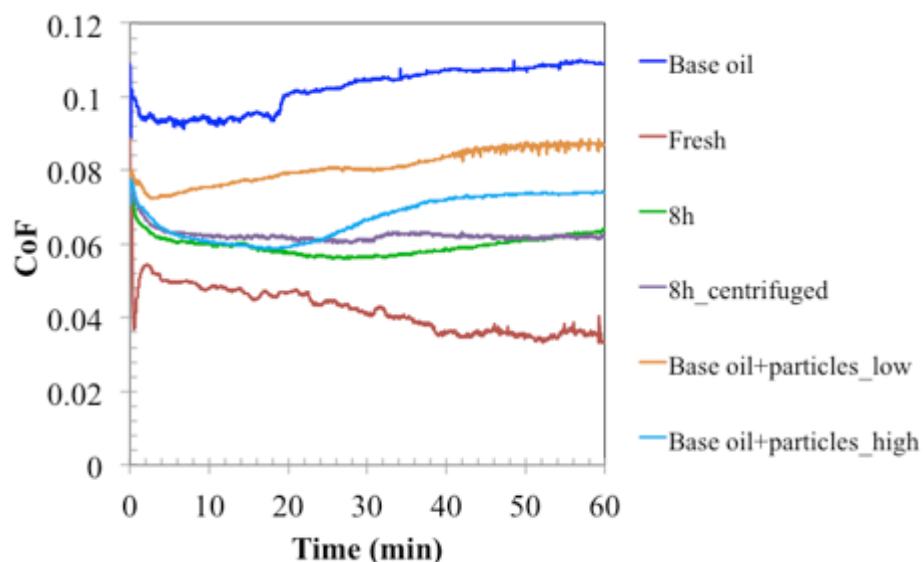
	Binding Energy (eV)	FWHM	Species	at (%)
Mo	231,4	2	$\text{MoS}_{2-x}\text{O}_x$	7,4
	232,9	2	Mo-oxide	3,1
S	163,2	2,4	Oxi-Sulfide	5,5
	168,4	1,7	Sulfate	9,1
O	530,6	1,9	Oxide	18,5
	531,7	1,5	$\text{C=O}$	19,7
	532,3	2,3	$(\text{SO}_4)^{2-}$	36,7

Tab. 4.4. Atomic composition for the top surface of the particles produced during thermo-oxidative degradation (8 hours of ageing).

## 3.5. Tribological results

### 3.5.1. Linear reciprocating Tribometer

In **Figure 4.9** is reported the friction coefficient in function of test time obtained employing different lubricants.



**Fig. 4.9.** Friction curves recorded using aged oils with and without particles. The tribometer employed facilitates the particles to be in the contact during the tribo-test carried out for 1 hour at 100°C and using a load of 8 N.

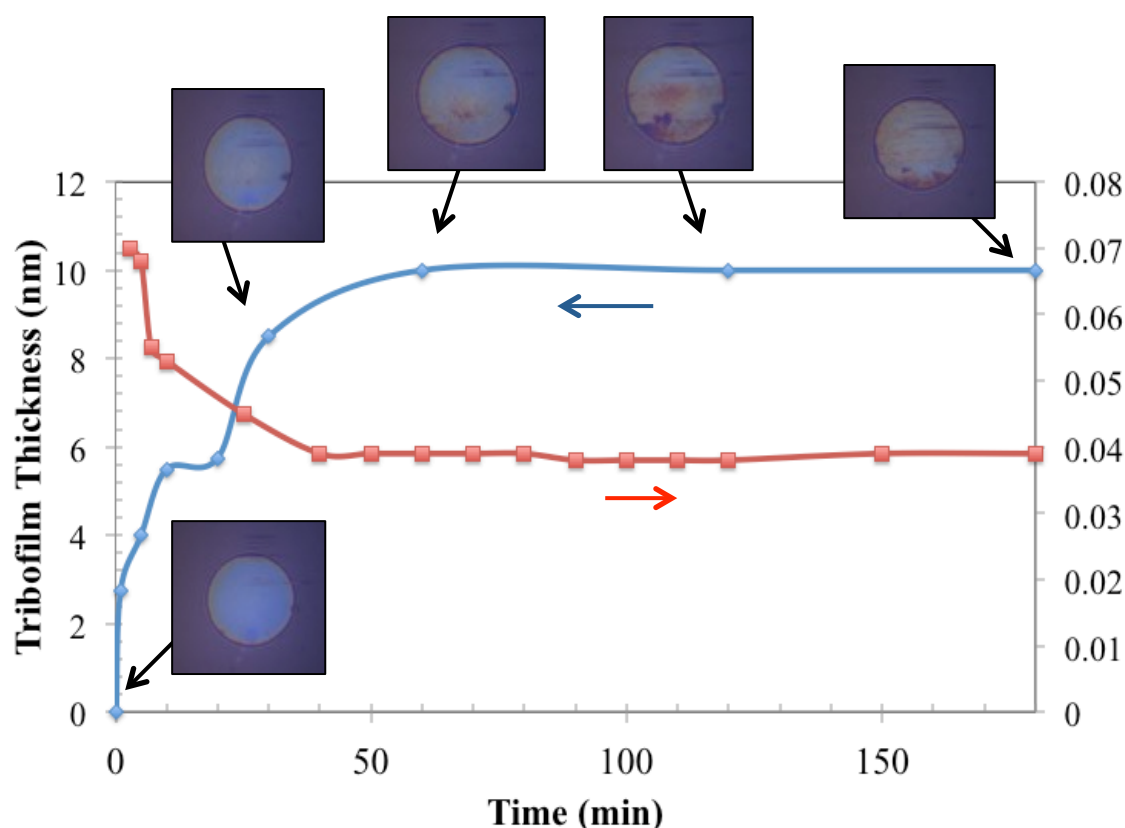
Also with this tribometer, it is clear that adding 1% in weight of MoDTC in base oil allow to obtain lower friction values. Moreover, it is possible to observe that when the oil is degraded for 8 hours, the reduction in friction is less important but still quite substantial. The reduction in friction seems to be the same also for the oil without particles (8h\_centrifuged). However, it needs to take into account that the centrifugation may not be good enough to remove all the solid-like particles. In fact, it has been noted that, after few months, at the bottom of the flask containing the centrifuged sample, there was a thick layer of precipitated particles. However, the effect of particles on friction reduction is clear when they are blended directly to additive-free base oil. In fact, when the concentration of particles added to the base oil corresponds to the one of the oil aged for 8 hours (the quantity of base oil added is the same as the quantity removed by centrifugation) a relatively good reduction in friction is obtained (Base oil+particles\_low orange curve in **Figure 4.9**). Moreover, if the concentration of particles is increased (the quantity of base oil added is much less of the oil removed), the reduction in friction results to be the same as for the oil without centrifugation

(0.06) till half experiment, before showing slight increase at the end (Base oil+particles\_ high light blue curve in **Figure 4.9**).

### 3.5.2. MTM Results

#### Step 1 (Tribofilm formation)

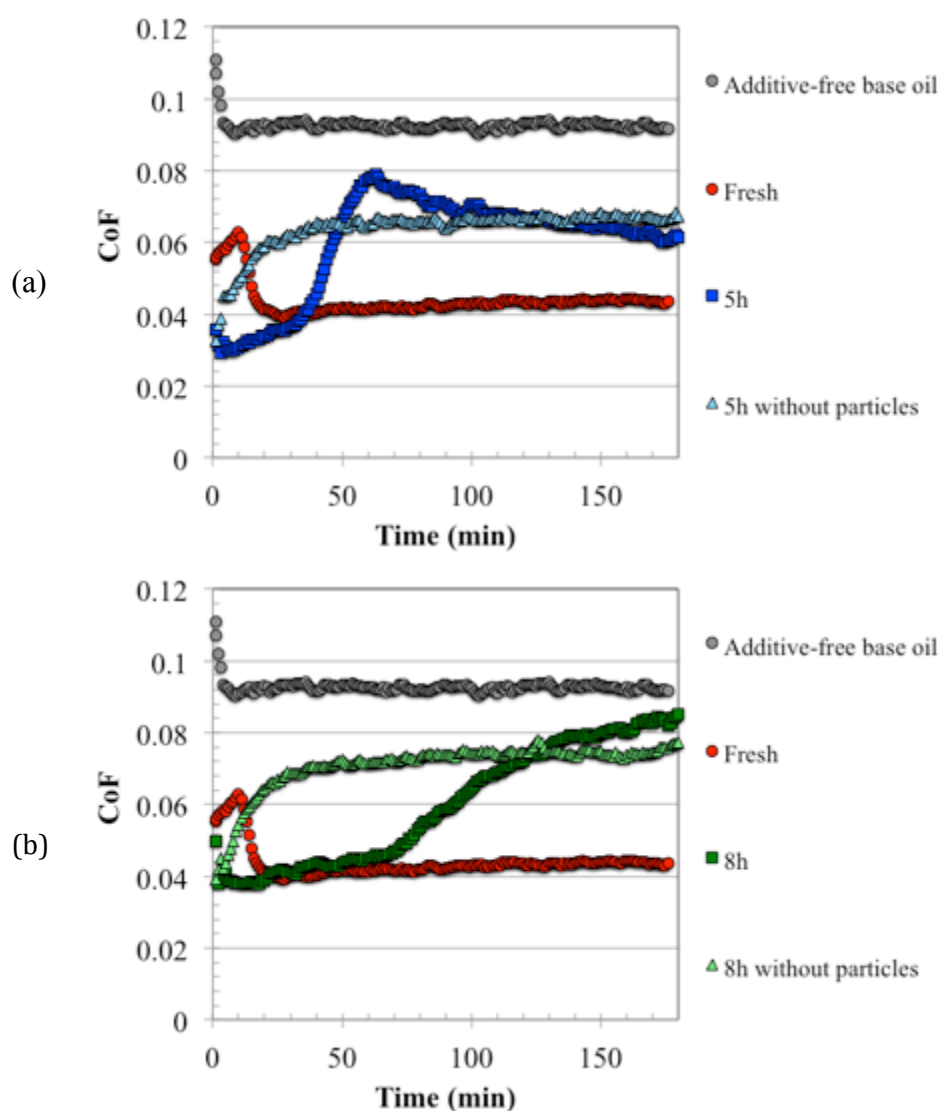
**Figure 4.10** plots the friction coefficient versus test time during the tribofilm-forming step for the fresh solution of 1% wt MoDTC in mineral oil (red curve).



**Fig. 4.10.** Friction behavior and tribofilm thickness for fresh MoDTC-containing base oil during the tribofilm formation (first step). The test is carried out for 180 minutes test under linear rolling-sliding with a speed = 50 mm/s and SRR = 5%, at 100°C with a load of 18 N.

The results show that, in the test conditions adopted, the addition of MoDTC additive leads to considerable friction-reduction. Images insert in the **Figure 4.10** displays a series of *in-situ* optical interferometry micrographs, showing the build-up process of the tribofilm on the steel counterpart. Tribofilm thickness values obtained from these images are reported in **Figure 4.10** (blue curve). The stabilization of friction response using fresh MoDTC-containing oil was achieved after 30 minutes of testing and the friction coefficient was around 0.04 although the tribofilm thickness was only 10 nm thick. **Figure 4.11** displays the

comparison between the friction values recorded during the first phase of MTM test for the fresh and aged oil, for 5 and 8 hours respectively. In both Figures, it is possible to note that the presence of particles in the contact (oil not centrifuged) leads to a better friction reduction during the first test hour. In fact, considering the oil aged for 5 hours (**Figure 4.11(a)**), for example, during the first 40 minutes experiment, even better value than fresh oil is obtained (0.04). Afterwards, a gradual increase of friction till reaching ca. 0.07 is obtained. This behavior, obtained also with the oil aged for 8 hours (**Figure 4.11(b)**), might be caused by the escape of the particles from the contact.

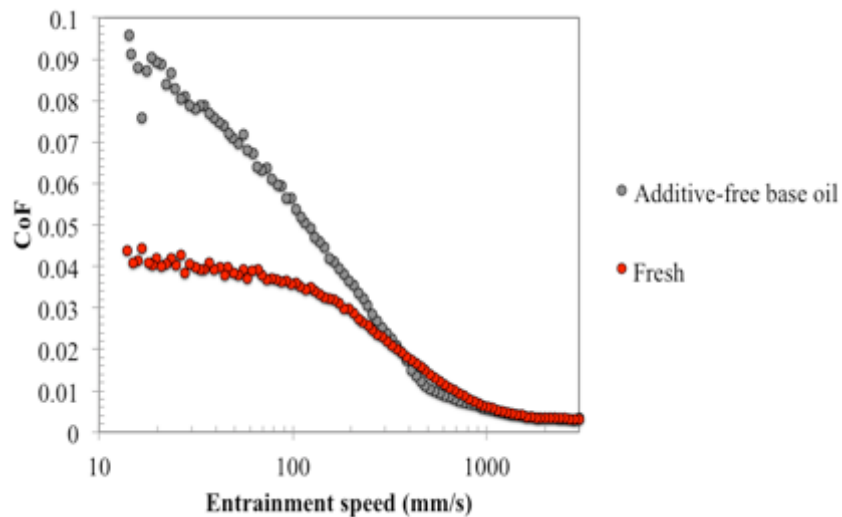


**Fig. 4.11. Friction curves for the oil aged for 5 (a) and 8 (b) hours with and without particles during the trobofilm formation (step 1). Tests carried out using MTM tribometer.**



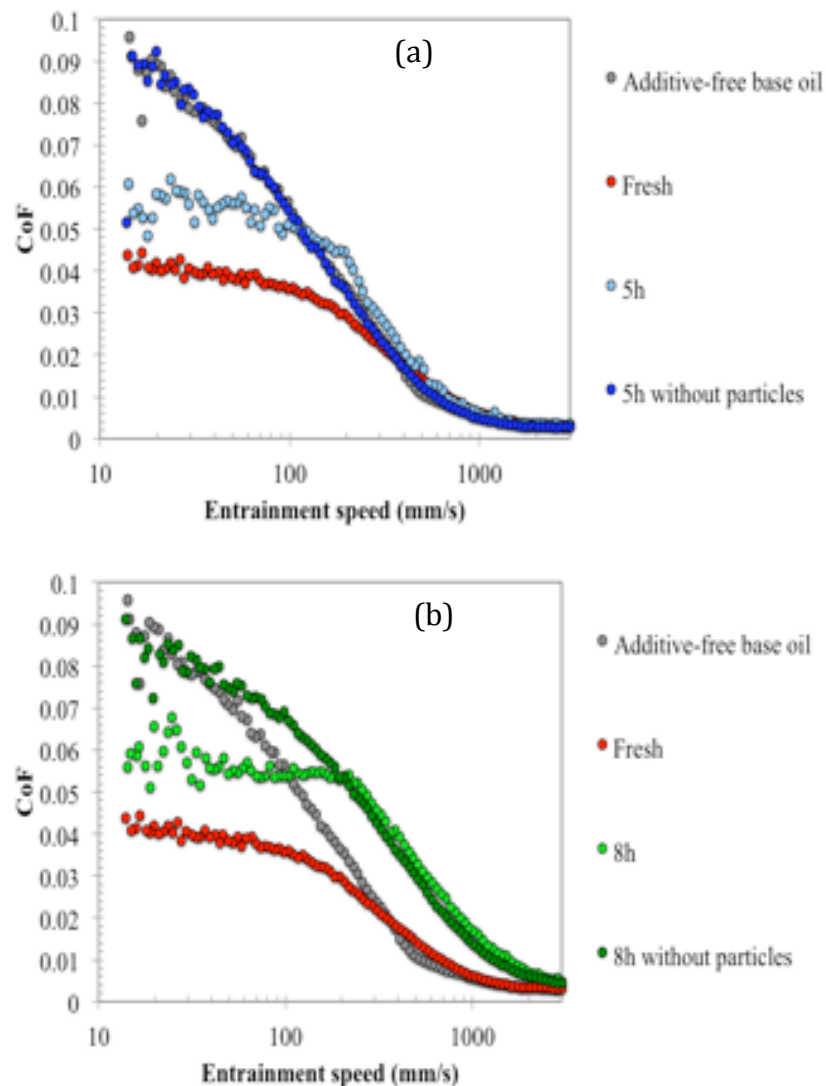
## Step 2 (Stribeck curve)

The comparison between the Stribeck curves obtained for additive-free base oil and for fresh MoDTC-containing oil is shown in **Figure 4.12**. The results indicate that at low speed (from 10 to 300 mm/s), using the working conditions employed, a relative important reduction in friction coefficient (CoF) is obtained in the presence of MoDTC. At speeds above 300 mm/s, a mixed/elasto-hydrodynamic film is formed between the two rubbing surfaces and no difference in friction is noted because essentially controlled by the rheological properties of the mineral base oil. Surprisingly, in this case, the friction values obtained are really low. However, considering that it has been obtained always the same value at high speed, only the trend of the curves will be considered and comparisons between values will be done with extremely attention.



**Fig.4.12.** Stribeck curves obtained with base oil and fresh MoDTC-containing oil (step 2). Tests carried out using MTM tribometer with SRR=5%.

In **Figures 4.13**, the curves obtained testing aged oils, 5 and 8 hours, are compared to the friction coefficient recorded using oil without solid particles.



**Fig. 4.13.** Stribeck curves obtained with aged oils, with and without particles (Step 2) after 5 hours (a) and 8 hours (b) of degradation process. Tests carried out using MTM tribometer.

These Stribeck curves show a similar pattern throughout the test: for both, 5 hours and 8 hours degraded oil, the oil sample (containing the MoDTC additive left, the reaction products and the particles) seems to be still active and it lowers the friction coefficient in the boundary lubrication zone. In fact, there is an almost constant friction coefficient in the low speed region, followed by a sharp and constant decrease all the way into the mixed regime. Also in this case, for speed in the range of 300 mm/s and 3000 mm/s, the presence of MoDTC does not influence the friction coefficient value, resulting similar to that obtained with additive-free base oil. The relevant aspect is that, when the test is carried out with the

centrifuged oils, in both cases, no friction reduction is obtained. These findings suggest that, although the particles are not able to reduce the friction coefficient at the same value of fresh MoDTC-containing base oil, they could clearly act as solid friction modifiers. It seems, in fact, that the reduction obtained should be generated by the particles and not because of the MoDTC left in the base oil.

## 4. DISCUSSION

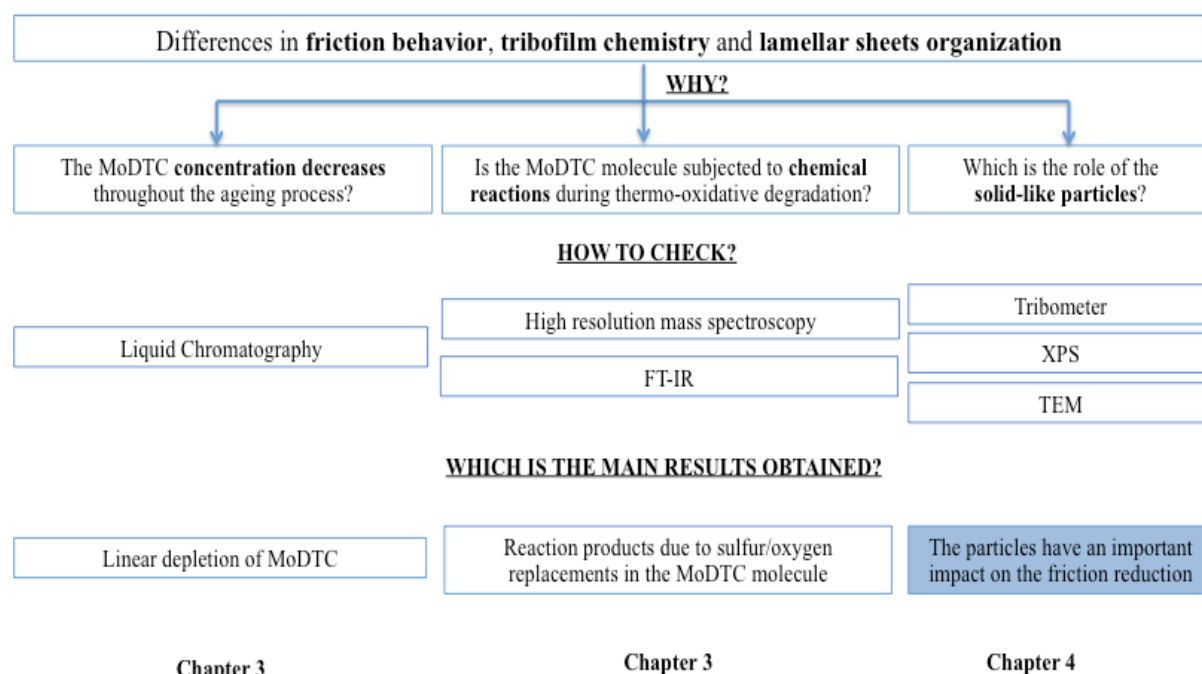
To further elucidate the reactions happening during the simulated degradation process hypothesized in the chapter 3, the attention has been focused on the investigation of the solid-like particles formed during the ageing.

After recuperation of the particles from the aged oils by centrifugation, DLS analysis has been conducted in order to estimate their size. It is possible to suppose that the values measured with this technique referred to the agglomeration dimensions and not to the single particle. It has been evaluated that the oil degradation after 2 hours yielded an agglomerated formation of approximately 37  $\mu\text{m}$  as nominal diameter. The agglomerated size seems to decrease with the increases of degradation time. In fact, the agglomerated obtained after 5 hours and 8 hours appear smaller having a nominal diameter of 20 and 15 respectively. For this reason, further morphological characterizations have been carried out by means of TEM. Moreover, also in this case, the particles inspection resulted to be complicated largely because of this agglomerated formation. However, putting the samples in an ultrasonic bath for 30 minutes, it has been possible to detect the basic units of some nearly spherical particles with diameters often in the range of 1 micron. Of great interest the TEM/EDX results, which revealed the presence of molybdenum, oxygen and sulfur elements in a carbonaceous matrix. XPS technique has been employed to obtain more information about the chemical characterization of the top surface of those particles. The photo-peaks clearly showed the presence of  $\text{Mo}_x\text{S}_y\text{O}_z$  species confirming the EDX analysis. It can be assumed that the chemical pathway supposed in the previous chapter is validated and the core of the MoDTC molecule can precipitate into carbonaceous matrix forming the solid suspension through the degradation process.

Based on the results obtained using these characterization techniques, it has been decided to give special emphasis to determine if these degradation products could be seen as “lubricant particles”. This was achieved by investigating their effect on the tribological properties in both, pure sliding and sliding/rolling configurations. The tribological experiments carried

out with the linear tribometer revealed the importance of the solid-like particles in friction reduction. The most evident results have been obtained blending these particles to additive-free base oil and obtaining a substantial reduction in friction. Similar results are achieved with the MTM tribometer. Also in sliding/rolling motion (Step 1, tribofilm formation) an important reduction in friction has been recorded in the boundary lubrication zone when aged oils were tested while, using centrifuged samples, similar values to additive-free base oil were recorded.

The findings summarized in this chapter allow to conclude that the reduction in friction obtained when degraded oil is employed, could be considered as a combination of different factors (**Figures 4.14**).



**Fig. 4.14.** Summary of the main difference between the results obtained with fresh and aged oil underlined in the chapter 2 and the possible explanations shown in chapter 3 and the principal conclusion obtained from the chapter 4.

Considering that in the previous chapter it has been underlined that the MoDTC additive is depleted through the degradation process and some reactions products are formed during the chemical path-way proposed, it is clear that the friction coefficient is lowered thanks to the action of the additive left into the oil and that the reaction products could play an important role in the reduction in friction. However, at the same time, the influence of the solid-like particles produced through the degradation process cannot be overlooked. In this chapter, in fact, it has been demonstrated that, depending on the contact type, the particles are able to

act as “solid lubricant”, showing marked friction reduction ability (although not as good as fresh MoDTC blend or MoS<sub>2</sub> nanoparticles tested in other conditions [2,3]).

The contribution of these particles to the overall friction behavior should be relativized for many reasons:

- they are not able to reach friction coefficient as low as MoDTC containing base oil;
- due to their tendency to form agglomerations, it could be difficult to have them into the contact;
- we should be careful comparing the influence of these particles on the tribological behavior and the results shown in the chapter 2. In fact, as already previously underlined, the configuration of the two tribometers employed could strongly influence the friction values. The smaller ball counter part and the use of only one single drop of sample allow the particles to enter into the contact in a much easier way than the situation with the tribometer used in the previous chapter (ANNEXE A). The important aspect of these results is mainly the trend of the curves and not the exact friction values.

Based on these results it could be of great interest the investigation of binary combinations using ZDDP, antioxidant and dispersant. These additives could strongly influence the MoDTC depletion, the chemical reactions happening during the degradation process and the particle formation. For this reason, the chapter 6 will be focused on the study of binary combinations of these additives.

## 5. CONCLUSIONS

In this chapter, special emphasis is given to the characterization of the solid particles produced during the degradation process and their effect on friction reducing properties of MoDTC has been investigated.

- The solid-like particles have been characterized by means of X-ray photoelectron spectroscopy (XPS) and Transmission electron microscopy (TEM) and both of the techniques shown that the lubricant degradation process causes the formation of solid-like particles made of molybdenum sulfur and oxygen in a carbon matrix.
- The particles seems to positively influence the friction reduction in both sliding and rolling/sliding motion.
- The reduction in friction obtained when aged oils are tested seems to be the consequence of different aspects: first of all, the influence of MoDTC reaction

products formed during the degradation process and the consequent concentration of MoDTC additive left in the sample (aspects investigated in the chapter 3) and, at the same time, the solid-like formation which could definitely have an important role in the friction reduction (**Figure 4.14**).

To obtain more information about the role of the solid particle in the friction reduction, further surface analyses (XPS and FIB/TEM) are needed.

## **6. BIBLIOGRAPHY**

- [1] Murdock R.C., Braydich-Stolle L., Schrand A.M., Schlager J.J., Hussain S.M., Characterization of nanomaterial dispersion in solution prior to in vitro exposure using dynamic light scattering technique, *Toxicol Sci*, Volume 101, Pages 239-53, (2008).
- [2] Meheux M., Minfray C., Ville F., Le Mogne Th., Lubrecht A., Martin J.M., Lieurade H.P., Influence of slide-to-roll ratio on tribofilm generation, *Proceedings Of The Institution Of Mechanical Engineers, Part J: Journal Of Engineering Tribology*, Volume 222, Pages 325-334, (2008).
- [3] Lahouij I., Vacher B, Martin J.M., Dassenoy F., IF-MoS<sub>2</sub> based lubricants: Influence of shape and crystal structure, *Wear*, Volume 296, Pages 558–567, (2012).
- [4] Tannous J., Dassenoy F., Lahouij I., Le Mogne Th., Vacher B., Bruhács A., Tremel W., Understanding the tribo-chemical mechanisms of IF-MoS<sub>2</sub> nanoparticles under boundary lubrication, *Tribology Letters*, Volume 41, Issue 1, Pages 55-64, (2011).

# Chapter 5

---

## DLC-involving contact

---

*In this chapter it is reported a new mechanism explaining the severe wear subjected by DLC coatings when lubricated by MoDTC-containing base oil. It is based on the formation of molybdenum carbide species inside the contact due to a strong chemical interaction between the molybdenum-based species formed on the steel counter-body during the first cycles of tribo-test and the carbon of the DLC material during sliding.*

*Furthermore, in the second part of the chapter, the impact of degradation of MoDTC-containing base oil on the tribological properties of DLC coatings has been investigated.*

*This study is believed to give some insights about the mechanisms by which the DLC materials are worn out in presence of MoDTC-containing base oil.*

# Chapter 5

---

## DLC-involving contact

---

*Dans ce chapitre, un nouveau mécanisme expliquant la forte usure rencontrée par les revêtements DLC lubrifiés avec une huile de base contenant du MoDTC a été mis en évidence. Ce model d'usure est basé sur la formation d'espèces de carbure de molybdène à l'intérieur du contact, à cause d'une forte interaction chimique entre les espèces à base de molybdène formées sur la bille en acier au cours des premiers cycles du test de frottement et le carbone du DLC.*

*Dans la deuxième partie de ce chapitre, l'impact de la dégradation du MoDTC sur les propriétés tribologiques des revêtements DLC a été étudié.*

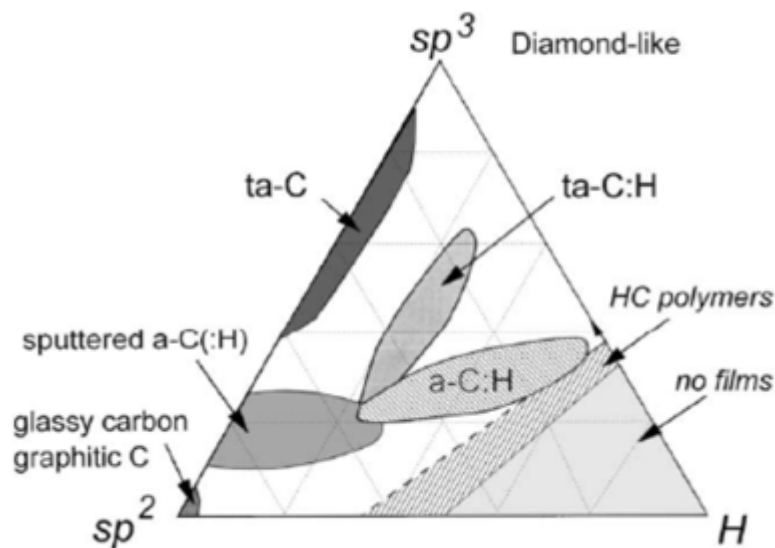
*Un mécanisme d'endommagement des matériaux DLC en présence de MoDTC est ici proposé.*



## 1. INTRODUCTION

To improve fuel economy and lower gas emissions, innovative and environmentally sustainable technologies for automotive engines are employed. In particular, cutting-edge coating and surface treatment technologies are increasing in importance. Recently, Diamond-Like Carbon (DLC) coatings have attracted large attention due to low friction, high hardness, good wear and corrosion resistance, high thermal and chemical stability. They represent one of the highest produced volume of coatings for applications in the combustion engine industry.

The DLC term describes metastable amorphous carbon coatings containing a variable fraction of  $sp^3$  and  $sp^2$  bonds. It includes hydrogen-free amorphous carbon coatings (a-C), hydrogenated amorphous carbon coating (a-C:H), tetrahedral amorphous coatings (ta-C) and hydrogenated tetrahedral amorphous coatings (ta-C:H). These different types of coatings can be represented on a ternary phase diagram (**Figure 5.1**) [1,2].



**Fig. 5.1.** Ternary phase diagram of bonding in hydrogen-containing amorphous carbon coating [2].

A significant number of techniques exist to deposit DLC coatings. Ion beam deposition, sputtering, cathodic arc, pulsed laser deposition and plasma enhanced chemical vapor deposition (PECVD). Sputtering is widely used for industrial application of hydrogen-free DLC material, while PECVD is preferred for deposition of hydrogenated DLC for laboratory investigations. All these depositions processes are well described in several review papers [2-3].

To take the maximum advantage of their beneficial properties, it is needed to understand their chemical interactions with the lubricant components. A lot of research has been performed on the effect of molybdenum-based additives on the boundary lubrication of DLC coatings in order to obtain even lower friction coefficient thanks to their combination. However, it has been widely shown that the tribological performances obtained in presence of MoDTC are poorer than those for steel/steel contact. Kosarieh S. *et al.* [4], for example, correlate the high wear of DLC to the molybdenum containing products decomposed from MoDTC. They found that DLC wear depends on the MoDTC concentration in the lubricant and that the addition of ZDDP additive to a certain extent could mitigate this wear.

An abrasive wear mechanism for DLC material when lubricated by oil additivated with MoDTC friction modifier was proposed by Shinyoshi *et al.* [5] and confirmed by Haque T. *et al.* [6]. In these studies it has been hypothesized that there is an interaction between the DLC coating and the MoO<sub>3</sub> particles, derived from MoDTC decomposition [7,8]. However other authors [9] have already demonstrated that there is no direct correlation between DLC wear and MoO<sub>3</sub> concentration. Other investigations [10,11] have shown that the re-hybridization change of carbon bonding from sp<sup>3</sup> to sp<sup>2</sup> bonding due to high temperature, pressure and mechanical stresses in the contact could play a key role in the wear of DLC material. It was proposed that these changes in the DLC structure cause the delamination of the soft amorphous carbon layer formed on the top of the DLC, showing increased sp<sup>2</sup>-content [11]. All these studies showed that DLC material suffers strong wear when it is lubricated by the MoDTC blended into the base oil. However, the wear mechanisms leading to the coating removal are not fully understood yet.

The principal aim of this chapter is an accurate investigation of the surface chemical modification undergoing on the lubricated DLC coatings in presence of MoDTC additive. To address the question of the strong wear of DLC materials, five different coatings were chosen. The DLC coatings selected differ in terms of hydrogen content and hardness. At the same time, it has been decided to study also the influence of doping agents. In fact, to enhance the properties of DLC films, different chemical elements or compounds (nitrogen, silicon, titanium, tungsten etc.) could be added into the coating [12,13]. Among all of them, amorphous hydrogenated silicon- and oxygen-doped DLC films (a-C:H:Si:O) have been selected because, during the last years, they have attracted special attention due to their ability to decrease the residual internal stress and to stabilize the sp<sup>3</sup>-bonding without sacrificing the hardness of the coating [14,15]. This is because such a coating has improved resistance to oxidation and adhesion to metal alloys, steels and glasses, leading to better high

temperature stability [16-18]. Due to these interesting properties, great effort has been expended to apply this type of DLC in different fields. Recently, it has been proposed to develop a carbon-based coating containing silicon and oxygen to be employed in automotive parts. Therefore, it is extremely important to optimize the interaction between a-C:H:Si:O DLC and the MoDTC additives to further reduce its already low friction coefficient.

Based on the experimental and analytical results presented in this chapter, a new wear mechanism has been proposed.

Finally, to develop a further understanding of the interaction between DLC and MoDTC additive, the effect of lubricant degradation on the DLC/steel contact has been investigated.

## 2. MATERIALS AND METHODS

### 2.1. DLC coatings

Five different types of DLC coatings supplied by OERLIKON Balzers France were investigated in this work. The main properties of these coatings are given in **Table 5.1**.

DLC type	DLC detailed name	Denomination	H [%]	Si [%]	Average top layer DLC thickness [μm] (total thickness)	Hardness [GPa]	Deposition technique
a-C:H	a-C:H Process 1	a-C:H	-	-	2.0 (3.5)	21	PACVD
a-C:H	High hydrogen a-C:H Process 2	HHS	33	-	0.9 (1.9)	22	PACVD
a-C:H	Low hydrogen a-C:H Process 2	LHS	29	-	1.5 (2.3)	20	PACVD
ta-C:H	Hard ta-C:H	ta-C:H	30	-	1.3 (3.0)	38	PACVD
a-C:H:Si:O	DLC doped with Si and O a-C:H Process 2	Si-doped	34	14	1.2 (2.3)	18	PACVD

**Tab. 5.1.** Main characteristics of DLC coatings used in this work. (H & Si content measured by ERDA/RBS).

### 2.2. Tribological experiments

Tribological experiments were performed using the tribometer described in the ANNEX A, employing the same conditions listed in the chapter 2. The AISI 52100 steel ball (6.7 mm radius) is reciprocated for one hour against the DLC-coated flat coupon with an applied load

of 8 N (maximum initial Hertzian pressure of 800 MPa), a sliding speed of 50 mm/s and a stroke length of 5 mm. These conditions were selected to compare the results obtained on DLC/steel to those reported in the chapter 2 using a steel/steel contact. The wear of DLC was obtained by following method. After the tribotest, the surface profile of the worn surface was measured using interferometry techniques to obtain the worn area. The wear coefficient ( $\text{m}^3/\text{Nm}$ ) of the DLC was calculated by dividing the averaged worn area at the wear track ( $\text{m}^3$ ) by the load (N) and the total sliding distance (m).

### 2.3. Surface post-mortem analysis

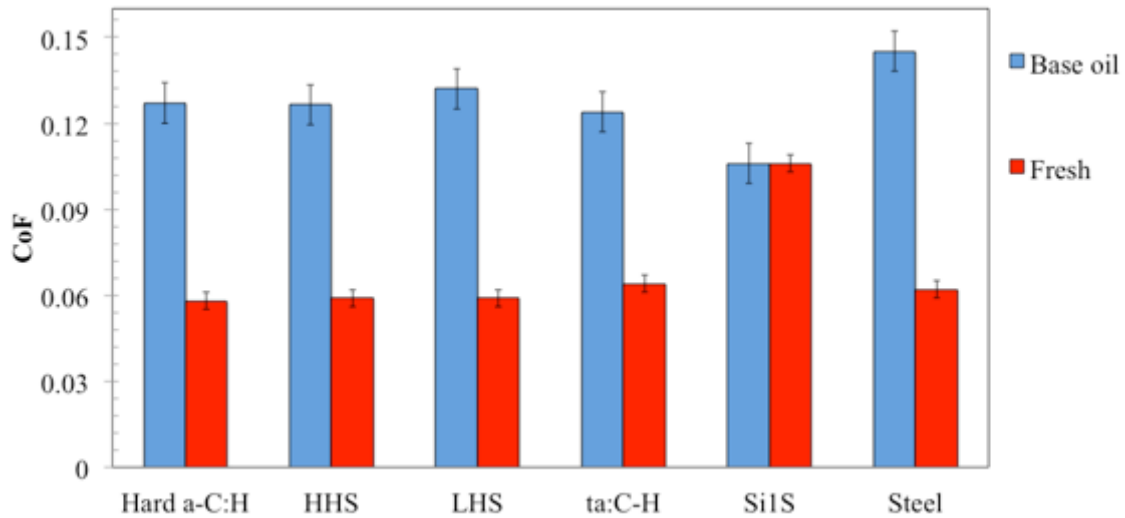
The worn surfaces of the steel balls and DLC-coated coupons were analyzed by SEM/EDX to get images of surface topography of the wear scar and information about its observed chemical composition. Further XPS analyses have been performed to investigate the chemical composition of the rubbed surfaces.

The detailed microstructural characterization of the tribofilm formed on the worn steel ball rubbed against the DLC coating was performed using the FIB cross-section. Microstructural observations were performed using Transmission Electron Microscope (JEOL 2010F HR-TEM) at 200 kV acceleration voltage equipped with Energy Dispersive X-Ray Spectroscopy (EDX). Thus, the four complementary techniques have been employed: Selected Area Electron Diffraction (SAED) for the crystallographic determination of the crystallized compounds; High Resolution Imaging; Elemental chemical mapping using EDX spectroscopy and High Annular Dark Field imaging (HAADF) for chemical compound revelation.

## 3. RESULTS

### 3.1. Friction performance

The value of the steady state friction coefficient (CoF) as a function of the different DLC coatings for the oil with and without MoDTC additive are given in **Figure 5.2**. All the DLC coatings except the one doped with silicon and oxygen show the same friction behavior: the blending of MoDTC into the base oil lowers the friction coefficient until reaching a value similar to that of a steel/steel contact. The Si-doped coating behavior is unique giving no friction reduction at all.



**Fig 5.2. Steady-state friction coefficient for different DLC coatings lubricated by base oil with and without MoDTC additive (steel ball slid against DLC coated coupon).**

As already underlined, the investigations so far indicate that when DLC-coated samples are tested in the presence of MoDTC-containing oils, it is very important to carry out wear measurements together with friction values [5-8].

## DLC-coated coupon characterization

### 3.2. Wear measurements

Optical images of wear scars on DLC-coated flats are shown in **Figure 5.3**. Almost invisible wear was observed for the first four DLCs when employing base oil with and without MoDTC. In fact, as shown in **Figure 5.3**, only a gradual polishing wear is noticeable. However, blending MoDTC additive in base oil leads to a really high wear for Si-doped DLC. The wear rate of DLC-coated flat coupons calculated from the depth/volume ratio of the wear scar measured by interferometry is shown in **Figure 5.4**. A huge difference in the wear rates between the Si-doped DLC and the other four coatings has been confirmed, almost more than two orders of magnitude. The results are in good agreement with the wear scar images shown in **Figure 5.3**, confirming the higher wear rate for the Si-doped DLC compared to the other DLC coatings and to the steel/steel contact.

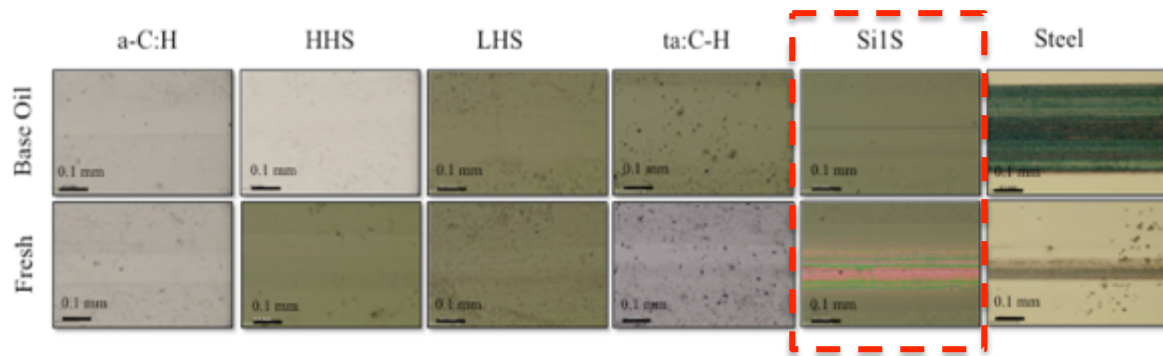


Fig 5.3. Optical images of wear scars formed on DLC coatings lubricated by base oil with and without MoDTC additive. (Steel ball slid against DLC coated coupon).

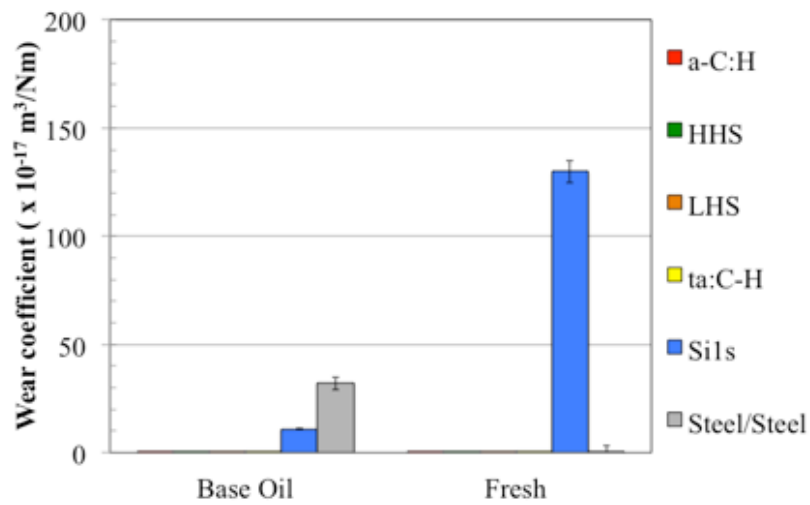
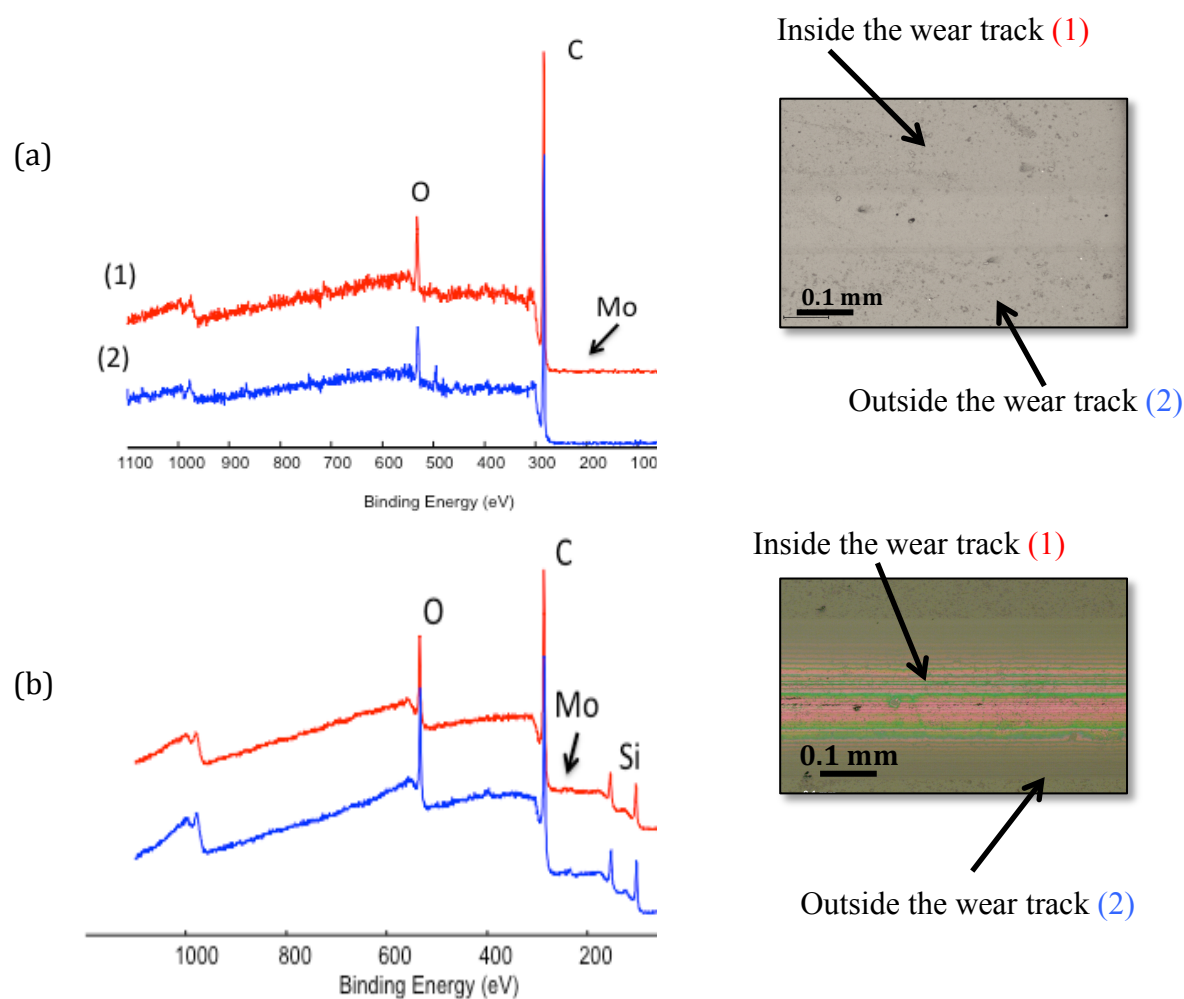


Fig 5.4. Wear coefficient of the DLC flat coupons and steel calculated by means of interferometry.

Taking into account that the tribological behaviors (friction and wear) of 4 of the DLC coatings seem to follow the same trend, it has been decided to focus further analyses on two DLCs, i.e., the a-C:H DLC (a promising coating for the automotive industry) and the silicon and oxygen doped DLC (with high friction and wear). The comparison between these two DLCs is believed to provide better understanding of the DLC wear mechanisms in the presence of MoDTC additive.

### 3.3. X-ray photoelectron spectroscopy (XPS)

The survey spectra obtained both inside (1) and outside (2) the wear track on the a-C:H (a) and Si-doped DLC (b) flat coupons after experiments with fresh MoDTC-containing base oil are shown in **Figure 5.5**. The amount of molybdenum species detected on both DLC coated flats seems negligible due to the absence of tribofilm formation.



**Fig 5.5.** Survey spectra recorded on a-C:H DLC coated flat (a) and silicon-doped DLC (b) lubricated by fresh MoDTC-containing oil.

### 3.4. Scanning Electron Microscopy/Energy Dispersive X-ray (SEM/EDX)

Figures 5.6 and 5.7 show SEM images and EDX analyses of rubbed and non-rubbed surfaces for a-C:H DLC coated flat and Si-doped DLC coupons, respectively.

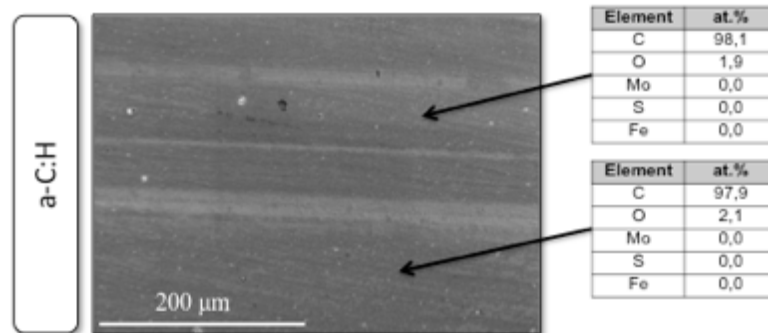


Fig 5.6. SEM micrograph of the wear scar on a-C:H DLC-coated flat and the corresponding EDX atomic composition inside and outside the wear track.

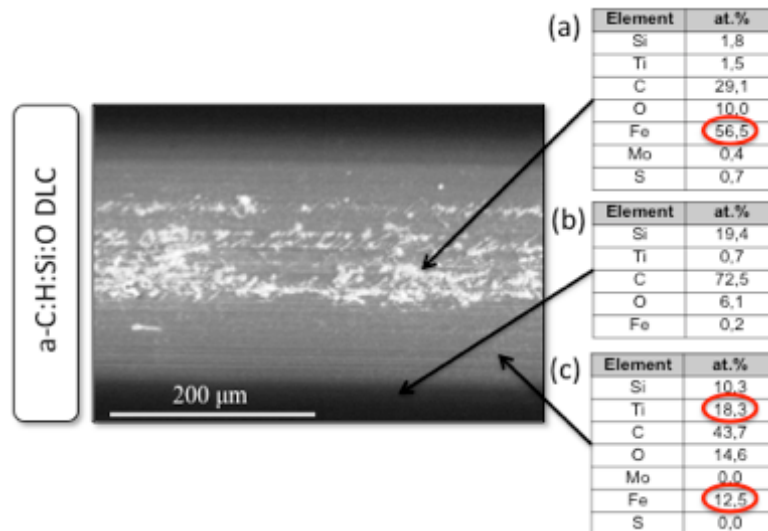


Fig 5.7. SEM micrograph of the wear scar on Si-doped DLC-coated flat and the corresponding EDX atomic composition inside and outside the wear track.

According to the SEM image (**Figure 5.6**), the a-C:H DLC flat has a smooth appearance with only few slightly inhomogeneous zones on the wear scar. Carbon is the major element inside and outside the wear scar. In the Si-doped DLC (**Figure 5.7**), three different areas can be recognized revealing that high wear is produced:

- (a) white patchy areas reveal that the DLC is completely worn out and the steel substrate has started to emerge (area rich in Fe).
- (b) a black area representing the original non-rubbed DLC, which is made of carbon and almost 20% of silicon;



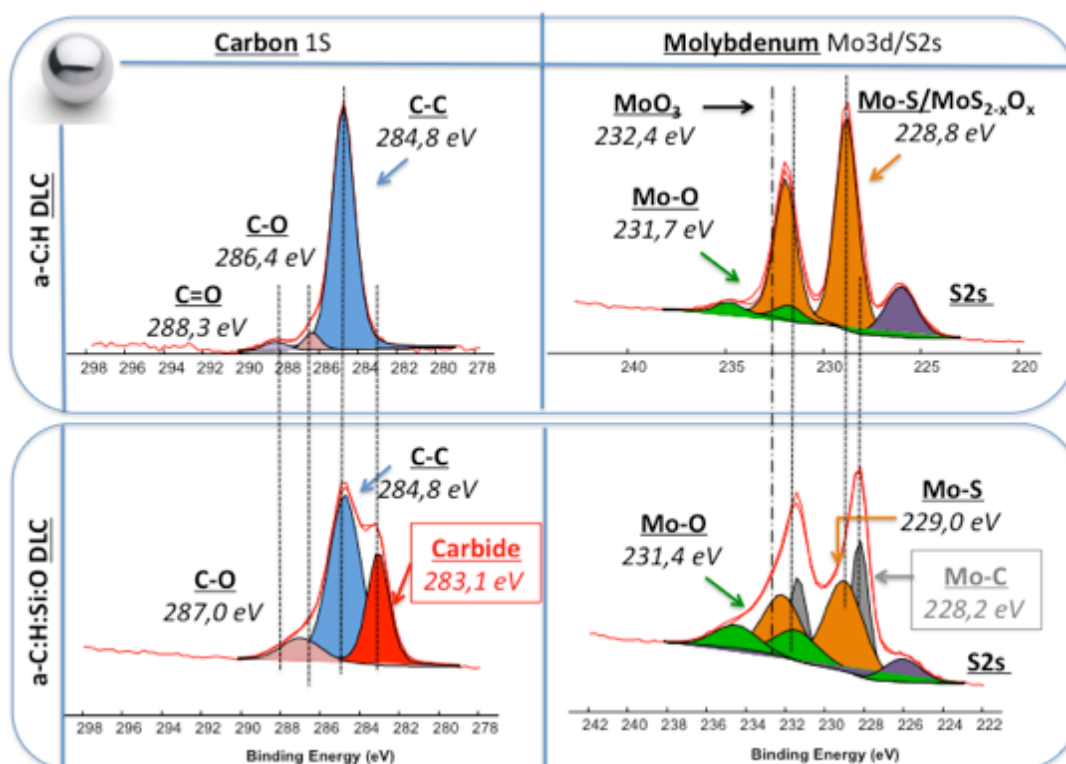
(c) grey areas in the wear scar made of titanium (sub-layer) and few percent of silicon (the DLC coating is still present);

## Naked steel ball counterpart

### 3.5. X-ray Photoelectron Spectroscopy (XPS)

Considering that the amount of molybdenum detected on the coated surface was negligible (no tribofilm formed on the DLC samples), it was decided to perform a surface analysis also on the worn steel counter-ball surfaces.

The C1s photo-peaks recorded on the steel balls slid against the a-C:H DLC and the a-C:H:Si:O doped DLC flats are presented in **Figure 5.8**.



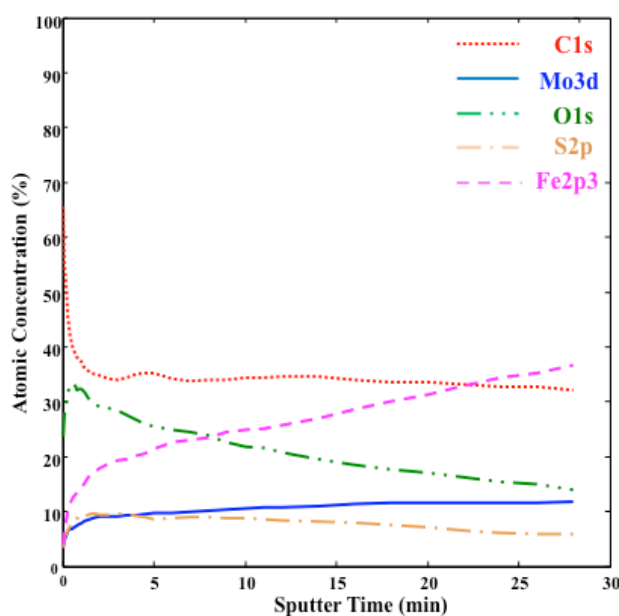
**Fig 5.8.** XPS Curve fitting of C1s and Mo3d photoelectron peaks recorded on tribofilm formed on the steel counterparts rubbed against a-C:H and a-C:H:Si:O DLCs using fresh MoDTC-containing oil.

The carbon peak related to the a-C:H DLC experiment clearly exhibits three contributions: the main peak at 284.8 eV, characteristic of the alkyl chain C-C, and two others located at 286.4 eV and at 288.3 eV assigned to C-O bonds. In the case of a-C:H:Si:O DLC, the binding energies for C1s were found to be at 284.8 eV and 287.0 eV, also corresponding to C-C and C-O bonds. However, in this case, a third contribution located at 283.1 eV was

needed to fit the experimental spectrum properly. According to the literature, this new peak position is attributed to carbide species [19]. The Mo3d XPS spectrum detected on the wear track of the steel ball sample rubbed against a-C:H DLC, both Mo-S and Mo-O doublets are observed at 228.8 eV and 231.7 eV, respectively, with an FWHM of 1.4 eV (**Figure 5.8**). In the case of the tribofilm formed on the steel ball slid against the Si-doped DLC, the Mo3d fitting showed that besides the formation of these doublets located at 229.0 eV (Mo sulfide) and 231.4 eV (Mo oxide), molybdenum carbide is also clearly detected, as suggested by the presence of a peak with binding energy at 228.2 eV.

Therefore, it seems that the molybdenum carbide species are formed on the steel counter part during the tribological experiment carried out on the Si-doped DLC.

To obtain more information about the Mo and C element distribution inside the tribofilm formed on the steel ball slid against the a-C:H:Si:O, XPS depth profiles were taken (**Figures 5.9** and **5.10**). It can be seen that after 40 sputter cycles (28 minutes), the majority of the carbon contamination has been removed, while the peak corresponding to the carbide species becomes more important. Moreover, considering that the contribution related to carbide species is still clear in the Mo3d photo-peaks also after the sputtering time, it is possible to confirm the presence of Mo-C species all over the tribofilm formed on the steel ball.



**Fig. 5.9.** XPS depth profiles of the tribofilm formed on the steel ball rubbed against a a-C:H:Si:O DLC coating.

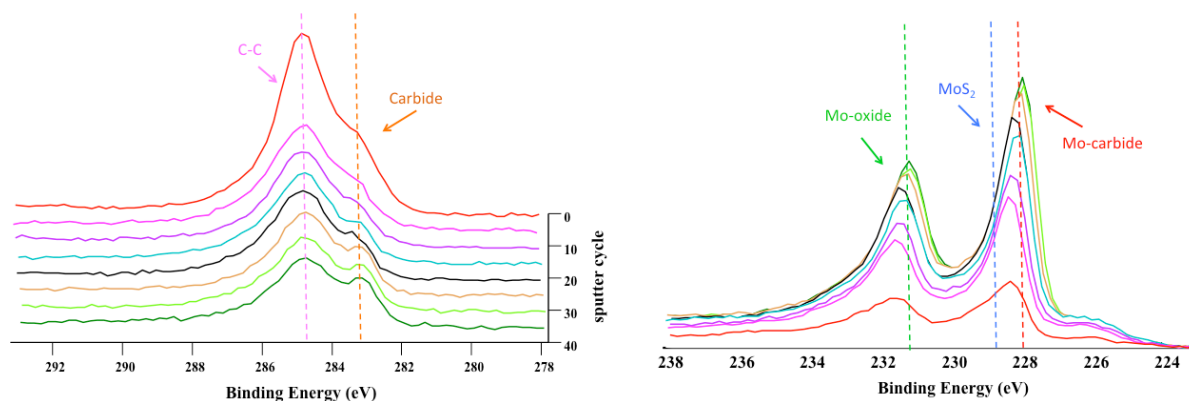


Fig. 5.10. XPS spectra zoomed in the molybdenum and carbon energy region (each color is associated with a sputter cycle number).

### 3.6. Scanning Electron Microscopy/Energy Dispersive X-ray (SEM/EDX)

**Figure 5.11** shows SEM images and the chemical composition of the worn surface on the steel ball after rubbing against Si-doped DLC. Following the EDX analysis results, the elemental composition in the dark grey region on the ball wear scar is dominated by iron, demonstrating that the ball was worn out at this region (no tribofilm formed). The elemental composition of the white areas of the scar (more evident in the zoomed picture) suggests that there is the formation of a tribofilm mainly containing carbon, molybdenum and iron.

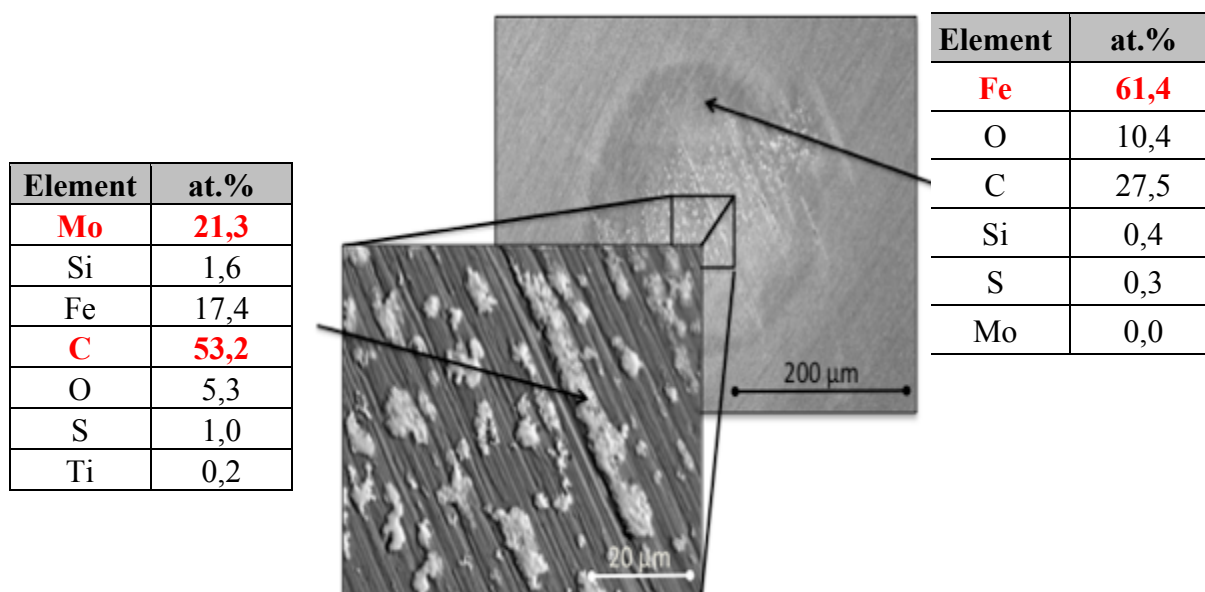
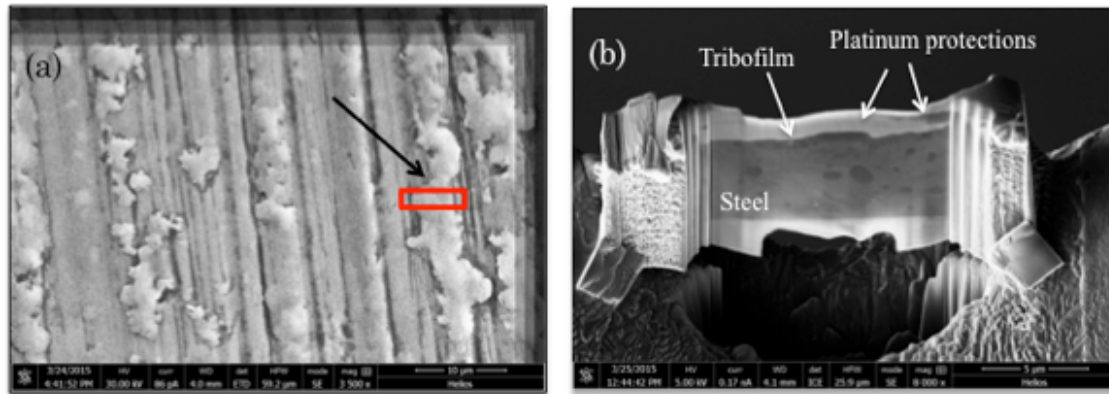


Fig 5.11. SEM micrograph of the tribofilm formed on the steel ball rubbed against Si-doped DLC and EDX composition.

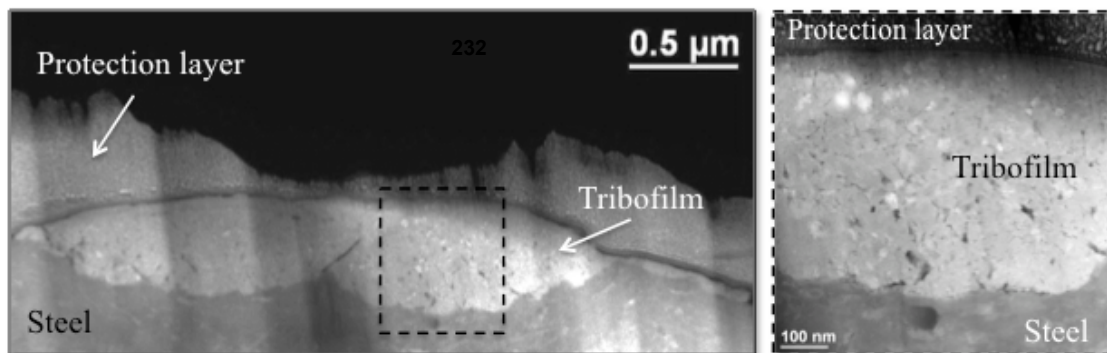
### 3.7. Transmission Electron Microscopy/Energy Dispersive X-ray (TEM/EDX)

The ability to directly image a cross-section of the tribofilm formed on a steel ball by means of FIB coupled with TEM and the possibility to monitor its chemistry using EDX analysis have been employed to obtain more information about the interaction between the DLC coating and MoDTC additive. The TEM specimen has been prepared by selecting a specific region of the steel ball surface to include the white patchy areas (see red rectangle in **Figure 5.12**).



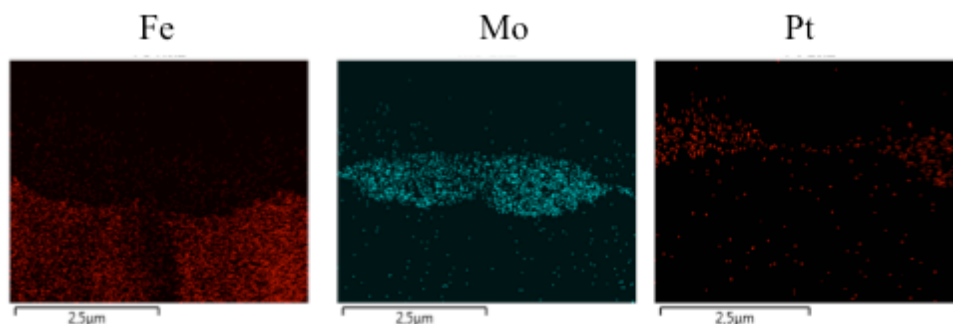
**Fig. 5.12.** SEM images of the tribofilm formed on the steel ball after a tribotest against the a-C:H:Si:O DLC (a) and cross-section of the layered structure of the cross-section performed in the zone

**Figure 5.13** shows a high angle annular dark field (HAADF) image of the tribofilm formed on the steel ball. A strong Z-contrast of elements is shown in the tribofilm (the lowest is the atomic number, the darker is the contrast), and the transverse bands are due to thickness variations of the FIB thin foil. Different layers can be distinguished in the zoomed image in **Figure 5.13**: the region on the top represents the platinum protection layer used to avoid damage during the sample FIB production, the 0.5 micron thick area represents the tribofilm, and the last layer is the steel.



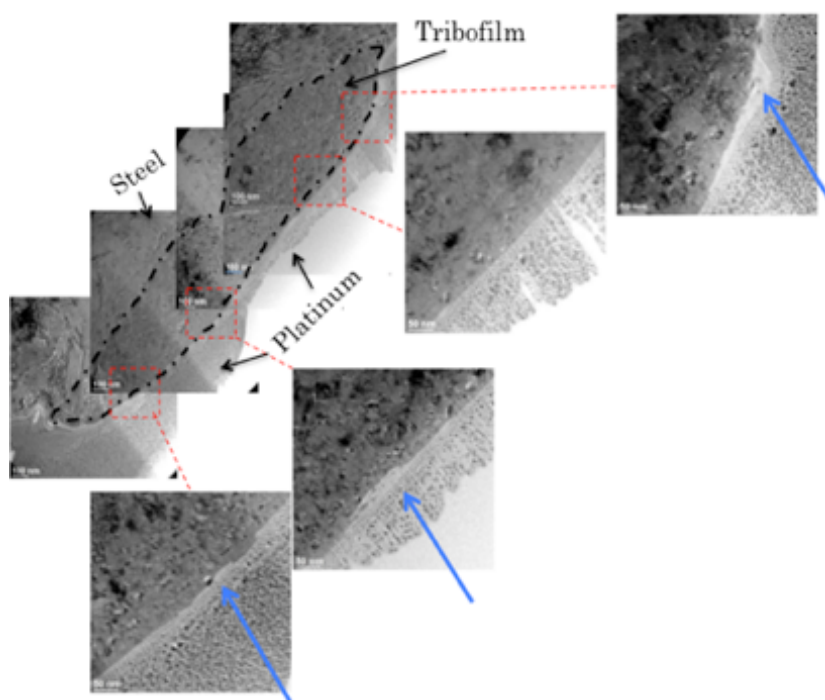
**Fig. 5.13.** HAADF images of tribofilm formed on the steel ball rubbed against an a-C:H:Si:O DLC coated flat coupon. (zoomed region on right).

HAADF imaging is commonly performed in parallel with EDX acquisitions. The corresponding chemical maps (**Figure 5.14**) depict the composition for the layered structure of the cross-section. Thanks to this technique, it has been possible to confirm the presence of molybdenum all over the tribofilm.

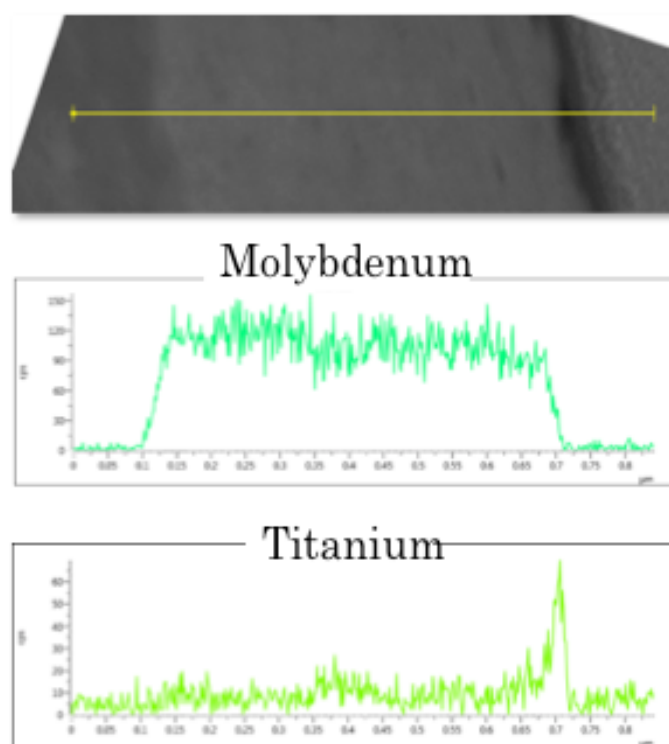


**Fig. 5.14. TEM/EDX mapping. Chemical composition of the structure of the tribofilm cross-section.**

Higher-magnification TEM images taken on this FIB cross-section (**Figures 5.15**) indicate that on the top part of the tribofilm, there is a heterogeneous extra layer. Surprisingly, an EDX line scan experiments (**Figure 5.16**) conducted on the tribofilm/platinum interphase, revealed titanium as the main component. This could be explained by supposing that the removal of DLC from the coated coupon onto the steel ball is so catastrophic in some places that it causes even the transfer of the titanium sub-layer after the complete removal of the DLC material.

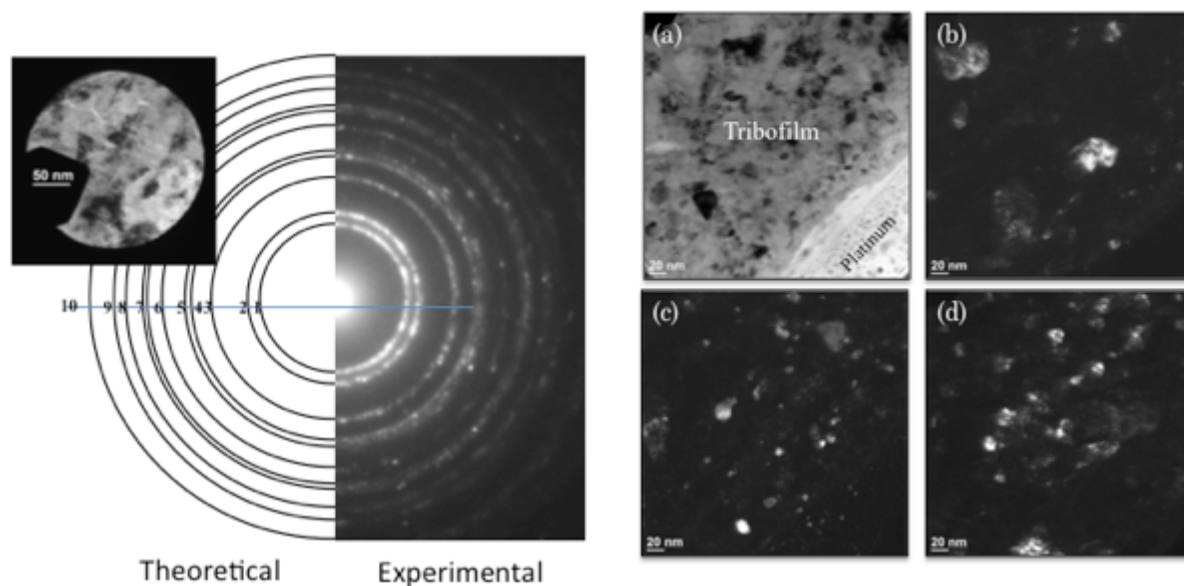


**Fig. 5.15. Low magnification TEM image for the tribofilm formed on the steel ball. A series of higher resolution images are also shown. The blue arrows point the extra-layer identified at the tribofilm/platinum interface.**



**Fig. 5.16.** Molybdenum and titanium EDX line scans recorded across the tribofilm formed on the steel ball.

A selected-area electron diffraction (SAED) pattern (ca. 250 nm diameter) was obtained in the tribofilm material, as shown in **Figure 5.17**.



**Fig. 5.17.** SAED pattern for the area of the tribofilm shown in the inset . A bright-field image (a) and a series of dark-field images (b,c,d) performed on the tribofilm formed on the steel ball.

The diffraction pattern obtained from the area shown in the inset is representative of a Debye-Scherrer type diffraction, where the diffraction rings are the result of numerous fine crystals lit up by the electron beam. It has been overlaid with the theoretical pattern of the MoC phase, having a face-centered cubic lattice (fcc), as identified in the JPDS file [20]. A good correlation is observed between the experimental SAED pattern of the tribofilm and the theoretical pattern for the MoC phase, clearly confirming the presence of molybdenum carbide species. A bright-field (BF) image of the tribofilm (a) and a series of dark-field (DF) TEM images (b, c and d) are also shown in **Figure 5.17**. The TEM-DF cross-section images are obtained after a selection of a small part of the two first rings. These images reveal a small fraction of the crystallite grains appearing bright with a nano-crystalline structure for the tribofilm with a carbide crystallites grain average size varying between ca. 10 nm and ca. 60 nm.

**Table 5.2** displays the comparison between the theoretical and experimental numerical results for the d-spacing of the rings. This confirms that the electron diffraction pattern obtained can be directly interpretable as crystalline molybdenum carbide compounds.

N°	d <sub>exp</sub> (nm)	d <sub>CMo</sub> (nm)	{hkl}
1	0.2473	0.2472	111
2	0.2148	0.214	200
3	0.1507	0.1514	220
4	0.1285	0.1291	311
5	0.122	0.1236	222
6	0.1066	0.107	400
7	0.096	0.0982-0.0957	331-420
8	0.0866	0.0874	422
9	0.0815	0.0824	511
10	0.071	0.07135	333

**Tab. 5.2.** Experimental Miller indices perfectly matching with the molybdenum carbide theoretical values (JPDS 03-065-8092).

An accurate analysis of the SAED pattern conducted on the tribofilm (**Figure 5.18**) revealed extra spots, which can be interpreted as crystalline graphitic-based material.

In fact, comparing the approximate experimental and theoretical (JCPDS 00-026-1079 [21]) values for the d-spacing of the rings (**Table in Figure 5.18**), it can be clearly seen that there is good matching between the structure present inside the tribofilm and the graphitic-based material (even if it is in a much smaller amount in comparison to the MoC species).



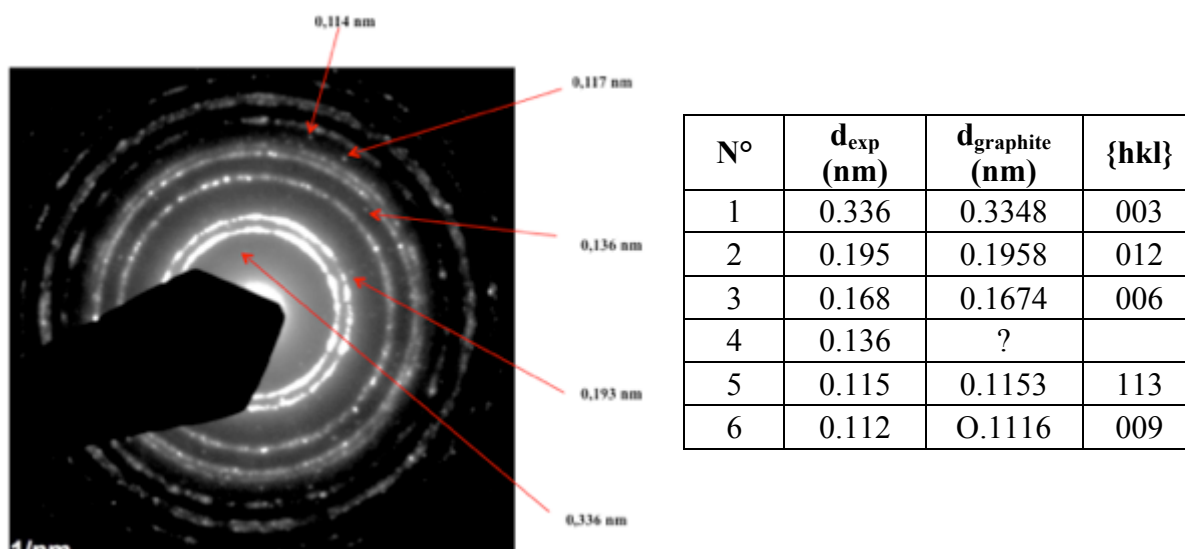


Fig. 5.18. SAED pattern of the tribofilm showing the extra spots present in the pattern (a). Some experimental Miller indices may match the graphite theoretical values (JCPDS 00-026-1079)(b).

A high-resolution TEM micrograph of an isolated grain is shown in **Figure 5.19**.

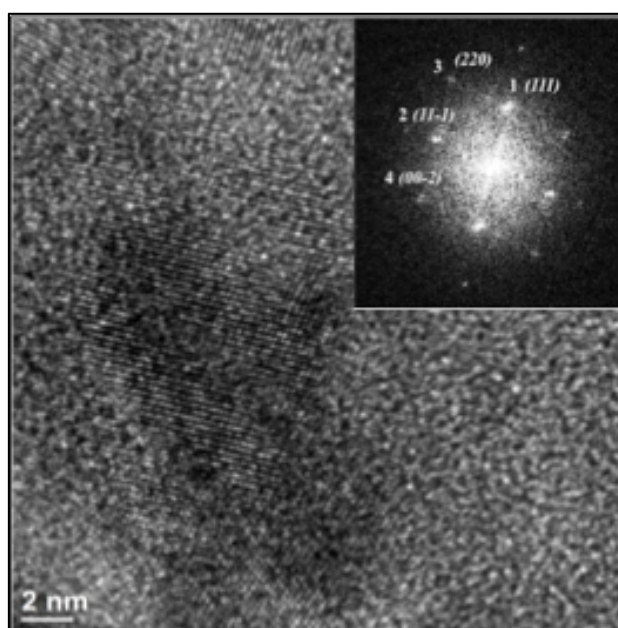


Fig. 5.19. High resolution TEM image recorded on the tribofilm formed on the steel ball during the tribotest and the indexed Fast Fourier Transform (FFT) of the micrograph.



Fringes in the image and the corresponding spots in the Fourier transform (inset in **Figure 5.19**), confirm that the tribofilm formed on the steel ball has a crystalline structure and that the inter-reticular distances (**Table 5.3**) match those of the MoC compound. However, the angles of the reticular planes do not match perfectly with an fcc lattice. This could be explained considering some crystal deformations as a result of internal stresses or by supposing that there is a specific superposition of two crystals of MoC.

N°	d <sub>exp</sub> (nm)	d <sub>graphite</sub> (nm)	{hkl}	Angles <sub>(exp)</sub>	Angles <sub>(theory)</sub>
1	0.248	0.2472	111	0°	0°
2	0.239	0.2472	111	78.8°	70.5°
3	0.157	0.151	220	39.5°	35.3°
4	0.200	0.214	200	126.7°	125.3°

**Tab. 5.3.** Comparison between experimental and theoretical interreticular distances and angles of MoC (JCPDS 03-065-8092).

## 4. DISCUSSION

### 4.1. Experimental results

To study the antagonistic interaction of the MoDTC additive and DLC materials, different types of DLC coatings have been tested in the presence of base oil, with and without MoDTC additive, with a steel ball counter-face. The comparison of the steady-state friction coefficients and wear rates obtained for the different steel/ DLC combinations (**Figure 5.2** and **5.4**) indicates that the 4 DLCs displayed similarly good tribological performance (the addition of MoDTC leads to lower friction values similar to those obtained testing steel/steel contact). However, the Si-doped DLC exhibits completely different behavior, showing high friction and catastrophic wear.

SEM images taken on the a-C:H DLC/steel and the a-C:H:Si:O DLC/steel tribopair suggested that a-C:H DLC is not damaged during the experiment while the doped coating is completely worn out in some zones. At the same time, the EDX analysis made on the Si-doped DLC confirm the extremely high wear produced during the experiment, as suggested by the zone enriched in iron and titanium (DLC sub-layers). Furthermore, on the steel ball rubbed against the Si-doped DLC were observed white patchy zones, rich in molybdenum and carbon.

The XPS analysis carried out after the friction experiments revealed that the  $\text{MoS}_{2-x}\text{O}_x$  compounds, main responsible for lowering the friction coefficient, are present only into the tribofilm formed on the steel counterpart. Indeed, the amount of molybdenum detected on the surface of the DLC coating was negligible. These results are coherent with the literature that has reported the absence of a tribofilm on the coated flat [4]. Using XPS results, it was not possible to observe a direct correlation between the wear produced on the DLC coating and the Mo-oxide species detected. For this reason, in the conditions employed in this work, the Shinyoshi's model cannot be validated [5]. However, an interesting feature was observed on the C1s and Mo3d photo-peaks: new contributions at approximately 283.1 eV and 228.2 eV, respectively, were detected only on steel ball rubbed against Si-doped DLC (**Figure 5.8**). According to the XPS database, they can be attributed to Mo carbide species. This finding is consistent with the EDX analysis obtained on the Si-doped DLC/steel tribopair, which revealed the presence of molybdenum and carbon into some white spots.

Deeper characterization of tribofilm formed on the steel ball slid against the DLC-coated flat has been performed in order to confirm the formation of carbide species.

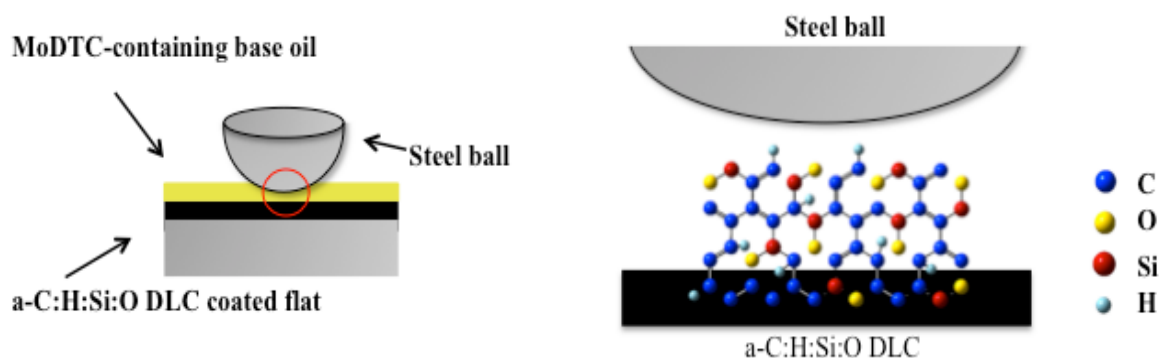
The investigation of the tribofilm with HR-TEM clearly suggests the growth of multi-phase tribofilm containing MoC species, in a matrix made of carbon and relative small amount of molybdenum sulfide and molybdenum oxide species. At the same time, the formation of fcc Mo-C species in the relatively thick and continuous tribofilm formed on the steel ball is stated by the good correlation between the SAED experimental data and the corresponding JCPDS files. Adopting this multi-techniques approach, the presence of molybdenum carbide crystallites has been demonstrated. They have face-centered cubic structure and a grain size varying between 5 nm and 60 nm.

## **4.2. Proposal of new wear mechanism**

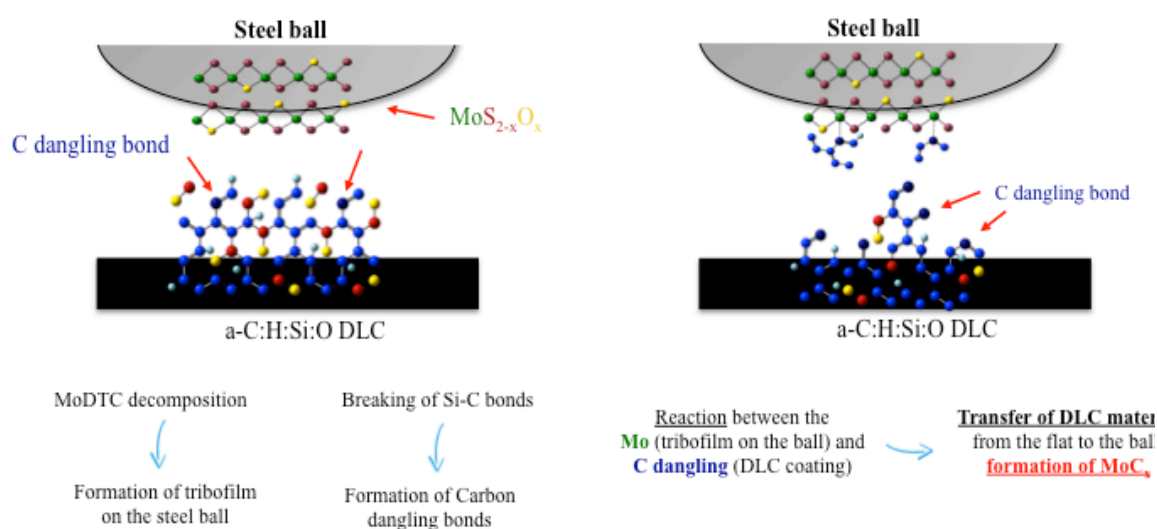
The comparison between tribological experiments, XPS, SEM/EDX and TEM/EDX analyses presented in this chapter, provides valuable insights into the wear mechanism of DLC coating. These findings suggest that when strong wear of DLC occurs, molybdenum carbide species could form on the steel counterpart. This carbide compound could result from the reaction between the molybdenum present in the tribofilm formed on the steel ball counterpart during the first cycles of the friction experiment and the dangling carbon bonds resulting from the breaking of Si-C bonds on the DLC surface.

According to the results detailed in the previous sections, a new mechanism for the wear of DLC in the presence of MoDTC-containing oil can be proposed. This new wear model is schematized in **Figure 5.20**.

### Initial situation



### Principal Wear Mechanism



**Fig 5.20. Schematic representation of the new wear model proposed.**

The first phase of the scenario involves two, probably simultaneous, steps. The formation of a molybdenum and sulfur-based tribofilm on the steel surface could be supposed as first step, justifying the low friction coefficient recorded during the friction test. At the same time, during the friction experiment, the temperature and the mechanical stresses could lead to the breaking of Si-C bonds network present in the Si-doped DLC structure. Subsequently, the molybdenum contained in the tribofilm formed on the steel ball may react with the carbon dangling bonds created on the DLC surface, resulting in the molybdenum carbides ( $\text{MoC}$ ) formation on the naked steel ball. In other words, it is supposed that there is a chemical

grabbing of carbon from the DLC coating through the steel counterpart caused by the reaction with molybdenum species present into the steel ball tribofilm.

### 4.3. Model validation

To confirm the wear scenario proposed above, additional friction experiments and further surface analyses need to be carried out.

#### 4.3.1. a-C:H DLC vs. a-C:H:Si:O DLC

The first important point to discuss is why high wear is produced on the Si-doped DLC while the a-C:H DLC (likewise the other three DLC coatings studied in this work), in the same test conditions, does not show similar behavior. To answer this question, the Bond Dissociation Energy (E) (or Potential Energy) could be considered. It is possible that, due to the complexity of the DLC structures, under the conditions employed in the friction experiment (temperature, pressure and time), the energy dissipated inside the contact is enough to break only C-Si bonds and not the other chemical bonds. The decomposition of silicon-carbon bonds in the worn Si-doped DLC surface due to the tribo-process has already been reported [22]. The authors investigated the performances of the pure DLC and Si-doped DLC coatings in dry conditions and found that there is a strong interaction between Si-doped DLC and the steel counter body, inducing a higher wear rate in comparison with the non-doped DLC coating. To verify this theory, experiments applying higher loads were carried out in order to check if the dissipation of more energy at the a-C:H DLC/steel tribo-pair interface could lead to higher wear with molybdenum carbide formation. The wear rates measured for a-C:H DLC as a function of the applied load are reported in **Figure 5.21**.

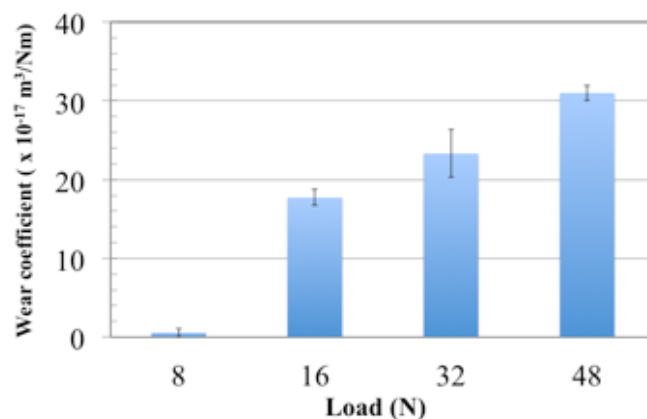
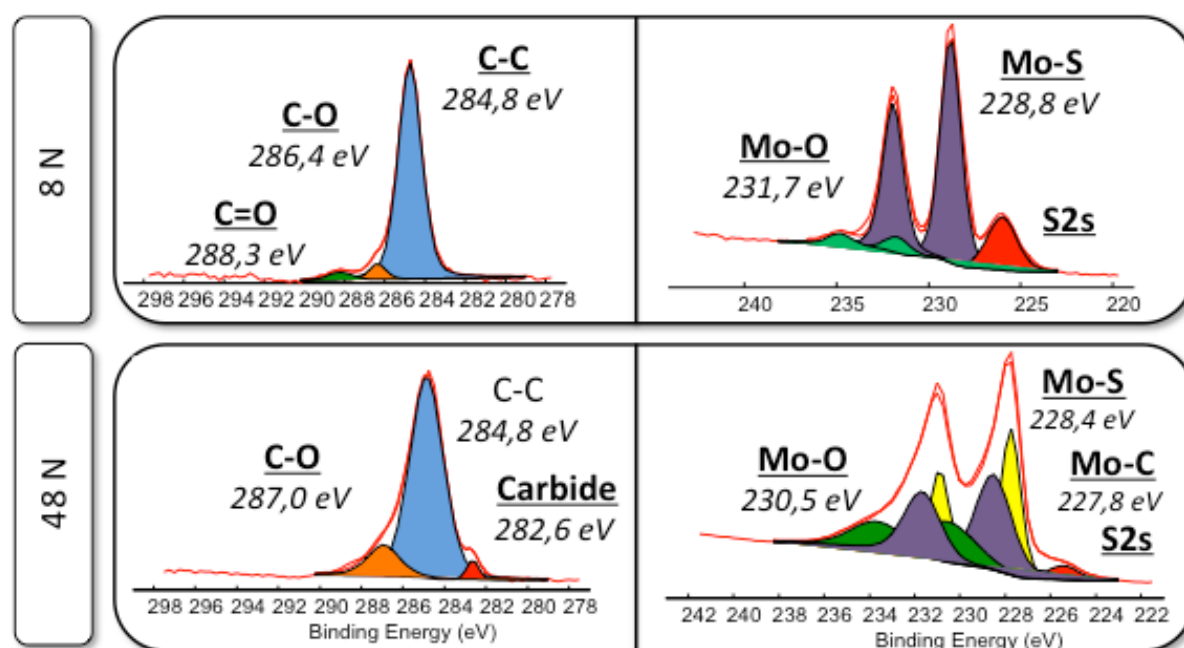


Fig 5.21. Wear coefficient vs. load for the a-C:H DLC coating.

As expected, there is a clear correlation between the load and wear rate: the higher the load applied, the higher the wear rate is. The comparison of the C1s and Mo3d photo-peaks recorded on the steel ball counterparts after tests carried out at 8 N and 48 N confirm the presence of carbide compounds when higher loaded test are carried out (**Figure 5.22**). This result could be explained by a more important interaction between the DLC and the reaction products of the MoDTC degradation. A detailed thermodynamic investigation is required to confirm this hypothesis and future simulation work could be carried out to prove the assumptions.



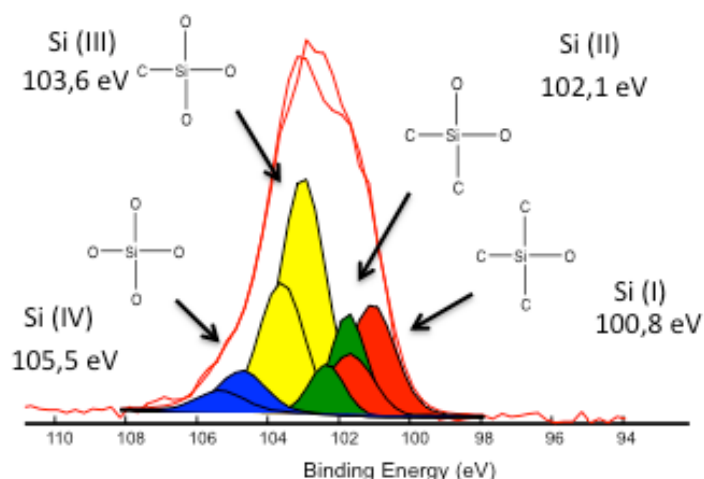
**Fig 5.22.** XPS curve fitting of C1s and Mo3d contributions obtained from the analysis of tribofilm formed on the steel counterpart rubbed against a-C:H DLC coated flat using fresh MoDTC-containing oil. The tests are carried out using 8 N and 48 N Loads.

#### 4.3.2. Characterization of pristine a-C:H:Si:O DLC coating

A preliminary study was conducted to investigate the structure of the DLC film, in terms of elemental chemical composition and bond hybridization. It is important to confirm the presence of Si-C bonds on the DLC top surface. In fact, in some studies [23, 24], silicon-doped coatings are believed to have two different networks, silica and carbon based. More in particular, it has been reported that the amorphous structure containing a mixture of  $sp^2$  and  $sp^3$  bonds is interpenetrated with  $SiO_2$  network [23, 24].

### 4.3.3. XPS analysis on DLC coating prior the tribological experiments

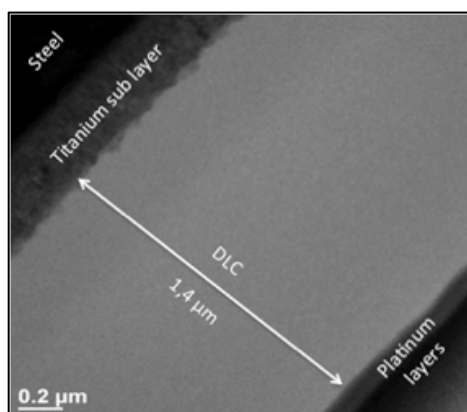
The Si2p photo-peaks recorded on the DLC-coated flat coupon prior to the tribo-test are shown in **Figure 5.23**. The fitting has been done using four contributions at 100.8 eV, 102.1 eV, 103.6 eV and 105.5 eV, corresponding to the different oxidation states of silicon.



**Fig. 5.23.** XPS spectrum for Si2p for the a-C:H:Si:O DLC coating prior to the tribological characterization.

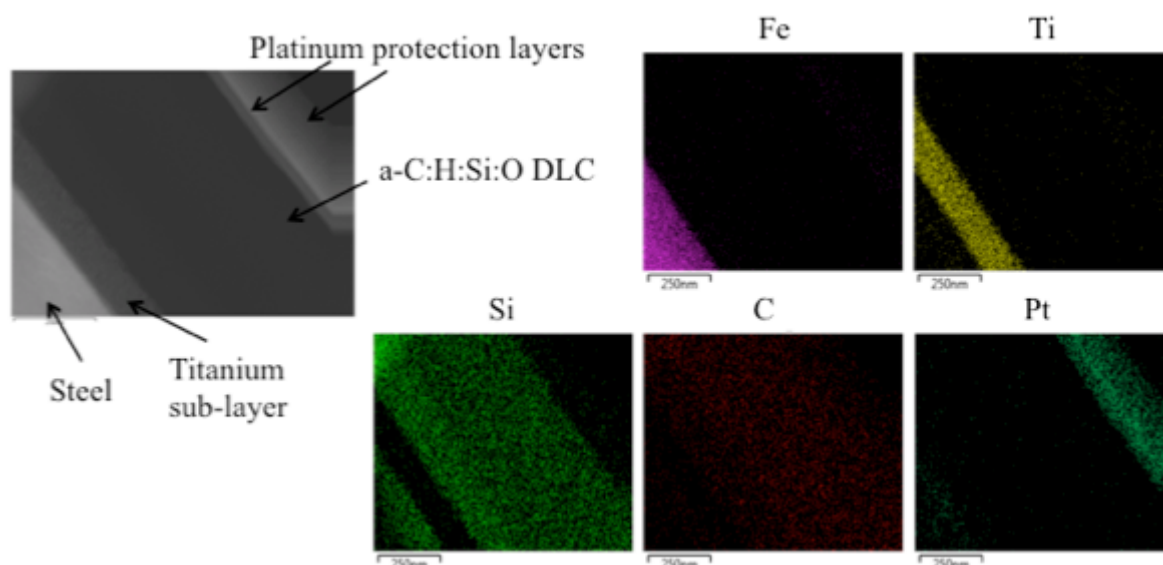
### 4.3.4. TEM observations

The low magnification image of silicon and oxygen doped DLC coating displayed in **Figure 5.24** shows the multi-layers structure of the sample. The first layer, starting from the top-left, is the steel substrate, followed by a titanium interlayer used to improve adhesion. Finally, below the black platinum layers deposited to protect the surface during FIB specimen preparation, the 1.4 micron thick DLC layer can be identified.



**Fig. 5.24.** Low magnification TEM image of DLC coating cross-section.

To obtain more information about the DLC structure, EDX component maps were generated for carbon (C), oxygen (O), silicon (Si), titanium (Ti) and platinum (Pt) (**Figure 5.25**).

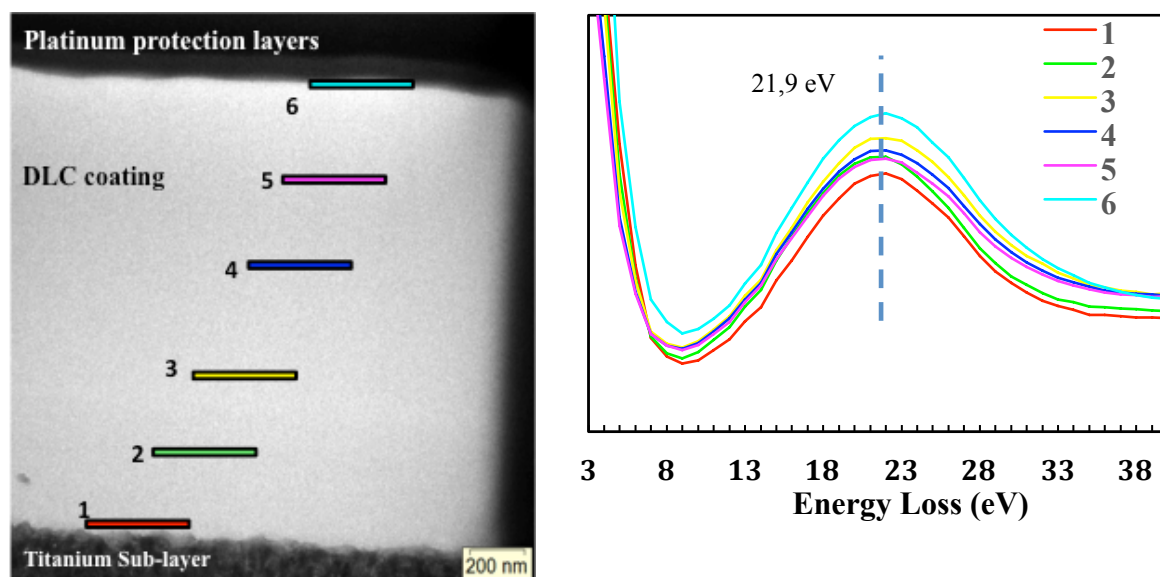


**Fig. 5.25.** EDX mapping revealing the multi-layered structure of DLC cross-section.

Due to the presence of contaminants, meaningful maps could not be obtained for the carbon. However, it is possible to obtain an elemental distribution within the region of interest. It can be noted, that silicon is present in the whole DLC coating. To obtain information about the carbon bonding of the DLC coating, TEM coupled with the low-energy loss spectroscopy (EELS) has been employed. The EELS measurements were carried out using a LEO 912 TEM operating at 120 kV acceleration voltage, equipped with integrated EELS spectrometer. The technique is explained in details in Egerton's book [25]. In this case, the attention was mainly focused to the plasmon-loss energy region corresponding to  $(\sigma+\pi)$  collective excitation valence electrons in order to get more information about the physical properties of DLC film prior the tribological experiment. The maximum energy of this plasmon peak is related to the fraction of  $sp^2$  hybridization of the material [25, 26]. It makes, in fact, possible to determine with high spatial resolution the ratio between  $sp^2$  and  $sp^3$  carbon in the coating with an accuracy of 10%.

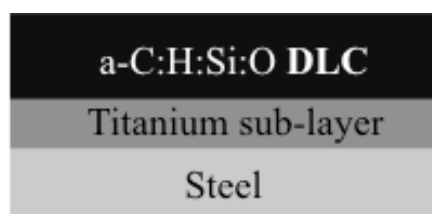
A series of spectra are obtained in different zones (electron probe size approximately 2 nm) along the DLC cross-section (**Figure 5.26**). Position 1 (red curve) corresponds to the titanium/DLC interface, while number 6 (light blue curve) is the DLC/platinum interface.

Comparing the energies of the plasmon loss peaks, it can be seen that there is no shift in these values, revealing again the homogeneity of the physical properties along the coating.



**Fig. 5.26.** Comparison between the low-energy loss spectra carried out in different areas of the coating cross-section.

According to these XPS analysis and the TEM characterizations, it is possible to accurately depict the multi-layer structure of the DLC coating studied in this work (**Figure 5.27**).



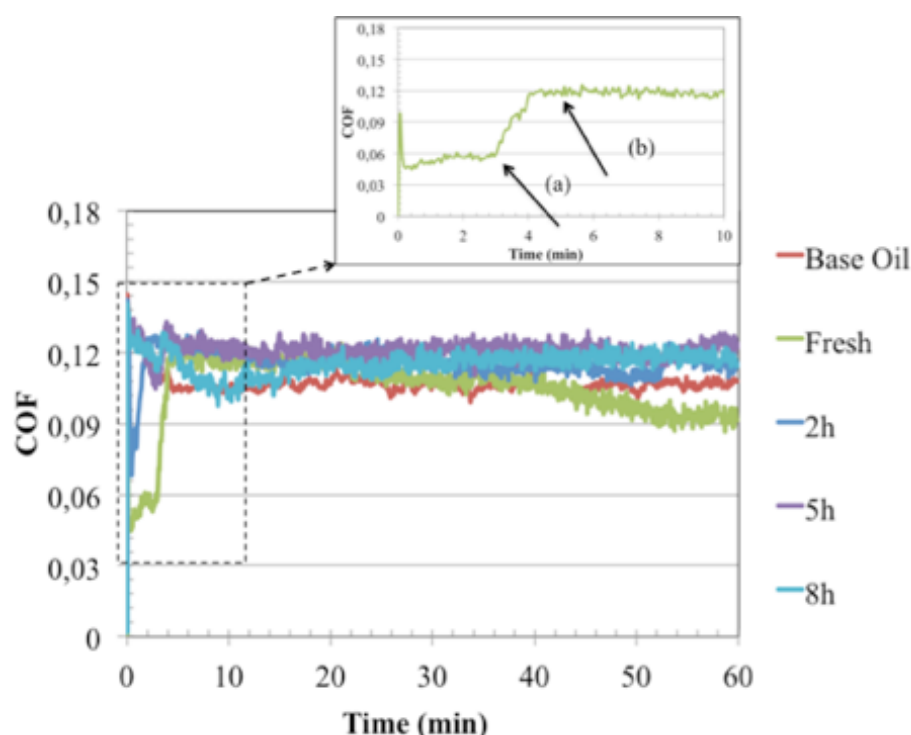
**Fig. 5.27.** DLC multi-layer structure.

More in particular, it has been demonstrated that the DLC coating studied in this work presents a complicated network, formed by carbon, hydrogen, silicon and oxygen atoms, thus also containing Si-C bonds all along the coating thickness.



### 4.3.5. Variable duration tests

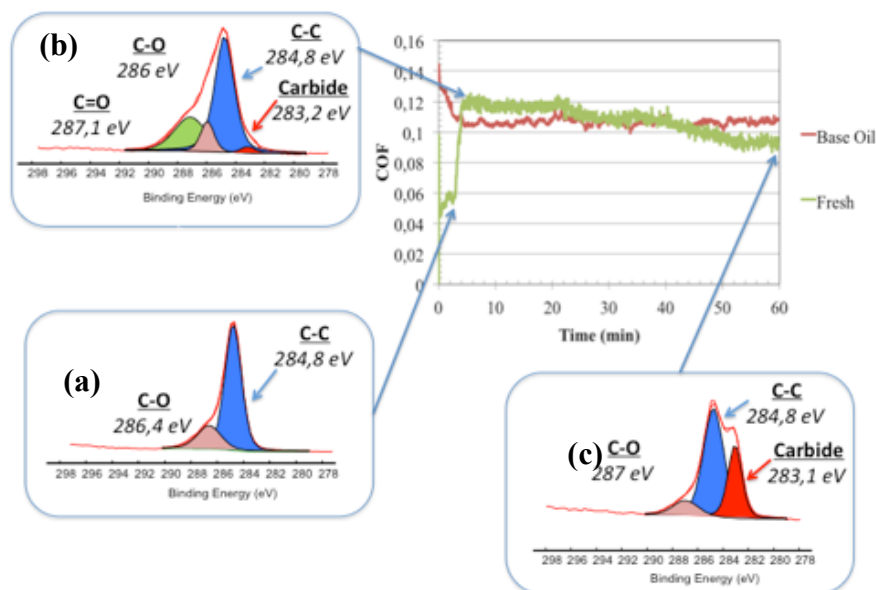
The hypothesis about the formation of  $\text{MoS}_2$  and/or  $\text{MoS}_{2-x}\text{O}_x$  compounds on the steel counterpart during the first cycles of the experiment and the consequent reaction between the molybdenum and carbon from the DLC leading to the formation of molybdenum carbide species inside the contact is supported by considering the “variable duration tests” for the Si-doped DLC/steel tribopair. **Figure 5.28** shows the evolution of the friction coefficient as a function of the test duration for the different oils tested.



**Fig 5.28.** Friction behaviour for the Si doped DLC for fresh and aged MoDTC-containing oils. In the zoom it is visible the low friction regime (a) and the high friction regime (b).

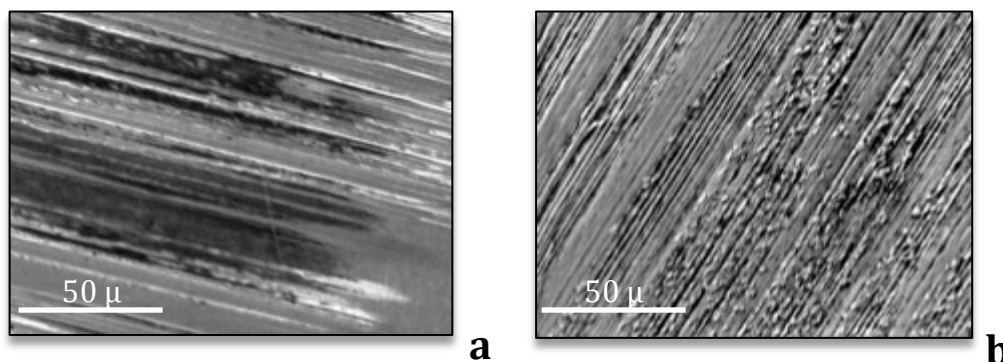
As can be noted, in the beginning of the test carried out with fresh oil there is an immediate and significant reduction in friction, followed by a sharp increase, reaching value similar to that of the additive-free base oil (0.12). The “variable duration tests” consist of stopping the test in the “low friction regime (a)” and when the friction coefficient starts to be high “(b)”.

The XPS spectra recorded on the steel ball wear tracks after these short tests against the Si-doped DLC coating (**Figure 5.29**) clearly show that during the first cycles, when the friction coefficient is relatively low due to the formation of MoS<sub>2</sub> compounds, no carbide formation is detected on the steel ball counterpart (**Figure 5.29(a)**). The peak corresponding to the carbide starts to appear only when the high friction regime is reached (**Figure 5.29(b)**) and it increases with the sliding duration (**Figure 5.29(c)**).



**Fig 5.29.** Curve fitting of C1s photopeaks recorded on tribofilm formed on the steel ball counterpart rubbed against Si-doped DLC in the presence of fresh MoDTC-containing oil. The test is stopped during the low (a) and high (b and c) friction regimes.

The relation between the carbide occurrence inside the contact and the high friction regime is further confirmed by the SEM images of the worn surface of the steel balls after sliding against Si-doped DLC (**Figure 5.30**). Indeed, the presence of white patchy zones, rich in molybdenum and carbon, is only evidenced when the high-friction regime is reached (**Figure 5.30(b)**).



**Fig 5.30.** SEM images of the wear scar on the steel ball counterpart rubbed against Si-doped DLC after variable test duration: low-friction regime (a) and high-friction regime (b, c).

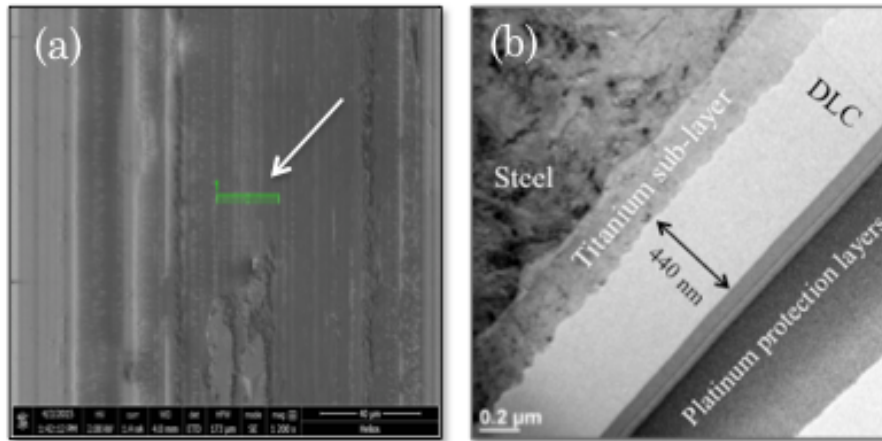
## 4.4. Questions arising from the results presenting above

Although the findings presented in the previous paragraphs are coherent to the proposed model, there are still some points to be discussed:

- a) Plasmon Electron Energy Loss Spectroscopy (PEELS) analysis have been performed to determine whether the hybridization change of carbon onto the DLC plays a key role in accelerating the coating failure mechanisms.
- b) Furthermore, to evaluate if the MoC<sub>x</sub> containing tribofilm formed on the steel ball is much harder than DLC coating, nano-indentation tests have been performed on the tribofilm in order to demonstrate whether the DLC wear is caused by an abrasive mechanism or not.
- c) PEELS and HR-TEM measurements are performed also on the wear debris collected after the tribotest to verify if any structural modification in the DLC carbon network occurs.
- d) Finally, the key role of steel counterpart in the proposed mechanism has been validated by considering the DLC/DLC contact configuration.

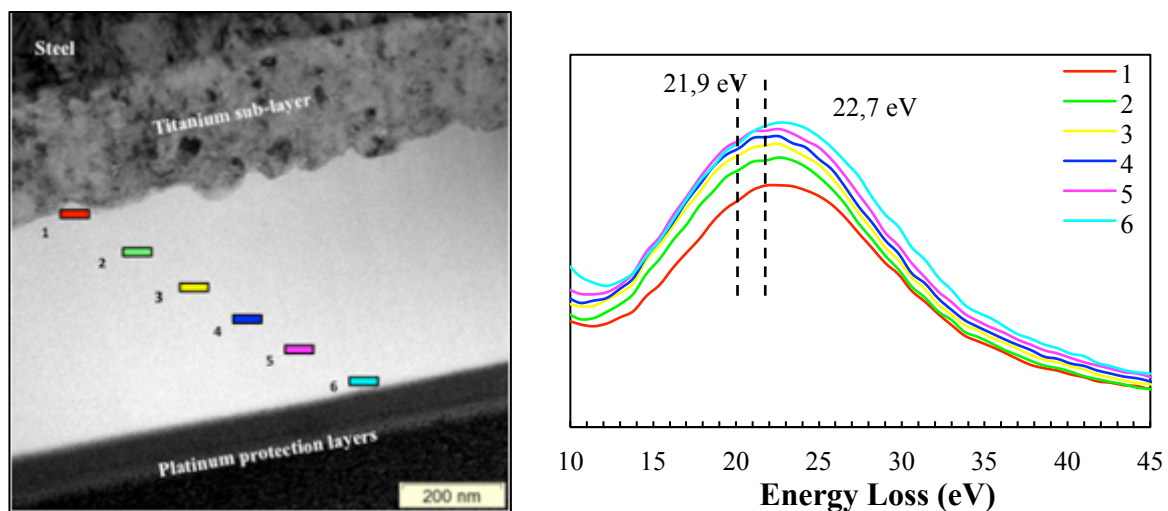
### 4.4.1. PEELS analysis

As has already been discussed previously, it is thought that structural changes may occur to the carbon hybridization of the DLC, resulting in the easier wear removal of the more graphite-based layer that is formed. The wear tracks were analyzed after tribological experiment by means of TEM to determine if the DLC wear mechanism involves this hybridization process. **Figure 5.31(a)** shows the SEM images for the coated flat coupon after the tribotest, which shows the catastrophic damage on the DLC coating. The zone pointed to by the arrow corresponds to the area where the FIB cross-section has been produced.



**Fig. 5.31.** SEM images for the DLC coated flat coupon (a) and DLC coating cross-section after the tribotest (b). The zone where the cross-section has been performed is evidenced in green and pointed to by the arrow.

It can be observed that the DLC coating is much thinner than before (one-third of the original thickness), confirming the high wear produced during the tribotest, although no adhesion failure/delamination was observed. Although the cross-section morphology after the tribotest (**Figure 5.31(b)**) is similar to the previously analyzed untested coating (**Figure 5.24**), the EELS study performed on this cross-section (**Figure 5.32**) shows that the  $sp^2/sp^3$  carbon ratio does not change significantly along the DLC film. In fact, the measurement done on the extreme surface of the remaining DLC coating (light blue curve in **Figure 5.32**) presents just a slight shift to higher electron energy loss values, and thus only a small graphitization can be hypothesized at the top of the DLC coating.

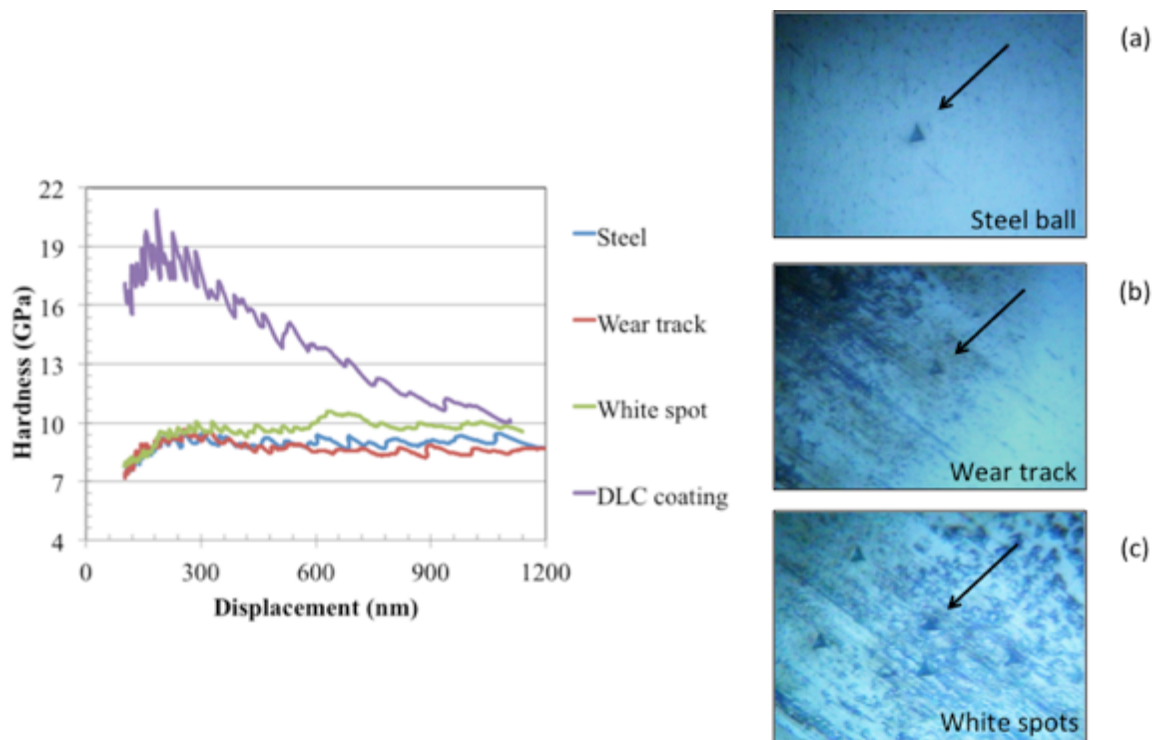


**Fig. 5.32.** Comparison between low-energy loss spectra carried out in different areas of the coating cross-section after the tribotest.

#### 4.4.2. Nano-indentation

Molybdenum carbide is widely used for cutting tools and abrasive materials [24, 27], due to its high hardness (15.5-24.5 GPa) [28]. For this reason, nano-indentation has been employed to evaluate the mechanical properties of the MoC-containing tribofilm formed on the steel ball to know if abrasive wear should be taken into consideration during the observed wear process. The nano-indentation experiments have been carried out by means of MTS nano-intender, equipped with an optical microscope thanks to which is possible to choose a desired area where to perform the measurement. The indentations were carried out using a Berkovich type tip geometry in a dynamic mode (loading rate of  $0.03 \text{ s}^{-1}$ ). Hardness vs. penetration-depth curves were taken using a maximum load of 450 mN. The experiments were performed at least three times on the different locations chosen.

**Figure 5.33** shows the hardness of the different zones identified on the tribofilm. For each indentation performed, the sample was imaged after the test (**Figures 5.33a, 5.33b, 5.33c**).



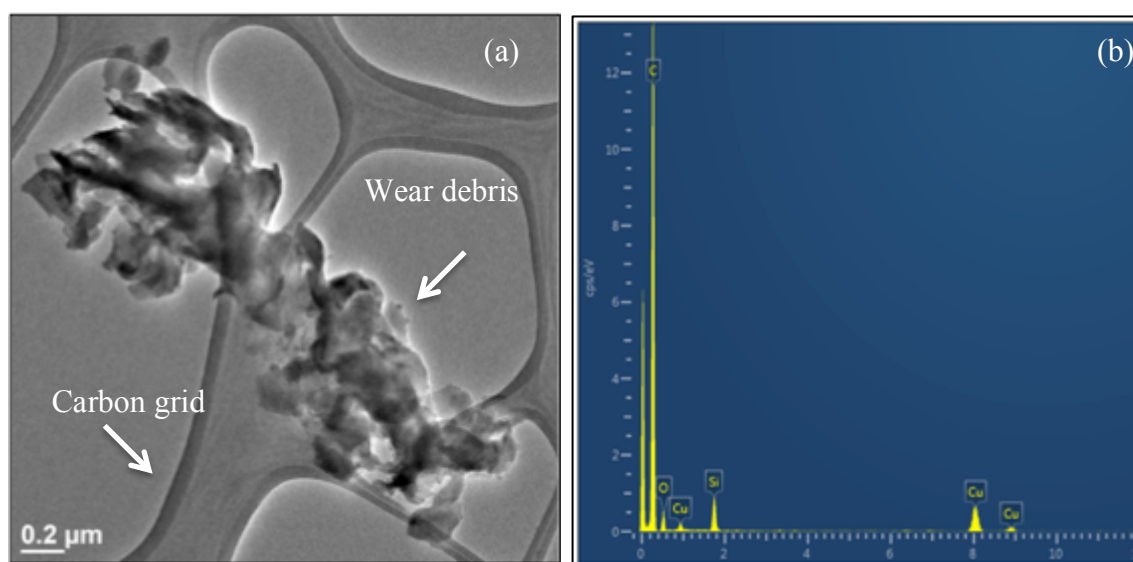
**Fig. 5.33.** Nano-indentation curves for the selected areas: steel substrate (a), wear track (b) and white spots (c).

The values obtained in the 200 nm displacement zone are assumed to be representative of the hardness for the DLC analyzed (19 GPa) and the 100C6 steel substrate used (8-10 GPa). It may be observed that the DLC coating is harder than both the MoC-containing tribofilm

and the standard heat-treated 100C6 steel substrate (62 HRC = approximately 10 GPa). The enhanced hardness value measured for the DLC coating suggests that the abrasive wear of DLC coating by MoC cannot be taken into account in the wear mechanism.

#### 4.4.3. TEM characterization of wear debris

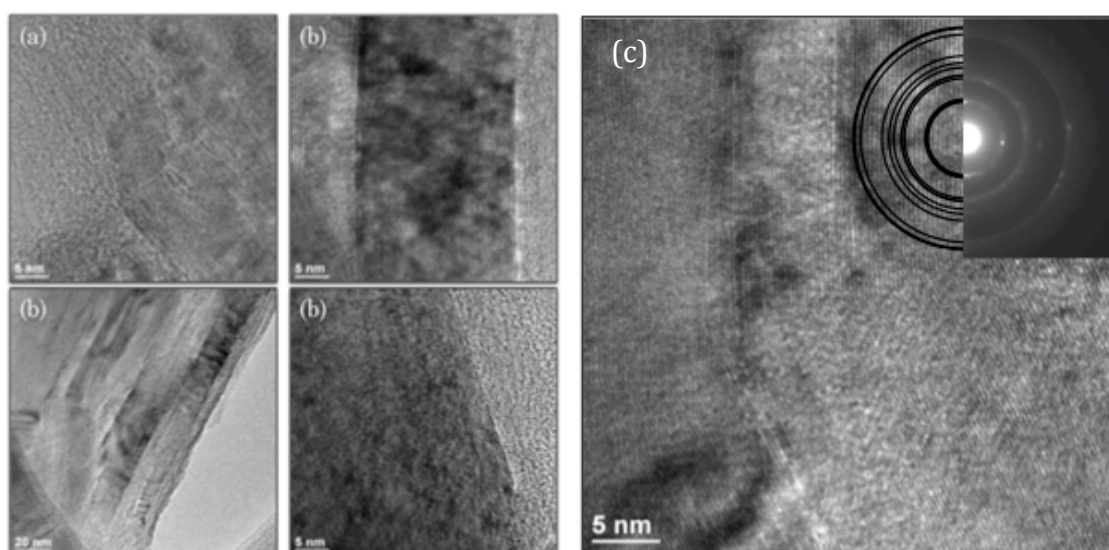
Wear debris was collected from the steel ball after the tribotest and were analyzed by means of TEM/EDX. **Figure 5.34** presents a low-magnification TEM image of the wear debris (a) deposited on a copper grid layered by a holey amorphous carbon film and the EDX spectrum (b), revealing that the particles are mainly made of carbon, with relatively small amounts of silicon and oxygen.



**Fig. 5.34.** Low-resolution TEM image of the wear particles collected from the steel ball slid against the silicon- and oxygen-doped DLC (a). TEM/EDX spectrum carried out on the wear debris (b).



The high-magnification observations (**Figure 5.35**) revealed the presence of crystalline clusters in the particles, having a shape similar to the graphite material.



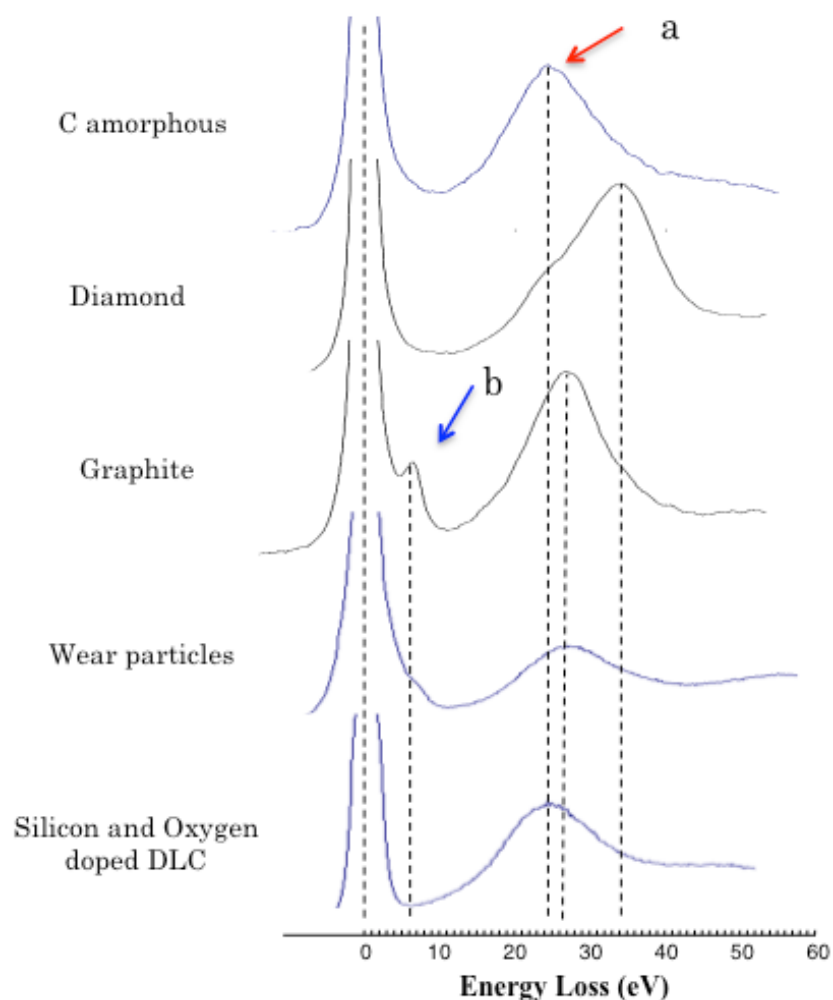
**Fig. 5.35.** High-resolution TEM images of particles inside debris. Note the lattice fringes spaced of 0.34 nm apart and the angular connections between crystals (a) and (b). In inset, the SAED pattern is compared to the theoretical one for graphite.

TEM micrographs exhibit periodic fringes spaced roughly 3.4 Å, which is characteristic of the (0002) lattice planes of graphite. The SAED pattern shown in the inset in the **Figure 5.35(c)** and the comparison between the experimental and theoretical values for the d-spacing of the rings (**Table 5.4**) confirm the graphitic nature of the crystals.

N°	$d_{\text{exp}}$ (nm)	$d_{\text{graphite}}$ (nm)	{hkl}
1	0.395	0.3395	0002
2	0.209	0.2139	10-10
3	0.200	0.2040	10-11
4	0.169	0.1697	0004
5	0.124	0.1235	11-20

**Tab. 5.4.** Comparison between experimental (inset in Figure 5.36) and theoretical d-spacing for graphite.

**Figure 5.36** displays a comparison between the EELS spectra recorded on the cross-section of the virgin DLC and on the wear particles. Spectra recorded on amorphous carbon, diamond and graphite standard materials are also shown for comparison.

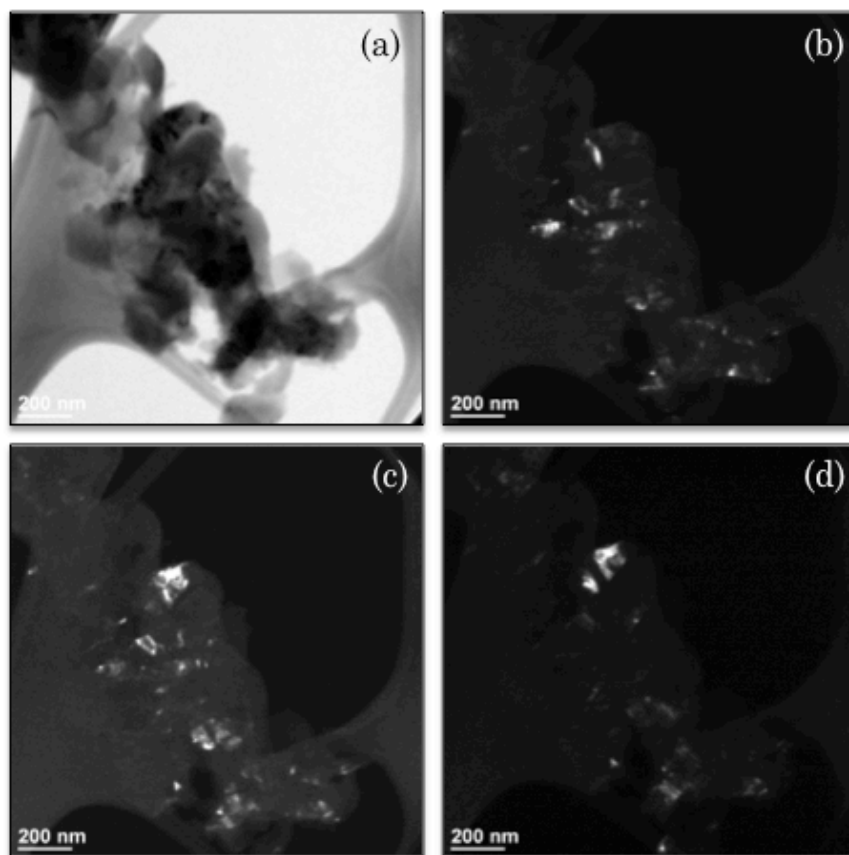


**Fig. 5.36.** Comparison between the EELS spectra recorded on the FIB cross-section of the studied amorphous DLC and the wear particles collected from the steel ball after the tribotest. Amorphous carbon, diamond and graphite spectra are shown for comparison.

As expected, the DLC coating showed similar low energy loss peak (at approximately 24 eV) to that obtained for the amorphous carbon, revealing the amorphous  $sp^2$  carbon rich nature of the coating. However, it is relevant to note that the location of plasmon peak recorded for the wear particles is close to the one of graphite, displaying the mean peak (pointed with red arrow in the **Figure 5.36**) at  $27.0 \pm 0.5$  eV, attributable to  $(\sigma+\pi)$  electron collective excitation [23, 29, 30]. It is also possible to note the presence of a characteristic small peak at approximately 6 eV (pointed with blue arrow in the **Figure 5.36**) due to  $\pi$  electron excitation, which is typically shown by graphite-based material [23, 29, 30]. To



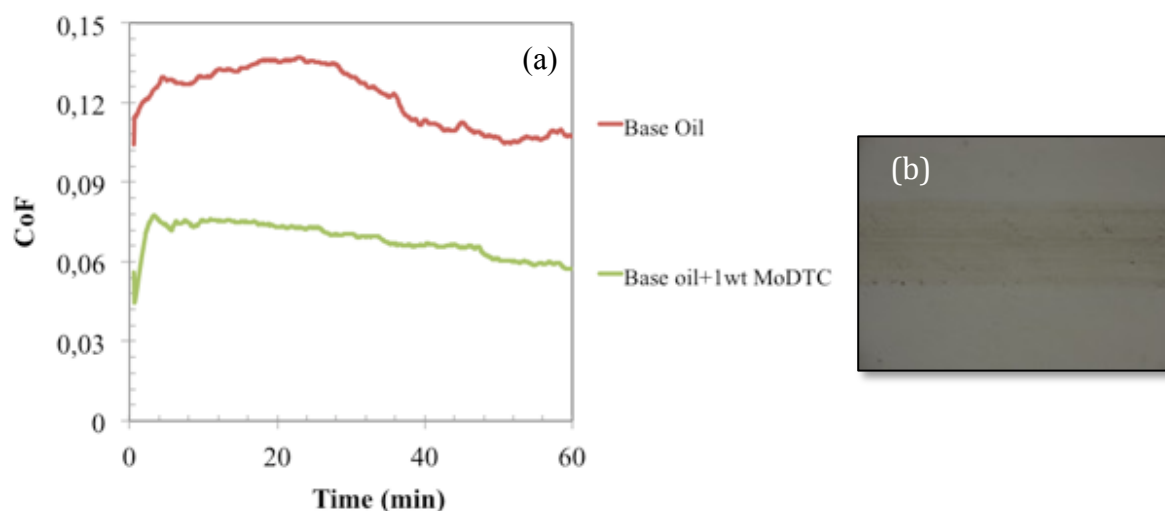
individuate the phase differentiation and the crystal size in the debris specimen, dark-field imaging was used (**Figure 5.37**). The graphitic nano-crystalline structure of the wear particles is evidenced and the crystallite size was found to be in the range of 30 – 100 nm.



**Fig. 5.37.** A bright-field image (a) and a series of dark-field images (b,c,d) taken of the wear particles collected from the steel ball.

#### 4.4.4. Tribological behavior of DLC/DLC tribo-pairs

To study the catalytic role of the steel in the DLC wear mechanisms, the DLC/DLC tribo-pair configuration has been tested. The friction coefficient versus time curves obtained in the presence of base oil alone and with MoDTC-containing base oil are plotted in **Figure 5.38**. The base oil gave a relatively high friction coefficient, approximately 0.12, a value similar to those obtained for the steel/steel and steel/DLC configurations. However, blending 1% in wt. of MoDTC into the base oil leads to a consistent reduction in friction. In this case, the wear produced on the silicon-doped DLC-coated flat coupon is much less significant than that in the previous steel/steel configuration (**Figure 5.38 (b)**).



**Fig. 5.38.** Friction behavior of a-C:H:Si:O DLC/ a-C:H:Si:O DLC tribo-pairs configuration lubricated by MoDTC-containing base oil (a). Friction wear track on the silicon-doped DLC flat coupon (b). Value to be compared to Figure 5.1 and 5.2.

The results shown in this chapter validate the hypothesis that testing steel/DLC configuration the tribofilm was generated by a chemical reaction between the molybdenum atoms adsorb on the steel ball and the carbon of the DLC coating. Moreover, using TEM characterization it has been possible to demonstrate that graphitic-based material could be present as well in the tribofilm (steel/DLC contact). This result could be explained supposing that the parts of DLC transferred on the steel ball after the reaction with the molybdenum, show a graphitization due to the temperature and/or the mechanical stresses induced during the tribotest. However, an alternative pathway involving the hydrogenated-DLC as a carburizing reagent can be proposed. Based on the work of Wang *et al.* [31] on the synthesis of molybdenum carbides, direct carburization of  $\text{MoO}_3$  by  $\text{C}_2\text{H}_6/\text{H}_2$  gas mixture produces  $\text{MoC}_x$  with excess graphitic carbon. This could be proved investigating hydrogen-free carbon coatings and showing that they are less sensitive to chemical wear by MoDTC.

These findings allow the authors to propose for the first time a multi-steps wear model, schematized in **Figure 5.39**. In particular, it has been confirmed that the principal cause of the wearing out of DLC when lubricated with MoDTC is the formation of molybdenum carbide crystallites on the steel ball, during the tribotest against a-C:H:Si:O DLC. The key role of steel in the wear mechanism has also been demonstrated. In fact, the test performed using the DLC/DLC configuration gave lower friction reduction and much lower wear was obtained for the DLC. In this case, no molybdenum carbide compound was detected on the rubbed surfaces. The origin of this interesting tribological behavior (DLC/DLC lubricated by MoDTC oil) was not further investigated here.

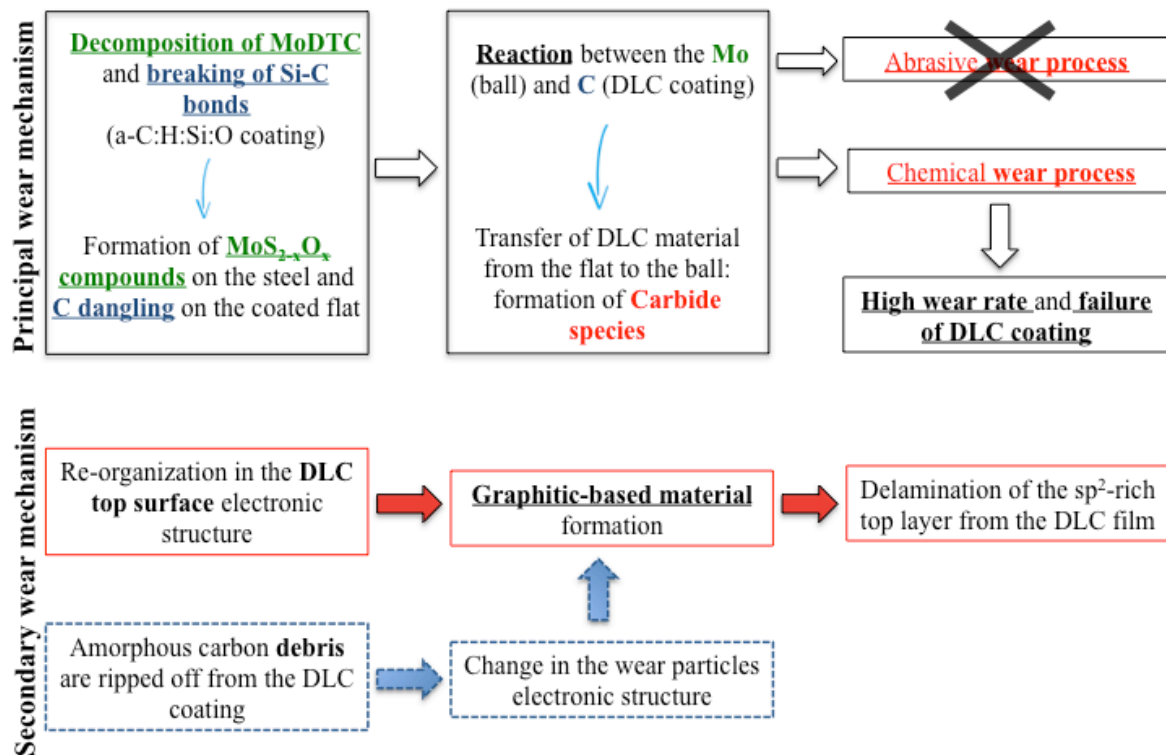


Fig. 5.39. Schematic representation for the new proposed wear model

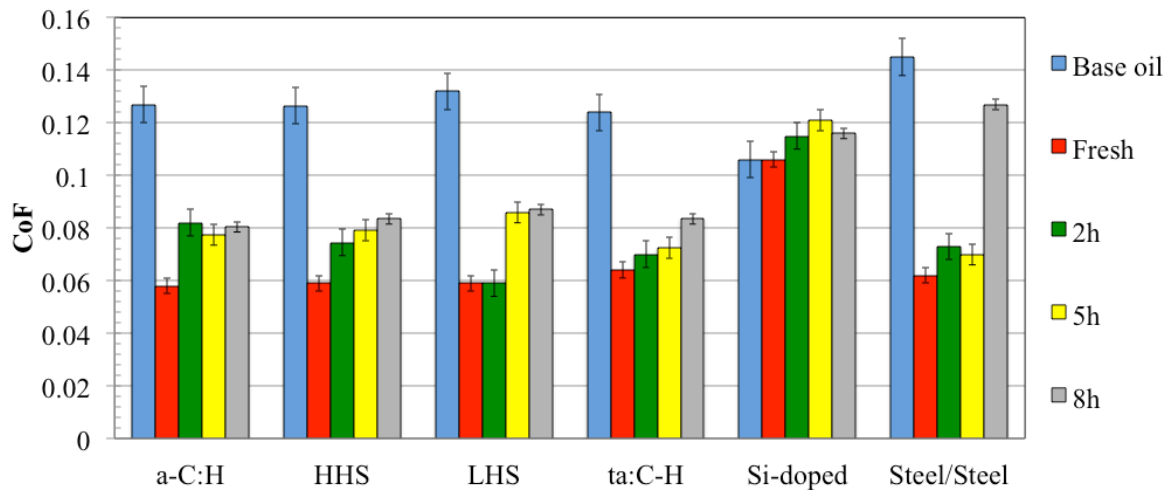
The  $\text{sp}^3 \rightarrow \text{sp}^2$  re-hybridization during the tribological test could be considered a secondary process in the wear mechanism in comparison to the chemical reaction leading to the formation of the carbide compound. In fact, almost no difference in  $\text{sp}^2/\text{sp}^3$  ratio has been clearly detected along the coating in the DLC cross-section after friction. However the presence of graphitic material in the wear debris was clearly evidenced. Two different methods for the formation of graphitic carbon can be proposed. It can be hypothesized that the temperature and the mechanical stresses induced during friction cause the re-hybridization of the carbon bonding on the top DLC surface. Then, the resulting softer graphitic top layer can be easily removed from the surface of the DLC coating producing a slight delamination of the DLC (red path in **Figure 5.39**). However, it could also be supposed that amorphous DLC debris are ripped off from the coating surface because of the severe conditions in the contact and that, during the shearing, there is a re-hybridization in the amorphous carbon network, leading to graphite crystallites formation (blue path in the graph). However, based on the results obtained, it is difficult to fully explain the transformation of the coating structure from amorphous DLC to polycrystalline graphite that is clearly observed in the tribofilm formed on the steel ball and in the wear debris collected.

## 4.5. Influence of MoDTC degradation on DLC/steel-involving contact

In order to get further understanding on the interaction between DLC and MoDTC additive, the effect of lubricant degradation on the DLC/steel contact has been investigated and it is presented in the following.

### 4.5.1. Friction and wear performance

The values of steady state friction coefficient (CoF) as a function of different DLC coatings for fresh and aged oils are given in **Figure 5.40**.

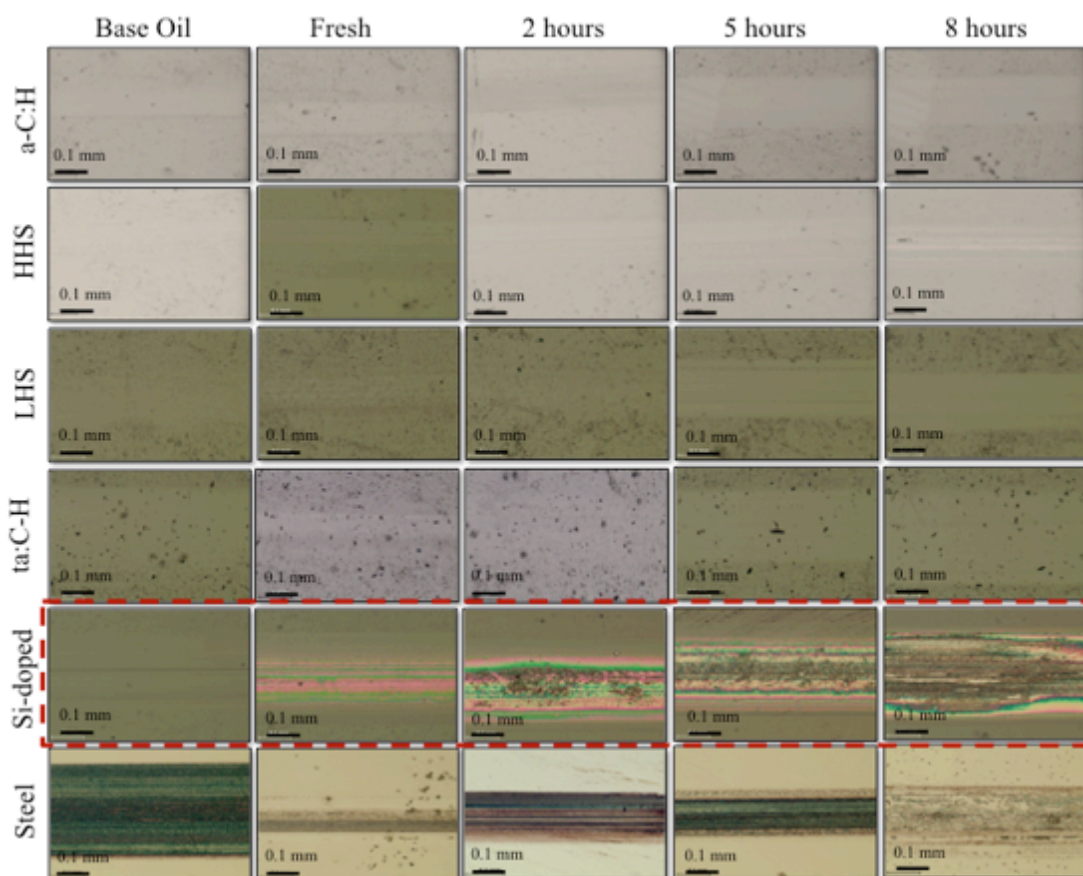


**Fig 5.40.** Steady-state friction coefficient for different DLC coatings lubricated with for fresh and aged oils.

The comparison of the degraded MoDTC-containing base oil on different DLC coatings (**Figure 5.40**) indicates that the ageing process can lead to slightly poorer MoDTC performance. In particular, employing aged oil the steady-state friction coefficient obtained was around 0.08, instead of 0.06-0.07 for steel/steel contact for both fresh and aged oil. At the same time, it can be noted that the oil ageing process impacts less on DLC/steel contact than steel/steel one. In fact, the DLC coating gave lower friction coefficient than steel/steel also during test with 8 hours degraded oil. However, by comparing wear data, it was found that the oil degradation tends to accelerate their wear rates.

The optical images of wear scar on DLC coated flats are shown in **Figure 5.41**. Almost invisible wear was observed for the first four DLCs, when employing low oxidized oil, only a gradual polishing wear is noticeable. The brighter color of wear track suggests that high-

oxidized oils cause higher wear. The Si-doped DLC coating is completely worn out, regardless of the ageing time.



**Fig 5.41. Optical images of wear scars formed on DLC coatings along with degradation time.**

By comparing wear data for the DLC-coated flats lubricated with fresh and aged oils, it was found that, also in the case of degraded oils, the Si-doped DLC shows catastrophic wear (**Figure 5.42**).

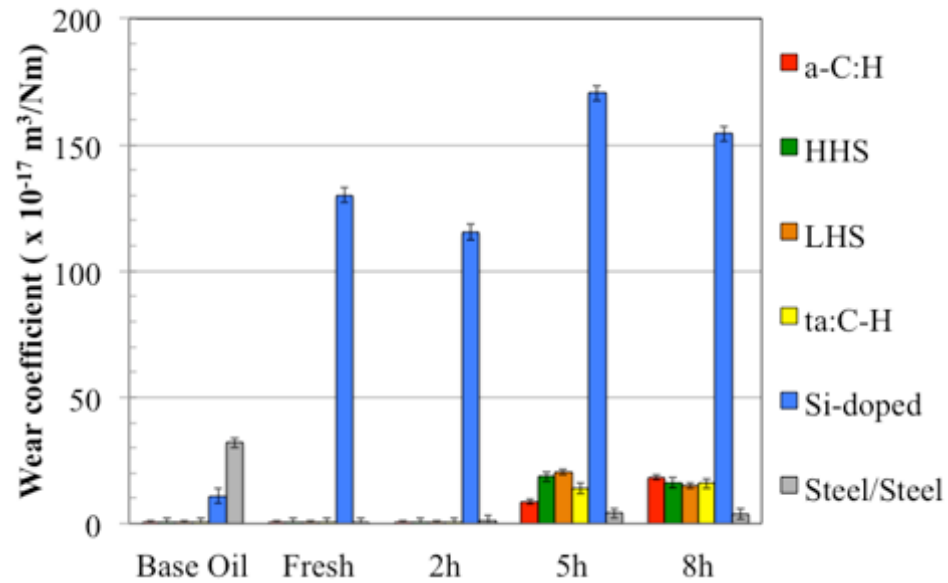


Fig 5.42. Wear coefficient of DLC flats and steel calculated by means of interferometry.

To compare the wear data, the wear coefficient related to a-C:H:Si:O DLC has been removed from the graph (Figure 5.43). It is possible to note that the oil degradation tends to accelerate their wear rates.

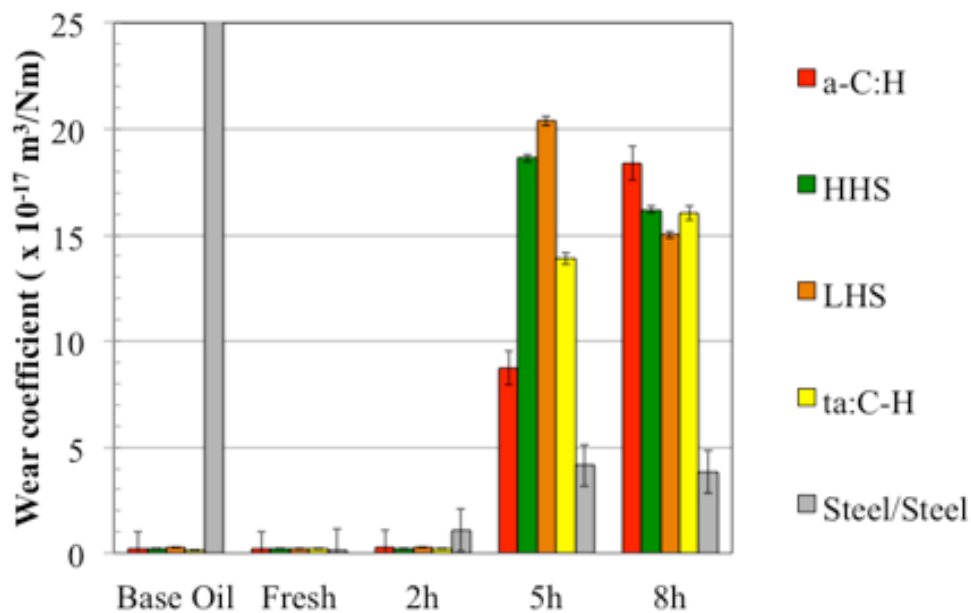


Fig 5.43. Wear coefficient of DLC flats and steel calculated by means of interferometry without a-C:H:Si:O DLC.

The results are in good agreement with the wear scar images shown in Figure 5.41, confirming that the longer time for oil ageing, the higher the wear coefficient results are. The wear coefficient are also higher if compared to the one showed with steel/steel contact.

## 5. CONCLUSIONS

In this study, the boundary lubrication of different DLC coatings is investigated in mild wear conditions in the presence of MoDTC additive. A number of these coatings show the effective performance of the MoDTC additive in reducing friction coefficient compared to additive free base oil. However, the silicon and oxygen doped DLC coating (a-C:H:Si:O DLC) is the only one showing relatively high friction combined with dramatic wear.

The severe wear of DLC coatings lubricated with MoDTC has been widely reported in the literature by different authors, but the major cause of it has not been clearly identified yet. All the tribological experiments and analytical results presented in this chapter provide strong support for the conjecture that the formation of a molybdenum carbide compound is an important step in the mechanism governing the wear of DLC coatings sliding against a steel counterpart in the presence of MoDTC additive. The formation of this carbide compound is evidenced for the first time on the steel counterpart surface. A new wear scenario has been proposed, consisting of different steps:

- During the initial running-in period, the MoDTC additive reacts preferentially with the steel surface, forming a  $\text{MoS}_2$  and/or  $\text{MoS}_{2-x}\text{O}_x$ -based tribofilm on the steel, compounds able to lower the friction coefficient;
- During further sliding, this molybdenum-based tribofilm interacts with the carbon surface dangling bonds of the Si-doped DLC generated by the breaking of the Si-C bond network;
- The reaction between the molybdenum present in the tribofilm formed on the steel counterpart and the carbon of the DLC coating leads to the formation of molybdenum carbide ( $\text{Mo}_x\text{C}$ ) species, resulting in an increase in the friction and wear rate as suggested by the surface analyses.

To gain insight into drastic DLC wear induced by MoDTC lubrication, post-mortem analyses have been performed and the following findings have been obtained.

The presence of molybdenum carbide ( $\text{MoC}$ ) on the steel counterpart that was slid against silicon-doped DLC has been evidenced by the TEM/EDX analysis of FIB cross-section samples. Important understandings were obtained through crystallographic studies.

To prove the importance of the chemical wear in comparison to the abrasive wear, the tribofilm hardness value is obtained from the nano-indentation curves. Considering that the tribofilm's mechanical properties are similar to those of the steel substrate, it is believed that no abrasive wear is produced during the tribo-test. Nevertheless, the thickness of the

tribofilm doesn't allow an accurate measurement of the hardness and most probably MoC hard particles are embedded in the tribofilm so their hardness would not be representative of the nano-hardness measurements.

The key role of iron in the proposed mechanism has been confirmed by the DLC/DLC configuration tribotest, showing that a lower friction value and less significant wear have been obtained in this last case. It has also been shown that the re-hybridization of the carbon network seems to not act fully as a DLC failure and possibly only facilitates the initialization of the reaction leading to the generation of the molybdenum carbide species on the steel counter-part.

It seems that the degradation of MoDTC-containing base oil has less impact on the DLCs/steel contact than the steel/steel one. Indeed, after 8 hours of oil ageing it is still possible to have friction reduction with some DLC coatings even if higher wear is produced in comparison with the fresh oil.

At this stage it is complicated to go deeper into the exact chemical wear mechanisms. Further thermodynamic studies and especially molecular dynamic and quantum chemistry simulations could help to elucidate the complex chemistry behind the molybdenum carburizing process and the graphitic re-hybridization of the amorphous DLC coating. In addition, it would be possible to deeply investigate the effect of the Si element introduction inside the amorphous DLC network on this carburizing process.

Although the chemical wear mechanisms remain unclear, these results might be helpful in developing a new MoDTC-containing lubricant (considering interactions with other additives) and a different DLC composition or structure compatible with the MoDTC friction modifier. More information about binary additive combinations effect on DLC wear will be reported in the following chapter.



## 6. BIBLIOGRAPHY

- [1] Jacob W., Moller W., On the structure of thin hydrocarbon films, *Applied Physics Letters*, Volume 63(13), Pages 1771-3, (1993).
- [2] Robertson J. Diamond-like amorphous carbon. *Materials Science & Engineering R-Reports.*, Volume 37, Pages 129-281, (2002).
- [3] Hainsworth S.V., Uhure N.J., Diamond like carbon coatings for tribology: production techniques, characterization methods and applications. *Int Mater Rev.*, Volume 52(3), Pages 153- 74, (2007).
- [4] Kosarieh S; Morina A; Lainé E; Flemming J; Neville A., The effect of MoDTC-type friction modifier on the wear performance of a hydrogenated DLC coating. *Wear*, Volume 302, Pages 890-898, (2013).
- [5] Shinyoshi T, Fuwa Y., Ozaki Y., Wear analysis of DLC coating in oil containing Mo-DTC, *JSAE 20077103*, SAE 2007-01-1969.
- [6] Haque T., Morina A., Neville A., Kapadia R., Arrowsmith S., Effect of oil additives on the durability of hydrogenated DLC coating under boundary lubrication conditions, *Wear*, Volume 266, Pages 147-157, (2009).
- [7] Kubo K., Mitsuhiro N., Shitamichi T., Motoyama K., The effect of ageing during engine running on the friction reduction performance of oil soluble molybdenum compounds, *Proceeding of the international tribology conference*, Yokohama, (1995).
- [8] De Barros Bouchet M.I., Martin J.M., Le Mogne Th., Bilas P., Vacher B., Yamada Y., Mechanisms of MoS<sub>2</sub> formation by MoDTC in presence of ZnDTP. Effect of oxidative degradation. *Wear*, Volume 258, Pages 1643, (2005).
- [9] Masabumi M., Takuya O., Saiko A., Akihito S., Hirotaka I., Friction and wear characteristics of DLC coatings with different hydrogen content lubricated with several Mo-containing compounds and their related compounds, *Tribology International*, Volume 82, part B, Pages 350–357, (2015).
- [10] Sugimoto I., Honda F., Inoue K., Analysis of wear behavior and graphitization of hydrogenated DLC under boundary lubricant with MoDTC, *Wear*, Volume 305, Issues 1–2, Pages 124-128, (2013).
- [11] De Barros Bouchet M.I., Matta C., Vacher B., Le-Mogne Th., Martin J.M., J. von Lautz, Ma T., Pastewka L., Otschik J., Gumbsch P., Moseler M., Energy filtering transmission electron microscopy and atomistic simulations of tribo-induced hybridization change of nanocrystalline diamond coating, *Carbon* 06, 87, (2015).

- [12] Voevodin A.A., O'Neill JP, Zabinski JS. Tribological performance and tribochemistry of nanocrystalline WC/amorphous diamond-like carbon composites. *Thin Solid Films*, Volume 342, Pages 194-200, (1999).
- [13] Singh V., Jiang J.C., Meletis E.I., Cr-diamondlike carbon nanocomposite films: Synthesis, characterization and properties. *Thin Solid Films.*, Volume 489, Pages 150-8, (2005).
- [14] Wu W.J., and M.H. Hon, The effect of residual stress on adhesion of silicon containing diamond- like carbon coatings, *Thin Solid Films*, Volume 345, Pages 200-207, (1999).
- [15] Camargo Jr S.S., A.L. Baia Neto, R.A. Santos, F.L. Freire Jr., R. Carius, and F. Finger, Improved high-temperature stability of Si incorporated a-C:H films, *Diamond and Relat. Mater*, Volume 7, Pages 1155-1162, (1998).
- [16] Camargo Jr S.S., A.L. Baia Neto, R.A. Santos, F.L. Freire Jr., R. Carius, and F. Finger, Improved high-temperature stability of Si incorporated a-C:H films, *Diamond and Relat. Mater.*, Volume 7, Pages 1155-1162, (1998).
- [17] Grossiord C., Varlot K., Martin J.M., Le Mogne Th., Esnouf C., Inoue K., MoS<sub>2</sub> single sheet lubrication by molybdenum dithiocarbamate. *Tribol Int*; Volume 31, Pages 737–43, (1998).
- [18] Schriver, Atkins, Langford. *Inorganic chemistry*. 2nd ed.Oxford University Press; (1994).
- [19] Katsuhiko Oshikawa , Masatoshi Nagai and Shinzo Omi, Characterization of Molybdenum Carbides for Methane Reforming by TPR, XRD, and XPS, *J. Phys. Chem. B*, Volume 105 (38), Pages 9124–9131, (2001).
- [20] E. Rudy, F. Benesovsky and L. Toth, Untersuchung der Dreistoff systeme der Va und VIa-Metalle mit Bor und Kohlenstoff, *Z. Metallk.*, Volume 54, Pages 345, (1963).
- [21] Holcombe C.E., USAEC Oak Ridge Y-12 Plant Report, Y-1887 (1973)
- [22] Oguri K. and Arai T., Tribological properties and characterization of diamond-like carbon coatings with silicon prepared by plasma-assisted chemical vapor deposition, *Surface and coating Technology*, Volume 47, Pages 710-721, (1991).
- [23] Neerincx D., Diamond-like nanocomposite coatings for low-wear and low-friction applications. *Diam Relat Mater*; Volume 7, Pages 468-71, (1998).
- [24] Scharf T.W., Ohlhausen J.A., Tallant D.R., Prasad S.V., Mechanisms of friction in diamond-like nanocomposite coatings, *J Appl Phys*, Volume 101, (2007).

- [25] Egerton R.F., *Electron Energy Loss Spectroscopy in the Electron Microscope*, Plenum Press, NewYork, (1986).
- [26] Joly-Pottuz L., Matta C., De Barros Bouchet M.I., Vacher B., Martin J.M., Sagawa T. Superlow friction of ta-C lubricated by glycerol: An electron energy loss spectroscopy study. *J Appl Phys*, Volume 102, Pages 1–9, (2007).
- [27] T. Hachisuka, Role of Molybdenum Carbide in Promoting Densification During Sintering of TiC-TiN-Mo sub 2 C-Cr sub 3 C sub 2 Ceramic Composite, *Journal of the Japan Society of Powder and Powder Metallurgy*, Volume 38, Pages 145-152, (1991).
- [28] Hugh O. Pierson, *Handbook of refractory carbides and nitrides: properties, characteristics, processing, and applications*, William Andrew, Pages 106, (1996).
- [29] Fink J., Muller Th. Heinzerling, J. Pflüger, B. Scheerer, B. Dischler, P. Koidl, A. Bubenzer, R.E. Sah, Investigation of hydro-carbon plasma generated carbon films by electron energy loss spectroscopy, *Phys. Rev. B*, Volume 30(8), Pages 4713–4718, (1984).
- [30] Prawer S., Rossouw C.J., Structural investigation of helium ion- beam-irradiated glassy carbon, *J. Appl. Phys.*, Volume 63 (9), Pages 4435–4439, (1988).
- [31] Wang X.H., Hao H.L., Zhang M.H., Li W., Tao K.Y., Synthesis and characterization of molybdenum carbides using propane as carbon source, *Journal of Solid state Chemistry*, Volume 179, Pages 538-543, (2006).



# Chapter 6

---

## Binary Additive Combinations

---

*In this chapter, the preliminary study on the interaction between MoDTC and three additives (ZDDP, antioxidant and dispersant) is reported. It has been noted that when fully formulated lubricant is aged, no suspended product is obtained even after a long degradation period (more than 150 hours). To understand how an additive is able to avoid/reduce particle formation in the fully formulated oil, the behavior of MoDTC in binary combinations with other additives has been analyzed. The MoDTC concentration in these blends has been followed by means of liquid chromatography and the possible formation of reaction by-products has been monitored using mass spectroscopy. At the end, the impact of the binary combinations on the tribological behavior has been studied, using both steel/steel and DLC/contact.*

# Chapter 6

---

## Binary Additive Combinations

---

*Dans ce chapitre, nous avons rapporté l'étude préliminaire sur l'interaction entre le MoDTC et trois autres additifs (le ZDDP, un antioxydant et un dispersant). Il a été noté que, lorsque le lubrifiant entièrement formulé est vieilli, nous n'avons pas obtenu de produits de dégradation en suspension (type particule), même après une longue période (plus de 150 heures). Pour comprendre quels additifs sont capables d'éviter/réduire la formation de particules dans l'huile entièrement formulée, nous avons analysé le comportement du MoDTC dans des combinaisons binaires avec d'autres additifs. Nous avons suivi la concentration du MoDTC dans ces mélanges avec la chromatographie liquide et la formation possible de sous produits de réaction a été contrôlée en utilisant la spectroscopie de masse. L'impact des combinaisons binaires sur le comportement tribologique a été étudié ensuite, dans le cas du contact acier/acier, mais aussi du contact DLC/acier.*

# 1. INTRODUCTION

Recently, great attention has been paid to the investigation of MoDTC performance when blended into an additive package since its effectiveness may be strongly affected by synergistic or antagonistic effects from the interactions with other lubricant additives.

## 1.1. Zinc Dialkyl Dithiophosphate (ZDDP)

A significant number of papers have addressed the interactions between MoDTC and the most commonly used anti-wear additive in engine oil [9, 10], the zinc dialkyldithiophosphate (ZDDP). Although the mechanisms of friction reduction based on the interaction of those two additives is still not fully understood, the different authors agree upon the fact that the lubricant performance is improved when the combination is tested in comparison to single-additivated base oil. It has been widely reported, in fact, that when MoDTC is blended to ZDDP, a synergistic effect on friction and wear performance is observed [1, 2, 14-17]. Muraki *et al.* has suggested that the reaction products of ZDDP decomposition have a key role in enhancing wear resistance and promoting the formation of MoS<sub>2</sub> [3]. Grossiord *et al.* reported that a glass-like film derived from ZDDP prevented the oxidation of MoS<sub>2</sub> lamellar sheets [4]. This hypothesis is confirmed by Iwasaki *et al.*, who labeled the ZDDP molecule with <sup>34</sup>S isotope and demonstrated that about 40% of the sulfur in MoS<sub>2</sub> formed on the rubbing surfaces was generated by ZDDP [5]. Yagishita *et al.* [6] has proposed the scenario shown in **Figure 6.1** for MoDTC exchange with ZDDP. Mo(DTC)<sub>2</sub> and Zn(DTP)<sub>2</sub> exchanges reversibly intermediate products Mo(DTC)(DTP) and Zn(DTP)(DTC) and further, reversibly, to Mo(DTP)<sub>2</sub> and Zn(DTC)<sub>2</sub>.

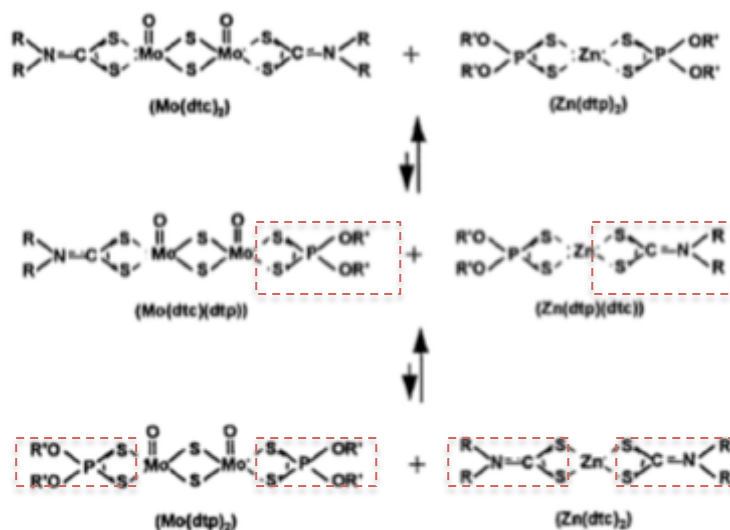


Fig. 6.1. Ligand-exchange reactions in the MoDTC/ZDDP mixture from [6].

Minami, *et al.* [12] has shown that the addition of sulfur-containing additives may improve the friction-reducing properties of the molybdenum-containing lubricant. The same hypothesis has been proposed by De Barros M.I. *et al.* [13]. Both authors suggested that the addition of sulfur results in an increased concentration of MoS<sub>2</sub> as a reaction product. They suggested that the ZDDP molecule provides sulfur atoms to complete the sulfuration of lamellar sheets, reducing the possibility to follow the pathway leading to MoO<sub>3</sub> formation (Figure 6.2).

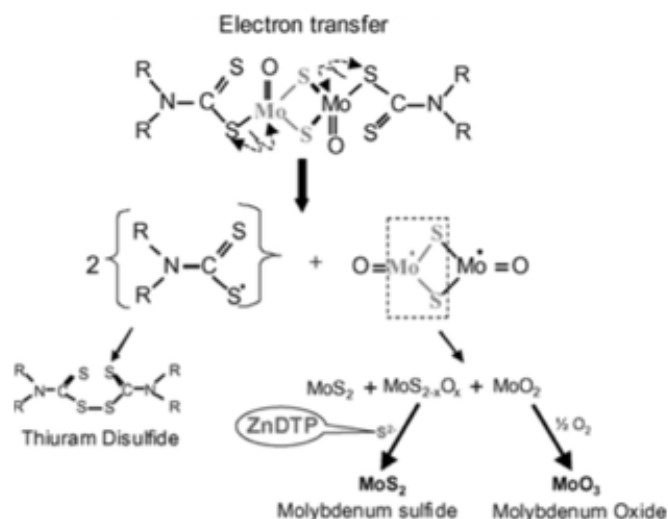


Fig. 6.2. Chemical process of MoS<sub>2</sub> formation in the presence of ZDDP additive [13].

## 1.2. Antioxidant

Kubo *et al.* reported that some antioxidants are able to enhance the friction-reducing capabilities of soluble molybdenum-containing additives [8]. This could be in agreement with the oxidation mechanisms proposed in this thesis. It has been suggested, in fact, that the MoDTC additive oxidizes in preference to the base oil and therefore it is depleted along the degradation process. MoDTC additive depletion might be limited in the presence of other antioxidants. To validate the supposed MoDTC depletion mechanisms, the investigation of the binary combination MoDTC+antioxidant could reveal important information.

## 1.3. Dispersant

It is also well known that molybdenum-containing additives have a low solubility in the base oil that prevents them from being used in many commercial formulations [7]. This drawback is overcome by combining them with dispersant additive. In the author's knowledge, the study of synergistic or antagonistic effect of such combinations has not been deeply



investigated. The only work addressed to MoDTC/dispersant combination is carried out by Wei and his co-authors [11]. They reported that the addition of a dispersant additive might enhance molybdenum additive response. It is evident that further analyses are needed to understand the effect of dispersant on the MoDTC performance.

## **2. OBJECTIVES**

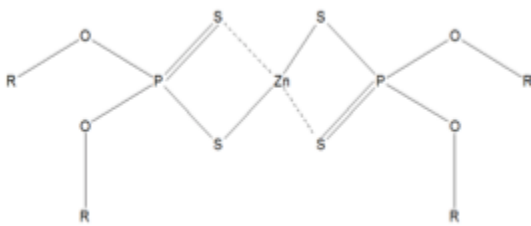

The main purpose of this chapter is to study the interactions between MoDTC and the three common additives presented above, used in commercial fully formulated lubricants and their impact on the degradation of MoDTC additive.

Initially, the visual inspection is carried out in order to determine if the carbonaceous particle formation obtained during MoDTC-containing base oil degradation is avoided (or at least reduced) by the addition of another additive. Further analyses have been done by means of liquid chromatography and mass spectroscopy in order to get more information about the possible chemical interactions between the different molecules present in the binary mixtures. At the end, the effects of those interactions on the tribological performance of their blends are evaluated in steel/steel contact and DLC/steel contact.

### 3. MATERIALS

Three different additives were blended to the MoDTC-containing base oil in order to investigate their influence on MoDTC durability.

It has been decided to study the addition of a commercial ZDDP mixture composed of three different ZDDP compounds (**Table 6.1**), and also of an amine antioxidant and a dispersant. The mixtures are prepared following the same procedure described in the chapter 2. The general chemical structures of ZDDP additives used for this study are shown in **Table 6.1**.

Schematic ZDDP molecular structure	Alkyl group	MW
(a) 	C <sub>6</sub>	661
	C <sub>8</sub>	773
(b) 	C <sub>8</sub>	1191

**Tab. 6.1. General chemical structures of the three ZDDP species present in the mixture**

The antioxidant and the dispersant have been provided by Total, but little information was available about their chemical composition.

The additive concentrations for the binary combinations are listed in **Table 6.2**.

Binary combinations	MoDTC	ZDDP	Antioxidant	Dispersant
<b>A</b>	1%	1%	-	-
<b>B</b>	1%	-	1%	-
<b>C</b>	1%	-	-	5%

**Tab. 6.2. Mixtures composition**

## 4. METHODS

It has been decided to analyze the impact of binary combinations employing liquid chromatography and mass spectroscopy (for the methodology refers to chapter 3) in order to get a better understanding of the chemical interactions between additives. Afterwards, the impact of these mixtures on tribological properties has been studied: the influence of degradation process has been investigated using steel/steel contact (same methodology described in chapter 2) and DLC/Steel contact (same methodology described in chapter 4) to evaluate the possibility to reduce DLC wear during MoDTC-involving lubrication adding another additive.

## 5. RESULTS

### 5.1. Visual Inspection

As already reported earlier in this thesis, the first evidence of the MoDTC degradation is the color alteration. It has been shown that the mixture changes from light green for the fresh oil to completely black oil after 8 hours of ageing, mainly due to solid-like particle formation. It is important to point out that when fully formulated lubricant is aged, no suspended product is obtained even after much longer degradation time (more than 150 hours in the same oxidative conditions).

From **Figures 6.3**, it can be noted that adding the ZDDP or antioxidant additive to the mixture leads to a delay in the formation of particles. In fact, in the case of these two mixtures, after 8 hours the formation of solid suspensions is much reduced in comparison to MoDTC-containing base oil. However, the mixture MoDTC+dispersant, even after 8 hours of degradation, does not present any visible formation of particles.

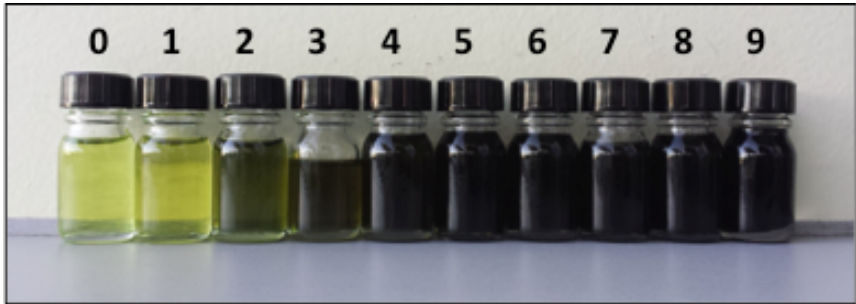

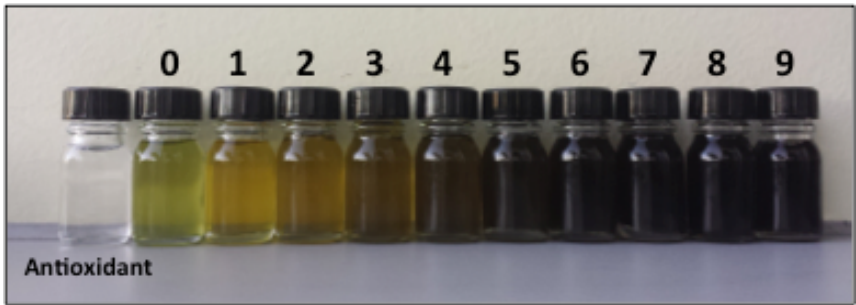
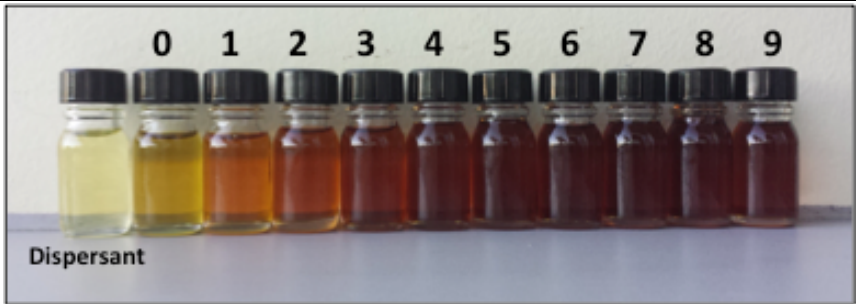
<p>Base oil + 1%wt <b>MoDTC</b></p>	
<p>(A) Base oil + 1%wt <b>MoDTC</b> + 1%wt <b>ZDDP</b></p>	
<p>(B) Base oil + 1%wt <b>MoDTC</b> + 1%wt <b>Antioxidant</b></p>	
<p>(C) Base oil + 1%wt <b>MoDTC</b> + 5%wt <b>Dispersant</b></p>	

Fig. 6.3. Visual inspection of the three mixtures analyzed in this chapter.

## 5.2. Liquid Chromatography

In **Figure 6.4**, the MoDTC additive depletion along the degradation time is plotted, measured by means of liquid chromatography for the different mixtures studied. It can be clearly noted that the addition of the ZDDP additive leads to a delay in MoDTC

consumption. In fact, after 8 hours, 60% of MoDTC is still present in the mixture. Even better results are obtained blending to the MoDTC-containing base oil 1% of antioxidant or 5% of dispersant. In fact, at the end of the thermo-oxidative process, the concentration of MoDTC in both mixtures seems to be above 80%.

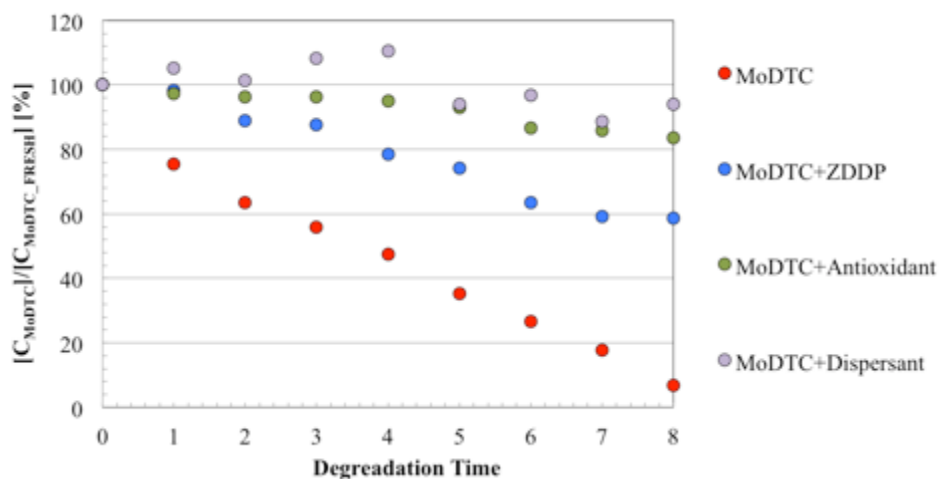


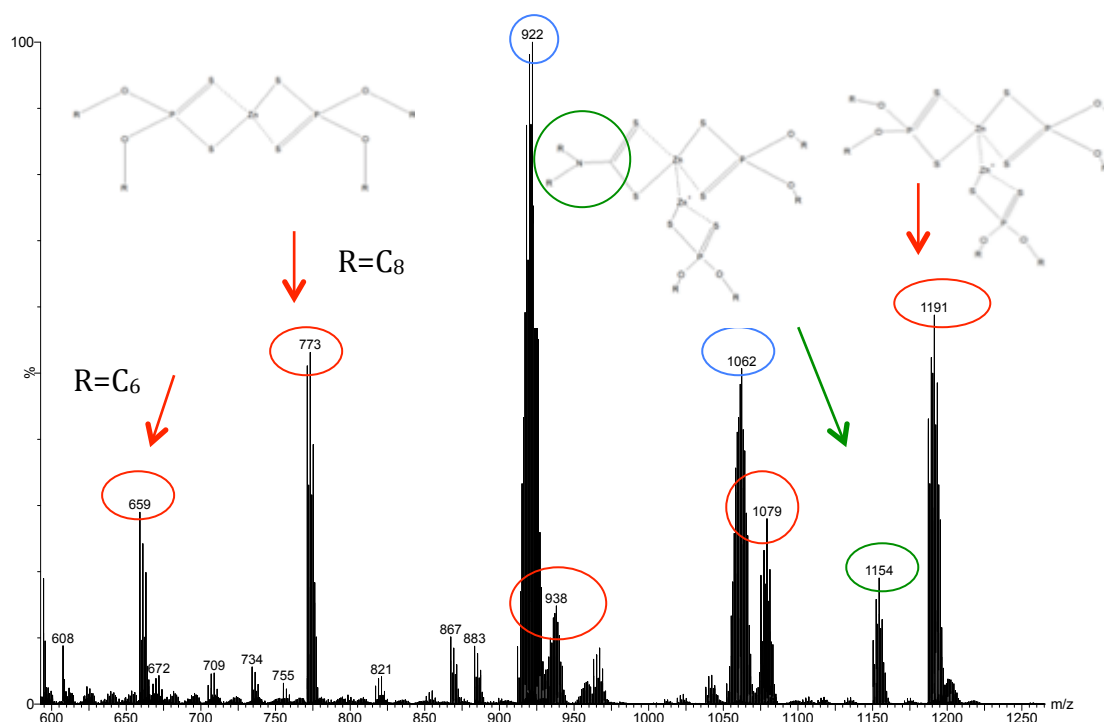
Fig. 6.4 MoDTC depletion throughout the degradation process in the binary combination mixtures.

### 5.3. Mass spectroscopy

The various mixtures are analyzed by means of mass spectroscopy in order to investigate the interactions between the additives from a chemical point of view, and to map possible reaction products formed throughout the degradation process.

#### (A) MoDTC+ZDDP

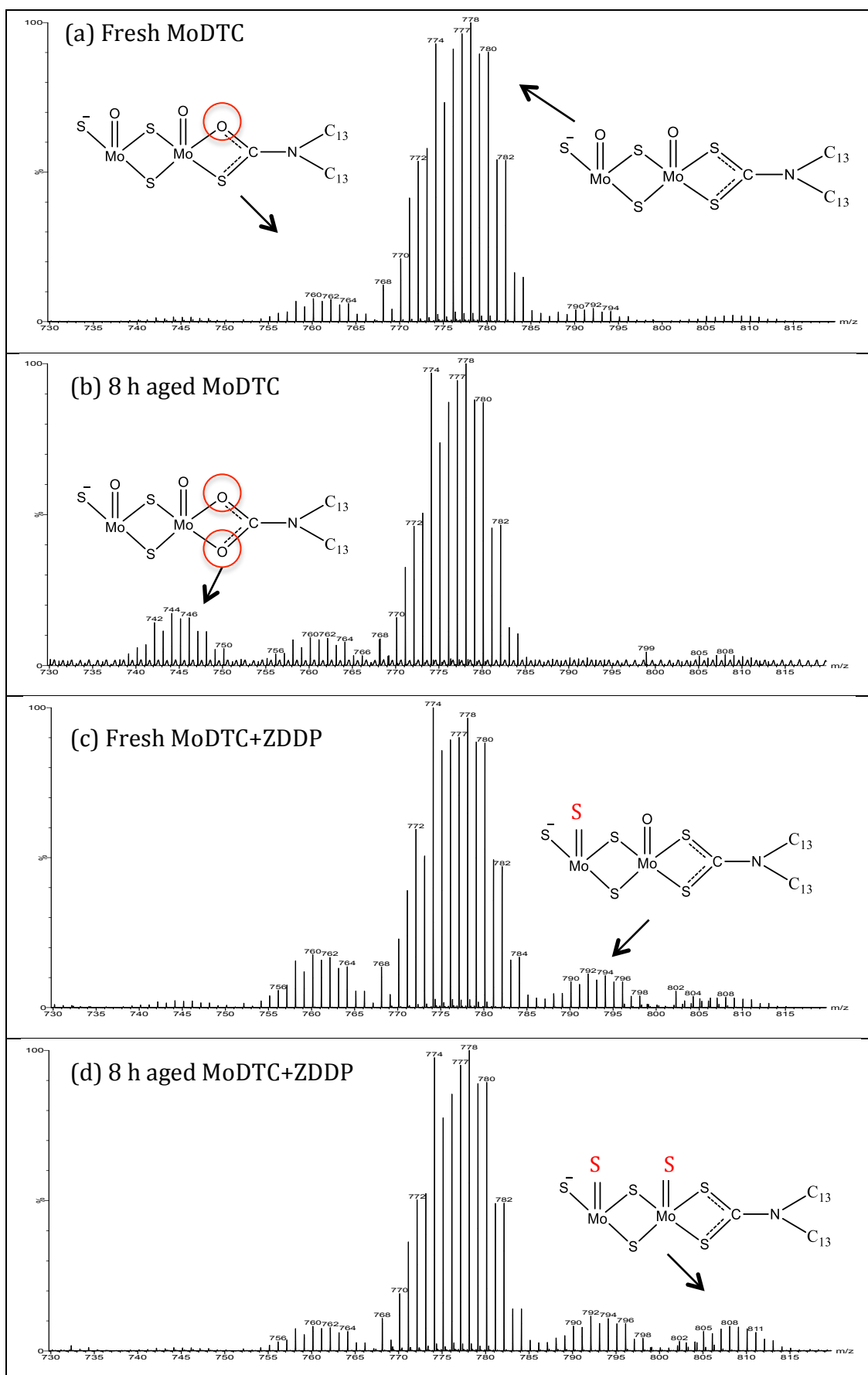
Figure 6.5 shows the mass spectrum for the fresh mixture MoDTC/ZDDP, obtained in positive ion mode. The measured molecular weight corresponding to MoDTC compounds are evidenced in blue (see chapter 3). The three peaks at  $m/z$  922, 1062 and 1202 Da, in fact, can be assigned to MoDTC with alkyl chains as  $R=C_8$ , 2  $R=C_8$  and 2  $R=C_{13}$ , or 4  $R=C_{13}$ , respectively. As expected, the addition of ZDDP additive causes the appearance of new peaks. The principal ones are given in red.



**Fig. 6.5.** Mass spectrum obtained for MoDTC/ZDDP fresh mixture in positive ion mode. The peaks with blue circles are related to the MoDTC, red and green circles are new peaks.

In the spectrum it is possible to recognize the three ZDDP compounds used in this study (peaks at  $m/z$  659, 773, 1191). It is interesting to point out that a new peak is detected at  $m/z$  1154 (evidenced with green circles). This peak has molecular weight 37 Da lower than the expected theoretical peaks. Considering that 37 Da is the same difference between nitrogen-carbon (N-C) group and oxygen-phosphorous-oxygen (O-P-O) group, this result could be explained supposing that the  $Zn_2(DTP)_3$  becomes  $Zn_2(DTP)_2(DTC)$ . However, no peak related to Mo(DTC)(DTP) has been detected, suggesting that only the ZDDP additive shows the chemical exchange of DTC/DTP group with the MoDTC friction modifier.

The comparison between the zoomed spectra obtained from MoDTC-containing base oil fresh (a) and aged (b) and MoDTC/ZDDP mixture fresh (c) and aged (d) is reported in **Figure 6.6**. Beside the peaks already described in the chapter 4, when ZDDP is blended to MoDTC-containing base oil a new peak appears. In fact, in addition to the ions at  $m/z$  768 and 762 (corresponding to MoDTC molecular fragments), there is a further peak at  $m/z$  794, thus 16 Da higher than the main peak (compare a to c). This could be explained supposing that while when MoDTC is alone in the base oil (a) the sulfur atoms present in the molecule are replaced by oxygen atoms (compare a to b, ref chapter 3), in the case of MoDTC/ZDDP mixture, there is the opposite exchange: it can be hypothesized that a sulfur atom replaces the oxygen (compare a to c).

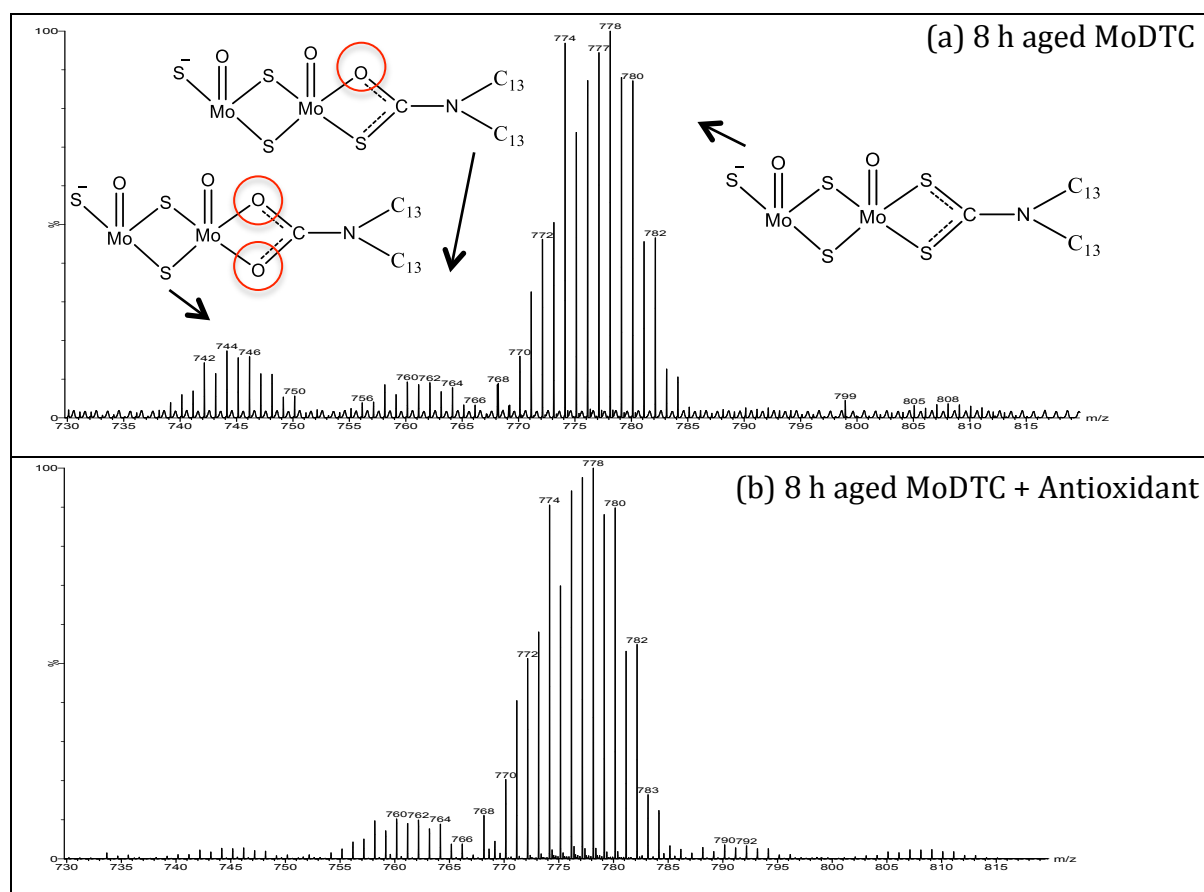


**Fig. 6.6. Comparison between mass spectrometers obtained for MoDTC-containing base oil fresh (a) and 8 hours aged (b), MoDTC/ZDDP mixture fresh (c) and 8 hours aged (d) in negative ion mode**

The spectra obtained with the aged oils (b and d) reveal that the MoDTC fragment containing two sulfur atoms substituted by oxygen atoms is not detected when ZDDP is added (no peak at  $m/z$  748 in the spectrum d). Furthermore, the presence of the new peak detected at  $m/z$  810 (spectrum d) could be explained supposing that the thermo-oxidative process of MoDTC/ZDDP mixture leads to the complete sulfurization of MoDTC (two oxygen atoms in the MoDTC molecule are exchanged with two sulfur atoms).

## (B) MoDTC+Antioxidant

The aged mixture MoDTC/antioxidant shows marked reduction in the peak intensity at  $m/z$  748, suggesting that the antioxidant additive is able to protect the MoDTC molecule from oxidation, limiting the sulfur/oxygen exchange (**Figure 6.7**).

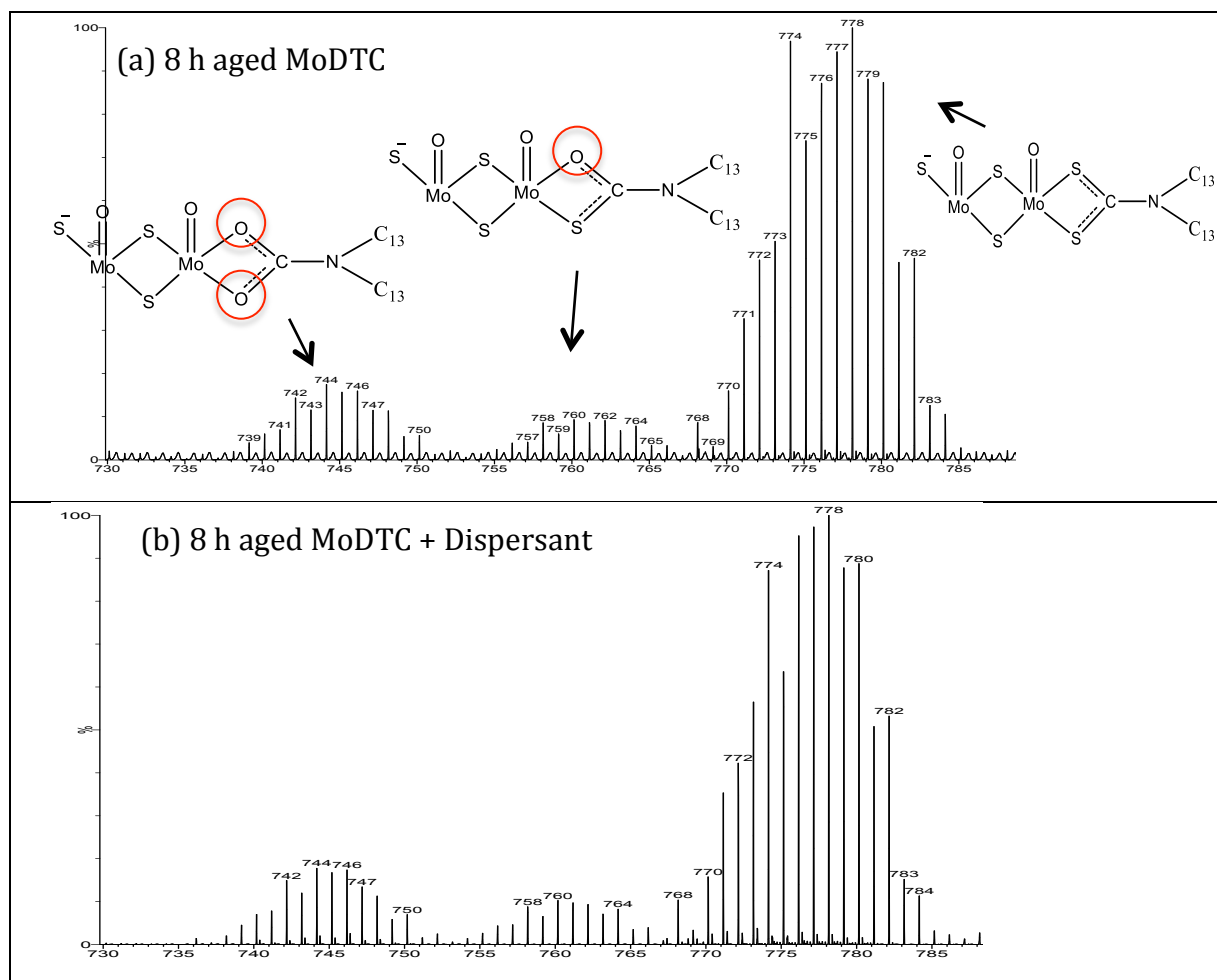


**Fig. 6.7.** Comparison between mass spectra obtained for 8 hours aged MoDTC-containing base oil (a) and 8 hours aged MoDTC/Antioxidant mixture (b) in negative ion mode.



### (C) MoDTC+Dispersant

When the dispersant is added to MoDTC-containing base oil similar peaks to the ones obtained using only the friction modifier additive are obtained (**Figure 6.8**). Although the hypothetical absence of the solid-like particles, in fact, after 8 hours of degradation, the peaks corresponding to the MoDTC fragments with one or two sulfur atoms replaced by oxygen atoms are evident.



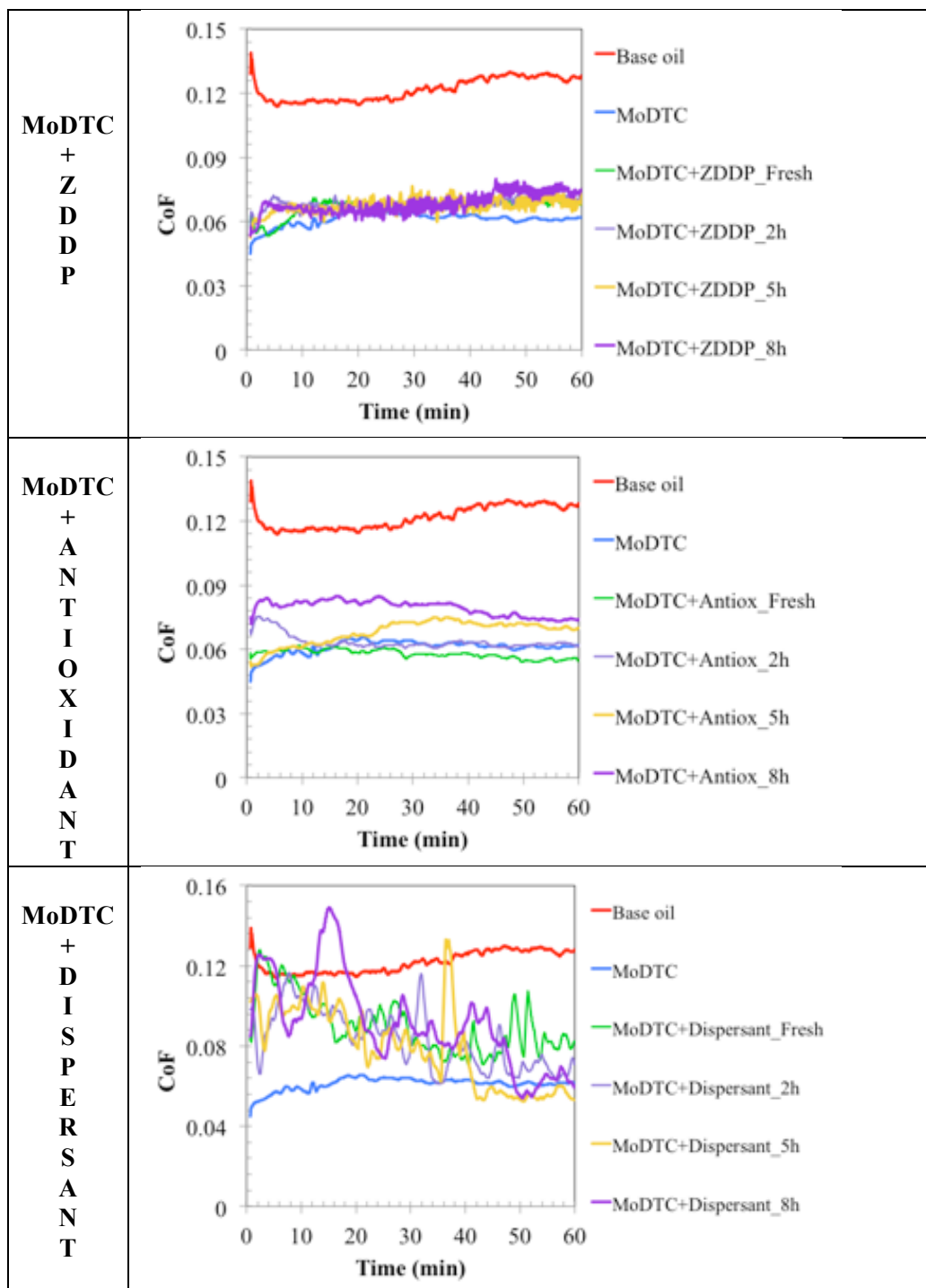
**Fig. 6.8.** Comparison between mass spectra obtained for 8 hours aged MoDTC-containing base oil (a) and 8 hours aged MoDTC/Dispersant mixture (b) in negative ion mode.

## 5.4. Tribological Experiments

The friction characteristics of these different binary combinations were evaluated with steel/steel and DLC/steel contact under the same conditions described in the previous chapters (Load = 32 N, T=100°C, speed=50 mm/s, Test duration = 1 hours, stroke length = 10 mm, frequency = 5 Hz).

### 5.4.1. Steel/Steel Contact

**Figure 6.9** reports the friction behavior of the three mixtures analyzed using steel/steel contact.



**Fig. 6.9** Friction behavior for MoDTC/ZDDP fresh and aged mixtures for steel/steel contact

### **(A) MoDTC+ZDDP mixture**

The friction coefficient obtained from the experiments carried out using fresh and aged mixtures for the binary combination (MoDTC+ZDDP) are very similar to the one obtained using only the MoDTC additive. Moreover, when ZDDP is employed, the reduction in friction is independent from the degradation time. In fact, the mixture lowers the friction coefficient even after 8 hours of ageing.

### **(B) MoDTC+Antioxidant mixture**

**Figure 6.9** reveals that the MoDTC tribological performance is not influenced by the addition of the antioxidant additive. Also in this case, the friction coefficient obtained is similar to those recorded employing only MoDTC additive. Furthermore, although the coefficient value increases from 0.06 to 0.08, a relatively important reduction in friction is still present also after 8 hours of ageing.

### **(C) MoDTC+Dispersant mixture**

Big scattering was recorded in the friction behavior for the MoDTC/dispersant combination. It suggests that the MoDTC performance is limited through a possible competition with dispersants either because of a chemical reaction happen between the two additives or because the dispersant additive adsorbs on the surface, just limiting the interaction between MoDTC and the steel surface. Both hypothesis, based on the friction modifier performance, lead to antagonistic behavior between MoDTC and the dispersant. It can be supposed that, due to the antagonism between these two additives, there is an effect of tribofilm formation/removal, which causes the big scattering in the friction coefficient value.

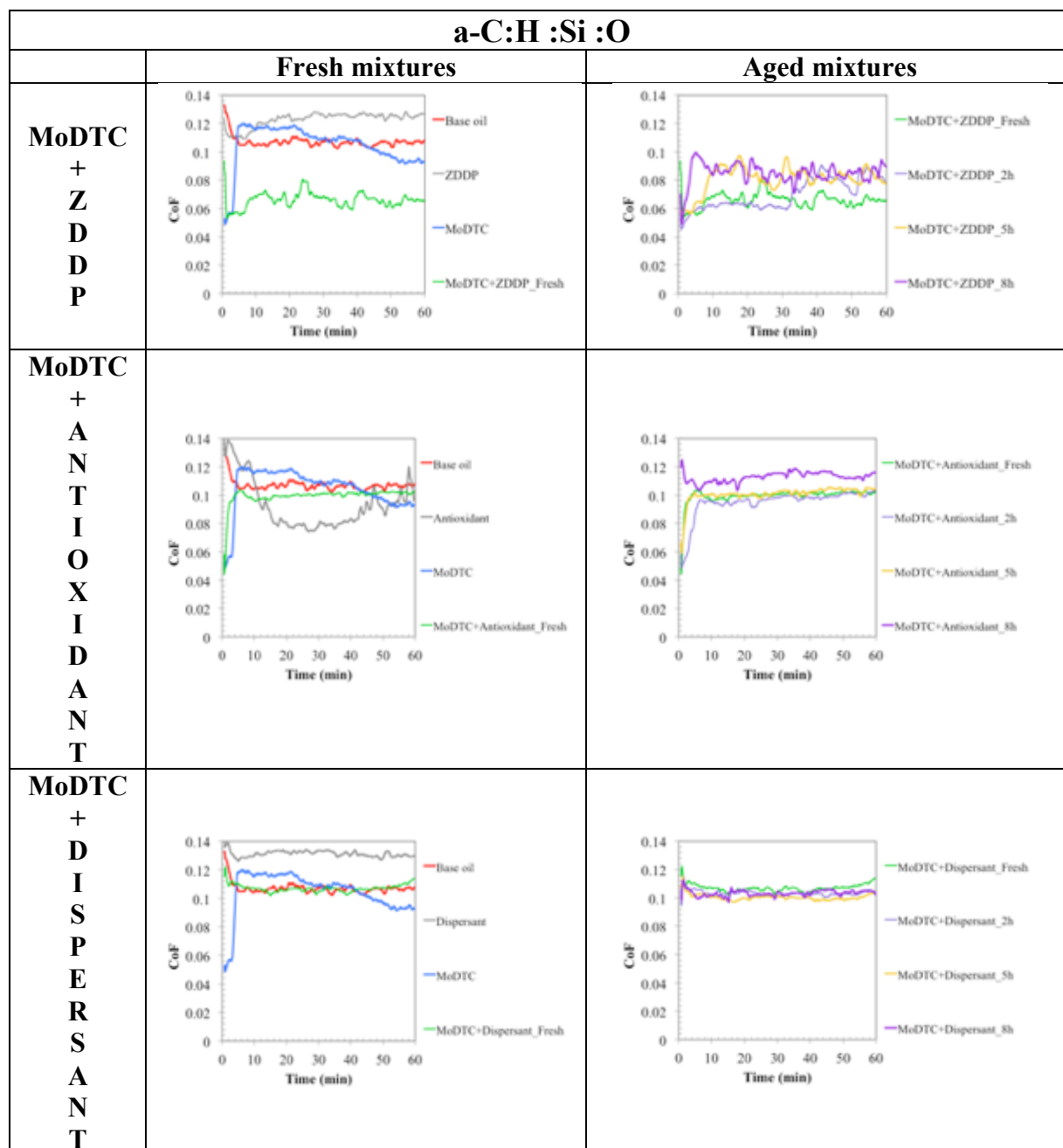
### 5.4.2. DLC/Steel Contact

Chapter 5 was dedicated to investigating of the antagonism between the MoDTC additive and the DLC coating surface. The combination of the results presented led to the proposal of a new DLC wear mechanism based on the formation of a molybdenum carbide species on the steel counterpart during the tribo-test. It is believed that the catastrophic wear is produced because of the reaction between the molybdenum compounds derived from the MoDTC decomposition formed on the steel sample and the carbon present on the DLC coated coupon.

This paragraph focuses on the effect of binary combinations on the friction and wear performance of two DLC coatings analyzed in chapter 5: the amorphous hydrogenated carbon (a-C:H) and the amorphous hydrogenated carbon doped with silicon and oxygen (a-C:H:Si:O). The main objectives are to evaluate the impact of lubricant degradation on DLC tribological performance changes with the addition of another additive. At the same time, the possibility to avoid/reduce the high wear produced on the a-C:H:Si:O DLC will be investigated. The test conditions employed for the experiments and properties of specimen used in this chapter are the same as listed in the previous chapters.

## Amorphous hydrogenated carbon DLC doped with Silicon and oxygen (a-C:H:Si:O)/Steel

The friction coefficient as a function of time for the a-C:H:Si:O/steel configuration using the three mixtures (both fresh and aged) is given in **Figure 6.10**.



**Fig. 6.10.** Friction behavior for MoDTC/Antioxidant and MoDTC/Dispersant mixtures, fresh and aged for a-C:H:Si:O DLC/steel contact

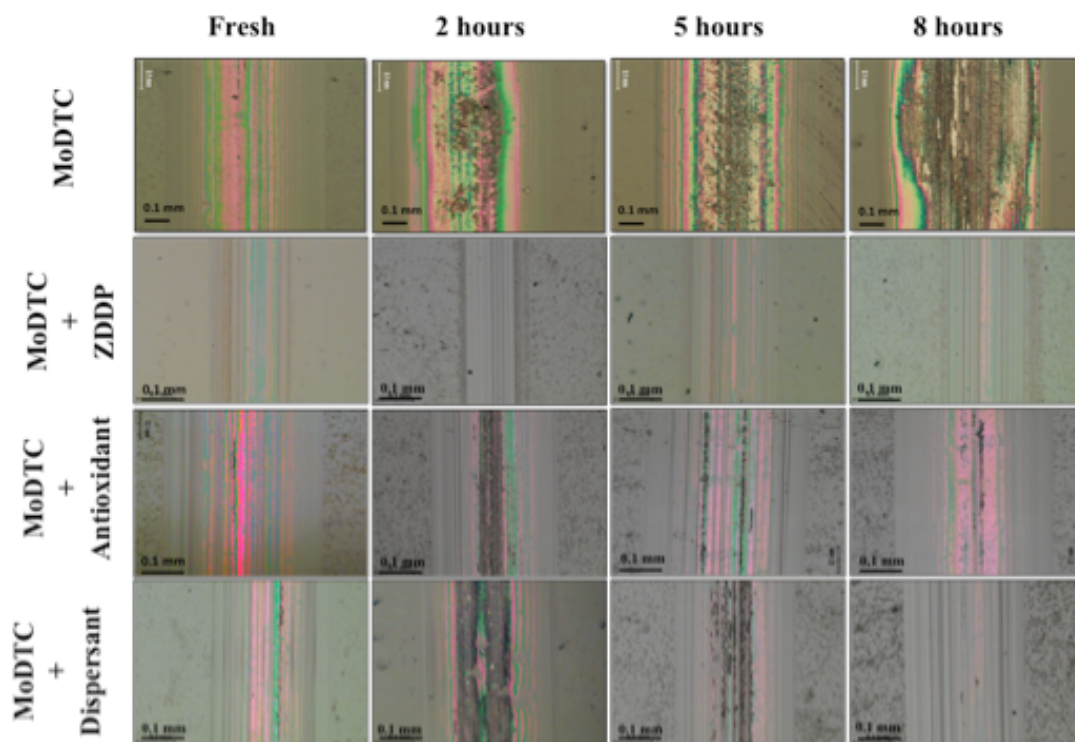
### **(A) MoDTC+ZDDP mixture**

Based on the friction curves shown in **Figure 6.10**, it can be affirmed that a drop in friction was observed when the ZDDP additive is blended into the MoDTC-containing base oil. The impact of thermo-oxidative degradation on the friction performance of the mixture is shown in the same figure. It can be seen that the aged oils have the same friction behavior compared to fresh mixture, although slightly higher friction coefficient has been obtained using oils aged for longer time (5 and 8 hours).

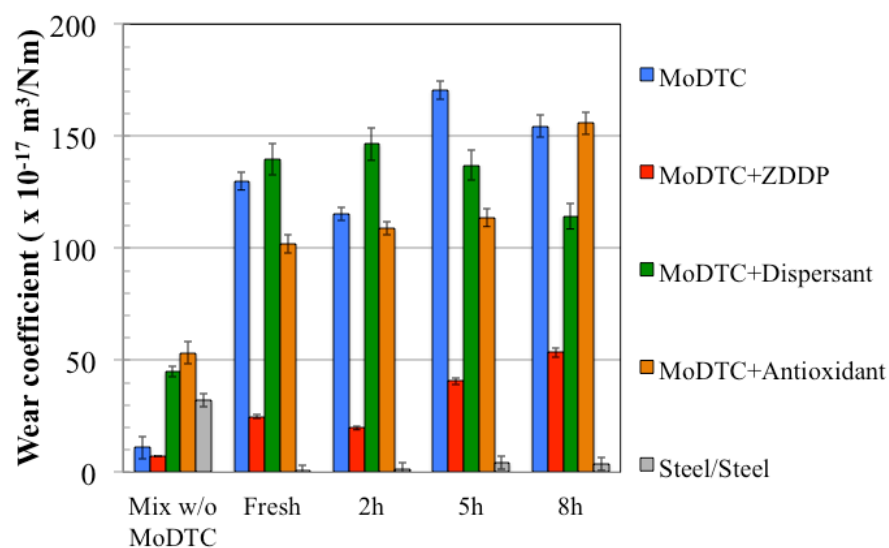
### **(B) MoDTC+Antioxidant and MoDTC+Dispersant mixtures**

**Figure 6.10** reports the interaction between MoDTC/antioxidant and MoDTC/dispersant considering their friction performance, analyzing fresh and aged mixtures. No significant differences are detected: every test condition gave a high friction coefficient and there is no influence of ageing time.

The wear of DLC coatings as a function of additive mixture and degradation time could be deduced from **Figure 6.11**. It is evident that a-C:H:Si:O DLC, despite the addition of antioxidant or dispersant, still shows catastrophic failure of the coating at multiple regions. However, the presence of ZDDP additive seems to considerably reduce the wear produced on the DLC coated flat. In fact, considering the interferometer results, it has been clearly observed that the DLC wear is much less in comparison to the MoDTC-containing base oil and to the other mixtures analyzed in this chapter (**Figure 6.12**).



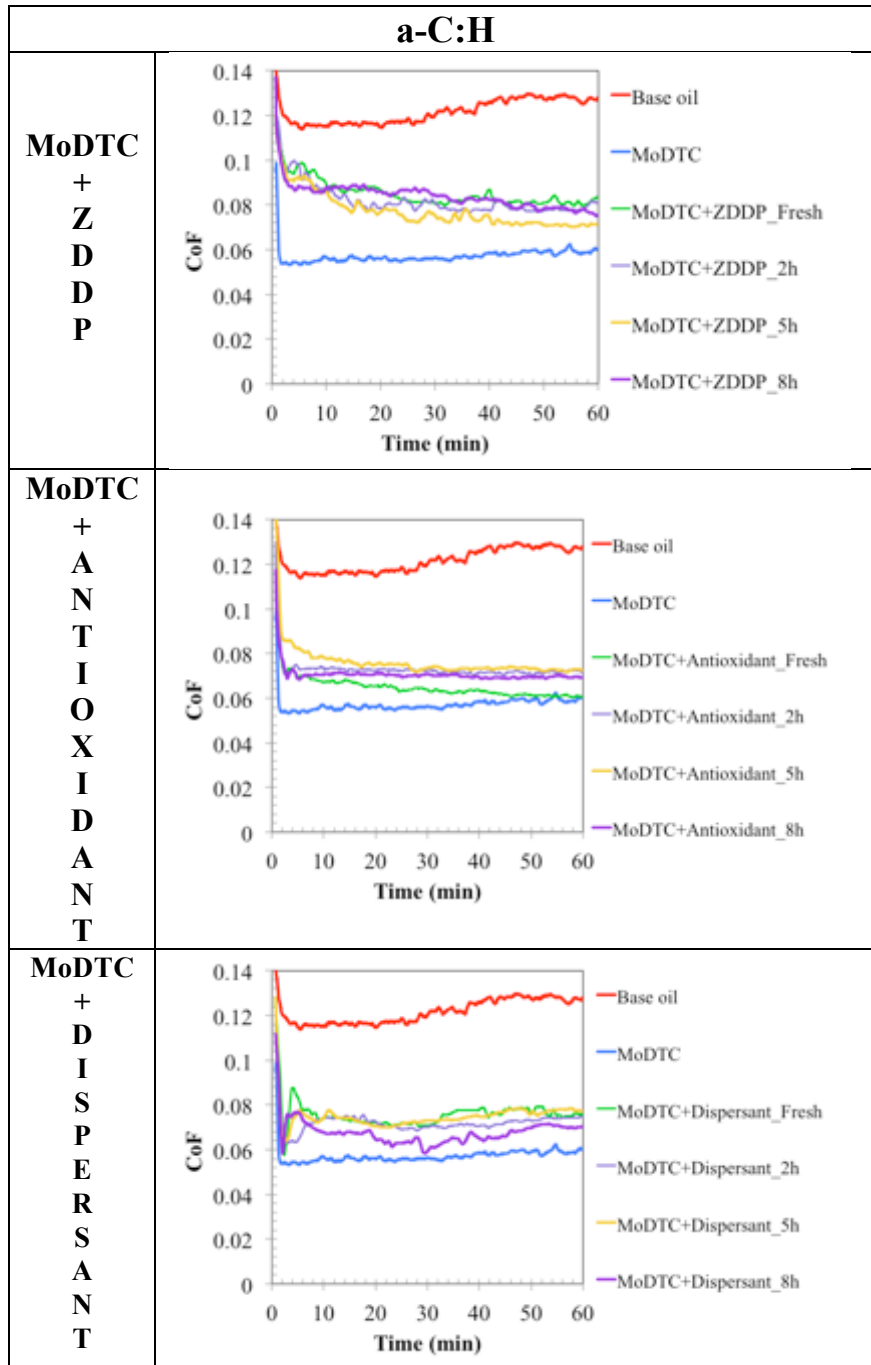
**Fig. 6.11.** Optical images for the a-C:H:Si:O DLC coated flats tested with fresh and aged samples.



**Fig. 6.12.** Wear coefficient for the a-C:H:Si:O DLC coated flats tested with fresh and aged mixtures.

## Amorphous hydrogenated carbon DLC (a-C:H)/Steel

To obtain some more elements of comprehension, the tribological experiments are performed also on the a-C:H DLC coating. **Figure 6.13** shows the lubrication properties of the hydrogenated amorphous DLC coating with MoDTC/ZDDP (a), MoDTC/antioxidant (b), MoDTC/dispersant (c) mixtures. The friction coefficients obtained testing the three binary combinations have slightly higher values than MoDTC-containing base oil. The friction coefficients tend to be independent of the degradation process.



**Fig. 6.13.** Friction behavior for the three mixtures analyzed in this chapter (fresh and aged) testing a-C:H DLC/steel contact.



## 6. DISCUSSION

To improve MoDTC performance it is necessary to better understand additive/additive interactions during the thermo-oxidative degradation process. Among all the possible combinations, it has been decided to investigate three different mixtures composed of the MoDTC friction modifier along with ZDDP, antioxidant or dispersant.

Liquid chromatography analysis using the **MoDTC/ZDDP** combination has shown that the anti-wear additive is able to extend the life of MoDTC. Mass spectroscopy, however, revealed two important features of this binary mixture: considering that it was not possible to find any evidence for the MoDTC molecule modification through ligand exchange, it seems that only the ZDDP undergoes in a such chemical change. However, as already hypothesized in literature, the MS results confirm that the ZDDP additive has a key role in promoting the formation of MoS<sub>2</sub>. Furthermore, for the first time, in this chapter it has been pointed out that the addition of ZDDP helps the formation of lamellar sheets representing a sulfur source through the replacement of an oxygen atom in the MoDTC molecule by one of sulfur. These MoDTC chemical changes might influence also its tribological performance and, therefore, the role of the blends in friction reduction has been highlighted. The friction behavior employing steel/steel contact of the MoDTC/ZDDP mixture seems to be coherent with the chemical analyses: the addition of an anti-wear additive improves the oxidation resistance of the MoDTC molecule allowing the formation of MoS<sub>2</sub> lamellar sheets formed through MoDTC decomposition in the contact also if the oil is degraded for a relatively long time. In fact, the friction value recorded using the mixture aged for 8 hours is similar to the performance obtained using the fresh mixture.

The chemical analysis done on the **MoDTC/antioxidant** combination revealed that the MoDTC additive is still detected in the base oil after 8 hours and its concentration seems to be similar to the initial value (approximately 85%). It is interesting to note the antioxidant protection shown by the MS technique. The peak related to the oxidized MoDTC, in fact, is much smaller than the one detected when the MoDTC is the only additive present in the base oil. For this reason, it can be concluded that the addition of antioxidant to MoDTC-containing base oil retards the depletion of the friction modifier molecule because the formation of oxidized MoDTC is strongly inhibited. Furthermore, this binary combination is able to lower the friction coefficient in steel/steel contact also if subjected to the thermo-oxidative degradation for 8 hours.

The influence of **dispersant** additive on the MoDTC tribological performance is not coherent with the chemical behavior of the mixture. In fact, the liquid chromatography results showed that also after being subjected for 8 hours to the thermo-oxidative degradation process, the concentration of MoDTC in the mixture is above 80% of the initial concentration. However, the MS spectra revealed that the dispersant is not able to avoid a certain MoDTC additive oxidation. In fact, the peaks associated with oxidized MoDTC are evident since the beginning of the degradation process. At the same time, the friction experiments performed employing steel/steel configuration revealed that the dispersant limits the MoDTC performance, showing an antagonism between the two additives. Several hypotheses could be proposed to explain the discrepancy in the results. It may be possible that the dispersant is not able to prevent the solid-like particle formation, but rather maintains smaller-scale particles suspended in the solution. An alternative scenario is that the MoDTC molecule reacts with the dispersant, leading to the formation of reaction products not able to interact with the surface and lower the friction coefficient. However, no new mass spectroscopy peak appeared when analyzing this mixture, suggesting that no chemical reactions happened between MoDTC and dispersant additive. An other possible explanation is that the dispersant molecules tends to encapsulate the MoDTC molecules, preventing its reaction with the steel surface.

The findings presented in this chapter obtained investigating **DLC/steel** contact, clearly show that the mixture ZDDP/MoDTC is able to extend the durability of the a-C:H:Si:O DLC coating. In fact, when this mixture is tested, much less wear was observed for the a-C:H:Si:O DLC. This could be explained by the presence of poly-sulfate species formed on the surfaces, causing the reduction of reactivity between the molybdenum compounds formed on the steel ball and the carbon of the DLC coating. This hypothesis is supported by the results obtained using the other binary mixtures. Indeed, despite the degradation of MoDTC molecules is limited thanks to the presence of the antioxidant or the dispersant, a catastrophic wear was found on a-C:H:Si:O DLC coated coupons, for both fresh and aged oils. It can be supposed that, even though the molybdenum oxi-sulfide species are formed in the contact, they are not embedded into a protective tribofilm, e.g. polyphosphate matrix in the case of ZDDP additive.

## 7. CONCLUSIONS

Studies of additive interactions in the bulk phase have been particularly useful in defining underlying causes for synergistic and antagonistic performance effects between MoDTC and three different classes of additives.

The following general conclusions can be drawn from the results presented above.

- The influence of additional additives on the MoDTC depletion has been investigated:
  - (A) MoDTC/ZDDP mixture: only a delay in the particle formation has been obtained and after 8 hours degradation, the MoDTC concentration is approximately 60% of the initial quantity;
  - (B) MoDTC/Antioxidant mixture: significant reduction of particle formation is observed and, at the end of the thermo-oxidative process, the MoDTC concentration is still above 80%;
  - (C) MoDTC/Dispersant mixture: it is complicated to confirm that the particles formation is avoided. It is more probable that the particles are extremely small size and they are kept suspended in the mixture thanks to the dispersant additive action. In this mixture the MoDTC depletion seems to be strongly reduced.
- The additive/additive combinations were further assessed from the tribological investigations.
  - o Steel/Steel contact
    - (A) MoDTC/ZDDP mixture: the addition of ZDDP increases the durability of MoDTC. In fact, also after being subjected to thermo-oxidative degradation for 8 hours, the mixture is able to lower the friction coefficient;
    - (B) MoDTC/Antioxidant mixture: blending antioxidant additive to MoDTC-containing base oil leads to an extension of the friction modifier life. Also in this case, in fact, the reduction in friction is still obtained when testing the mixture aged for 8 hours;
    - (C) MoDTC/Dispersant mixture: the tribological characterization of this mixture suggests the antagonism between the two additives. In fact, although at this stage it is difficult to give a detailed explanation, tests with fresh and aged binary combinations between MoDTC and dispersant gave no friction reduction. It can be supposed that the dispersant has a physical reaction with the MoDTC molecule, leading to the encapsulation of MoDTC and, consequentially, limiting the access of this additive to the steel surface.

- DLC/Steel contact
  - a-C:H:Si:O DLC/steel
- (A) MoDTC/ZDDP mixture: although still higher in comparison to the wear obtained when testing steel/steel contact, the DLC coated flat wear is considerably reduced when ZDDP is blended to MoDTC-containing base oil;
- (B) MoDTC/Antioxidant mixture: the addition of antioxidant does not bring significant improvement. In fact, the friction and wear are still really high;
- (C) MoDTC/Dispersant mixture: the tests carried out using this binary combinations show no friction reduction and high wear for both, fresh and aged mixtures.
- a-C:H DLC/steel
 

The friction experiments carried out on the amorphous carbon DLC employing the three binary combinations gave slightly higher values than those obtained with MoDTC-containing base oil. The values recorded using fresh mixtures are similar to those obtained with aged ones.

Summarizing all the results reported in this chapter, it can be concluded that MoDTC additives can be protected against thermo-oxidative degradation by the addition of an antioxidant additive (ZDDP or antioxidant) confirming the results of previous works. Although the concentration of MoDTC seems not to change throughout the degradation process when dispersant is blended to it, the mixture seems to not have friction-reducing capability.

## 8. PERSPECTIVE

While great progress has been made in recent years in understanding the structure of tribofilm derived from MoDTC-containing base oil, thanks to the improved quality of modern analytical tools, more information are needed to clarify the tribofilm formed with the binary mixtures. Clearly, a better understanding of the reactions happening into the contact and a deep study on their kinetics may allow some degree of control over the properties of MoDTC in engine oils when DLC coating is involved in the contact.

## 9. BIBLIOGRAPHY

- [1] Unnikrishnan R., Jain M.C., Harinarayan A.K., Mehta A.K., Additive–additive interaction: an XPS study of the effect of ZDDP on the AW/EP characteristics of molybdenum based additives, *Wear*, Volume 9, Pages 252:240, (2002).
- [2] Kasrai M., Cutler J.N., Gore K., Canning G., Bancroft G.M., The chemistry of antiwear films generated by the combination of ZDDP and MoDTC examined by X-ray absorption spectroscopy, *Tribol. Trans.*, Volume 41, Pages 69–77, (1998).
- [3] Muraki M., Yanagi Y., Sakaguchi K., Synergistic effect on frictional characteristics under rolling-sliding conditions due to a combination of molybdenum dialkyldithiocarbamate and zinc dialkyldithiophosphate. *Tribol. Int.*, Volume 30, Pages 69–75; (1997).
- [4] Grossiord C., Varlot K., Martin J.M., Le Mogne Th., Esnouf C., Inoue K., MoS<sub>2</sub> single sheet lubrication by molybdenum dithiocarbamate, *Tribol. Int.*, Volume 31, Pages 737–43, (1998).
- [5] Iwasaki H. TOF-SIMS analysis of MoS<sub>2</sub> formed on the rubbing surface for MoDTC and ZnDTP synthesized by using 34S isotope, *Proceedings of Japanese Society of Tribologists Tribology Conference Takamatsu*. Pages 359–60, (1999).
- [6] Yagishita, K., and Igarashi, J., Analysis of ligand-exchange reaction among sulfur containing complexes, *Prep JAST Tribology Meeting, Fukuoka*, Pages 673-6, (1991).
- [7] P.C.H. Mitchell, Oil soluble Mo–S compounds as lubricant additives, *Wear*, Volume 100, Pages 281, (1984).
- [8] Kubo K., Nagakari M., Shitsmichi T., and Motoyama K., The Effect of Ageing During Engine Running on the Friction Reduction Performance of Oil Soluble Molybdenum Compounds, *Proc. Intern. Trib. Conf. Yokohama*, Pages 745-750, (1995).
- [9] Stachowiak G., and Batchelor A.W., *Engineering Tribology*, Elsevier, Butterworth Heinemann, Pages 832 (2005).
- [10] Spikes H.A., The History and Mechanisms of ZDDP, *Tribology Letters*, Volume 17(3), Pages 469-489, (2004).
- [11] Wei D., Song H., Wang R., An investigation of the effect of some motor oil additives on friction and wear behavior of oil soluble organo molybdenum compounds, in: *Proceedings of the 7<sup>th</sup> International Colloquium on Automotive Lubrication*, Paper 3.14, Esslingen, West Germany, (1990).

- [12] Minami I., Kitayama N. and Okahe H., Synthesis and Evaluation of Sulphurized MoDTP, Japanese Journal of Tribology, Volume 37, Pages 13-19, (1992).
- [13] De Barros Bouchet M.I., Martin J.M., Le Mogne Th., Bilas P., Vacher B., Yamada Y., Mechanisms of MoS<sub>2</sub> formation by MoDTC in presence of ZnDTP: effect of oxidative degradation, Wear, Volume 258, 1643–1650, (2005).
- [14] F.G. Rounds, Effect of organic molybdenum compounds on the friction and wear observed with ZDP-containing lubricant blends, Tribol. Trans., Volume 33, Pages 345–354, (1990).
- [15] Kubo K., Moriki Y., Kibukawa M., Friction behavior of lubricants containing organo-molybdenum compounds. Part 1. Application to sulfur–phosphorus type gear lubricants, J. JSLE 313, Pages, 309, (1988).
- [16] Kubo K., Hamada Y., Moriki Y., Kibukawa M., Friction behavior of lubricants containing organo molybdenum compounds. Part 2. Application to the lubricants containing zinc dialkyl dithio phosphate, J. Jpn. Soc. Tribol. Volume 34, Pages 185, (1989).
- [17] Muraki M., Yanagi Y., Sakaguchi K., Frictional properties of organo molybdenum compounds in the presence of ZnDTP under rolling–sliding conditions: Part 1. Effect of surface hardness of roller, J. Jpn. Soc. Tribol. Volume 40, Page 40, (1995).



# Chapter 7

---

## Conclusions and Perspective

---

*This chapter summarizes the conclusions that have been drawn from the research described in this work. It also makes suggestions for further works in the MoDTC additive investigation.*



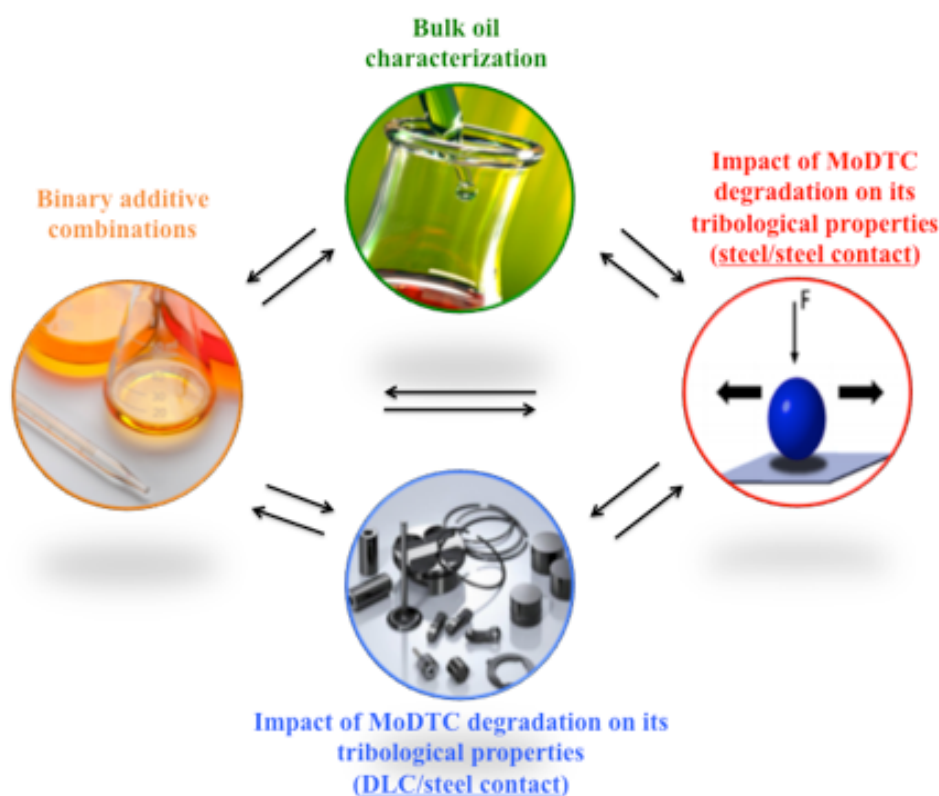
## CONCLUSIONS AND PERSPECTIVE

Molybdenum Dithiocarbamate (MoDTC) additive has been the subject of both fundamental and applied research, because of its importance as a friction modifier in modern lubricants. The principal intent of this thesis was to further investigate the MoDTC-containing base oil behavior, covering its two main drawbacks. A crucial factor in practical MoDTC research related to engine lubricant is the lifetime of its friction-reducing capability. At the same time, to date, the antagonism existing between MoDTC and DLC coatings leading to a catastrophic wear is not fully understood yet. A fundamental approach to better understand the behavior of MoDTC when subjected to thermo-oxidative degradation is obtained through a combination of tribological experiments with steel/steel and DLC-involving contacts, surface characterization techniques (XPS, FIB/TEM/EDX, Raman, SEM) and bulk oil characterizations (Liquid Chromatography, Mass spectroscopy, FT-IR). A direct link between the tribofilm composition and the hypothetical chemical pathway followed by the MoDTC additive during the ageing process has been discussed. The findings reported in this thesis allow to hypothesize the formation of molybdenum oxi-sulfides lamellar sheets in the contact together with well-known  $\text{MoS}_2$  sheets. These  $\text{MoS}_{2-x}\text{O}_x$  species strongly influence the MoDTC friction performance. In the light of the results presented in this manuscript, it is highly probable that the formation of the  $\text{MoS}_{2-x}\text{O}_x$  species is promoted by the gradual oxidation of the MoDTC molecule happening directly in the bulk oil. Moreover, it has been experimentally established that the addition of traditional ZDDP anti-wear additive has a double effect. It slows down the MoDTC depletion preventing its oxidation and it induces an additional sulfurization of the molecule, which enables to maintain the reduction of the friction coefficient even after long degradation time for the lubricant.

As mentioned above, commonly, the modern additives are designed to be used on ferrous-based surfaces. It is therefore essential to simultaneously optimize the lubricants and coatings to enhance their performance. For the first time, it has been proposed a wear model for the hydrogenated DLC lubricated by MoDTC-containing base oil, involving the formation of molybdenum carbide imbedded into the tribofilm formed on the steel surface. At this stage it results complicated to individuate the exact mechanisms due to the many parameters involved in the process. However, it is believed that the high wear produced on the DLC material is due to a chemical reaction between the molybdenum-based species produced on the steel counterpart and the carbon of the hydrogenated DLC-coated flat coupon. The formation of molybdenum carbide seems to be facilitated by the presence of

silicon inside the hydrogenated DLC material. Moreover tribo-chemical hybridization change of carbon ( $sp^3$  towards  $sp^2$ ) has been studied experimentally by HR-TEM and electron energy loss spectroscopy (EELS) on wear debris collected on the contact zone. Surprisingly, even under severe tribological conditions, a strong graphitization of the DLC wear debris was clearly detected.

The main and complementary topics of the thesis are summarized in **Figure 7.1**.



**Fig. 7.1.** Schematic summary of the thesis.

The perspective works should be split into short-term investigations considering the next steps from the results presented in this thesis, and in the long term, more fundamental approaches for looking at MoDTC additive degradation in full-scale engines.

We believe that there is a great deal of molecular simulation work that could immediately follow on from the findings presented in this thesis. This would enable a better comprehension of MoDTC behavior in bulk-aged oil and directly in the contact. To allow the implementation of chemical simulation, an improvement on the accuracy of the information derived from this thesis is necessary. In fact, it is acknowledged that fairly basic fixed parameters have been used during this work. Despite this, the investigation of the influence of the MoDTC chemical structure and test parameters on the different

hypothesized mechanisms shown in this study could bring further important information. For example, it could be extremely useful to investigate the influence of the MoDTC configuration, focusing on the sulfur content in the core of the molecule and on the length of the alkyl chains.

The synergistic impact of binary additives mixtures with MoDTC, especially the combination with ZDDP, on both the tribological performances and the MoDTC degradation resistance, would deserve to be thorough. Indeed, the dual role of ZDDP, as sulfur provider for MoDTC and responsible of the formation of the phosphate-based glass protective layer, needs to be furthered in the oil formulation.

Although aware of the complexity of the system, it is also believed that the understanding of MoDTC performance in full-scale real-life components should also be attempted.

## CONCLUSIONS AND PERSPECTIVE

L'additif dithiocarbamate de molybdène (MoDTC) a fait l'objet de nombreux travaux de recherche fondamentaux et appliqués visant à mieux comprendre les mécanismes de réduction du frottement dans un contact lubrifié. Mais cette réduction du frottement est peu durable dans le temps car elle est fortement affectée par la dégradation du lubrifiant. Un antagonisme fort entre les revêtements DLC et le MoDTC engendrant une usure catastrophique a également été mis en évidence à plusieurs reprises.

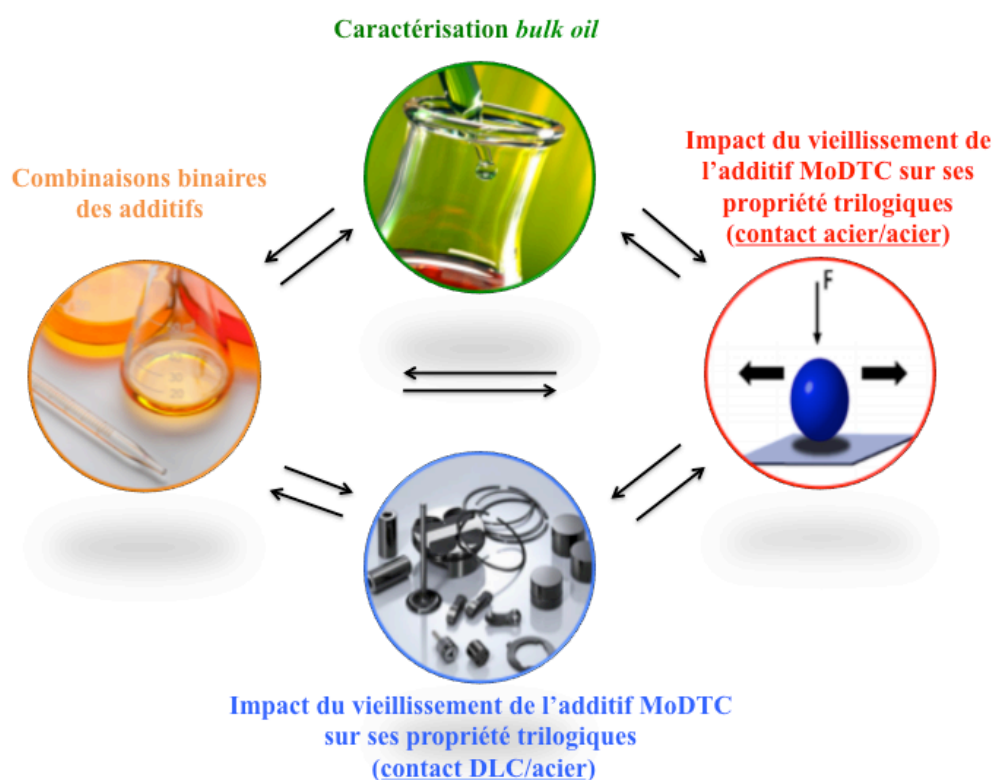
L'objectif principal de cette thèse était donc de mieux comprendre le comportement tribologique (frottement et usure) d'une huile de base contenant du MoDTC en fonction de la dégradation du lubrifiant pour des contacts acier/acier et DLC/acier.

L'approche utilisée pour mieux comprendre le comportement du MoDTC lorsqu'il est soumis à une dégradation thermo-oxydative consiste à combiner des expériences tribologiques, à des caractérisations de surface (XPS, FIB / TEM / EDX, Raman, SEM) et à des caractérisations chimiques des huiles (chromatographie en phase liquide, spectroscopie de masse, FT-IR). Un lien direct et cohérent entre la composition du tribofilm et la voie de décomposition chimique de l'additif MoDTC proposée a été mise en évidence. Les résultats présentés dans cette thèse ont permis de confirmer le bas frottement observé en régime de lubrification limite en présence de MoDTC pouvant s'expliquer par la formation de feuillets lamellaires de MoS<sub>2</sub> bien connus, mais aussi par la formation de feuillets d'oxy-sulfure de molybdène. Ces dernières espèces MoS<sub>2-x</sub>O<sub>x</sub> influencent donc la performance en frottement du MoDTC. À la lumière des résultats présentés dans ce manuscrit, il est fort probable que la formation de l'espèce MoS<sub>2-x</sub>O<sub>x</sub> soit favorisée par l'oxydation progressive de la molécule de MoDTC qui se produit directement dans le cœur du lubrifiant pendant le vieillissement. En outre, il a été établi expérimentalement que l'addition de l'additif anti-usure traditionnel ZDDP a un double effet. Il ralentit l'épuisement du MoDTC en empêchant son oxydation et, en même temps, il induit une sulfuration complémentaire de la molécule, ce qui permet de maintenir la réduction du coefficient de frottement même après un long temps de dégradation du lubrifiant.

Comme mentionné ci-dessus, généralement, les additifs modernes sont conçus pour être utilisés sur des surfaces à base de fer. Il est donc essentiel d'optimiser simultanément les lubrifiants et les revêtements pour améliorer leurs performances. Dans cette thèse, un modèle d'usure du revêtement DLC hydrogéné lubrifié en présence de MoDTC a été proposé. Nous avons établi à l'aide de plusieurs techniques, que l'usure est due principalement à la

formation de carbure de molybdène présent dans le tribofilme formé à la surface de l'acier. A ce stade, il reste encore compliqué de décrire les mécanismes exacts d'usure. Cependant, la forte usure produite sur le matériau de DLC est probablement due à une réaction chimique entre les espèces à base de molybdène produites sur la surface en acier et le carbone du DLC hydrogéné. De plus, la formation de carbure de molybdène semble être facilitée par la présence de silicium à l'intérieur du DLC hydrogéné. Par ailleurs, le changement d'hybridation de carbone ( $sp^3$  vers  $sp^2$ ) a été étudié expérimentalement par HR-TEM et spectroscopie de perte d'énergie des électrons (EELS) sur les débris usés collectés dans la zone de contact. De manière surprenante, à cause des conditions tribologiques relativement sévères (spécialement en cisaillement), une forte graphitisation des débris d'usure de DLC a été clairement détectée.

Les principaux aspects étudiés lors de la thèse sont résumés dans la figure ci-dessous.



Des perspectives futures visant à une meilleure compréhension du comportement du MoDTC soumis à un vieillissement thermo-oxydatif peuvent être proposées et classées en deux catégories:

des analyses à court terme à partir des résultats présentés dans cette thèse,  
des travaux à plus long terme avec une approche plus fondamentale et à grande échelle, en étudiant la dégradation du MoDTC directement dans les moteurs.

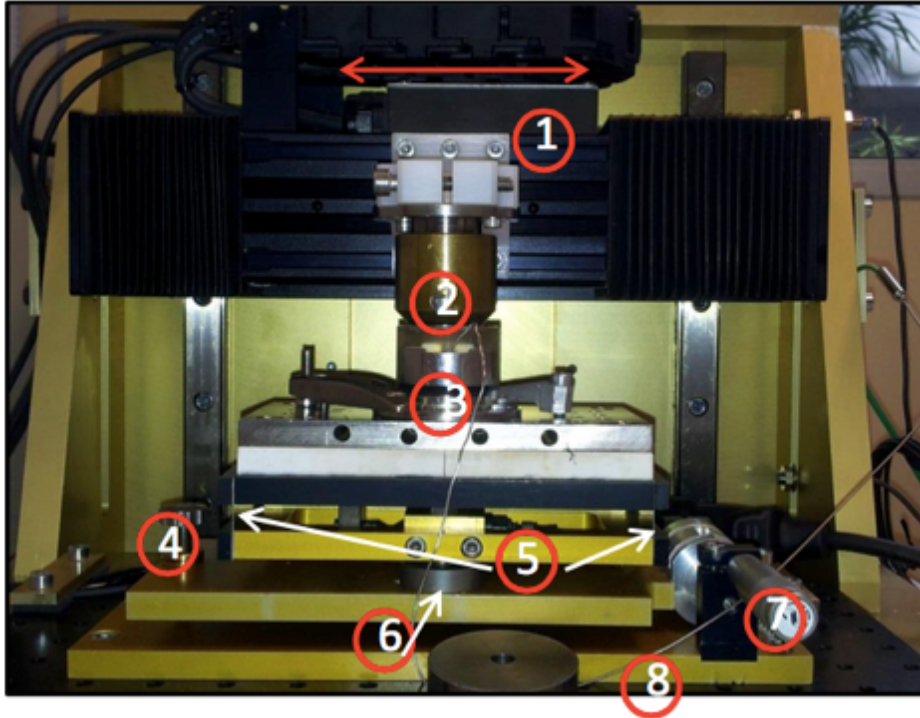
Un travail de simulation moléculaire pourrait suivre immédiatement les résultats présentés dans cette thèse. Cela permettrait une meilleure compréhension du comportement du MoDTC au sein du lubrifiant et directement dans le contact. Pour permettre la mise en œuvre de la simulation chimique, il est nécessaire d'améliorer la précision des résultats obtenus dans cette thèse, parce qu'au cours de ce travail, nous avons utilisé des paramètres fixes. L'étude de l'influence de la structure chimique du MoDTC et des conditions de tests effectués sur les différents mécanismes supposés, pourrait apporter d'autres informations importantes. Par exemple, il pourrait être très utile pour étudier l'influence de la structure chimique du MoDTC, en se concentrant sur la teneur en soufre dans le cœur de la molécule ainsi que sur la longueur des chaînes alkyles.

L'impact synergique des mélanges binaires du MoDTC avec d'autres additifs, en particulier la combinaison avec le ZDDP, tant sur ses performances tribologiques que sur sa résistance à la dégradation, mériterait d'être approfondi. En effet, le double rôle de ZDDP, à la fois comme fournisseur de soufre pour la molécule du MoDTC et comme responsable de la formation de la couche de protection en verre de phosphate, doit être creusé.

Bien que conscient de la complexité du système, la compréhension de la performance du MoDTC vieilli en situation réelle dans un moteur devrait également être étudiée.

## APPENDIX A

**Figure 1** shows the linear tribometer used to carry out the tests presented in the chapters 2, 5 and 6.

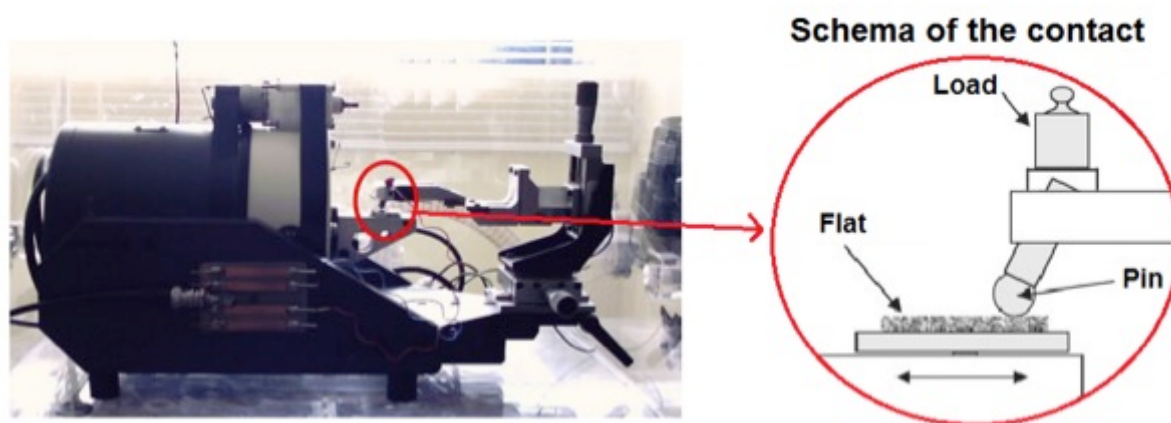


**Fig.1. Linear Tribometer employed to carry out the tests shown in the chapters 2, 5 and 6.**

1. Alternating electric motor
2. Sample holder (ball)
3. Sample holder (plane)
4. Screw used to regulate the inclination of the plane
5. Piezoelectric sensor and bi-lame (tangential force)
6. Strain gage (normal force)
7. Screw used to regulate the plane in the z direction
8. Thermocouple type K

## APPENDIX B

A picture of the linear tribometer and a schema of the contact can be observed in **Figure 2**. The friction coefficient is measured by a piezoelectric force transducer placed against the heater block supporting the lower specimen holder. The particularity of this home-made tribometer is the possibility to use a small ball and to perform the experiments using only a drop of lubricant.



**Fig.2.** Linear Tribometer employed to carry out the tests shown in the chapters 4.



## ACKNOWLEDGEMENTS

There are many people without whom I would have been unable to achieve the things I have done during the last three years.

I would like to thank my supervisor **Clotilde Minfray** for the precious discussions and suggestions since the beginning of the project. Thanks also to Maria Isabel de Barros for being my second supervisor and for her discussions both job-related and personal ones. Their guidance and support, and mostly their enthusiasm for research have been a constant encouragement to complete this work.

The work presented in this thesis has been supported by the European Commission FP7 Marie Curie Initial Training Network (MC ITN) through **ENTICE** (Engineering Tribochemistry and Interfaces with a Focus on the Internal Combustion Engine) research training network. The project has also given me the opportunity to collaborate with different research groups and I would like to thank them all for what I have learned and how much I have enjoyed it. In particular, I would like to thank my “questions machine” **Benoit Thiebaut** from Total, I enjoyed the discussions with you, always constructive and motivating and **Anne Neville** from Leeds University, You inspired me every meeting we had, if one day I will have half of your strength I can consider myself a winner.

My warmest thanks also to **Rossana**, I will never stop to thank you for making all this possible. Everything started with your interview and I will be grateful to you for all my life.  
*Ti voglio veramente bene.*

I extend my acknowledgements also to other people in the different ENTICE partners. Without your help this thesis would not been possible. Special thanks to the other fellows, it was a privilege and a pleasure to work with all of you. I hope to meet each of you somewhere in the world.

Ecole Centrale de Lyon has provided a creative and challenging working environment. Everybody is to thank:

- **Thierry** who introduced me to the XPS technique. His explanations and discussions were of the greatest help during this project;
- **Beatrice** for the help with TEM analysis;
- **Mathieu** for the help with the tribometer;

- **Didier** for his technical support;
- **Helene** for her administrative assistance and for sharing chocolate-breaks;
- **Gaetan** for his kindness every time I was disturbing him with my technical problems;
- **Mickael** for the informatics problems.

I would like to acknowledge also all my colleagues in ECL: I cannot but mention **Paule** who was an excellent colleague and even better friend. I miss you since the first day you left ECL. Many thanks also to all the people who gave me a personal support during the last three years after-work. I must acknowledge the “French” ones, **Arnaud**, **Arthur**, **Morgan**, **Leo** and **Idriss** for their great advice about life and for the evening spent together. I would like to thank also my “foreigner” friends for being always so enthusiastic about everything I do. Especially to **Gennarina** and **Gaetano**, always there to listen my complains, **Antonio**, **Karmen** and **Elvira** for the messages which remind me that even if I am faraway I left a piece of my life which will be always there when I need it; thank you also to **Stefano** and **Marco** for the whatsapp moral support and thank you to **Rosita** and **Giovanna** for coming over for my thesis defense; thank you also to all my ex-colleagues from the university especially to **Dante**, **Gianfranco** and **Francesco**. My warmest thanks to **Tiago**, for being so caring from so far away and for all his great advice about work and life.

Last but not least, I would like to thank my family (big hug to my grandmother) for their constant support and confidence under all circumstances.

## AUTORISATION DE SOUTENANCE

Vu les dispositions de l'arrêté du 7 août 2006,

Vu la demande du Directeur de Thèse

Madame M-I. DE BARROS BOUCHET

et les rapports de

Monsieur C. GEANTET

Directeur de Recherche - Institut de Recherche sur la Catalyse et l'Environnement de Lyon (IRCELYON) -  
UMR 5256 CNRS/Université LYON 1 - 2 avenue Albert Einstein - 69626 Villeurbanne

Et de

Monsieur A. ERDEMIR

Professeur émérite - Argonne National Laboratory - Energy Systems Division - 9700 South Cass Avenue -  
Building 212 - Room D222 - Argonne - IL 60439 - USA

**Monsieur DE FEO Modestino**

est autorisé à soutenir une thèse pour l'obtention du grade de **DOCTEUR**

Ecole doctorale **MATERIAUX**

Fait à Ecully, le 14 décembre 2015

P/Le directeur de l'E.C.L.  
La directrice des Etudes







## Abstract

European legislation on vehicle emissions continues to become more severe to minimize the impact of Internal Combustion Engines (ICE) on the environment. One area of significant concern in this respect is the reduction of friction losses resulting in reduced emissions and as well as higher fuel efficiency and lower fuel consumption. To decrease these losses, several approaches have been made particularly at design of mechanical parts stage and at experimental level to optimize lubricant components. A great contribution to solve the problem can be given by the optimization of the additives package blended into the engine lubricants. The molybdenum dithiocarbamate (MoDTC) is the additive showing the best tribological performance by acting as friction modifier. It decomposes under high temperatures and pressure, forming layered structures on the engine surfaces. However, the use of effective friction reducing additives to achieve low boundary friction coefficient is not enough to have great engine fuel efficiency. In addition, in fact, it is needed also to maximize their durability, preventing premature consumption or depletion of these additives. It has been shown, in fact, that the friction reduction performance of MoDTC is sensitive to engine operating time and that is related to the degradation of MoDTC itself. In the first part of my thesis we tried to get a good comprehension of the chemical mechanisms of MoDTC ageing and to study the impact on the tribological properties. The chemical bulk oil characterization of MoDTC blended into the base oil when subjected to thermo-oxidative degradation allowed to propose a new hypothetical chemical pathway followed by the friction modifier molecules during the ageing process. At the same time, these findings were linked to the impact of the MoDTC degradation on its tribological properties. As reported in literature, another MoDTC drawback is its strong antagonism with DLC coating. In fact, when DLC-involving contacts are lubricated by MoDTC-containing base oil, a catastrophic DLC wear is produced. For this reason, in the second part of the project a multi-techniques approach has been adopted to get a better understanding of this wear mechanism. The combination of all the findings allowed to propose for the first time a new wear mechanism based on the formation of molybdenum carbide species inside the contact. A strong chemical interaction between the molybdenum-based species formed on the steel counter-body and the carbon of the DLC material has been supposed, leading to the formation of MoC species. All the results found are discussed to clarify the correlation between degradation time, tribological performance and tribofilm characterizations in both steel/steel and DLC/steel contact.

## Résumé

La législation européenne sur les émissions des véhicules devient de plus en plus sévère et ceci afin de minimiser l'impact sur l'environnement de la pollution occasionnée par les moteurs à combustion interne. La réduction des pertes par frottement et une plus faible consommation du carburant représentent différents aspects sur lesquels il est possible d'intervenir dans ce sens. Pour diminuer les pertes par frottement, plusieurs approches ont été utilisées, soit au niveau du design des pièces mécaniques, soit au niveau de l'optimisation du lubrifiant pour un contact considéré. Le dithiocarbamate de molybdène (MoDTC) est l'un des additifs modificateur de frottement permettant d'atteindre les plus faibles coefficients de frottement pour un contact acier/acier lubrifié en régime limite. La molécule se décompose dans le contact à des températures et des pressions élevées, en formant des feuillets lamellaires de MoS<sub>2</sub> sur les surfaces frottantes. Cependant, il est nécessaire d'optimiser la durée de vie de ces additifs, en empêchant leurs appauvrissements ou dégradations prématurés dans le lubrifiant. Il a été montré, en effet, que les performances du MoDTC sont sensibles au temps de fonctionnement du moteur et sont donc liées à sa dégradation.

L'objectif principal de cette thèse était donc de mieux comprendre le comportement tribologique (frottement et usure) d'une huile de base contenant du MoDTC en fonction de la dégradation du lubrifiant pour des contacts acier/acier et DLC/acier. L'approche utilisée pour mieux comprendre le comportement du MoDTC lorsqu'il est soumis à une dégradation thermo-oxydative consiste à combiner des expériences tribologiques, à des caractérisations de surface (XPS, FIB / TEM / EDX, Raman, SEM) et à des caractérisations chimiques des huiles (chromatographie en phase liquide, spectroscopie de masse, FT-IR). Un lien direct et cohérent entre la composition du tribofilm et la voie de décomposition chimique de l'additif MoDTC proposée a été mise en évidence.

Les additifs modernes sont conçus pour être utilisés sur des surfaces à base de fer. Il est donc essentiel d'optimiser simultanément les lubrifiants et les revêtements pour améliorer leurs performances. Dans cette thèse, un modèle d'usure du revêtement DLC hydrogéné lubrifié en présence de MoDTC a été proposé. Nous avons établi à l'aide de plusieurs techniques, que l'usure est due principalement à la formation de carbure de molybdène présent dans le tribofilm formé à la surface de l'acier.

**Key words :** MoDTC, friction modifier, degradation, DLC coating

**Mots Clé :** MoDTC, modificateur de frottement, vieillissement, couche mince DLC